

**Elucidation of the Role of DNA-Damage Response
Genes in the Tumor Microenvironment and
Molecular Characterization of a “Tropical” Chronic
Lymphocytic Leukemia Cohort**

Inaugural-Dissertation

zur

Erlangung des Doktorgrades

philosophiae doctor (PhD)

der Medizinische Fakultät

der Universität zu Köln

vorgelegt von

Benedict Sackey

aus Sekondi, Ghana

Cologne University Publication Server (KUPS), Köln

2023

Betreuerin/Betreuer: Prof. Dr. Christian P. Pallasch

Referentin/Referent : Prof. Dr. Björn Schumacher

Prof. Dr. Olaf Utermöhlen

Prof. Dr. Peter Nürnberg

Datum der Mündlichen Prüfung: 13.06.2023

Table of Contents

I.	Acknowledgment	7
II.	Abstract of Dissertation	8
III.	Zusammenfassung	10
1	Introduction	12
1.1	Cancer pathogenesis and epidemiology	13
1.2	Risk factors to tumorigenesis	14
1.3	Cancers of the blood and lymphatic systems	15
1.4	The leukemias	15
1.5	The Lymphomas	18
1.5.1	Hodgkin Lymphomas (HL)	18
1.5.2	The Non-Hodgkin's Lymphomas (NHL)	18
1.6	The Role of DNA Damage in Carcinogenesis	20
1.6.1	Types and Mechanisms of Endogenous DNA Damaging Agents	21
1.6.2	Types and Mechanisms of Exogenous DNA damaging agents	22
1.7	The DNA Damage Response (DDR) System	23
1.8	Types of DNA Damage Repair Pathways	23
1.8.1	DNA Double Strand Break Repair Mechanisms	23
1.8.2	Other forms of DNA Damage Repair Mechanisms	26
1.8.3	Role of DDR Genes in Cell Cycle Progression	28
1.8.4	Role of DDR Genes in Cellular Apoptosis	30
1.8.5	Role of DDR Genes in Cellular Senescence	31
1.8.6	Deregulated DDR Genes; a Cause of Tumorigenesis	32
1.8.7	The Role of DDR Genes in Cancer Treatment Failures	33
1.8.8	Tumor Microenvironment Mediates Acquired Treatment Resistance	34
1.9	Contemporary Treatment Strategies in Cancers	40
1.9.1	Surgical Treatment of Cancers	40
1.9.2	Cancer Radiotherapy	40
1.9.3	Cancer Chemotherapy	40
1.9.4	Cancer Immunotherapy	42
2	Aims and Objectives	50
2.1	Problem statement	50
2.2	Aims of the Research	50
2.2.1	Specific objectives	51
3	Materials and Reagents	52
3.1	Devices	52
3.2	Disposable Materials	54
3.3	Chemicals	55
3.3.1	Cell culture	55
3.3.2	Cloning	55
3.3.3	Western Blot	56
3.4	General	57
3.4.1	Buffer, Media and Solution composition	57
3.5	Kits	58
3.6	Cytokines, Primer and Enzymes	59
3.6.1	Cytokines	59

3.6.2	Oligo sequences for shRNA	59
3.6.3	Enzymes	59
3.7	Antibodies	59
3.7.1	Primary Antibodies	59
3.7.2	Secondary Antibodies	60
3.7.3	Fluorochrome Conjugated Antibodies	60
3.8	Inhibitors and Chemotherapeutic Agents	62
3.8.1	Inhibitors	62
3.8.2	Chemotherapeutic Agents	63
3.8.3	Other Reagents	63
3.9	Cell Lines, Primary Cells and Mouse Strains	63
3.9.1	Cell Lines	63
3.9.2	Primary Cells	63
3.9.3	Mouse Strains	64
3.9.4	Bacteria Strands	64
3.10	Software	64
4	Methods	65
4.1	Generation of short hairpin ribonucleic acid (shRNA) mediated knock downs of the M552-MyD88 cell line	65
4.1.1	shRNA design	65
4.1.2	Short hairpin Ribonucleic Acid (shRNA) plasmid cloning	65
4.1.3	Subcloning of shRNA from MLS backbone into MLP backbone	66
4.1.4	Dephosphorylation of recipient MLP vector	66
4.1.5	Ligation of shRNA to MLP	67
4.1.6	Transformation of DH5- α competent <i>E.Coli</i>	68
4.1.7	DNA Sequencing	68
4.1.8	Transfection of retroviral producing ecotropic phoenix cell line	69
4.1.9	Transduction of MyD88 cell line with viral supernatant	69
4.1.10	Generation of cell lysates	70
4.1.11	Protein determination by Pierce Bicinchoninic acid (BCA) assay kit	70
4.1.12	Sodium dodecyl sulphate polyacrylamide gel electrophoresis (SDS-PAGE)	70
4.1.13	Western blotting	71
4.2	Primary cells isolation	71
4.2.1	Isolation of primary thioglycollate induced murine macrophages	71
4.2.2	Purity check	72
4.2.3	Isolation and differentiation of murine bone marrow derived macrophages	73
4.2.4	Macrophage phenotype staining and determination by flow cytometry	74
4.2.5	Peripheral blood mononuclear cell isolation from Ghanaian CLL patients	76
4.2.6	Phenotypic characterization of Ghanaian CLL patients	76
4.3	Functional cell culture experiments	79
4.3.1	Cytotoxicity of MyD88 parental and KD cells to selected chemotherapeutic agents	79
4.3.2	Generation of cells' secretome/conditioned media (CM)	79
4.3.3	Genotoxic stressed tumor cells	79
4.3.4	Antibody dependent cellular phagocytosis assay (ADCP)	79
4.3.5	Determination of non-opsonized phagocytosis (spontaneous phagocytosis)	81
4.3.6	Effect of genotoxic stress and effector cell contact on immune checkpoint antigens	82
4.3.7	Immune checkpoint antigen inhibition in co-culture of MyD88 cells	82
4.4	Total exosome isolation from cell culture media	83
4.4.1	Functional effect of exosomes on tumor cells- macrophages co-culture	84
4.5	Statistical analysis and data illustration	84
5	Results: The role of DNA damage response in the tumor-macrophage interaction	85
5.1	Functional impact of DNA damage response genes deregulation on phagocytosis and efficacy of immune checkpoint inhibitors in a murine model of ABC-like DLBCL	85
5.1.1	Introduction	85

5.2	Characterization of the E μ -Myc and OSU-CLL cell lines for <i>in vitro</i> assessment of DDR on phagocytosis	86
5.2.1	OSU-CLL cells inappropriate for studying Fc-gamma-mediated phagocytosis due to inherent stickiness	87
5.2.2	High Cd20 antigen expression of E μ -Myc cell is critical to genotoxic substance-induced ADCP	89
5.2.3	E μ -Myc cells inappropriate for studying Fc-gamma-mediated phagocytosis due to in vitro loss of Cd20 expression	91
5.2.4	E μ -Myc cells show reduced Fc- γ mediated phagocytosis relative to other B-cells	92
5.2.5	E μ -Myc cells downregulate expression of CD20 antigens	94
5.3	Characterization of Myloid Differentiation Primary Response Protein 88 (MyD88) cell line for functional genetic studies	96
5.3.1	Baseline characteristics of Cd20 expression, genotoxic sensitivity, antibody dependent cellular phagocytosis (ADCP) and proliferation of MyD88 clones	96
5.3.2	Genotoxic pretreatment increases phagocytosis of M552 cells under anti-CD20 treatment	99
5.3.3	Generation and characterization of M552 cell line with knockdown of DNA damage response genes	101
5.3.4	Knockdown of DNA damage response genes changes proliferation pattern of M552 cells	103
5.3.5	Knockdown of DNA damage response genes alter sensitivity of M552 cells to genotoxic treatment	105
5.4	Genes in DNA damage response pathway are crucial for effective tumor cell phagocytosis	107
5.4.1	Phagocytic function of peritoneal macrophage is impaired by knockdown of critical DNA damage response genes in tumor cells	107
5.4.2	Similar DDR genes regulate tumor cells phagocytosis in primary macrophages from different anatomic compartments	113
5.4.3	Knockdown of identified DDR genes impair phagocytic capacity of Bone Marrow-Derived Macrophages	113
5.4.4	Downregulation of DDR genes also influence phagocytic capacity of J774.1A macrophage cell line	115
5.4.5	Peritoneal, bone marrow-derived and J774.1A macrophages show shared DDR genes dependencies in phagocytosis of tumor cells with downregulated DDR genes	116
5.4.6	Abrogation of critical DDR genes impair phagocytosis through changes in functional effects of cellular secretome (conditioned media)	119
5.4.7	Genotoxic stress orchestrates DNA damage response gene-mediated secretory phenotype in tumor cells	123
5.5	M552 lymphoma cell model of ABC-subtype DLBCL express high levels of immune checkpoint antigens	126
5.6	Immune checkpoint inhibitors further enhance phagocytosis of anti-CD20/mafosphamide treated tumor cells	128
5.6.1	Anti-CD47 promotes phagocytosis predominantly through interruption of CD47/Sirp- α interaction	131
5.6.2	Treatment refractory DDR gene KD cells differ in immune checkpoint expressions	134
5.6.3	Immune checkpoint inhibitors overcome impaired phagocytosis of DDR genes KD cells	137
5.6.4	Immune Checkpoint inhibitors bolster phagocytosis of other effector cells	140
5.7	Tumors with downregulated DDR genes influence phenotypic characteristics of macrophages	143
5.8	<i>TP53</i> is required for functional extracellular vesicles composition and optimum outcome of immune checkpoint inhibitors	147
5.9	Unraveling the Molecular Signature of “Tropical” African Chronic Lymphocytic Leuemia (CLL) – The Ghanaian Cohort	149
5.9.1	General introduction and objectives	149
5.9.2	Demographic characteristics of recruited CLL patients	150
5.9.3	Hematological profile of CLL patients	152
5.9.4	Ghanaian CLL patients present with advance clinical stages of the disease at diagnosis	155
5.9.5	Challenges of geographic specific hematology reference ranges and Binet staging system	156
5.9.6	Expression of surface immunoglobulin IgM and IgD in CLL	156
5.9.7	ZAP-70 and CD38 expression in CLL patients	161
5.9.8	Expression of immune checkpoint antigens on peripheral CD19+CD5+ CLL cells	166
5.9.9	Clinical stage in CLL is independent of immune checkpoint and prognostic parameters	169
6	Discussion	172
6.1	Functional impact of DNA damage response genes deregulation on phagocytosis and efficacy of immune checkpoint inhibitors in a murine model of ABC-like diffuse large B-cell lymphoma (DLBCL)	172
6.1.1	Introduction	172

6.1.2	Eμ-Myc cells downregulate Cd20 expression precluding use for DNA damage response genes functional assays utilizing anti-Cd20 mediated phagocytosis	172
6.2	Evaluation of MyD88 cell line for functional assays elucidating DNA damage response genes regulation of macrophage phagocytic functions under chemo-immunotherapy	174
6.2.1	Downregulation of DNA damage response genes influence proliferation of M552 KD cells	175
6.2.2	Downregulation of DNA damage response genes alter sensitivity of M552 cells to genotoxic treatment	177
6.3	Tumor cells phagocytosis is influenced by DDR genes downregulation	181
6.3.1	Abrogation of critical DDR genes impact phagocytosis through changes in functional effects of cellular secretome	184
6.3.2	Importance of KD cells to cellular secretome composition	188
6.3.3	Expression of high levels of immune checkpoint antigens promote tumor cell phagocytosis with checkpoint inhibitors-based chemo-immunotherapy	188
6.3.4	Anti-CD47 promotes phagocytosis through CD47-Sirp-α disruption	190
6.3.5	Poorly phagocytosed DDR KD cells show different immune checkpoint antigen expression upon genotoxic treatment	191
6.3.6	Immune checkpoint inhibitors circumvent impaired phagocytosis of DDR genes KD cells	192
6.3.7	Tumors with downregulated DDR genes influence phenotypic characteristics of macrophages in vitro	193
6.3.8	<i>TP53</i> is required for packaging extracellular vesicles and optimum outcome of immune checkpoint inhibitors	195
6.4	Demographic of CLL cohort and Presentation at Diagnosis	197
6.4.1	Ghanaian CLL patients present with advanced diseases at diagnosis	198
6.4.2	Good prognosis of CLL cohort thwarted by late poor clinical stage at diagnosis	199
6.4.3	Surface immunoglobulin (sIg) pattern and their correlation to other biologic variables	201
6.4.4	Expression of Immune checkpoint and their correlation to prognostic factors	204
7	Conclusion	205
7.1	Elucidation of the role of DNA-damage response in the tumor microenvironment interaction	205
7.2	Molecular characterization of a “Tropical” Chronic Lymphocytic Leukemia cohort	205
8	Outlook	207
9	References	208
10	Appendices	273
	Abbreviations	279
	List of Figures	287
	List of Tables	289
	Erklärung	290
	Overview of publications	290
	Curriculum vitae	291

I. Acknowledgment

I express my immense thanksgiving to Prof. Dr. Christian Pallasch for the opportunity to work in his research group and the enormous support accorded me in guidance, advice, technical support, critique and inspiration to undertake this study.

I thank Prof. Björn Schumacher and Prof. Utermöhlen for being my tutors in the IPHS graduate school and their helpful, constructive comments and inputs regarding this project.

I am also grateful to Prof. Badu-Addo, the nurses, and CLL patients of the Hematology Clinic of Komfo Anokye Teaching Hospital and Mr. Oppong Agyeman, Renate Asare, Dr. Albert Dompere and Eugene for support during my field trips to sample the CLL patients' in Ghana.

My special thanksgiving to the postdocs in AG. Pallasch group especially, Drs. Stuart James Blakemore, Daniela Vorhort, and Elena Izquierdo for being a fortress of support in technical assistance, in resolving challenges related to my work and constructive engagement and encouragement throughout my study.

Michael Michalik, Reinhild Brinker, and Olaf, I am immensely grateful for the support and pieces of expert advice you provided me throughout my work.

To all my colleagues and friends in the whole Hallek family especially Max, Daniel, Verena, Anna, Hien, Natascha, Heidi, Alex, Henning Feldkötter, Oleg, Günther, Lukas, I shall forever treasure the memories we shared at data clubs, retreats, kika competitions and the workplace that kept us all going in pursuit of our goals and made the working environment conducive to all.

This study was sponsored and financed by DAAD-MoE Ghana scholarship without which this work would not have been possible. I remain forever grateful for such a seed in my life.

Many thanks to ALL.

II. Abstract of Dissertation

In most human cancers such as diffuse large B cell lymphoma (DLBCL) and Richter's transformation of chronic lymphocytic leukemia (CLL), major genomic components of the DNA damage response (DDR) complex such as p53, suffers inactivating mutations and dysregulation that impairs critical DNA repair processes and apoptotic pathways relevant to therapeutic treatment. The advent of chemoimmunotherapy (CIT) has improved treatment outcomes of many B-cell malignancies within the last few decades. However, despite the successes of CIT as frontline therapy, many highly aggressive, relapsed/refractory B-cells malignancies still remain a major clinical challenge as therapy resistance account for 90% of cancer related death. The tumor microenvironment (TME) has been shown to mediate therapeutic resistance. Protumorigenic TME promotes complex molecular crosstalk of tumor with surrounding stroma cells that facilitate tumor survival, proliferation, immune escape and metastasis. In CLL which is characterized by accumulation of neoplastic CD5⁺/CD19⁺ expressing B-cell clones', differences in disease biology and clinical outcomes reported among different racial groups and geographical settings may reflect interplay of different genetic and environmental factors.

This research sought to elucidate the role of DNA damage response genes (DDR) in TME interactions, and decipher the molecular signature of "tropical" CLL in an African cohort by measuring molecular informative markers of the malignant B-cells. Using an ABC-subtype of DLBCL cell line (Myd88, clone M552), we show that, downregulation of *TP53* and *ATX* genes in tumor cells impair antibody dependent cellular phagocytosis (ADCP) under CIT treatment. We identified the cellular secretome as a communicating conduit affected by gene downregulation that causes impaired tumor cells killing in CIT treatment and demonstrated that CD47/Sirp- α axis blockade with checkpoint inhibitors in combination with CIT overcome impaired phagocytosis of *TP53* and *ATX* downregulated cells.

CLL patients' in tropical Africa (Ghana) showed predominantly females than males' incidence (51.1% vs 48.9%), had a median age of 59yrs with 42.2% < 55yrs compared to Western CLL patient who are predominantly males than females (2:1), have a median age of 71yrs, with 5-11% below 55yrs. Despite 80% of patients showing good prognosis according to ZAP-70 and CD38 assessment, 88.4% of CLL patients presented with late clinical stage based on Binet criteria at diagnosis. Peripheral CD5⁺/CD19⁺ B-cells of CLL patients expressed higher proportion (54.5%) of monotypic surface IgM B-cell receptor (BCR) than dual IgM⁺/IgD⁺ (34.1%) BCR unlike the Western CLL patients who predominant express dual surface IgM⁺/IgD⁺ BCR. Thus, p53 and *ATX* genes of DDR are critical for therapeutic success of CIT. Anti-CD47/Sirp- α or anti-PDL1/PD-1 combination with CIT overcome tumor killing failures caused by dysregulated DDR genes, providing the rational for addition of immune-checkpoint

inhibitors to current frontline CIT treatment. Also, clinical and molecular features differ in CLL presentations among African population compared to that in developed Western countries with high proportion of African CLL patients presenting with late stage clinical disease at diagnosis.

III. Zusammenfassung

Bei den meisten menschlichen Krebsarten wie dem diffusen großzelligen B-Zell-Lymphom (DLBCL) und der Richter-Transformation der chronischen lymphatischen Leukämie (CLL) sind wichtige genomische Komponenten des DNS-Schadensreaktionskomplexes wie p53 inaktiviert und dysreguliert, wodurch wichtige DNS-Reparaturprozesse und apoptotische Wege, die für die therapeutische Behandlung relevant sind, beeinträchtigt werden. Die Einführung der Chemoimmuntherapie (CIT) hat in den letzten Jahrzehnten die Behandlungsergebnisse bei vielen bösartigen B-Zell-Tumoren verbessert. Trotz der Erfolge der CIT als Erstlinientherapie stellen viele hochaggressive, rezidivierende/refraktäre B-Zell-Malignome nach wie vor eine große klinische Herausforderung dar, da Therapieresistenz für 90 % der krebbsbedingten Todesfälle verantwortlich ist. Es hat sich gezeigt, dass die Tumormikroumgebung (TME) die Therapieresistenz vermittelt. Das protumorigene TME fördert eine komplexe molekulare Wechselwirkung des Tumors mit den ihn umgebenden Stromazellen, die das Überleben, die Vermehrung, die Flucht vor dem Immunsystem und die Metastasierung des Tumors erleichtern. Bei der CLL, die durch eine Anhäufung neoplastischer CD5+/CD19+ exprimierender B-Zell-Klone gekennzeichnet ist, könnten die Unterschiede in der Krankheitsbiologie und den klinischen Ergebnissen, die zwischen verschiedenen ethnischen Gruppen und geografischen Gegebenheiten berichtet wurden, das Zusammenspiel verschiedener genetischer und umweltbedingter Faktoren widerspiegeln.

In dieser Studie wurde versucht, die Rolle von DDR-Genen bei TME-Interaktionen aufzuklären und die molekulare Signatur der "tropischen" CLL in einer afrikanischen Kohorte zu entschlüsseln, indem informative molekulare Marker der malignen B-Zellen gemessen wurden. Anhand eines ABC-Subtyps der DLBCL-Zelllinie (Myd88, Klon M552) zeigen wir, dass die Herunterregulierung von p53- und ATX-Genen in Tumorzellen die Phagozytose unter CIT-Behandlung beeinträchtigt. Wir identifizierten das zelluläre Sekretom als eine kommunizierende Leitung, die von der Herunterregulierung von Genen betroffen ist, die eine beeinträchtigte Abtötung von Tumorzellen bei der CIT-Behandlung verursacht, und zeigten, dass die Blockade der CD47/Sirp- α -Achse mit Checkpoint-Inhibitoren in Kombination mit CIT die beeinträchtigte Phagozytose von herunterreguliertem p53 und ATX überwindet.

CLL-Patienten im tropischen Afrika (Ghana) sind überwiegend weiblich (51,1 % gegenüber 48,9 %) und haben ein Durchschnittsalter von 59 Jahren, wobei 42,2 % jünger als 55 Jahre sind, im Vergleich zu westlichen CLL-Patienten, die überwiegend männlich sind (2:1) und ein Durchschnittsalter von 71 Jahren haben, wobei 5-11 % jünger als 55 Jahre sind. Obwohl 80 % der Patienten gemäß der ZAP-70- und CD38-Bewertung eine gute Prognose aufwiesen, befanden sich 88,4 % der CLL-Patienten zum Zeitpunkt der Diagnose in einem späten klinischen Stadium gemäß den Binet-Kriterien. Die

peripheren CD5+/CD19+ B-Zellen der CLL-Patienten wiesen einen höheren Anteil (54,5 %) an monotypischen Oberflächen-IgM-B-Zellrezeptoren (BCR) auf als duale IgM+/IgD+ (34,1 %) BCR im Gegensatz zu den westlichen CLL-Patienten, die überwiegend duale Oberflächen-IgM+/IgD+ BCR exprimieren.

Somit sind die p53- und ATX-Gene der DDR entscheidend für den therapeutischen Erfolg von CIT. Die Kombination von Anti-CD47/Sirp- α oder Anti-PDL1/PD-1 mit CIT überwindet das Versagen der Tumorabtötung, das durch dysregulierte DDR-Gene verursacht wird, und liefert die Begründung für die Ergänzung der derzeitigen CIT-Behandlung durch Immun-Checkpoint-Inhibitoren. Außerdem unterscheiden sich die klinischen und molekularen Merkmale der CLL in der afrikanischen Bevölkerung von denen in den westlichen Industrieländern, wobei ein hoher Anteil der afrikanischen CLL-Patienten zum Zeitpunkt der Diagnose ein spätes Krankheitsstadium aufweist.

1 Introduction

Evolving understanding of tumor biology over the years has led to the recognition that, the tumor microenvironment (TME) is a site of complex intercellular and molecular interaction that leads to the development of the malignant phenotype of cancer (1). Tumors driven by genetic and epigenetic changes influence their microenvironment through complex multi-directional crosstalk leading to re-organization of microenvironmental components that favour tumor cell survival, proliferation, immune escape, metastasis and treatment refractory (2). The tumor microenvironment thus act as a functional ecosystem to promote interaction of tumor cells with their microenvironment stromal elements comprising mesenchymal, vascular and immune cells through complex signaling networks within the extracellular matrix.

Tumor cells and their products within the TME influence and alter gene expression in non-tumor cells residing in or infiltrating into the microenvironment to influence their functions (3, 4). Stromal cells such as fibroblasts and endothelial cells are co-opted to perform tumor supporting functions as cancer-associated fibroblast (CAF) and transition into mesenchymal cells involved in tumor metastasis (EMT). Infiltrating tumor-antagonizing immune cells, known to play major roles in tumor killing, are suppressed through inhibition of cytotoxic functions through numerous mechanisms including upregulation of inhibitory checkpoint proteins to induce tumor escape from immune surveillance (5, 6). Additionally, Immune cells such as macrophages and lymphocytes are coerced into protumorigenic roles within the TME as tumor-associated macrophages (TAM) and tumor infiltrating lymphocytes (TILs) where their presence have been correlated to worse prognosis in a number of studies (7-9).

The extracellular matrix (ECM) and its related enzymes and chaperone proteins (10) normally provides both physical scaffolds to maintain tissue structure and biochemical signals to modulate cellular function. However, within the TME, ECM secreted by both tumor and stromal cells could promote tumor proliferation, metastasis and treatment resistance. Increase in deposition of extracellular matrix such as collagen, fibronectin, hyaluronan and laminin promote invasion of tumor cells (11, 12).

Survival of a species depends on fidelity in transmission of the genetic material to its progeny. Accumulation of genomic mutation could result in cancer, premature aging and chronic inflammation which are detrimental to the survival of an organism. Thus, organisms develop complex mechanism to detect, avoid and resolve genomic mutation to prevent transmission of erroneous genetic information and to interrupt occurrence of neoplastic transformation. Within the

permissive tumor microenvironment, progressive acquisition of genetic lesions underpins clonal evolution of tumor heterogeneity with multi-drug resistant acquisition that promote tumor progression and metastasis (13). More importantly, DNA damage response mechanism, detect genetic lesions, arrest cell cycle progression to effect repairs and commit affected cell to apoptosis or permanent replicative arrest when genomic damage is irreparable, is particularly targeted for inactivation or dysregulation in numerous human cancers (14, 15). Impaired DNA damage response exacerbate existing gene deletions, chromosome losses, rearrangements, and aberrant features that characteristically enable tumor progression, metastasis, and drug resistance (16). The resulting genomic instability drives heterogeneous tumor evolution that is refractory to current therapeutic drugs as observed in cancers such as diffuse large B-cell lymphoma (DLBCL) where up to 40% of patients progress under current treatment regimen (17) or sudden change of course of progression from indolence to a rapidly aggressive tumor phenotype such as transformation of chronic lymphocytic leukemia (CLL) to Richter's syndrome (mainly DLBCL) with very poor treatment outcomes and reduced survival (18, 19).

The DNA damage response can also arouse immune system through mediation of soluble immune signaling factors whose secretion is orchestrated by different components of the DDR (20). Recently, chemotherapy-mediated genotoxic damage was shown to induce soluble factors that potentiate enhanced tumor cells killing through antibody-dependent cell mediated phagocytosis in TME of an aggressive “double-hit” lymphoma model (21).

An understanding of the underlying genes of DDR mechanism mediating cellular and molecular interactions of tumor cells with its microenvironment could provide a channel to disrupt such dependence interplay as a therapeutic treatment strategy.

1.1 Cancer pathogenesis and epidemiology

Cancer is a term to describe a plethora of malignancies characterized by abnormal cellular proliferation, growth and differentiation with potential to invasively metastasis from primary sites of origin in to secondary anatomic niches. Cancer is a disease caused by the accumulation over time of changes to the normal DNA sequence resulting in alterations, loss, amplification, or changes in expression of genes important for normal cellular functions and growth properties, including proto-oncogenes and tumor suppressor genes.

According to Global Cancer Incidence, Moratlity and Prevalence (GLOBOCAN) reports, global estimate of cancers keep increasing from 18.1 million cases with 9.6 million cancer-associated mortality in 2018 to 19.3 million cases and 10 million cancer-related deaths (22, 23) . It is further

predicted that, cancer related mortality would displace that of infectious diseases as the leading rank of mortality in the 21st century.

Cancer etiology in its modern concept is viewed as a multi-step genomic mutations that alter normal cellular control of molecular networks responsible for cell proliferation, differentiation and apoptosis, inducing a state of functional autonomy of the clonally transformed cells in a supportive microenvironment (24, 25). Clones from the mutation modified cell multiply into a tumor capable of invading the boundaries of other tissues and organs in the body (26-28). The cancer inducing genetic mutations predominantly occur in proto-oncogenes, tumor suppressors and DNA damage repair genes in the somatic cells and less commonly, in germline cells which predispose to inheritable genetic lesions (14). The evolution of the malignant phenotype in cancer is not only mutation driven but heavily influenced by the dynamic heterogeneous tumor microenvironment (TME) where interactions of tumor cells with stromal cells shapes the pro-tumorigenic niche that facilitates survival, immune escape and metastasis of cancers (29, 30).

1.2 Risk factors to tumorigenesis

A close collaboration of environmental factors with genetic mutations shape the cancer phenotype. Exogenous factors found to potentiate tumorigenesis include chemical related factors such as tobacco smoke which is associated with more than 90% of lung cancer cases (31). Interestingly, diet and obesity have also been found to predispose to tumorigenesis of solid cancers and hematologic malignancies including multiple myeloma, Hodgkin lymphoma, non-Hodgkin lymphoma (NHL), and leukemia although the exact mechanisms mediating this risk remain elusive (32, 33). Nonetheless, dietary portions such as excessive fats, salt and contaminant due to preparation including aflatoxins are protumorigenic whereas vegetables, whole grain products and citrus fruits are anti-tumorigenic (34-36).

Another critical risk factor identified in tumorigenesis is biological agents such as infectious agents. Infections associated with higher viral titers are associated with induction of genetic damage that predispose to carcinogenesis. Typical examples of these include Epstein-Barr virus in Burkitt's lymphoma (37), human lymphotropic virus I in T-cells leukemia/lymphoma (38), hepatitis B and C in hepatocellular carcinomas (39), human papilloma virus subtypes 16 and 18 in cervical cancers (40). Furthermore, exposure to radiations are linked to carcinogenesis of certain malignancies such acute myeloid leukemias, myelodysplastic syndrome (41), whereas sunlight and ultraviolet (UV) radiations have been linked to certain melanomas (42) and squamous cell carcinomas (43).

Notably, causative roles in malignant transformation has been determined for biologic agents such as human lymphotropic virus type-1 in lymphomas/leukemias of T-cells (38, 44), Epstein Barr virus in Burkitt's lymphoma (37), human papilloma viruses (HPV16 and 18) (40) in cervical cancers and hepatitis B and C in hepatocellular carcinoma.

Disease entities, distinct in etiology, genetic characteristics, progression patterns and treatment that emanate from the ectoderm or endoderm are classified as carcinomas whereas tumor cells which arises from the mesoderm of fetal germ layer is called sarcoma (45)

1.3 Cancers of the blood and lymphatic systems

Hematologic malignancies consist of cancers that originate from the blood cells and the lymphatic systems. Lymphoid malignancies are generally classified as leukemia if they involve primarily the blood and bone marrow and as lymphoma if they present as tumors in lymph nodes or other organs. Often, these cancers are also called liquid tumors since they do not form lumps or masses to distinguish them from all other cancer associated with formation of masses which are called solid tumors (46, 47).

1.4 The leukemias

Leukemias are non-epithelial tumors that affect blood cells in the bone marrow with a spill-over into the general blood circulatory system and can develop at any stage in the hematopoietic process. Two distinct types of leukemia are recognized depending on the maturation status of the malignant cells. Leukemias associated with immature cells or blast that lack differentiation are classified as "acute" whereas those associated with relatively more mature or differentiated cells are referred to as "chronic" leukemias. Thus, based on the affected progenitor cells whether lymphoid or myeloid, leukemias can be sub-divided into Acute Myelogenous Leukaemia (AML), Chronic Myelogenous Leukemia (CML), Acute Lymphocytic Leukemia (ALL) and Chronic Lymphocytic Leukemia (CLL) (48, 49).

AML is characterized by rapid proliferation of blast cells within the bone marrow and also into peripheral circulation. Two major types of genetic events have been described that are crucial for leukemic transformation of AML. First, mutation of Fms-like receptor tyrosine kinase 3 (FLT 3) in the internal tandem domain or activating loop of the tyrosine kinase domain (ITD) (50). These mutations found in a third of the AML patients and over 50% of those with t(15;17) chromosomal translocation (51) disrupt the kinase auto-inhibitory function thereby rendering signal transduction through intermediates molecules constitutively active to drive aberrant cell proliferation (50, 52).

Secondly, mutations that target transcription factors and primarily impair hematopoietic differentiation. Such point mutations confer the capacity to convert α -keto-glutarate to R2-hydroxyglutamate by isocitrate dehydrogenase enzyme. R2-hydroxy-glutamate, an onco-metabolite subsequently inhibits α -keto-glutarate dependent enzymes such as histone and DNA demethylases impairing cell differentiation (53).

CML on the other hand arises from a reciprocal translocation of breakpoint cluster region (BCR) gene on chromosomes 22 and the proto-oncogene c-Abelson (ABL) on chromosome 9 (54). The t(9;22) (q34;q11) translocation results in formation of BCR-ABL fusion gene on truncated chromosome 22 called the Philadelphia chromosome (Ph) which when transcribed, leads to formation of defective constitutively active receptor tyrosine kinase (24). In CML, aberrant myeloid cell proliferation, survival and apoptosis inhibition activities are mediated by interaction of the defective constitutively active receptor tyrosine kinase with main signal transduction pathways, such as Rat sarcoma/mitogen-activated protein kinase (RAS/MAPK), phosphatidylinositol-3 kinase (PI3K), mammalian-Abelson murine leukemia viral oncogene homolog 1 (c-ABL) kinase pathways, Janus Kinase/signal transducer and activator of transcription (JAK-STAT) and the proto-oncogene, non-receptor tyrosine kinase (Src) pathways. Inhibition of apoptosis is thought to result from activation of the PI3K and RAS pathways with induction through protein kinase B (AKT) of Myc and B-cell leukaemia/lymphoma 2 (BCL-2) (55). CML progresses through chronic, accelerated and terminally acute leukemia “blastic” phases where spill-over of blast cells are detectable in peripheral circulation (56). In a minority of Philadelphia-negative CML (5-10%), cryptic BCR-ABL rearrangement and complex chromosomal karyotype has been reported (57, 58).

ALL arises from genetic mutation at the pluri-potent stem cell level or committed stem cell with less self-renewal capacity. The lineage of the precursor lymphoid neoplasm could be B-cells or T-cells in which case the blast cells form >20% of total cells in the bone marrow. ALL shows four times higher incidence in children than adults. ALL is associated with mutations that block lymphoid cells differentiation and drive aberrant proliferation and survival of the undifferentiated cells. Some of the driver genomic aberrations of ALL include chromosomal polyploidy and structural abnormalities such as translocations t[12;21], [1;19], [9;22], [4;11] and rearrangement (MYC, mixed lineage leukaemia (MLL) genes) which are augmented by additional cooperating lesion necessary for the disease phenotype (59, 60).

CLL is characterized by the accumulation of functionally incompetent, apoptosis-resistant, mature B-lymphocytes in the peripheral blood, bone marrow and lymphoid tissues (61). The B-cells neoplastic clones express cluster of differentiation CD⁵⁺, CD¹⁹⁺, CD²³⁺ surface markers (62). CLL represents a very heterogeneous disease, with various forms of manifestation, ranging from lymphadenopathy to an isolated leukemic phenotype (63). Furthermore, treatment response and disease course vary dramatically between patients: Some patients live for decades and do not require any therapeutic intervention, while others suffer from rapidly progressive and refractory disease (63) which could transform into a malignant lymphoma called Richter's syndrome with poor survival (64). Despite the development of novel chemo-immunotherapies as well as novel targeted therapeutic agents, there is currently no curative approach besides allogeneic stem cell transplantation. Principal genetic abnormalities found in CLL include chromosomal deletion (6q21, 11q22.3, 13q14 and 17p13), trisomy (12q13, 3q26, 8q24) and translocation (14q32) (65). Additionally, recurrent mutations in neurogenic locus notch homolog protein 1, exportin-1, splicing factor 3b subunit 1 and myeloid differentiation primary response gene 88 (*NOTCH1*, *XPO1*, *SF3B1* and *MYD88* respectively) genes have also been reported (66). Interestingly also, CLL-cells have been shown to interaction with the microenvironment through their B-cell receptors (BCR), CD40, complement receptors, cytokine/chemokine receptors, Toll-like receptors (TLR) and major histo-compatibility classes (MHC) (67) to trigger numerous cellular responses, including survival, proliferation, cell cycle progression and apoptosis inhibition.

Whiles antigenic stimulation of BCR may not be the sole mechanism in CLL development, as buttressed by evidence of antigen independent B-cell signaling in some cases of the disease (26), the relevance of BCR to the malignant phenotype is highlighted by the prognostic value of the BCR sequencing of the immunoglobulin heavy chain variable gene (*IGHV*) locus. CLL subtype carrying mutated IgHV gene offers good prognosis, whiles those with unmutated IgHV gene offers poor prognosis(68). Additionally, expression of higher level of zeta chain of T-cell receptor associated protein kinase 70 (ZAP-70) and CD38 markers also associated with poorer disease outcomes (69).

Thus, the persistence of low frequencies of candidate driver mutations coupled with a wide clinical heterogeneity in presentation and biased use of immunoglobulin heavy chain variable region genes (IgHV) support the evidence of genetic-environmental factors interaction in CLL ontogeny. Despite the typically indolent nature of CLL, some patients rapidly develop a transformed, highly aggressive NHL, which has been described as Richter syndrome (RS) Transformation typically displays the histo-morphological characteristics of a diffuse large B cell

lymphoma (DLBCL) whose aggressiveness requires intensive therapeutic intervention.

1.5 The Lymphomas

Lymphomas are a diverse group of tumors that arise from the cells in the lymphatic system such as lymph nodes, spleen, bone marrow or the thymus. The lymphomas are generally classified into Hodgkin (HL) and Non-Hodgkin Lymphomas (NHL).

1.5.1 Hodgkin Lymphomas (HL)

Hodgkin lymphomas are lymphoid neoplasm of B cells in which the malignant cells are admixed with a heterogeneous population of non-neoplastic inflammatory cells. Hodgkin's lymphomas are further sub-divided into classical variant (cHL) comprising; nodular sclerosing, mixed cellularity, lymphocyte depleted, and lymphocyte rich sub-types and the non-classical variant of nodular lymphocyte predominant Hodgkin's lymphoma (NLPHL). Common to all sub-types of HL are malignantly transformed cells called Reed-Sternberg (RS) cells. RS cells are large polynuclear post-germinal center B-cells that have failed immunoglobulin gene re-arrangement processes within the germinal center. RS cells constitute 1-2% of the tumor cell mass (70) but critically maintains a decisive interplay with the cellular infiltrate in HL to create an environment that suppresses cytotoxic immune responses while enabling cellular interactions and cytokines secretions that support the growth and survival of RS cells. Specifically, apoptosis bound RS cells are rescued through constitutively active nuclear factor kappa-light chain-enhancer of activated B-cells (NF- κ B) signaling sustained by CD30, CD40, tumor necrosis factor alpha (TNF- α) and notch-1 pathways engagements (71-73).

Conversely, secretions such as interleukin 10 (IL-10), transforming growth factor beta (TGF- β) and CD95 ligands by RS cells shapes the tumor microenvironment by elimination of CD8⁺ cytotoxic T-cell and T-helper type 1 (Th1) cells (74, 75)

Thus, in cHL subtypes, inflammatory infiltrates comprise predominantly of T-regulatory cells (Tregs) and T-helper type 2 (Th2) cells while as in NLPHL variant, lymphocytic and histiocytic cells are the predominant infiltrates (76).

1.5.2 The Non-Hodgkin's Lymphomas (NHL)

Non-Hodgkin lymphoma (NHL), the most prevalent hematologic cancer, represent a diverse group of malignant tumors of lymphoid tissues variously derived from the clonal expansion of B-cells, T-cells, natural killer (NK) cells or precursors of these cells.

As a heterogeneous disease entity, NHL comprise over 30 different disease subtypes, making 60%

of all lymphomas and are classified based on the type of lymphoid cells involved. However, NHL could also be sub-divided based on the rate of growth of the tumor cells into less aggressive or indolent and aggressive phenotypes.

Diffuse large B-cell lymphoma (DLBCL) is the commonest subtype of NHL, accounting for 60% of NHL and 35% of all newly diagnosed lymphomas (77, 78). DLBCL represent a highly heterogeneous group of diseases both genetically and clinically with variable treatment outcomes. The putative mature B-cells involved in DLBCL pathophysiology are germinal center experienced and show monoclonal rearrangement of immunoglobulin heavy (IGH) and light chain (IG-IG λ) genes. However, gene expression profiles of the putative cells could sub-classify DLBCL into germinal center (GC)-like DLBCL and activated B-cells (ABC)-like DLBCL (79)

GC-like DLBCL constitute about 40-50% of DLBCL and shows a highly hyper-mutated immunoglobulin gene with indication of ongoing somatic hyper-mutation (SHM), an increased in B-cell lymphoma 6 (BCL6) and CD10 expressions. Generally, GC like DLBCL subtype shows better prognosis upon treatment with frontline therapy, R-CHOP (rutiximab-based, cyclophosphamide, doxorubicin, vincristine and prednisone) compared to the ABC like DLBCL subtype (80). Nonetheless, better and worse prognostic subsets are still found within both groups irrespective of the cells of origin. ABC-like DLBCL subset shows no evidence of ongoing SHM but rather, an up-regulation of genes required for plasma cell differentiation such as interferon regulatory factor 4 (IFR4) and multiple myeloma oncogene 1 (MUM1). Additionally, ABC-like DLBCL shows a hallmark of activated NF- κ B and B-cell receptor pathways while downregulates germinal center associated genes. Based on the putative cell of origin alone, a minority (10-15%) of DLBCL termed unclassified, cannot be apportioned into ABC- or GC- like DLBCL subtypes.

Distinct repertoires of genetic aberrations associated with origin of the tumor cells are preferentially used by different subtypes of DLBCL in the disease pathophysiology (81).

For instance, the GC-like DLBCL subtype, often present mutations involving methylation or acetylation of histone (enhancer of zeste 2 polycomb repressive complex 2 subunit (EZH2), histone acetyltransferase p300 (EP300), cyclic adenosine monophosphate response element binding protein (CREBBP), lysine methyltransferase 2 D (KMT2D)), B-cell homing (G protein subunit alpha I3 (GNA13), GNAI2, sphingosin-1-phosphate receptor 2 (SIPR2)), phosphoinositide-3-kinase (PI3K) pathway signaling, and the Janus-associated kinase – signal transducer and activator of transcription (JAK-STAT) pathway. B-cell lymphoma 2 (BCL-2) and

MYC proto-oncogene (MYC) are mostly preferentially deregulation through a t(14;18)(q21;q32)/IGH-BCL2 and 8q24 with IGH, IGK, IGL or none immunoglobulin loci translocations respectively (82, 83)

In contrast, genetic abnormalities that result in activation of B-cell receptor signaling and the Toll-like receptor signaling pathways, ultimately resulting in constitutively active nuclear factor kappa beta (NF- κ B) pathway activation, are more common in the ABC subtype (myeloid differentiation primary response factor 88 (MYD88), CD79A/B, caspase recruitment domain family member 11 (CARD11), mucosa-associated lymphoid tissue lymphoma translocation protein 1 (MALT1), BCL10, tumor necrosis factor alpha induced protein-3 (TNFAIP3), and deletions in B-lymphocytes induced maturation protein-1 (PRDM1/BLIMP1) responsible for terminal inhibition of differentiation of ABC-like B cells into plasma cells selectively occur in ABC-subtype of DLBCL. Also, translocations involving BCL-6 locus are more common in ABC-like subtype than GC-like subtype (82, 84).

But perhaps, the most distinguishing feature of the ABC-like subtype of DLBCL is constitutive activation of NF- κ B, a transcription factor that mediate several cellular processes including inflammation, proliferation, differentiation and apoptosis inhibition. Activated NF- κ B translocates into the nucleus where it transactivates several target genes including BCL2, IL6 and IL10. Diverse pathways converge on NF- κ B activation including gain-of-function mutations in signal transduction components of the BCR (CD79a and CARD11) and toll-like receptor (MYD88) signaling pathways or Loss-of-function mutation or deletions in the NF- κ B negative regulator TNFAIP3/A20.

1.6 The Role of DNA Damage in Carcinogenesis

DNA is the only polymer that contains the blueprint information for synthesizing all the molecules that form the structures of an organism. The preservation of the genetic information in its original state requires not only accuracy in copying during DNA replication but also timely proficiency in repairing events of compromised integrity. Multicellular organisms must faithfully replicate and transmit complete set of genes as DNA, the basic unit of inheritance to their progeny to ensure genetic continuity of their species. Loss of fidelity in DNA replication results in transmission of mutations to daughter cells which may have adverse consequences on the evolutionally potential of succeeding generations and aging (85). Whilst mutations in some cases improve fitness for survival, in others, it results in deregulation of critical cellular pathway control mechanisms resulting in cancer. Among the characteristic hallmarks of cancer, is a lack of genomic stability

which underlies continuous selection of treatment unresponsive, refractory clones with high metastatic tendencies (86).

In the context of genome stability, DNA damaging agents pose the greatest risk to alteration of the genetic information. DNA is highly reactive molecule and myriad of DNA damaging agents of both exogenous and endogenous origins constantly induce damage to the genetic material. Additionally, the enzymes involved in replication and repairs (the DNA polymerases) do commit errors which may jeopardize the integrity of the genomic material. To forestall loss of genomic integrity therefore, damage to the DNA triggers complex cellular mechanisms for detection and repair collectively called the “DNA damage response system” aimed to reduce the deleterious effect of genomic damage (87). To sum up the extent of genomic assault, Lindahl *et al* (88) reported that, per single day, a human cell experiences over 10^5 DNA lesions most of which are of endogenous sources occurring as a result of normal cellular processes. DNA damage can trigger changes in gene expression, inhibits cell division, induce cell death or introduce mutations into the genetic code when damaged DNA is replicated (89).

1.6.1 Types and Mechanisms of Endogenous DNA Damaging Agents

Endogenous causes of DNA damage are cellular intrinsic-potentially aggressive factors produced by normal cellular metabolism which are capable to induce genetic lesions. These include chemical modification of DNA bases due to hydrolysis of backbone phosphodiester bonds (90), hydrolytic deamination of DNA bases, or hydrolytic cleavage of the glycosidic bonds which hold the nucleobases to the sugar-phosphate backbone termed depurination or depyrimidination depending on the base involved (91, 92). Additionally, incidence of non-canonical pairing where DNA base hydrolysis leads to conversion into another or rare DNA base which pair with other bases in a manner not in conformity to the base-pairing rules. Additionally, small organic molecules such as alkylating agents can react with DNA at multiple sites to impair accurate read-out of DNA sequences and so have profound biological consequences (93). Alkylating agents contain electrophilic centers capable of cross-linking nucleophilic centers in DNA duplex to block transcription thus making them exceptionally useful as anti-cancer treatment drugs (94). Similarly, DNA base modification such as alkylation and methylation can alter the chromatin architecture. For instance, methylation of cytosine residues at CpG islands leads to stable silencing of genes. DNA is also damaged by free radical oxygen species and nitrogen intermediates that occur as by-product of mitochondria respiration. Free radicals such as hydroxyl, peroxy, and superoxide

abstract hydrogen atoms from the deoxyribose sugar of DNA or readily react with the heterocyclic bases of DNA to induce damage (95, 96). Another form of DNA damaged occurs during normal cellular metabolism. Here, ribonucleotides (rNTP) bearing reactive 2'-hydroxyl (OH) group rather than deoxyribonucleotide (dNTP) are erroneously incorporated into the growing DNA chain either at initiation of DNA synthesis or during DNA repairs (97, 98). Reactive hydroxyl group of ribonucleotides could attack sugar-phosphate backbone of nucleic acid to induce strand breaks when inappropriate incorporated into the DNA strand (99).

1.6.2 Types and Mechanisms of Exogenous DNA damaging agents

Exogenous DNA damaging agents consist of both physical and chemical factors external to the cell capable of altering the integrity of the genetic information contained in the DNA. From the time of DNA discovery in 1869 by Friedrich Miescher (100) and prior to its molecular structure elucidation in 1953 by Watson and Crick (101), it was known that routine exposure to exogenous substances such as ultraviolet (UV) light, X-rays and various chemicals can cause DNA damage and promote cancer (102). A number of environmental agents are linked to DNA damage; some of which such as chemical mutagens and radiation can transcend cell membranes, nuclear pores to interact directly with cellular DNA. Ionizing radiations (IR) such as X-ray causes rapid elevation of free radicals and reactive oxygen species in the tissues. Excess radicals not neutralized induce oxidative stress and structural and sequence damage to the DNA. However, the most tragic DNA lesions caused by IR is the induction of DNA double strand breaks which can lead to chromosomal rearrangements (103).

Similarly UV radiation can cause formation of dimers among the DNA bases. For instance, while the ozone layer absorbs much of the harmful portion of UV radiation (UV-C), other UV component of sunlight (UV- A and UV- B) can cause formation of pyrimidine dimers of the DNA bases. Unrepaired pyrimidine dimers containing cytosine residues could be deaminated resulting in replacement of cytosine with thymine in the DNA sequence (104).

which when left unrepaired to induce double strand breaks and could further generate radiation-induced free radicals in a manner similar to ionizing radiation (105, 106). Alkylating agents have been the oldest class of anticancer drugs and play key role in the treatment of several types of cancers (107). Alkylating agents which are monofunctional forms DNA adducts with nitrogen and oxygen atoms of the DNA bases to impair replication and transcription leading to DNA damage. Bifunctional alkylating agents such as nitrogen mustards (melphalan, chlorambucil, cyclophosphamide, and ifosfamide) and chloroethylnitrosoureas on the other hand induce complex

damage to the DNA by forming adducts of chloroethyl, intra and interstrand cross-linkages leading to DNA double strand breaks (DSB). DNA DSB are among the most lethal genomic damages and organism lacking efficient DSB repair mechanism are more sensitive to alkylating agents (108). Notably also, the role of polycyclic aromatic hydrocarbons (PAH) ubiquitously found in the environment and enriched in cigarette smoke as a potent carcinogenic substance has been documented (109, 110). PAH can be metabolized into reactive intermediate which covalently bind to purine bases as stable adduct, whilst it could also form unstably adducts which depurinate to form apurinic sites in DNA (111).

1.7 The DNA Damage Response (DDR) System

In order to maintain the integrity of the DNA passed on to subsequent generations, living organisms employ diverse mechanisms to detect, signal and promote repairs of the genomic lesions caused by endogenous and exogenous agents (87). The complex network of integrated pathways activated to sense damage, transduce signals and activate effectors to orchestrate appropriate DNA repair program and resolution of replication challenges is collectively termed DNA damage response (DDR) (112). The DDR is activated regardless of the type of genomic damage to repair the DNA damage and facilitate DNA replication through coordination of cell cycle checkpoint. The DDR response thus includes activation of DNA repair pathways, cell cycle checkpoints mechanisms, cell senescence and apoptotic pathways.

1.8 Types of DNA Damage Repair Pathways

There are several pathways employed to resolve specific types of damage to the DNA. The main repair pathways are homologous recombination repair (HR) and non-homologous end joining repair (NHEJ) – adapted to DNA double strand breaks, and base excision repair (BER), nucleotide excision repair (NER), and base mismatch repair (MMR) - adapted to other forms of DNA damage.

1.8.1 DNA Double Strand Break Repair Mechanisms

DNA double strand breaks (DSB) do occur under different exogenous and endogenous conditions. These include damaging effects of ionizing radiation, treatment with certain chemotherapy, chromosomal stress, reactive oxygen species (ROS) at the ends of chromosomes due to defective metabolism. Also, despite the challenges DSBs pose to genomic integrity, it is also deliberately generated by site-specific nuclease composed of recombination-associated gene 1 and 2 nucleases (RAG1 and RAG2) proteins for the defined purpose of variable, diversity and joining genes

(V(D)J) recombination in developing B and T-lymphocytes to generate the antigen binding diversity of the immunoglobulin and the T-cell receptors (113). Two major pathways are involved in repair of DNA DSBs in eukaryotes. These repair pathways are homologous recombination (HR) where DNA damage is sensed by MRN (Mre11–RAD50 homolog – Nijmegen breakage syndrome 1(NBS1)) complex which recruits Ataxia telangiectasia mutated (ATM) to the site of damage (114), single-strand annealing (SSA) and non-homologous end-joining (NHEJ) where DSBs are sensed by Ku proteins (Ku70–Ku80) which recruits DNA-dependent protein kinase catalytic subunit (DNA-PKcs) to the damage site (115). Both ATM and DNA-PKcs are part of phosphatidylinositol 3-kinase-related kinase (PIKK) family of serine/threonine kinases which phosphorylated a number of downstream substrates.

1.8.1.1 DNA Repair by Homologous Recombination Mechanism

Homologous recombination pathway repairs DSBs using genetic information retrieved from the undamaged homologue (sister chromatid) to repair the break by reconstituting the original sequence. Critically, nucleolytic processing or resection of the ends of the DSBs to generate extended 3'-end ssDNA filament covered with replication protein A (RPA) and the recombinase Rad51 is a deciding point that tilts the repair machinery in favor of homologous directed recombination (116, 117). Several nucleases including meiotic recombination 11 (Mre11) exonuclease 1 (Exo1), DNA replication helicase/nuclease 2 (DNA2) in addition to Bloom syndrome helicase (BLM) coordinate the resection of the ends of DSB whereas DSBs blocked or chemically modified ends require the activity of Mre11/Rad50/Nijmegen breakage syndrome 1(NBS) constituting the MRN complex to initiate recognition and resection (118, 119). The NBS1 shuttle the MRN complex to the nucleus recruiting ataxia telangiectasia mutated (ATM) or ATR (ATM-and Rad3-related) proteins, members of phosphatidylinositol-3 kinase (PI3K) family, which activate a signaling process that leads to cell-cycle checkpoints and pauses cell-cycle progression (120). Two crucial substrates of ATM and Ataxia telangiectasia and RAD3 related (ATR) are checkpoint 1 and 2 kinases (Chk1 and Chk2), respectively: Once phosphorylated, these are able to induce cell cycle arrest, thus guaranteeing time for damaged cells to repair.

Another initial step for the DSB repair (DSBR) is the ATM phosphorylation of the histone, H2AX in the vicinity of DSBs, leading to the formation of γ H2AX foci (120). These foci act as a signal to recruit other repair proteins in order to allow the assembly of DSB repair complexes (121). H2AX phosphorylation can also be mediated by DNA-PK, the kinase complex that is formed once the NHEJ pathway of DSBR is activated and which acts both as sensor and as effector of DSBR (122).

Initiation of the DDR pathway is dependent on phosphorylation of histone H2A variant X (H2AX) at serine 139 to form γ -H2AX by phosphoinositide 3-kinase like kinases including ATM, ATR and DNA-PK (123, 124). Presence of γ -H2AX act as a molecular marker to the site and surroundings of DNA damage to permit MRE11/RAD50/NBS1 (MRN) complex which is involved in the early steps of DSB ends processing prior to repair by multiple pathways by maintaining broken ends of sister chromatids in close proximity (125). The Mre11 induces a nick on the 5'-end filament to allow entry of resection nucleases-exonuclease 1(Exo1), Dna2 and Bloom syndrome DNA helicase (BLM) initiate long range resection from 5' – to -3' direction whiles the MRN complex execute short range resection from 3' – to -5' direction. This nick-dependent mechanism for resection is activated in S and G2/M phases through the cyclin-dependent kinase 1 (Cdk1) dependent phosphorylation of retinoblastoma-binding protein 8 (CtIP) (126, 127). Another multi-faceted adaptor proteins recruited to the site of DNA damage is Mediator of DNA Damage Checkpoint 1 (MDC1) which initiate recruitment of critical DDR proteins including breast cancer gene1 (BRCA-1), p53 binding protein 1 (53BP1) and MRN complex (128, 129). Thus, MDC1 propagates the spread of γ -H2AX in the chromatin to form repair foci on chromatin-based platform for aggregation of DNA repair factors around the break. Also, damage to the DNA could also be detected by 53BP1, a conserved protein in eukaryotes which directly recognize DSB-specific histone code as changes to the chromatin and this forms the stimulus that recruit ATM to the site of damage (130) where it is converted from inactive dimers to active monomers through auto phosphorylation (131). 53BP1 also act as a mediator that links the upstream kinase ATR (ATM and Rad3 related) to the downstream kinases CHK2 and CHK1. Following DSB-induced phosphorylation by ATM, 53BP1 recruits replication timing regulatory factor 1 (RIF1), the Shielding complex and the CST/ Pol α -Prim complex that fills in the resected DNA end, restoring double strand DNA (dsDNA) and allowing NHEJ (132).

More recently, Hartlerode et al (133) demonstrated that DNA-PKcs could substitute for ATM in facilitating local chromatin responses during DNA DSB and that ATM recruitment to site of DSB and activation could occur without MRN or DNA-PKcs recruiting protein Ku70/80.

ATM and DNA-PKcs are activated by DSBs to phosphorylate downstream targets in all stages of the cell cycle, however, ATR is activated following single strand-DNA (ssDNA) break generated at stalled replication forks and ssDNA generated via DSB processing.

1.8.1.2 DNA Repair by Non-homologous End-Joining (NHEJ) Mechanism

The NHEJ pathway is a less fidelity mechanism of DNA DSBs repair which does not require the use of homologous sequence from an intact sister chromatid (134). However, NHEJ is described to

occur in two forms; a resection-dependent DSB prior to ligation and resection independent process (135). NHEJ is the predominant DNA DSBs repair mechanism employed by most vertebrate to repair DSB at all stages of the cell cycle including G₀, G₁, and S phases of the cell cycle (136) and V(D)J recombination (137). Following DNA DSB, the heterodimer Ku70/80 complex (KU) are the first proteins to bind the ends of the DNA DSB to form a platform for the recruitment of downstream proteins such as DNA-PKcs (138), a nuclease resects the ends of the broken double strand, artemis (135) and other double strand end-processing enzymes involved in NHEJ (139, 140). Ku is also reported to bind single-ended DSBs occurring during DNA replication (141). Functionally, the Ku-DSB end complex assembly a series of specialized proteins with scaffolding and/or enzymatic activities which partake in protection of the DNA ends, synapse formation, DNA ends processing and ligation. The processing of broken ends of double strand DNA is carried out by artemis following which template dependent and independent DNA synthesis is carried out by DNA pol λ and μ polymerases (142). The final step of ligation is catalyzed by a complex of Ligase IV, X-ray repair cross-complementing protein 4 (XRCC4), and XRCC4-like factor (XLF) (137, 143, 144).

1.8.2 Other forms of DNA Damage Repair Mechanisms

1.8.2.1 Base Excision Repairs (BER)

Nucleotide bases of DNA damaged as a result of hydrolysis, oxidation, deamination or alkylation are repaired by nucleotide base excision mechanism (145). The small base lesions do not significantly distort the DNA helical structure; however they have the potential to cause cancer, aging and neurodegeneration (146, 147). The damaged base is recognized and removed by DNA glycosylase enzyme (a base-lesion specific evolutionally conserved enzymes that cleave the bond between deoxyribose and a modified or mismatched DNA base) leaving an abasic site that is further processed through incision and end processing by specific endonuclease and exonuclease, repair synthesis and gap filling by polymerase and final ligation by ligase resulting in repaired by either short-patch (a single base replacement) or long-patch (2-10 bases replacement).

1.8.2.2 Nucleotide Excision Repair (NER)

Often, damage to DNA affects more than just a base and potentially distorts the helix structure of DNA. Such bulky DNA adducts caused by agents such as UV radiation, environmental mutagens and some drugs such as chemotherapeutics are best eliminated by nucleotide excision repair mechanism (148). NER eliminate DNA damage by the excision of single-strand oligonucleotides sequence (about 24–32 nucleotides) from a damaged DNA strand, followed by restoration of an

intact double helix by DNA repair synthesis using the undamaged strand as template. In Eukaryotic, NER is orchestrated by two distinct pathways: global genomic NER (GG-NER) and transcription-coupled (TC-NER). GG-NER detects and eliminates bulky damages in the entire genome, including untranscribed regions and silent chromatin. Here, heterotrimeric protein complex comprising XPC-RAD23-CETN2 is used to recognize the damage site on the DNA (149, 150). On the other hand, TC-NER resolves damage to a transcribed DNA strand when damage of nucleotide bases limit DNA transcription activity by RNA polymerase II which recognizes the DNA damage (151, 152). Timely removal of DNA damage is necessary to prevent collapse of the replication fork and activation of p53 dependent apoptosis triggered by prolonged stall of the replication machinery. Defects in NER has been implicated in the development of some autosomal diseases such as xeroderma pigmentosum (XP) (153), Cockayne syndrome, trichothiodystrophy, and UV-sensitive syndrome (154). On the basis of clinical presentation of xeroderma pigmentosum compared to Cockayne syndrome and trichothiodystrophy (TTD) others argues that, GG-NER is more important for suppression of UV-induced mutagenesis and carcinogenesis (155).

1.8.2.3 DNA Mismatch Repairs (MMR)

DNA mismatch repair is an evolutionary conserved post-transcription system that recognizes erroneous insertions, deletions, incorporation of nucleotide base-base mispairs, and corrects these in the newly synthesized strands by excision and subsequent replacement (156). Mismatch repair therefore is required to reduce the number of replication-associated error of DNA and its deregulation or inactivation is associated with increase of spontaneous mutations leading to hereditary and sporadic cancers. DNA nucleotide mismatch arises from DNA replication errors and recombination, as well as from some types of base modifications. The MMR mechanism in eukaryotes uses two families of MMR proteins: heterodimeric homologs of bacterial MutS (MSH) or MutL (MLH). The MutS family of proteins (MSH2, MSH3, and MSH6) recognizes base-base mismatches and small nucleotide insertion/deletion. The activity of MutS dimers at the DNA mismatch site is dependent on interactions with the proliferating cell nuclear antigen (PCNA) which is an important cofactor that participates in both DNA replication and repair mechanisms (157, 158). PCNA is loaded onto the DNA by replication factor C (RFC) where it interacts with both MutS α and MutS β dimers.

MutL homolog family proteins such as MLH1 and PMS2 endonuclease, constituting the MutL α heterodimer. The MutS α heterodimer binds to the altered region and recruits the MutL α heterodimer which subsequently engages the enzymes required for the mismatch repairs.

In prokaryotes, the daughter DNA strand is discriminated from the parent strand by hemimethylation of dGATC sites. However, in human cells daughter DNA strand is not distinguished from parent strand by hemimethylation of dGATC site, rather, MutH-dependent nick suffice as a discriminatory signal to identify the daughter strand.

Following recruitment and activation by MutS and MutL in the presence of adenosine triphosphate (ATP), MutH specifically incises a nick into the hemimethylated dGATC to provoked excision at the identified mismatch site (159, 160). Helicase II is then loaded at the nick to unwind the double strand DNA in a direction towards the mismatch. The resultant single stranded DNA is protected by single strand DNA binding protein from nuclease attack. A bi-directional excision approach (5'→3' or 3'→5') (161) is undertaken by exonucleases after which repair DNA re-synthesis and ligation is performed by polymerase δ and DNA ligase I (161, 162).

1.8.3 Role of DDR Genes in Cell Cycle Progression

The cell cycle consists of a series of events in which cellular components are doubled and accurately divided into two daughter cells. The cell cycle checkpoints are integral components of DNA damage repair and coordinate the arrest of cell cycle progression to permit DNA repair in order to avert transmission of altered genome to progeny. In this way, cell cycle checkpoints provide more time for repair of damaged DNA before DNA replication or mitosis.

The cellular DNA damage response mechanism which detect DNA damage also signal downstream effectors kinases which directly activate the cell cycle checkpoints (163). Progression through the phases of the cell cycle consists of periodic activation and inactivation of cyclin-dependent Serine/Threonine kinases (Cdks) whose activation depends on binding to their cognate cyclin. For instance, cyclin A/B bind to Cdk1 to activate G1-S phase checkpoint and it is deactivated by E3-ubiquitin ligase mediated degradation of cyclin A/B, small inhibitory proteins or inhibitory tyrosine phosphorylation. (164). Similarly, CDK2/cyclin E complexes drive a cell across the G1/S-phase border; CDK2/cyclin A, mediate DNA replication; and CDK1/cyclin B, control entry into mitosis (165).

The cell cycle is characterized by two major events; one at the S phase (synthesis) where the genome DNA is duplicated and the other at the M phase (Mitosis) where duplicated chromosomes are distributed among daughter cells. Between the S and M phases, however are “gap” phases consisting of G₁, G₂ and G₀. At the end of each phase exists cell cycle checkpoint for controlling

entry into subsequent phases. The G1 phase precedes the DNA replication (S phase) and it is a period for increased cellular biosynthetic activity such as protein synthesis, organelles formation and cell growth. The G1 checkpoint regulated by the G1/S cyclins at this stage determines continuity to S-phase, or commit to G0 phase of replicative dormancy. The G2 phase occurs after DNA replication. A number of activities including protein synthesis, organization of microtubules into a spindle and review of cellular genomic integrity at the G2 checkpoint, regulated by the tumor suppressor gene p53 are carried out.

The DDR is intricately linked to the control of the cell cycle machinery. In the event of genomic lesion, the cellular response involves complexes of protein interactions that govern cell cycle checkpoint arrest and repair of the DNA lesions. Sensors of the DNA damage transduce signals rapidly to ATM (in response to double strand breaks) and ATR (in response to variety of DNA lesions including single strand breaks and stalled replication fork) which functions as the central regulators of these response pathways to arrest the cell cycle to allow for lesion repairs (166). ATM mediates phosphorylation activation of a number of substrates including CHK2 kinase, p53 and BRCA1 (166). Additional kinases such as DNA-dependent protein kinase (DNA-PKcs), Polo-like kinase-3 (PLK3) and promyelocytic leukemia protein (PML) are reported to mediate activation of Chk2 kinase (167-170). Activated Chk2 phosphorylate breast cancer susceptibility proteins BRCA1 and BRCA2 which promote DNA homologous recombination and also participate in DNA base excision repair processes (171-174). Most importantly, CHK2 arrests the cell cycle at G1/S and G2/M by several mechanisms.

First, Chk2 kinase prevents dephosphorylation activation of Cdk2 kinase required for G1/S and S-phase progression through phosphorylation and subsequent proteasomal degradation of Cdc25A phosphatase needed to activate Cdk2 (175). Next, the cell cycle arrest is sustained by Chk2 and ATM activation of p53, a transcription factor which initiate increased expression of p21, an inhibitor of cyclin-dependent kinases to reinforce G1/S transition arrest (176). Additionally, CHK2 phosphorylate retinoblastoma tumor suppressor protein (pRb) to enhance formation of transcriptionally inactive pRb/E2F-1 complex causing G1/S arrest and apoptosis repression (177). At the G2/M transition, Chk2 together with ATM/ATR are reported to phosphorylate an RNA polymerase-II binding protein called Chk-1 which further promotes p53 transcription and G2/M checkpoint activation (178). However, regulation of the G2/M cell cycle checkpoint comes under the direct control of Chk1 protein kinase which is activated by ATR, a member of phosphatidylinositol 3-kinases that respond to DNA single strand break and stalled

replication. G2-M transition is initiated by Cyclin-dependent activating kinase (CAK) activation of Cdk2 to form a complex with cyclin-B.

In the event of stalled replication or DNA single strand break (ssDNA), activated ATR targeted to the RPA-coated ssDNA by its interacting protein ATRIP in connection with proliferating cell nuclear antigen (PCNA) related clamp and a loading protein, replication factor C complex, activates a number of substrate in the signaling pathway including RPA, Rad17, TopBP1, Claspin, and Chk1. Chk1 initiate cell cycle arrest at G2/M checkpoint by inactivating cyclin B on one hand and inhibiting Cdk2 activation through phosphorylation of Cdc25 phosphatase which promotes its ubiquitinated proteosomal degradation (179). The absence of Cdc25 phosphatase to remove inhibitory phosphorylation of CAK induced by Wee1 or mitosis inhibitor protein kinase 1 (Mik1) kinases under phosphorylative activation of Chk1 leads to establishment of G2/M checkpoint to halt the cell cycle for DNA repair.

1.8.4 Role of DDR Genes in Cellular Apoptosis

Recent understanding of the DNA damage repair mechanisms in cell cycle has demonstrated a crosstalk between DNA damage and cellular apoptotic machinery. In 1991, the wild-type p53 was shown to induce apoptosis in leukaemic cells (180). It was further shown that pro-apoptotic function of p53 plays a more important role in its antitumor effect than its cell cycle arrest in a mouse model with specific p53 mutant (181). The first step in DNA damage response is the recognition of the lesion which rapidly triggers mediators and effectors to arrest cell cycle and commence repairs to avoid lesion inheritance. However, cells with irreparably compromised genome are committed to senescence (permanent cell cycle arrest) or apoptosis (programmed cell death). Cellular senescence and apoptosis is mediated by p53 acting as a tumor suppressor protein and a transcription factor at the convergent fulcrum of signals transmitted by DNA DSBs pathway mediators (182). p53 is activated by all the sensor PI3-K kinases involved in DDR including ATM, ATR, DNA-PK, CHK1 and CHK2 leading to p53 stabilization and accumulation in the nucleus where it functions as a transcription factor (182, 183). In the absence of DNA damage, the levels of p53 is controlled by murine double minute 2 (MDM2), an ubiquitin ligase, which forms a negative feedback loop with p53 by mediating its expulsion for proteosomal degradation upon activation by p53(184). However, in DNA damage, ATM and CHK2 phosphorylation of p53 on serine 15 and 20 disengage MDM2 from p53 (185). This enables p53 to activate its target genes involved in diverse cellular processes such as DNA damage repair, cell cycle arrest, and apoptosis

induction.

A marked increase in the levels of p53 upregulate cell cycle proteins such as growth arrest and DNA damage-inducible 45 (GADD45) and p21 to triggers G1 or G2/M phase arrest (186, 187). However, if DNA repair cannot restore cells to normalcy, elevated p53 transcribe pro-apoptotic genes such as p53 upregulated moderator of apoptosis (PUMA) to antagonize anti-apoptotic BCL2 proteins thus freeing Bcl-2 Associated X protein (BAX) or BCL2 Antagonist/Killer (BAK) to induce apoptosis through the intrinsic-mitochondria mediated pathway (188).

In the BCL-2-regulated apoptotic pathway, apoptosis is initiated by transcription and/or post-transcription upregulation of the pro-apoptotic Bcl-2 homology domain 3 (BH3)-only members of the BCL-2 protein family including Bcl-2 interacting mediator o cell death (BIM), PUMA, BH3 interacting-domain death agonist (BID), Bcl-2 modifying factor (BMF), Bcl-2-associated agonist of cell death (BAD), BCL2 Interacting Killer (BIK), NOXA, Harakiri BCL2 interacting protein (HRK). The BH3-only proteins bind and inhibit the pro-survival BCL-2 proteins such as BCL-2, B-cell lymphoma-extra large (Bcl-xL), myeloid cell leukemia-1 (MCL-1), Bcl-2-like protein 2 (BCL-W) and BCL2-related protein A1 (A1/BFL1) thereby unleashing the cell's death effectors of pro-apoptotic proteins Bax and Bak (189). Bax and Bak activation induce mitochondria membrane permeability and leading to escape of apoptogenic factors such as cytochrome C, apoptosis-inducing factor (AIF), second mitochondria-derived activator of caspase/Direct inhibitor of apoptosis binding protein with low pI (SMAC/DIABLO), high-temperature requirement A2 (Htra2/Omi) , which triggers cascade of executioner caspase which dismantle the cell (190, 191). Beyond it role in transcription mediated apoptosis induction, p53 is also reported to mediate transcription-independent pathways of apoptosis initiated by stress-induced accumulation of p53 in the cytosol or mitochondria leading to direct activation of Bax and Bak pro-apoptotic proteins (192).

1.8.5 Role of DDR Genes in Cellular Senescence

Cellular senescence is a cell-cycle arrest mechanism used to impose replicative dormancy on cells deemed to have sustained DNA damage, depleted nucleotide for DNA synthesis, badly impacted by ROS, or exhausted limited proliferative lifespan (193, 194). Senescence is an irreversible process and is characterized by distinct morphology, gene expression pattern, and secretory phenotype whiles the cells remain viable and metabolically active (195). Two mechanisms of cellular senescence have been described. Replicative senescence occurs as a result of progressive

shortening of telomeres to a critical length resulting in collapse of the protective structures and exposure of uncapped chromosomal ends (196, 197). On the other hand, stress-induced premature senescence (SIPS) is caused by cellular stimulations, including activated oncogenes, cytokines, reactive oxygen species, DNA damage, or nucleotide depletion (193). Regardless of the origin, whether telomere attrition or stress factors, DNA damage response is triggered by exposed or fused chromosome ends which may result in multiple outcomes including induction of cellular senescence (198). p53 is shown as the pivotal gene which moderate cell fate by controlling processes leading to cell cycle arrest, DNA repairs, cellular senescence or apoptosis aimed to limit tumor progression (199, 200). Thus, p53 links the cellular senescence mechanism to the initiator kinase of DDR such as ATM, ATR, DNA-PK, CHK1 and CHK2 which directly activate p53 through phosphorylation (201). Additionally, multiple stress signals such as chemotherapeutic drugs and oncogenes activation are able to induce senescence by activating p53 and/or the p16^{INK4A} pathways. The p16^{INK4A} protein inhibits the activity of cyclin-dependent kinases Cdk4/6, to prevent phosphorylation of retinoblastoma (Rb) protein. Thus accumulation of hypophosphorylated retinoblastoma protein (pRb), induce cell cycle arrest and senescence through inhibition of E2F transcription (202). These stressors also trigger DNA damage regulated by either ATM-Chk2 or ATR-Chk1 pathways and thus transactivates p53 and p21^{CIP1}. Moreover, p21^{CIP1} protein levels may lead to inhibition of Cdk4/6 activity, which contribute to the G1 arrest and induction of senescence (203).

1.8.6 Deregulated DDR Genes; a Cause of Tumorigenesis

A healthy genome is essential for the survival of an organism. In normal cells, the genome integrity is maintained by the DDR network comprising of the cell cycle checkpoints and the DNA damage repair pathways. Loss of genome integrity due to inactivation of DDR genes may enhance the risk of accumulating mutations in genes that promote cancer development. Defects in DNA repair or response to DNA damage caused by endogenous or exogenous sources results in an increased rate of genetic mutations, often leading to the development of a number of human diseases including cancers (87, 204), neurodegenerative diseases and aging (205-207). Additionally, deregulation of DNA repair and cell cycle genes influence resistance of cancer cells to a number of DNA damaging agents used in cancer treatment (208, 209).

In the DDR pathway, DNA damaging signals from the PI3-K kinases (ATM, ATR, DNA-PK) and the checkpoint kinases (CHK1, CHK2) ultimately converge on the tumor suppressor protein p53 which act as the central mediator of the DNA damage-induced transcriptional response. Here, the

critical role played by p53 as a tumor suppressor is attested to by its mutation or inactivation in almost every type of cancer at rates varying between 10% in hematopoietic malignancies (15) and up to 100% in high-grade serous carcinoma of the ovary (210). Additionally, while the mutant p53 lacks the ability to bind DNA in a sequence-specific manner to activate transcription of canonical p53 target genes involved in cell cycle arrest, DNA repair, senescence, apoptosis, energy metabolism and response to oxidative stress (211, 212); it is also reported that mutant p53 protein exerts dominant-negative effects over co-expressed wild-type p53, largely by forming mixed tetramers that are incapable of DNA binding and transactivation. Moreover, mutant p53 is reported to demonstrate gain of function capabilities that increase genomic instability and risk of cancer development. For instance, disruption of normal spindle checkpoint control by mutant p53 leads to accumulation of cells with polyploid genomes (213). Other reported cancer-related gain of function activities include increased frequency of centrosome amplification and aberrant mitoses (214), aberrant centrosome amplification and non-reciprocal chromosome translocations (215), and augmented cell migration and invasion (216).

Moreover, deregulation of genes involved in specific DNA damage response pathways have also been linked to carcinogenesis. For instance, disabling mutations in the homologous recombination pathway which affects BRCA1, BRCA2, ATM, CHK2, RAD50, RAD51C have been recurrently identified in numerous cancers such as lung cancer, ovarian carcinomas, pancreatic ductal adenocarcinoma, and chronic lymphocytic leukemia (CLL) (217-219). Also, defect in NER is identified as the cause of the hereditary disease, Xeroderma pigmentosum (XP) while a variant of XP is also associated with inherited defects in polymerase eta (pol η), that specializes in translesional synthesis of nucleotides across stalled damaged regions of the DNA (220, 221). Another cancer predisposing condition related to the DDR pathway is mutation which affects the ATM gene. ATM is a central signaling protein in the DNA damage response, and cells lacking ATM demonstrate abnormalities in all major DNA damage repair and cell checkpoints, G1, S, and G2/M pathways (222). Alterations of ATM result in Ataxia-telangiectasia (AT), a disease of pleiotropic abnormalities, including cerebellar degeneration, cancer predisposition, progressive pulmonary dysfunction, and profound radiosensitivity (223).

1.8.7 The Role of DDR Genes in Cancer Treatment Failures

Cancerous cells adapt a number of mechanisms to resist the potency of drug treatment. Drug resistance occurs when cancer cells become tolerant to pharmaceutical treatment. Drug resistance and refractory drug treatment are responsible for up to 90% of the cancer-related deaths (224,

225). In 2020 alone, almost 10 million cancer-related mortality were recorded globally (23). Most cancer associated mortality was due to failure of cancer therapy associated with acquired and intrinsic resistance mechanisms. These mechanisms include altered drug transport and metabolism (226), mutation and amplification of drug targets (227), impaired apoptosis pathways (228), tumor heterogeneity (229), and acquired or possession of therapy resistance features (230). Intrinsic resistance are the innate resistant mechanisms pre-existing before drug treatment while the acquired resistance is induced after therapy (231, 232). Whilst intrinsic drug resistance may be due to the presence of mutation(s) of genes involved in cancer cell growth and/or apoptosis, acquired resistance may be due to activation of second proto-oncogene which then becomes the driver mutation (226), mutated or altered expression of drug targets (233) or changes in the tumor microenvironment (TME) following treatment (234). DNA double-strand breaks are the critical lesions mediating tumor cell killing by many chemotherapeutic drugs and majority of ionizing radiation. Thus, the ability of tumor cells to elicit a DNA damage response via activation of DNA repair and cell cycle checkpoints, promotes tumor cells resistance and survival (235). Treatment resistant human colon cancer cell lines for example, have been associated with upregulation of genes involved in DNA repair, such as flap endonuclease 1 (FEN1), Fanconi anemia complementation group G (FANCG), RAD23 homolog B nucleotide excision repair protein following 5-fluorouracil (5-FU) treatment. Additionally, p53-target genes on DNA damage response and repair were upregulated causing reduced cell cycle arrest and apoptosis thus ensuring survival of the tumor cells (236). On the other hand, deregulation of DDR may increase the risk of developing new mutations due to genomic instability, the accumulation of which may initiate a new round of carcinogenesis.

1.8.8 Tumor Microenvironment Mediates Acquired Treatment Resistance

Tumour microenvironment (TME) is a functional ecosystem of tumor cells and stromal elements that interact through signaling molecules to promote tumor survival and metastasis. Primarily, the stroma consist of a histological unit of peri-tumoral cells such as mesenchymal, vascular and immune cells within an extracellular scaffold and is critical to the development of the malignant phenotype of cancer (237). Chemoresistance is influenced by genetic and epigenetic alterations which affect drug uptake, metabolism and export of drugs at the cellular levels. A number of mechanisms have been identified to contribute to chemoresistance including; tumor heterogeneity, drug inactivation, apoptosis evasion, enhanced DNA repair, increased drug efflux, epithelial-to-mesenchymal transition and the involvement of the tumor microenvironment (238). Growing

evidence have highlighted the critical role the tumor microenvironment plays to induce therapy resistance in cancer (239, 240). The TME is dynamic and heterogeneous in cellular composition of both cancers and stromal cells, extracellular matrix (ECM) composition, soluble factors such as cytokines and growth factors and levels of tissue oxygenation and acidity (241, 242). The ECM, consisting of glycoproteins, proteins and proteoglycans are the non-cellular component of the TME secreted by both tumor and stromal cells.

The ECM provides the physical scaffold for cell anchor in addition to provision of signals necessary for cellular growth, migration and differentiation. The remodeling of ECM by several degrading enzymes such as metalloproteinases, lysyl oxidase (LOX), tissue inhibitors of metalloproteinases (TIMPs) and cathepsins in cancer perturbs ECM homeostasis leading to treatment resistance and metastasis (243, 244). In peripheral neuroblastic tumors for instance, the ECM, could create a barrier that limits drug availability to tumor cells within the TME (10). Also, in drug resistance metastatic ovarian cancers, certain ECM-associated metalloproteinases mediates treatment resistance within the TME (245).

The activities of a number of tumor-associated myeloid cells such as tumor-associated macrophages (TAMs), tumor-associated neutrophils (TANs) and myeloid-derived suppressor cells (MDSCs) reduce the efficacy of therapeutic treatment and are associated with more aggressive disease phenotype and poor prognosis (9, 246, 247). MDSCs are a heterogeneous population of immature myeloid cells consisting of a small group of myeloid progenitors and immature mononuclear cells, which arise due to chronic inflammatory environment associated with tumors (248, 249). MDSC produce arginase and nitric oxide and support expansion of local T-regulatory cells (Treg) populations to suppress anti-tumor immune responses of activated T-cells and natural killer (NK) cells within the TME (250-252).

Anti-tumorigenic cells such as fibroblasts and macrophages acquire tumor-promoting tendencies, releasing soluble factors such as growth factors and proteases needed by tumor cells to burrow through the ECM and so support progressive tumor growth (243). Under the influence of transforming growth factor beta (TGF- β) and platelets derived growth factor (PDGF) fibroblasts and macrophages are converted to cancer-associated fibroblasts (CAF) and tumor associated macrophages (TAM). CAF induce homeostatic deregulation by synthesis and deposition of enormous ECM fibers, fibronectin, periostin and release of matrix metalloproteases to promote epithelial–mesenchymal transition. Deposition of stiff ECM in the microenvironment induces tumor progression, malignancy and treatment resistance through integrin signaling in a variety of cancers such as breast cancer (244, 253).

Proliferating tumors require oxygen, nutrients, and growth factors for sustenance, however, in most solid tumors, blood vasculature is disorganized and leaky creating an environment of nutrient deprivation (254). Tumor cells thus orient energy source to anaerobic glycolysis which generate metabolic acidosis, oxidative stress and trigger extracellular matrix (ECM) changes within the TME with negative repercussion on treatment effectiveness (255, 256).

In hematological malignancies, indolent lymphoma cells could be transformed into an aggressive lymphoma through neurogenic locus notch homolog protein (Notch) signaling to demonstrate that mal-adapted tumor-associated vascular endothelial cells could confer stem cell-like activity to indolent tumor cells (257). Additionally, proximity to sprouting vasculature support proliferation of tumor cells and awakening of dormant malignant cells through provision of periostin (POSTN) and transforming growth factor- β 1 (TGF- β 1) in the TME to induce treatment resistance (258). Within the bone marrow, trafficking of mitochondria through tunneling nanotubes from bone marrow mesenchymal stromal cells (BMSC) to different cell types such as acute myeloid leukemia (AML) cells has been reported as one of the intercellular communication associated with chemoresistance (259). Similar mitochondria transfer is reported in multiple myeloma where increased oxidative phosphorylation leads to CD38-driven mitochondrial transfer (260). In leukemia, an adaptive mechanism where leukemic stem cells switch from oxidative phosphorylation to enhanced fatty acid oxidation to increase fitness toward chemotherapy resistance is also reported (261). These reports highlights the challenge of targeting only one metabolic pathway as treatment strategy since tumor cells could escape through adaptation.

1.8.8.1 The Role of Tumor-Associated Macrophages in TME

As earlier highlighted, the growth of malignant cells in both solid tumors and hematologic malignancies is facilitated by non-tumor cells such as stromal, vascular, immune and mesenchymal stem cells present in the tumor microenvironment. Macrophages are the predominant immune cells to infiltrate the tumor microenvironment. As critical innate immune cells specialized in immune surveillance and phagocytosis, macrophages are highly heterogeneous in morphology, biochemistry, phenotypes, and functions (262). Macrophages can be stimulated by lipopolysaccharide (LPS), granulocyte-macrophage colony stimulating factor (G-MCSF) and interferon-gamma (IFN- γ) into classically activated macrophages (M1) or stimulated by interleukin-4 (IL-4), transforming growth factor beta(TGF- β), macrophage-colonystimulating factor (M-CSF), postagladin F, vitamin D3 and interleukin-13 (IL-13) into alternative activated macrophage (M2) (263). Whilst M1-polarized macrophages are strongly pro-inflammatory and

anti-tumorigenic, M2-polarized macrophages are rather anti-inflammatory, tissue damage repair promoting and tumor supportive (264-267). The distinct functional differences arises from the unique cytokine profiles of the polarized macrophages. For example, polarized M2-macrophages secretes high levels of interleukin -10 (IL-10), IL-13, TGF- β , metalloproteinase 2 (MMP-2), arginase -1 and vascular endothelial growth factor A (VEGF-A). IL-10 for instance, promotes T-helper 2 cells (Th2- cells) to secrete high levels of interleukin - 4 and 13 (IL-4 and IL-13) (268). IL-4 activates type -1 arginase enzyme to metabolize L-arginine to form ornithine and polyamines used for synthesizing collagen, a major component of ECM, thus promoting tissue repairs and building (269) . Comparatively, IFN- γ activated M1-macrophages secretes high levels of IL-12, IL-6, IL-1 β , tumor necrosis factor-alpha (TNF- α) and IL-23. IL-12 promote the differentiation of naïve CD4⁺ T-cells to Type-1 T-helper cells (Th1 cells) which are characterized by secretion of pro-inflammatory cytokine interferon gamma (IFN- γ) and IL-23 promotes development and expansion of Th17 cells which secrete high levels of pro-inflammatory IL-17 (266, 270). The M1 and M2 polarized states represent two extremes of the macrophages activation phenotypes, however, there exist a continuum of varied activation states between these ends.

Immune cells such as lymphocytes and macrophages are reported to infiltrate the tumor microenvironment at all stages of tumor development (271). The immune infiltration of tumor is closely related to clinical outcomes and the composition of infiltrating immune cells serves as a biomarker for treatment response (272). Macrophages are the most predominant immune cells infiltrating the tumor microenvironment, where they acquire distinct characteristics as a result of environmental cues to become tumor-associated macrophages (TAM). TAM could constitute up to 50% of the tumor mass in some cases and express M2-phenotype due to signals in the microenvironment such as IL-4 and TGF- β (273) which suggest that macrophages could be polarized towards M2 inducibility within the TME where their role is essential to tumorigenesis. In a variety of tumors such as lymphomas, lung, gastric and gynecological cancer, infiltration of TAM positively correlate with poor clinical prognosis (273-277). The tumor microenvironment empressees a number of factors such as IL-4, IL-13, TGF- β , and IL-10 which polarize infiltrating macrophages into M2-like phenotype where they become pro-tumor supporting cells. Here, TAMs orchestrate various aspects of cancer, such as tumor progression, angiogenesis, tumor growth, metastasis, immunosuppression, matrix deposition, and remodeling culminating in poor prognosis and treatment failures. Depletion of TAM using Clodronate liposome has been shown to reduced blood vessel density, confirming the role of TAM in neo-angiogenesis (278). Also, mouse model

of cervical cancer showed that membrane metalloproteinase 9 (MMP-9) was a major TAM-derived metalloprotease that degrades extracellular matrix to promote angiogenesis and tumor growth (279). Adaptation of TAM to hypoxic TME induces a switch in expression of pro-angiogenic genes such as vascular endothelial growth factor (VEGF), fibroblast growth factor (pFGF), C-X-C motif chemokine ligand 8 (CXCL8), and glycolytic enzymes under transcription control of hypoxia-inducible factor 1 and 2 (HIF-1 and HIF-2) thus playing a prominent role in stimulating tumor angiogenesis and progression (280, 281).

1.8.8.2 TAM Mediated-Immunosuppression in the TME

Tumor immunosuppression serves as a mechanism to promote tumor growth through disarming critical immune function mechanisms necessary for immune surveillance and response. TAM are immunosuppressive; preventing tumor cell attack by natural killer and T cells during tumor progression and under chemoimmunotherapeutic (CIT) treatment through secretion of TAM-derived cytokines and proteases, such as TGF- β , IL-10, and arginase 1(282). TGF- β promotes TAM polarization to an M2-phenotype within the TME (283, 284). M2-polarized TAM further secrete TGF- β forming a cyclical feedback loop that cripples innate immune response through a number of mechanisms with dire consequence on adaptive immune activation. TGF- β maintains TAM in an anti-inflammatory state and inhibits cytolytic activity of natural killer cells (NK cells) (285, 286). Furthermore, TGF- β decreases dendritic cells (DCs) migration and promote their apoptosis (287) whilst increasing differentiation of regulatory T-cell (Tregs)(288), and induces CD4⁺ T cells differentiation into a type-2 helper T- cells culminating in increased immunosuppression (289, 290).

Another immunosuppression mechanism deployed by TAM is the secretion of interleukin 10 (IL-10). IL-10 is often present in the advanced stages of tumors and its serum levels is positively correlated to the progression of tumor, implying a critical role of this cytokine in the TME (291). As an anti-inflammatory, immunosuppressive interleukin, IL-10 impairs maturation of dendritic cells (DCs) by preventing upregulation of activation markers such as major histocompatibility class II (MHC II) and CD86, thus reducing presentation of tumor specific antigen to T-cells (292, 293). Additionally, IL-10 is reported to inhibit IL-12 and IFN- γ release with implications for naïve T-cell activation and differentiation into type 1 T-helper cells in the TME (294-296). IL-10 is thus associated with tumor immune escape and growth (291).

The main sources of IL-10 in the TME include the tumor cells, TAM and cytotoxic T-cells. Higher levels of IL-10 is observed in advanced metastases diseases (291, 297). IL-10 impairs presentation

of tumor antigens by inhibiting maturation of dendritic cells and Th-1 cells secretion activities (298, 299). Despite the known immunosuppressive functions of IL-10, contrarily evidence has also been shown to advance immuno-stimulatory function of IL-10 in TME. Here, IL-10 is reported to exhibit cytotoxic and cytolytic activities of immune cells while exhibiting strong inhibitory effect on angiogenesis thus favoring tumor regression (300, 301). Infiltration of tumor microenvironment by M2-like TAM is also associated with expression of high level of arginase-1. Stress induced from catabolism of arginine to polyamine and proline by arginase has emerged as a key immune escape mechanism in cancer to suppress tumour-specific lymphocytes. In fact, high levels of arginase activity is associated with dysregulated T-cell receptor signaling and unresponsive CD8⁺ T-cells function (302, 303). In acute myeloid leukaemia (AML) patients and mouse models, release of arginase into blood circulation deplete systemic arginine and inhibit T-cell proliferation and effector functions (304).

Similar to reports in leukemia, in both classical Hodgkin lymphoma (cHL) and Non-Hodgkin lymphoma (NHL), tumor-associated macrophages are critical inducers of lymphoma progression and predicts poor progression-free survival (PFS) and overall survival (305-307). Monocytes respond to colony stimulating factor -1 cytokine (CSF-1) to differentiate into macrophages. In cHL for example, it is observed that the percentage of TAM expressing the receptor for CSF-1 (CSF-1R) was inversely associated with survival (308), a finding corroborated by subsequent meta-analysis (309). Within the highly infiltrated microenvironment of cHL, where malignant Reed Sternberg (RS) cells constitute just about 1% with the remaining cells being immune cells, high program death ligand 1 or 2 (PD-L1/PD-L2) expressing TAM colocalize with PD-L1⁺ RS cells. Thus, interaction of PD-L1/PD-L2⁺ TAMs with PD-1⁺ T-cells and natural killer (NK) cells leads to suppression of effector functions of T-cells /NK cells activities leading to tumor evasion and progression (310).

Among the non-Hodgkin group of lymphomas, high expression of CD68⁺/CD163⁺ TAMs and absolute peripheral blood monocytes counts were associated with poorer overall survival and PFS in a group of 221 untreated, newly diagnosed diffuse large B-cell lymphoma (DLBCL) despite the biological and genetic heterogeneity present in this sub-group of lymphoma (311). These reports among others, highlights the crucial role TAM plays regarding tumor cells proliferation, invasion, angiogenesis, metastasis and suppression of anti-tumor immunity in many tumors (312).

1.9 Contemporary Treatment Strategies in Cancers

Cancer remain one of the major causes of death globally despite the advances made in the current diagnostic and treatment options. The International Agency for Research on Cancer (IARC) updated GLOBOCAN (2020) report indicated that the burden of cancer has risen to 19.3 million cases and 10 million cancer deaths recorded worldwide in 2020 (23). During cancer progression, tumors become highly heterogeneous, creating a mixed population of cells characterized by different molecular features and diverse responsiveness to therapies (313). Tumor cells heterogeneity is thus a key factor responsible for development of resistant/refractory phenotypes, often exacerbated by selective pressure upon treatment.

Currently, a number of different treatment strategies including surgery, chemotherapy, radiotherapy, immunotherapy, targeted therapy, hormonal therapy, stem cells therapy and precision therapy are employed for cancer management.

1.9.1 Surgical Treatment of Cancers

Surgery, a method of physical excision of cancer tissue from the body is used as a treatment strategy mainly in the solid tumors where metastasis of the malignant tumor from the primary site has not occurred. Surgical procedure is aimed at curative, debulking, diagnostic, palliative or prevention and may be combined with other cancer treatment option to achieve the desired aim (227, 314-316).

1.9.2 Cancer Radiotherapy

Radiotherapy uses high-energy beams of radiation from sources such as, X-rays, gamma rays, electron beams, or protons, to cure diseases. Similar to surgical intervention, radiotherapy is largely applied in non-metastatic or focal tumors where application of high doses of energy kill tumor cells through DNA damage and subsequent apoptosis induction. In hematologic malignancies, radiotherapy is used as either definitive therapy, as consolidation after chemotherapy, as part of bone marrow transplantation protocols, or in palliative care (317).

1.9.3 Cancer Chemotherapy

Chemotherapy is the use of chemically formulated drug with cytotoxic effect for the treatment of cancer and other diseases. Several types of chemotherapeutic drugs such as alkylating agents, mitotic inhibitors, antineoplastic antibiotics, anti-metabolites, topoisomerase inhibitors and ribonucleotide reductase inhibitor are used in cancer treatment (167, 318).

Alkylating agents are compounds such as mustard gas derivatives (including cyclophosphamide,

ifosfamide, melphalan, and chlorambucil), alkylsulphonates (Busulfan), Nitrosureas, and Metal salts (Carboplatin, Cisplatin, and Oxaliplatin) that react with electron-rich atoms in biologic molecules to form covalent intrastrand and interstrand bonds that cross-link DNA causing single or double strand breaks (319). This prevents normal function of DNA (DNA replication and consequent RNA transcription and translation) at all phases of the cell cycle. Alkylating agents are cell cycle non-specific and most potent in the resting phase of the cell thus combination with cell cycle specific agents enhance cytotoxicity of resting cells recruited into active division (320).

Anti-metabolites are cytotoxic agents that structurally resemble the purine and pyrimidine bases for DNA synthesis. However, their incorporation into the nucleic acids impairs functions of key enzymes resulting in strand breaks and premature termination of nucleic acid synthesis culminating in cell death (321).

Chemotherapies which exert cytotoxic effect through disruption of cellular mitotic process constitute the anti-mitotics. The current approved anti-mitotic drugs including vinca alkaloids (e.g. vinblastine and vincristine) and taxanes (e.g. paclitaxel, docetaxel) target microtubules thus interfering with formation of spindle fibers needed for chromosomal segregation at mitosis (322, 323). Taxanes are commonly used in the treatment of breast and ovarian cancers, whilst vinca alkaloids, such as vincristine, are often used in combination therapies to treat hematological malignancies. Vincristine usage is associated with induced neuropathy (324) generating controversy of its relevance as part of standard treatment for diffuse large B cell lymphoma (DLBCL). Accordingly, it has been shown that, omission of vincristine from rituximab-based CHOP (cyclophosphamide, doxorubicin, vincristine (VCR), and prednisone) did not affect disease-free or overall survival (325)

Topoisomerase inhibitors are chemical compounds that inhibit the activities of enzymes involved in a wide range of functions related to the maintenance of DNA topology during DNA replication, and transcription. Topoisomerase I preferentially binds to double-stranded DNA to induce a single-strand break, whilst topoisomerase II binds covalently to complementary strands of double-strand DNA, cleaving both strands to release torsional stress (326). Inhibitors of topoisomerases either prevent DNA strand breaks or impair re-ligation processes following DNA strand break thus activating cell cycle arrest and apoptosis mechanisms (327). High levels of topoisomerase II alpha is reported in the germinal center subtype of DLBCL and is associated with high tumor cell proliferation but also significant response to treatment, a strong basis for the use of topoisomerase II inhibitors in GC-DLBCL subtype (328).

Antineoplastic antibiotics are anticancer drugs that affect DNA synthesis and replication by a number of mechanisms which culminate in the elimination of tumor cells by cytostatic and cytotoxic actions (329). Identified mechanisms include; intercalating into DNA strands, free radical formation of highly reactive oxygen compounds such as superoxide, lipid peroxidation, DNA binding and alkylation and DNA cross-linkage that cause breakage of DNA strands. Examples of antineoplastic antibiotics include anthracyclines, doxorubicin, daunorubicin, bleomycin, mitomycin, actinomycin, dactinomycin, and guanorycin (329, 330).

1.9.4 Cancer Immunotherapy

Tumors develop through a combination of genetic and epigenetic alterations that facilitate immortality, but also formation and display of foreign neo-antigens, which should render neoplastic cells detectable by the immune system for destruction (13). However, tumor cells are able to evade the host immune surveillance through multiple resistance mechanisms, including local immune evasion, induction of tolerance, immune editing and systemic disruption of T-cell signaling (331, 332). Immunotherapy has become a standard treatment option for patients with various cancers, including melanoma, lymphoma, and carcinomas of the lungs, kidneys, bladder, and head and neck. The concept of cancer immunotherapy involves the artificial stimulation of the immune system aimed at improving on its ability to fight tumor cells. A number of approaches including; cancer vaccines, oncolytic viruses, adoptive transfer of ex-vivo activated T and natural killer cells (NK cells), administration of antibodies or recombinant proteins that either co-stimulate cells or block immune checkpoint pathways have been developed. These approaches could be classified into two major immunotherapeutic strategies of an active and a passive approach. The active immunotherapy approach involves the use of vaccines or chimeric antigen receptor T-cells (CAR-T cell), or targeted monoclonal antibodies to specifically target the tumor cells. A passive immunotherapy approach on the other hand, aims to enhance the ability of the immune system to attack tumor cells such as in the case of immune checkpoint inhibitors and the use of cytokines.

Immunotherapeutic strategies for diffuse large B-cell lymphoma (DLBCL) include monoclonal anti-CD20 antibody (rituximab), monoclonal anti-PD-1 antibodies (nivolumab and pembrolizumab), monoclonal anti-PD-L1 antibodies (avelumab, durvalumab, and atesolizumab) and chimeric antigen receptor (CAR) T-cell therapy.

Currently, monoclonal anti-CD20 antibody-based immunochemotherapy consisting of, cyclophosphamide, doxorubicin, vincristine, and prednisone (R-CHOP) is the treatment of choice

for DLBCL, being effective in about 60% of patients. The remaining 30-40% of DLBCL patients who relapse/progress on R-CHOP and high-risk DLBCL with MYC and BCL2 or BCL6 translocation who fail R-CHOP therapy are managed on high intensity, dose-adjusted regimen of rituximab, etoposide, prednisone, vincristine, cyclophosphamide, and doxorubicin (DA.R-EPOCH).

1.9.4.1 Monoclonal Antibody Therapy

The first anti-CD20 monoclonal antibody licensed by FDA (USA) for treatment of patients with advanced stage or relapsed low-grade non-Hodgkin lymphoma, in 1997 was rituximab (333). As a chimeric antibody of murine heavy and light chains variable regions and human IgG1 constant region, the variable regions selectively bind to the CD20 antigen expressed on the surface of both normal B and most malignant B-cells. The presence of a human constant region allows rituximab to bind to Fc receptors on human effector cells such as macrophages, and neutrophils to mediate both complement-dependent cytotoxicity and antibody-dependent cytotoxicity and phagocytosis as primary mechanisms of action (334). CD20 is a cell surface protein expressed on early pre-B cells through to later differentiation stages, but absent on terminally differentiated plasma cells. CD20 mediates Ca^{2+} influx across plasma membranes of the cells thus, maintaining intracellular Ca^{2+} concentration to allow for B cells activation. The success of rituximab has engendered the development of more efficacious anti-CD20 antibodies including; ocrelizumab (humanized mAb), ofatumumab (a fully human mAb) and obinutuzumab (a third generation glyco-engineered Fc fragment with enhanced Fc gamma receptor binding capability). Beside mAb against CD20 antigen, other mAb against different B-cell target such as anti-CD19 and anti-CD22 antibodies have been developed.

1.9.4.2 Immune Checkpoint Inhibitors

Anti-tumor immune responses, elicited through tumor antigen recognition by immune cells could be suppressed by immune checkpoint antigens on cells surfaces (335). In health, immune checkpoint antigens regulate the immune homeostatic balance through the use of co-stimulatory and inhibitory signals which constitute the immune checkpoint mechanisms. The immune checkpoint is thus critical to maintain self-tolerance and to avoid tissue damage from excessive inflammation and autoimmune diseases (332).

T-cells are primary mediators of immune effector functions as such, express multiple co-inhibitory receptors such as lymphocyte-activation gene 3 (LAG-3), programmed cell death protein 1 (PD-1) and cytotoxic T-lymphocyte-associated protein 4 (CTLA-4). The inhibitory receptors of T-cells,

modulate T-cell responses to self-proteins, tumor antigens and chronic infections (336). Nevertheless, tumor cells are able to adopt multiple mechanisms of immune suppression to prevent effective anti-tumor immunity. Such mechanisms of tumor immune escape include reduction in expression of tumor antigens, increasing expression of co-inhibitory antigens such as PD-L1, CTLA-4 (337, 338), secretion of immune suppressive cytokines and inducing immunosuppressive microenvironment (339). Monoclonal antibodies that target the inhibitory receptors have thus been explored to boost immune response to tumors.

1.9.4.2.1 Monoclonal anti-PD-1/PD-L1 Antibodies

PD-1/PD-L1 axis is one of the co-inhibitory mechanisms deployed to regulate effector T-cells activity. PD-1 (CD279) is an immunosuppressive molecule receptor of the CD28 and CTLA-4 immunoglobulin superfamily which interacts with two B7 family ligands including PD-L1 (CD274 and also known as B7-H1) and PD-L2 (CD273 and also known as B7-DC). PD-1 is expressed on the surface of mature activated T-cells in peripheral and tumor microenvironment. However, a number of other cells including B-cells, natural killer cells, macrophages and some tumor infiltrating lymphocytes (TILs) do express PD-1. PD-L1 is constitutively expressed by a wide variety of cells including tumor cells, antigen-presenting cells (APC), and a variety of non-hematopoietic cells (340) and its levels of expression can be upregulated by the presence of strong inflammatory signals. Pro-inflammatory cytokines including tumor necrosis factor α (TNF- α), IL-17, type I and type II interferons, and vascular endothelial growth factor (VEGF) could induce expression of PD-L1 (341-343). PD-L2 on the contrary has a low expression threshold and is expressed mainly by dendritic cells and macrophages (344) although expression could be induced by IL-4 and granulocyte-macrophage colony stimulating factor (GM-CSF) in immune and non-immune cells depending on the stimulus from the microenvironment (345, 346).

The binding of PD-L1/PD-L2 ligands to PD-1 induces the two structural motifs of the cytoplasmic tail of PD-1 (immunoreceptor tyrosine-based inhibitory motif (ITIM) and immunoreceptor tyrosine-based switch motif (ITSM)), which bind the Src homology region 2 domain-containing phosphatases-1 (SHP-1) and SHP-2. SHP-2 directly dephosphorylates PI3K, which inhibits downstream activation of protein kinase B (Akt) and thereby decreases production of inflammatory cytokines including IFN γ , TNF α , and IL-2 as well as cell survival proteins such as Bcl-xL (347, 348). Additionally, signaling through PD-1 decreases tyrosine phosphorylation of the T-cell receptor (TCR) ζ -chain and zeta-chain-associated protein kinase 70 (ZAP-70) and also inhibits the expression of transcription factors associated with effector cell functions, including

GATA-binding protein 3, T-box transcription factors T-bet and Eomes (349, 350). Thus, PD-1/PD-L1 interaction culminates in T-cell inactivation, inhibition of proliferation, suppression of cytokines secretion and promotion of cytotoxic T-cell apoptosis and regulatory T-cell differentiation (351, 352). Immune blockade of the PD-1/PD-L1 interaction by monoclonal antibodies can restore the antitumor activity of cytotoxic T-cells and has become a clinically validated treatment with durable objective responses and improved overall survival (OS) in both solid tumors and hematological malignancies. In DLBCL, monoclonal antibodies targeting the PD-1/PD-L1 pathway evaluated in clinical trials for refractory/relapse patients include PD-1 antibodies nivolumab and pembrolizumab and anti-PD-L1 antibodies, avelumab, durvalumab, and Atesolizumab. The efficacy of the PD-1/PD-L1 inhibitors have been evaluated in a multiple phase I/II studies in combination with other agents such as ipilimumab (NCT03305445), rituximab and chemotherapy (NCT03259529), varlilumab (anti-CD27) (NCT03038672), the IDO1 inhibitor epacadostat (NCT02327078), and lenalidomide (NCT03015896) in participants with DLBCL (353). It is acknowledged that, immune checkpoint blockade although potentially promising in DLBCL, manifest variable responses to single agent checkpoint therapy. Thus, combination with other agents such as co-inhibitory blockade, co-stimulatory agonist, anti-CD20 mAb and conventional chemotherapy may be the way to enhance their antitumor efficacy through synergistic interactions (354).

1.9.4.3 Chimeric Antigen Receptor T-cells Therapy (CAR-T cells)

CAR-T cells are autologous or allogeneic T-cells, genetically engineered to express a tumor-targeting receptor which direct the T-cells to bind a specific tumor antigen (355). The engineered T-cell has extracellular single chain variable fragment (scFv) domain that recognizes specific tumor antigen and an intracellular signaling domain, involved in T-cell activation. This arrangement permits CAR-T cells to achieve optimum activation independent of involvement of major histocompatibility complex (MHC) antigens (356). Different generations of CAR-T cells (first, second, third and fourth) developed differ in the intracellular signaling domains and cytokine secretion. Whilst the first generation of CAR-T cells lacked co-stimulatory domains to achieve sufficient activation of T-cells, subsequent generations of CAR-T cells were engineered with co-stimulatory domains to be effective against non-costimulatory antigen expressing tumor cell (357, 358). However optimum CAR-T cells activation was associated with increased release of cytokine storms which induce a number of pathologies in treated patients (359, 360). The challenges with cytokine storm is addressed in the fourth generation of CAR-T cells equipped

with inducible caspase 9 for rapid elimination of CAR-T cells through apoptosis induction (360, 361). Thus, fourth generation CARs utilize inducible expression of components to increase activation of T-cells whilst attracting other immune cells through cytokine secretion to target tumor antigen negative cancer cells. CAR-T cells immunotherapies have been most efficacious in B-cells acute lymphoblastic leukaemia patients (362, 363), however in a clinical trial of CD19-CAR-T cells (NCT02348216) undertaken by Kite Pharma, investigators showed that CAR-T cells was effective in treatment of refractory/relapse DLBCL and the most aggressive forms of DLBCL associated by double hit genetic lesions (364). Additionally, in one recent study, pretreated 22 advanced-staged lymphoma patients including 19 DLBCL with low-dose chemotherapy (cyclophosphamide and fludarabine) for two days followed by CAR-19 T-cells therapy. Among these patients group, overall response rate (ORR) was 73%, with 55% achieving complete remission (CR) and 18% achieving partial response (PR). This signifies that, CAR-19 T-cells are potentially an effective therapy for DLBCL patients (365). Nonetheless, challenges such as treatment limitation to only heavily pretreated patients with good performance status, complications of cytokine release syndrome, CAR T cell related encephalopathy syndrome, and the extremely high cost of treatment coupled with challenges of geographical scalability and quality maintenance limits access to CAR T cells therapy (366).

1.9.4.4 Cytotoxic T-lymphocytes Associated Protein 4 (CTLA-4) Inhibitors

T-cells activation which is the first step in mounting immune response, is achieved when antigen presenting cells (APCs) such as macrophages and dendritic cells present foreign antigens bound to their major histocompatibility class II molecule to host T-cells.

The binding of T-cell receptor (TCR) to the tumor antigens, is complimented by a co-stimulatory signal of CD28 on T-cells binding to CD80/86 of the antigen presenting cell (288). CTLA-4 is a transmembrane glycoprotein that is a homolog of CD28 but serve as the inhibitory receptor for the negative regulation of T-cells activation upon binding to CD80/CD86 on antigen presenting cells. CTLA-4 (CD152) is hardly detectable on the surfaces of resting T-cells because of a motif in its cytoplasmic domain that facilitates interaction with the clathrin pit adaptor complex (AP-50) causing its rapid internalization from the cell surface. However, following T-cells activation, CTLA-4 is induced to maximum expression within 48-72hrs (367). Here, binding of CTLA-4 molecules on T-cells by CD80/86 ligands results in decreased T-cells proliferation and IL-2 production (368). Thus, both CD28 and IL-2 signaling, independently upregulate CTLA-4 expression indicating that, the most potent signals for T-cell activation are also the most powerful inducers of CTLA-4 expression (368).

Overexpression of inhibitory ligands on lymphoma cells can suppress an effective antitumor T-cell response by reducing T-cell differentiation and proliferation. Thus, blockade of CTLA-4 interactions using anti-CTLA-4 mAbs increases T-cell responses (369).

CTLA-4 inhibits T-cell responses by competing with CD28 binding to CD28 ligands such as CD80/CD86 where CTLA-4 exhibit higher binding affinity than CD28. In its non-phosphorylated state, CD28 is associated with serine/threonine protein phosphatase 2A (PP2A). On T-cell stimulation, CD28 undergoes phosphorylation on its intracellular tyrosine residues (Y), leading to dissociation from PP2A and recruitment of phosphatidylinositol 3-kinase (PI3K) and growth factor-receptor-bound protein 2 (GRB2) (370). Activation of PI3K, which induces phosphorylation of phosphatidylinositol (PI) into phosphatidylinositol 3-phosphate (PIP3), promote activation of protein kinase B (PKB/Akt), followed by that of nuclear factor- κ B (NF- κ B), resulting in Bcl-2 and Bcl-XL upregulation that favors T-cell survival (371). Akt activation is additionally proposed stimulate interleukin-2 (IL-2) production (372).

CTLA-4 does not have ITIM, however contains two tyrosine that provide SH2-domain binding sites. CTLA-4 has a motif of tyrosine and proline rich residues which promotes its association with AP50 to limit surface expression of CTLA-4 by clathrin-dependent endocytosis (373). During T-cell receptor (TCR) stimulation, CTLA-4 undergo tyrosine phosphorylation by SRC kinases, however, increased T-cells CTLA-4 turnover at the plasma membrane is not stabilized to induce surface retention as CTLA-4 endocytosis was observed to continue (373). Upon engagement with B7 proteins, CTLA-4 is phosphorylated and binds phosphoinositide 3-kinase (PI3K) and Src homology 2 (SH2) -domain containing protein tyrosine phosphatase (SHP-2) (374), inhibits ZAP-70 microcluster formation (375). Activation of CTLA-4 reduces T-cell receptor (TCR)-dependent activation of the mitogen-activated protein (MAP) kinases ERK (extracellular signal-regulated kinase) and JNK (Jun N-terminal kinase), nuclear factor- κ B (NF- κ B), activator protein -1 (AP-1) transcription factor and nuclear factor of activated T-cells (NF-AT) which results in decreased cytokine production by T-cells and cell-cycle arrest (376). SHP2 additionally dephosphorylate CD3 complex (γ , δ , ϵ , and ζ chains) and inactivation of TCR-dependent signaling pathways. In one study, overall response rate of 11% among 18 patients with refractory/relapse NHL treated with anti-CTLA4 antibody ipilimumab (a fully human IgG1 mAb) was reported. Although the response was low, it remained durable in DLBCL, lasting beyond 31 months clearly demonstrating that CTLA-4 antagonists have limited activity as a single agent but may add to durable effect in combination therapy (377).

1.9.4.5 CD47/ Signal-Regulatory Protein Alpha (SIRP- α) Inhibitors

CTLA-4 and PD1 inhibitors have shown unexpectedly low efficacy in DLBCL patients compared to the Hodgkin lymphomas. This has necessitated the need for other immune checkpoint proteins to be explored as a therapeutic strategy in the case of about 40% of DLBCL patients who remain refractory/relapse on R-CHOP/EPOCH therapy. Mucin-domain containing molecule-3 (TIM-3) (378), T cell immunoglobulin and ITIM domain (TIGIT) (379) and B and T lymphocyte Attenuator (BTLA) (380) are potential immune blockade candidates of the adaptive immune system whilst CD47 is a promising candidate for the innate immune response. CD47 (previously, integrin-associated protein) is a cell surface glycoprotein ligand of the immunoglobulin family capable of sending a potent “don’t eat me” signal to prevent phagocytosis when it engages signal regulatory protein alpha (SIRP- α) molecule expressed on phagocytic cells of the monocyte/macrophage lineage (381). CD47 is generally expressed in low levels by nearly all cells of the body (382). However in a number of hematological malignancies such as DLBCL, chronic lymphocytic leukemia (CLL), follicular lymphoma (FL), mantle cell lymphoma (MCL), marginal zone lymphoma (MZL) and acute lymphoblastic leukemia (ALL), CD47 is variably expressed (383) and the benefit of anti-CD47 blockade has been explored (384). For example, in DLBCL, CD47 is overexpression on the activated B-cell subtype compared to the germinal center B-cells subtype. Overexpression of CD47 was associated with poorer R-CHOP treatment outcomes (385) and remains an independent predictor of disease progression in multivariate analysis with the international prognostic index for DLBCL. CD47 interaction with SIRP- α leads to activation of tyrosine phosphatases that inhibit myosin accumulation at the sub-membrane assembly site of the phagocytic synapse, resulting in phagocytosis blockade (386). The glycosaminoglycan (GAG) chain of CD47 mediates inhibition of T-cell receptor signaling following ligation of CD47 by its ligand thrombospondin-1(387).

1.9.4.6 Cancer vaccines

The use of cancer vaccines to treat malignancies stems from realization that cancer patients harbor CD4⁺ and CD8⁺ T-cells capable of recognition of tumor antigens. Unfortunately, a number of multifaceted issues had hindered development of effective anti-cancer vaccine to date (388, 389). Initial gap of understanding of role of dendritic cells as a critical antigen presenting cell coupled with the type of suitable tumor antigens to induce T-cell response impaired success of initial anti-

cancer vaccine trials. The use of short peptides, whole proteins and polyvalent tumor antigens from lysates of tumor cells attained minimal success due to poor pharmacokinetics, heterogeneity in expression among specific cancer group and inadequate immunogenicity respectively (390, 391). However, dendritic cell-based vaccines, where dendritic cells were ex vivo treated with fusion protein of prostatic acid phosphatase linked to granulocyte colony-stimulating factor (GM-CSF) achieved modest survival advantage enough to warrant US Food and Drug Administration (FDA) approval (392, 393). Cancer vaccine had been applied in lung carcinoma (394), melanoma (395) and metastatic prostate cancer with varied outcomes. However, in DLBCL after vaccination of a cohort of patients, significant elevation of CD4+ and CD8+ T-cells with corresponding reduction of lactate dehydrogenase and β 2-microglobulin levels were observed. The authors thus suggested that dendritic cell-based vaccine could be used for patients with poor response to chemical drug treatment (396).

1.9.4.7 Ribonucleotide Reductase Inhibitors

Ribonucleotide reductases (RNRs) catalyze the de novo conversion of nucleotides to deoxy nucleotides in all organisms, controlling their relative ratios and abundance. Ribonucleotide reductase inhibitors (RNRi) are drugs that inhibit activities of ribonucleotide reductase, the enzymes which catalyze de novo biosynthesis of deoxyribonucleoside triphosphates for DNA synthesis (397). Tumors are characterized by uncontrolled proliferation which increase demand for DNA in both replication and repairs (398). Enhanced DNA biosynthesis is associated with increased ribonucleotide reductase activity thus providing the rationale for use of RNRi in treatment of malignancies particularly of hematopoietic origin. Ribonucleotide reductase enzyme consists of two subunits, α and β , that associate to form the holoenzyme (399). The α subunit contains the catalytic site and two different allosteric sites whilst the β harbors a di-iron cofactor and tyrosyl radical essential for RNR activity (400).

Clinically available small-molecule RNRi fall into two classes; the inhibitors that target the α -subunit such as gemcitabine and clofarabine, bind to nucleotides and those that target the β -subunit which depends on a redox active metallocofactor and radical quencher (401).

2 Aims and Objectives

2.1 Problem statement

Interactions of tumor cells with their microenvironment (TME) is indicted in malignant feature acquisition that promote tumor proliferation, survival, immune evasion and treatment resistance. Macrophages are one of the major infiltrating immune cells of TME, with pivotal role to influence the course of disease through acquisition of protumorigenic phenotype as tumor-associated macrophages (TAM). The mediation of TAM in establishing immune suppressive niche that promote tumor survival, metastasis and treatment resistance, is evidenced by tumor regression and enhanced overall survival following clodronate liposome-mediated TAM depletion and monocyte-macrophages differentiation blockade by colony stimulating factor receptor -1 (CSFR1) inhibitors. It was shown recently that, suppressed effector functions of TAM can be restored through chemoimmunotherapy which induce tumor cells secretion of acute soluble factors capable of reprogramming TAM. This highlights the relevance of macrophages in cancer treatment and suggest critical role of the DNA damage response genes in the interactions within the tumor microenvironment. The impact of TME interactions influence heterogeneity in treatment outcomes of diseases such as seen in DLBCL where 40% of patients experience recurrent disease/treatment refractory on R-CHOP whilst 60% are cured. In CLL, dependence of tumor cells on genetic-microenvironmental interplay for pro-survival stimuli influence the disease ontogeny across different geographical settings. For instance, in the West, CLL shows male predominance of 2:1 and median incidence of 65yrs whilst in sub-Saharan Africa, youthful incidence, female predominance and poorer prognosis reported reflects differences in CLL biology.

2.2 Aims of the Research

This thesis aims to define the role of DNA damage response genes in the interaction between the tumor cells and macrophages within the tumor microenvironment and to characterize a “tropical” type of CLL by measuring informative molecular markers in a Ghanaian CLL patients’ cohort.

2.2.1 Specific objectives

Objective 1: Analyze the influence of alterations in the DNA-damage response genes in lymphoma cells towards the function and polarization of macrophages

To investigate the effect of alterations in the DNA damage response pathway by specific RNA interference (RNAi) mediated targeting of leukemia cells on the interaction between macrophages and malignant B-cells in the tumor microenvironment.

Objective 2: Investigate the specific effects of identified DDR alterations on microenvironment modulation in the context of therapeutic interventions

To analyze macrophage modulation in the context of specific mutations and address the role of tumor-associated macrophages (TAM) in therapeutic response for respective specific mutations

Objective 3: To characterize a “tropical” CLL patients’ cohort in Ghana by measuring informative molecular markers.

To measure expression of molecular markers relevant for CLL diagnosis, prognosis and immune interactions of a cohort of CLL patients from Ghana-West Africa.

3 Materials and Reagents

3.1 Devices

-150°C Freezer	Panasonic, Kadoma, Japan
-20°C and -80° Freezer	AEG, Stockholm, Sweden
4°C Fridge	AEG, Stockholm, Sweden
Analytic Balance	Satorius, Göttingen, Germany
Autoclave Systec VX-150	Systec, Bergheim, Germany
Biometra Compact S, M and L	AnalytikJena, Germany
CASY Cell Counter Model TTC	Roche, Basel, Switzerland,
Centrifuge 5415 R	Eppendorf, Hamburg, Germany
Centrifuge 5810 R	Eppendorf, Hamburg, Germany
CO ₂ Incubator for Cell Culture	Labotect, Göttingen, Germany
Easypet 3 Pipettboy	Eppendorf, Hamburg, Germany
Electrophoresis System DNA	BioRad, Hercules, CA, USA
Electrophoresis Power Supply EPS 3500	Pharmacia Biotech
FLUOstar Optima	BG Labtech, Ortenberg, Germany
Flow Cytometer MACSQuant VYB	Milentyi Biotech, Berg. Gladbach, Germany
Flow Cytometer MACSQuant X	Milentyi Biotech, Berg. Gladbach, Germany
Freezing Container “Mr. Frosty”	Nalgene, Neerijse, Belgium
Heater/Magnetic Shaker MR3001	Heidolph, Schwabach, Germany

Incline Incubator for Molecular Biology	VWR, Darmstadt, Germany
Laminar Flow Hood	Labogene, Lygne, Denmark
Leica DM IL LED fluorescent microscope	Leica Microsystem, Germany
Mini-Protean Tetra Vertical Electrophoresis Cell	BioRad, Hercules, CA, USA
Molecular Imager Gel Doc XR+System	BioRad, Hercules, CA, USA
NanoDrop 1000 Spectrophotometer	Thermo Scientific, Dubuque, IA, USA
Neubauer Hemacytometer	Laboroptic, Lancing, UK
Odyssey CLX Imaging System	LI-COR Biotech. Bad Homburg, Germany
PowerPac HC Power Supply	BioRad, Hercules, CA, USA
pH-Meter	Mettler-Toledo, Schwerzenbach, Germany
Pipettes Eppendorf Research Plus	Eppendorf, Hamburg, Germany
QuadroMACS Separation System	Miltenyi Biotech, Berg. Gladbach, Germany
QuantStudio 12K Flex Real-Time PCR System	Thermo Fisher Scientific, Waltham, MA USA,
Roller Mixer SRT9	Stuart, Bibby Scientific, Staffordshire, UK
Rotilabo®-Mini-Centrifuge	Carl Roth, Karlsruhe, Germany
Shaker IKA-VIBRAX-VXR	IKA, Staufen, Germany
Stratagene Ultraviolet 4000 UV Transilluminator	Ultraviolet Products, San Gabriel, CA, USA
T3000 Thermocycler	Biometra, Göttingen, Germany
Thermomixer Compact	Eppendorf, Hamburg, Germany
Vortex “Lab Dancer”	IKA, Staufen, Germany
Water Purification System Milli-Q	Millipore, Eschwege, Germany
Waterbath	Heidolph, Schwabach, Germany
ZOE fluorescent cell imager	BioRad, Hercules, CA, USA

Multitron Pro incubator shaker

INFORS HT, Switzerland

3.2 Disposable Materials

Cannula Introcan Safety (24G)

BBraun, Melsung, Germany

Cell culture chamber for microscopy

Ibidi, Martinsried (Munich), Germany

Cell Scraper 16cm

Sarstedt, Nümbrecht, Germany

Cell Scarper 25cm

Sarstedt, Nümbrecht, Germany

Cell Strainer 45 μ M, 100 μ M Nylon

Falcon/VWR, Darmstadt, Germany

Combitips 0.5ml

Eppendorf, Hamburg, Germany

CryoPure Tube 1.8ml

Sarstedt, Nümbrecht, Germany

Experimental Gloves

Paul Hartmann, Heidenheim, Germany

Experimental Tubes 15, 50ml

Sarstedt, Nümbrecht, Germany

Filtropour BT500 0.45, 500ml Bottle Top Filter

Sarstedt, Nümbrecht, Germany

Filtered Pipette Tips

Sarstedt, Nümbrecht, Germany

Flow Cytometry Tubes 5ml

Sarstedt, Nümbrecht, Germany

Inoculating Loops 10 μ L

VWR International LLC, Germany

Mini Trans-Blot Filter Paper

BioRad, Hercules, CA, USA

Multiwell Plates 6-, 12-, 24-, 48- and 96-well

Falcon/VWR, Darmstadt, Germany

Needles BD Microlance 0.4, 0.9mm

BD, Ranklin Lakes NJ, USA

Nitocellulose Membrane Hybond-C Extra

Amersham Biosciences, Amersham, UK

Parafilm

Echiney Plastic Packaging, Chicago, IL, USA

PCR Tubes 500 μ l

Labware, Wilmington, DE, USA

Pipette Tips 10, 100 and 1000 μ l

Sarstedt, Nümbrecht, Germany

Pre-filters 30 μ M

Milentyi Biotech, Berg. Gladbach, Germany

Puradisc FP Syringe Filter 0.45 μ M

GE Healthcare, Little Chalfont, UK

Receiver Bottle 500ml

Sarstedt, Nümbrecht, Germany

Reagent Reservoirs 60ml

Starlab, Hamburg, Germany

Safe-Lock Tubes "Eppi" 1.5 and 2ml

Eppendorf, Hamburg, Germany

Serological Pipettes 5, 10, 25 and 50ml

Sarstedt, Nümbrecht, Germany

Syringe Plasilpak 1ml

BD, Franklin Lakes, NJ, USA

Syringe Discardit 2, 5, 10 and 20ml

BD, Franklin Lakes, NJ; USA

Tissue Culture Dishes 10cm, 15cm

Falcon/VWR, Darmstadt, Germany

Tissue Culture Flask 250ml

Falcon/VWR, Darmstadt, Germany

Xplorer Multipipette

Eppendorf, Hamburg, Germany

3.3 Chemicals

3.3.1 Cell culture

ACK Lysis Buffer	Gibco/Thermo Fisher Scientific, MA, USA
Chloroquine Diphosphate Salt	Sigma, St. Louis, MO, USA
CD19 Micro Beads Mouse	Miltenyi Biotech, Berg. Gladbach, Germany
Dulbecco's Modified Eagle Medium (DMEM)	Gibco/Thermo Fisher Scientific, MA, USA
Dulbecco's Balanced Salt Solution (DPBS)	Gibco/Thermo Fisher Scientific, MA, USA
Fetal Calf Serum (FCS)	Gibco/Thermo Fisher Scientific, MA, USA
GlutaMAX	Gibco/Thermo Fisher Scientific, MA, USA
Iscove's Modified Dulbecco's Medium (IMDM)	Gibco/Thermo Fisher Scientific, MA, USA
MEM Non-Essential Amino Acids Solution	Gibco/ Thermo Fisher Scientific, MA, USA
Pancoll Solution	Pan Biotech GmbH, Germany
Penicillin/Streptomycin (PS) (5000 U/ml)	Gibco/Thermo Fisher Scientific, MA, USA
Puromycin	Invivo Gen, San Diego, CA, USA
RPMI 1640	Gibco/Thermo Fisher Scientific, MA, USA
Trypsin-EDTA (0.05%)	Gibco/Thermo Fisher Scientific, MA, USA
β -Mercaptoethanol	Gibco/ Thermo Fisher Scientific, MA, USA

3.3.2 Cloning

Acetic Acid	Carl Roth, Karlsruhe, Germany
Agarose	Sigma, St. Louis, MO, USA
Ampicillin	Carl Roth, Karlsruhe, Germany
Antartic Phosphatase (NEB #M0289)	NEB, MA, IpswichUSA
Bacteria Culture Tubes	Falcon/VWR, Darmstadt, Germany
Calcium Chloride Dihydrate (CaCl ₂)	Sigma, St. Louis, MO, USA
Disodium Phosphate (Na ₂ HPO ₄)	Carl Roth, Karlsruhe, Germany
EcoRI endonuclease (NEB #K0146L)	NEB, MA, Ipswich, USA
Gel Loading Dye Orange 6x	NEB, Ipswich, MA, USA
Gel Red Nucleic Acid Gel Stain	Biotium, Fremont, CA, USA
HEPES Molecular Biology Grade	AppliChem, Darmstadt, Germany
LB Agar	Carl Roth, Karlsruhe, Germany

LB Broth for Molecular Biology	Carl Roth, Karlsruhe, Germany
Magnesium Chloride (MgCl ₂)	Fermentas, Burlington, Canada
Polybrene	Sigma, St. Louis, MO, USA
Primer	Invitrogen/Thermo Fisher, Waltham, USA
Quick-Load 1kb Ladder	NEB, Ipswich, MA, USA
Quick Load 100 bp Ladder	NEB, Ipswich, MA, USA
T4 DNA Ligase 10x Buffer	NEB, Ipswich, MA, USA
Taq Buffer 10x	Fermentas, Burlington, Canada
Sodium Hydroxide (NaOH) 0.1M	AppliChem, Darmstadt, Germany
XhoI endonuclease (NEB #R0101L)	NEB, MA, Ipswich, USA

3.3.3 Western Blot

Acrylamid Rotiphorese Gel30	Carl Roth, Karlsruhe, Germany
Ammonium Persulfate (APS)	AppliChem, Darmstadt, Germany
Bromophenol Blue	Carl Roth, Karlsruhe, Germany
Bovine Serum Albumin (BSA)	PAA, Pasching, Austria
Complete Mini Protease Inhib. Tablets	Roche, Basel, Switzerland
1,4-Dithiothreit (DTT)	Carl Roth, Karlsruhe, Germany
DNase/RNase Free Water	Gibco/Thermo Fisher Scientific, MA, USA
Ethylendiamine Tetra Acetic Acid (EDTA)	Carl Roth, Karlsruhe, Germany
Glycine	Carl Roth, Karlsruhe, Germany
Hydrochloric Acid 37%	Carl Roth, Karlsruhe, Germany
Isopropanol	Carl Roth, Karlsruhe, Germany
Methanol Absolute	Th. Geyer, Renningen, Germany
Non-fat Milk Powder	Carl Roth, Karlsruhe, Germany
Nonidet P-40 (NP-40)	Roche, Basel, Switzerland
Odyssey Blocking Buffer	LI-COR Biotech. Bad Homburg, Germany
PageRuler Plus Prestained Protein Ladder	Thermo Fisher Scientific, Waltham, USA
PhosSTOP	Roche, Basel, Switzerland
Ponceau S	Carl Roth, Karlsruhe, Germany
RIPA Buffer (10x)	CST, Boston, MA, USA
Sodium Dodecyl Sulfate (SDS)	AppliChem, Darmstadt, Germany

TEMED 99%	Carl Roth, Karlsruhe, Germany
Tris HCL	Carl Roth, Karlsruhe, Germany
Tris	Promega, Madison, WI, USA
Tween-20	AppliChem, Darmstadt, Germany
Urea	GE Healthcare, Little Chalfont, UK
Mini-PROTEAN [®] TGX [™] Precast Protein Gels (4–20%)	BioRad, Hercules, CA, USA

3.4 General

Annexin V Binding Buffer	BD, Franklin Lakes, NJ, USA
Cell Fix 10x	BD, Franklin Lakes, NJ, USA
Dimethylsulphoxide (DMSO)	Sigma, St. Louis, MO, USA
Ethanol	Carl Roth, Karlsruhe, Germany
FACS Clean	BD, Franklin Lakes, NJ, USA
FACS Flow	BD, Franklin Lakes, NJ, USA
FcR blocking reagent anti-mouse/human	Miltenyi Biotech, Berg. Gladbach, Germany
Fluid Thioglycollate Medium	BD, Franklin Lakes, NJ; USA
Glycerol	Carl Roth, Karlsruhe, Germany
MACSQuant Running Buffer	Miltenyi Biotech, Berg. Gladbach, Germany
Nuclease Free Water	Ambion, Austin, TX, USA
Sodium Chloride (NaCl)	Carl Roth, Karlsruhe, Germany

3.4.1 Buffer, Media and Solution composition

Blocking Buffer	5% BSA or Milk in TBS-T
B-Cell Culture Medium (murine)	1% Penicillin/Streptomycin, 1% GluatMAX, 1% β -Mercapthoethanol, 10% FBS in IMDM /DMEM (1:1 ratio), MEM Non-Essential Amino Acids Solution (100X)
Cell Culture Medium (human)	1% Penicillin/Streptomycin, 10% FBS in RPMI 1640
Macrophage Culture Medium (murine)	1% Penicillin/Streptomycin, 10% FBS in DMEM

Macrophages Differentiation Medium	1% Penicillin/Streptomycin, 10% FBS, 15% Feeder 1 (L929 derived), 15% Feeder 2 (L929 derived) in DMEM
DNA Alkaline Buffer	10 ml, 1 M Tris (pH 8), 5ml 0,5M EDTA (pH 8), 1ml 5M NACL, 5ml 10% SDS, 29ml sterile H ₂ O
Freezing Medium	90% FBS, 10% DMSO
50x TAE Buffer	224g Tris, 57.1ml Acetic Acid 100%, 100ml 0.5M EDTA (pH 8), Add H ₂ O to 1L
10x TBS	0.2M Tris, 1.83M NaCl, HCl (pH 7.6), Add H ₂ O to 1L
TBS-T Wash Buffer	100ml 10x TBS, 0.1% Tween-20, Add H ₂ O to 1L
10x Towbin Buffer	0.25M Tris, 1.92 Glycine, Add H ₂ O to 1L
Transfer Buffer	200ml Methanol, 100ml 10x Towbin Buffer, Add H ₂ O to 1L
RIPA Buffer+Pi+PS	1ml RIPA Buffer (10x), 1 Tablet PhosSTOP, 1 Tablet Protease Inhibitor, Add H ₂ O to 1L
Running Buffer	100ml 10x Towbin Buffer, 0.1% SDS, Add H ₂ O to 1L
2x Urea Sample Buffer	8M Urea, 5% SDS, 200mM Tris-HCL, 0.1mM EDTA, 0.1% Bromphenol Blue
Separating Gel Buffer	1.5M Tris with HCL (pH 8.8), 04% SDS, add H ₂ O to 1L
Stacking Gel Buffer	0.5M Tris with HCL (pH 6.8), 0.4% SDS, Add H ₂ O to 1L

3.5 Kits

Fix & Perm Cell Permeabilization Kit	Invitrogen/ Thermo Fisher, Waltham, USA
Gel & PCR clean up Kit	Qiagen, Hilden, Germany
QIAquick Gel Extraction Kit	Qiagen, Hilden, Germany
Pierce BCA Protein Assay Kit	Thermo Fisher Scientific, Waltham, USA
Plasmid Plus Maxi Kit (25)	Qiagen, Hilden, Germany

Monach DNA Gel Extraction kit (T1020)	NEB, Ipswich, MA, USA
Pierce™ F(ab') ₂ Preparation Kit	Thermo Fisher, Waltham, USA

3.6 Cytokines, Primer and Enzymes

3.6.1 Cytokines

Recombinant murine M-CSF	Miltenyi, Berg. Gladbach, Germany
--------------------------	-----------------------------------

3.6.2 Oligo sequences for shRNA

Gene name	Gene ID	shRNA target sequences
P53	22059	CCACTACAAGTACATGTGTAA
ATM	11920	CACGAAGTCCTCAATAATCTA
ATR	245000	ACCTTTAATGAGTGTCTTAAA
ATX (SMG-1)	233789	CAGGCTGCATTCAATAACTTA
DNA-PKcs	19090	CAGGCCTATACTTACAGTTAA
P38	26416	CAGGTCTTGTGTTTAGGTCAA
CHK1	12649	CAGGAATATTCTGATTGGAAA
CHK2	50883	CAGAAACACATAATCATTTAA
Bim	12125	CACCCTCAAATGGTTATCTTA
Bak	12018	CCGGAACCTATGATTACTTGA
P21	12575	GACAGAGAGACAAGCTTACAA
MK2	17164	GTACCTGCACTCGATCAACAT

3.6.3 Enzymes

EcoRI	NEB, Ipswich, MA, USA
XhoI	NEB, Ipswich, MA, USA
T4 DNA Ligase	NEB, Ipswich, MA, USA
vent Polymerase	NEB, Ipswich, MA, USA

3.7 Antibodies

3.7.1 Primary Antibodies

Specificity	Host species	Order #	Company
α-Tubulin	Mouse Monoclonal	DM1A	Santa Cruz, Santa Cruz, CA, USA

β -Actin	Mouse Monoclonal	MAB1501	Millipore, Eschwege, Germany
ATM	Rabbit Monoclonal	2873	CST, Boston, MA, USA
ATR	Rabbit Monoclonal	13934	CST, Boston, MA, USA
ATX (SMG-1)	Rabbit Monoclonal	4993	CST, Boston, MA, USA
Bak	Rabbit (D2D3)	121055	CST, Boston, MA, USA
Bim	Rabbit	29335	CST, Boston, MA, USA
CHK1	Mouse Monoclonal	2360	CST, Boston, MA, USA
CHK2	Rabbit Monoclonal	2662	CST, Boston, MA, USA
DNA-PK	Rabbit Polyclonal	orb227986	Biorbyt Ltd, Cambridge, UK
GAPDH	Mouse Monoclonal	649201	Biologend, San Diego, CA, USA
MK2	Rabbit monoclonal	3042	CST, Boston, MA, USA
P21	Mouse monoclonal	11024	Santa Cruz, Santa Cruz, CA, USA
p38	Rabbit monoclonal	9212	CST, Boston, MA, USA
p53	Mouse monoclonal	2524	CST, Boston, MA, USA

3.7.2 Secondary Antibodies

IRDye 800CW Goat anti-Mouse	LI-COR Biotech., Bad Homburg, Germany
IRDye 800CW Goat anti-Rabbit	LI-COR Biotech., Bad Homburg, Germany
IRDye 680RD Goat anti-Mouse	LI-COR Biotech., Bad Homburg, Germany
IRDye 680RD Goat anti-Rabbit	LI-COR Biotech., Bad Homburg, Germany
IRDye 680RD Donkey anti-Goat	Santa Cruz, Santa Cruz, CA, USA

3.7.3 Fluorochrome Conjugated Antibodies

Specificity	Conjugation	Order #	Company
Annexin V	APC	31490016	Immunotools, Friesoythe, Germany
Annexin V	FITC	31490013	Immunotools, Friesoythe, Germany
Annexin V	Pacific Blue	640918	Biologend, San Diego, CA, USA
Annexin V	PE	31490014	Immunotools, Friesoythe, Germany
Arginase1	PE	IC5868P	R&D, Minneapolis, MN, USA
Arginase1	APC	IC5868A	R&D, MN, USA
CCL2	PE	505903	Biologend, San Diego, CA, USA
CD3	FITC	100203	Biologend, San Diego, CA, USA
CD4	APC	555349	BD, Franklin Lakes, NJ, USA

CD5	FITC	100605	Biolegend, San Diego, CA, USA
CD11b	APC	101211	Biolegend, San Diego, CA, USA
CD11b	PE/Cy7	101216	Biolegend, San Diego, CA, USA
CD11b	PerCP/Cy5.5	101227	Biolegend, San Diego, CA, USA
CD14	FITC	130098	Miltenyi Biotech., Berg. Gladbach, Germany
CD14	PE	123309	Biolegend, San Diego, CA, USA
CD16/32	PerCP/Cy5.5	101323	Biolegend, San Diego, CA, USA
CD19	APC/Cy7	115529	Biolegend, San Diego, CA, USA
CD19	BV421	302234	Biolegend, San Diego, CA, USA
CD19	FITC	363008	Biolegend, San Diego, CA, USA
CD19	PE/Cy7	115519	Biolegend, San Diego, CA, USA
CD19	PE/Cy7	302216	Biolegend, San Diego, CA, USA
CD20	PE	120201	eBioscience, San Diego, CA, USA
CD45	APC/Cy7	123981	Biolegend, San Diego, CA, USA
CD47	Pacific Blue	127514	Biolegend, San Diego, CA, USA
CD56	PE	362507	Biolegend, San Diego, CA, USA
CD64	PE	5170704221	Miltenyi Biotech., Berg. Gladbach, Germany
CD68	FITC	137006	Biolegend, San Diego, CA, USA
CD68	Brilliant Violet137017		Biolegend, San Diego, CA, USA
CD80	Brilliant Violet104725		Biolegend, San Diego, CA, USA
CD86	PerCP/Cy5.5	105025	Biolegend, San Diego, CA, USA
CD95	PE	120951	eBioscience, San Diego, CA, USA
CD184/CXCR4	PerCP/Cy5.5	146509	Biolegend, San Diego, CA, USA
CD200	PE	123807	Biolegend, San Diego, CA, USA
CD204	FITC	DSMB00487	RayBiotech, Norcross, GA, USA
CD206	FITC	141703	Biolegend, San Diego, CA, USA
CD282/TLR2	FITC	121805	Biolegend, San Diego, CA, USA
CD284/TLR4	PE/Cy7	145407	Biolegend, San Diego, CA, USA
CD335	APC	137607	Biolegend, San Diego, CA, USA
CXCL9	AF647	515606	Biolegend, San Diego, CA, USA
Dectin	PE	144303	Biolegend, San Diego, CA, USA
EGR-2	APC	REA869	Miltenyi Biotech., Berg. Gladbach, Germany
F4-80	APC	123115	Biolegend, San Diego, CA, USA

F4-80	PE	123110	Biolegend, San Diego, CA, USA
IL10	PE/Cy7	505025	Biolegend, San Diego, CA, USA
IL12	PE	505203	Biolegend, San Diego, CA, USA
iNOS	PE	1978214	Invitrogen, Waltham, USA
Ly6c	PerCP/Cy5.5	128011	Biolegend, San Diego, CA, USA
MHCII	FITC	107606	Biolegend, San Diego, CA, USA
TNF- α	FITC	506303	Biolegend, San Diego, CA, USA
TGF- β	APC	141405	Biolegend, San Diego, CA, USA
IgG1	FITC	400406	Biolegend, San Diego, CA, USA
IgG2a	PE	554689	BD, Franklin Lakes, NJ, USA
IgG2a	APC	2202669	BD, Franklin Lakes, NJ, USA
IgG2a	PerCP/Cy5.5	2321567	BD, Franklin Lakes, NJ, USA
IgG1	PE/Cy7	557872	BD, Franklin Lakes, NJ, USA
IgG2a	APC/Cy7	2223983	BD, Franklin Lakes, NJ, USA
PD1	Brilliant Violet	13256184	Biolegend, San Diego, CA, USA
PD-L1	PE-Cy7	124314	Biolegend, San Diego, CA, USA
Human			
IgG1	PE	400112	Biolegend, San Diego, CA, USA
IgG2a	FITC	400506	Biolegend, San Diego, CA, USA
IgG1	APC	400120	Biolegend, San Diego, CA, USA
IgG1	PerCP/Cy5.5	400150	Biolegend, San Diego, CA, USA
IgG2b	PE/Cy7	400617	Biolegend, San Diego, CA, USA
IgG1	APC/Cy7	400128	Biolegend, San Diego, CA, USA

Live/Dead Stains

7AAD	A1310	Thermo Fisher Scientific, Waltham, USA
Propidium Iodide (PI)	P3566	Thermo Fisher Scientific, Waltham, USA

3.8 Inhibitors and Chemotherapeutic Agents**3.8.1 Inhibitors**

KU 55933 (ATM Kinase Inhibitor)	Selleckchem, Houston, TX, USA
SB 203580 (p38 Inhibitor)	Selleckchem, Houston, TX, USA
PF-8380 (ATX inhibitor)	Selleckchem, Houston, TX, USA

3.8.2 Chemotherapeutic Agents

Bendamustine HCL	Selleckchem, Houston, TX, USA
Cyclophosphamide Monohydrate	Sigma, St. Louis, MO, USA
Doxorubicin Hydrochloride	Tocris Bioscience, Bristol, UK
Fludarabine Phosphate	Sigma, St. Louis, MO, USA
Mafosfamide Sodium Salt	Santa Cruz, Santa Cruz, CA, USA
Etoposide	Sigma-Aldrich Chemie GmbH, Steinheim

3.8.3 Other Reagents

Mouse monoclonal anti –CD20 antibody 18B12	Biogen, Cambridge, MA, USA
α -PD1	Gilead Sciences, CA, USA
Atezoluzumab (anti-PD-L1)	Roche, Basel, Switzerland
MIAP301 (anti-CD47)	Bio Cell, NH USA

3.9 Cell Lines, Primary Cells and Mouse Strains

3.9.1 Cell Lines

M552 MYD88-mutant ABC-DLBCL cells (p.L252P) expression with BCL-2 Knockin (402)	ABC-DLBCL, derived from conditional Myd88
J774A.1	Murine ascites derived macrophage cell line, ATCC, Manassas, VA, USA
L929 (NCTC clone 929)	Murine fibroblast derived cell line, ATCC, Manassas, VA, USA
Phoenix ecotropic (HEK293T derivate)	Embryonic kidney derived packaging cell line, Allele Biotech, ABP-RVC-10001

3.9.2 Primary Cells

Primary CLL cells	CLL-Biobank, Cologne, Germany
CLL peripheral blood mononuclear cells	CLL cohort, Kumasi, Ghana
Peritoneal Murine Macrophages	Wild type C57B/16-J, Charles River, USA
Bone Marrow Derived Macrophages	Wild type C57B/16-J, Charles River, USA

3.9.3 Mouse Strains

Strain	Background	Brief Description
Wild type	C57B/16 J	Wild Type Ctrl, Charles River, Wilmington, MA, USA

3.9.4 Bacteria Strands

One Shot® TOP10 Chemically Competent <i>E.coli</i>	Invitrogen/ Thermo Fisher, Waltham, USA Genotype: F- <i>mcrA</i> Δ (<i>mrr-hsdRMS-mcrBC</i>) Φ 80 <i>lac</i> Z Δ M15 Δ <i>lacX74</i> <i>recA1</i> <i>araD139</i> Δ (<i>araleu</i>) 7697 <i>galU</i> <i>galK</i> <i>rpsL</i> (StrR) <i>endA1</i> <i>nupG</i>
--	---

3.10 Software

Endnote	Thomson Reuters, Philadelphia, PA, USA
FlowJo	Treestar, Ashland, OR, USA
GENTle	M. Manske, University of Cologne, Germany
GraphPad PRISM	GraphPad Software Inc., La Jolla, CA, USA
ImageJ	W. Rasband, NIH, Bethesda, MD, USA
Image Studio Lite	LI-COR, Biotech. Bad Homburg, Germany
MACSQuantify Software	Miltenyi, Berg. Gladbach, Germany
Microsoft Office	Microsoft, Redmond, WA, USA
Rstudio	R Core Team, free software

4 Methods

4.1 Generation of short hairpin ribonucleic acid (shRNA) mediated knock downs of the M552-MyD88 cell line

4.1.1 shRNA design

The shRNAs were a gift from the lab of Michael T. Hermann (The Koch Institute for Integrative Cancer Research, MIT, Cambridge, Massachusetts, USA) where the hairpins were generated and used to accurately group diverse chemotherapeutics into established biochemical modes of action (403). Briefly, FASTA sequence of gene of interest of *Mus musculus* species was retrieved from the nucleotide database housed in reference sequence (RefSeq) of NCBI GenBank. In an siRNA scale software (http://gesteland.genetics.utah.edu/siRNA_scale), the FASTA sequence is pasted to generate a 21 mer oligonucleotide sequence whose antisense strand shows 0% remaining target gene mRNA following siRNA targeted cleavage. The 21 mer antisense strand is reverse complement converted and concatenated to sense strand by a loop sequence to form a hairpin whose correct folding is checked with a folding program ([# oligos = 1](http://katahdin.cshl.org:9331/homepage/siRNA/RNAi.cgi?type=shRNA)). The gene promoter sequence for the hairpin is then added at the 5' whilst the terminator of transcription sequence is added to the 3' ends. This is followed by addition of restriction site sequences to both the 5' and 3' ends of the hairpin. Gene sequence for antibiotic resistance and reporter proteins can be included under a dedicated gene promoter sequence. The generated construct is finally reverse complemented and submitted for DNA synthesis. However for optimum KD efficiency, a minimum of three (3) shRNA designs were generated and the most efficient selected.

4.1.2 Short hairpin Ribonucleic Acid (shRNA) plasmid cloning

shRNAs were cloned into the MSCV-LTR miR30-SV40 GFP (MLS ie: retroviral vector where the expression of the shRNA insert is under the control of Murine Stem Cell Virus-Long Terminal Repeat promoter and the expression of the reporter Green Fluorescent Protein gene is under the control of Simian Virus-40 promoter) plasmid backbone, for shRNAs targeting the Bcl2 family proteins: Bim and Bak, as well as the DNA damage response (DDR) genes: p53, ATM, ATR, ATX (SMG-1), DNA-PK, P38, P21, CHK1,CHK2 and MK2. Initially, the shRNAs stored on filter paper were eluted with 70ul DNase/RNase free H₂O in 1.5ml Eppendorf tubes at room temperature for 30 minutes. Dissolved plasmids were separated by centrifugation at 13,000 RPM for 1 minute and plasmid concentration determined by Nanodrop.

4.1.3 Subcloning of shRNA from MLS backbone into MLP backbone

To introduce an alternative selection marker other than GFP which was also expressed in the MyD88 parental cell line, shRNA for each target gene was subcloned from MLS backbone into a puromycin containing MLP backbone (ie: retroviral vector where the expression of the shRNA insert was under the control of Murine Stem Cell Virus-Long Terminal Repeat promoter and the expression of the Puromycin resistance selector marker gene was under the control of Phosphoglycerate kinase promoter. Parallel digestion of shRNA-MLS and MLP empty vector plasmids were carried out at 37°C for 4hrs using two different restriction enzymes to generate sticky ends.

shRNA-MLS vector digest	MLP vector digest
1.4µg DNA	1.4µg DNA
1.4µl EcoRI	1.5µl EcoRI
1.4µl XhoI	1.5µl XhoI
4µl NEB Buffer 2	4µl NEB Buffer 4
ddH ₂ O to 40µl	ddH ₂ O to 40µl

Digested products were mixed with 6X loading dye and loaded on to a 1.5% agarose gel containing 0.5µg/ml of red safe nucleic acid stain. Samples were electrophorized horizontally at 100V for 1hr in 1X TAE buffer using a 100bp and 1Kbp DNA ladder as references, respectively. Bands of the digested nucleic acids were visualized by UV light and shRNA inserts as well as linearized MLP empty vector excised from the gel with a scalpel. Excised nucleic acids were extracted using Monarch gel nucleic acid purification kit according to manufacturer's instructions and purity and concentration determined by Nanodrop absorbance analysis.

4.1.4 Dephosphorylation of recipient MLP vector

To prevent self-ligation of the linearized empty MLP vector, the phosphate groups at the ends of the vector were removed with Antarctic phosphatase (NEB #M0289, Biolabs). Briefly, 5µg of vector DNA was added to 1µl Antarctic phosphatase buffer. 1µl of Antarctic phosphatase enzyme was then added and incubated at 37°C for 15mins. The mixture was subsequently heated to 65°C for 5 minutes to inactivate the enzyme before ligation was carried out.

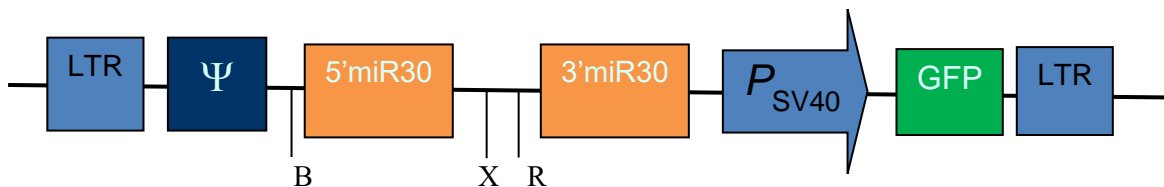
4.1.5 Ligation of shRNA to MLP

Gel purified shRNA of target genes were ligated to linearized MLP vector in reaction mixture which were incubated overnight at 16°C. The reactions were finally heat inactivated at 65°C for 10 minutes and chilled on ice for bacteria transformation.

Ligation mix

3µl gel purified shRNA product
 1µl digested backbone (MLP)
 0.5µl T4 DNA ligase
 1µl 10x T4 buffer
 Nuclease free H₂O to 10µl

a. MSCV-LTR miR30-SV40 GFP (MLS vector)



Unique sites:

B = Bgl II R = EcoR I X = Xho I

b. MLP Vector

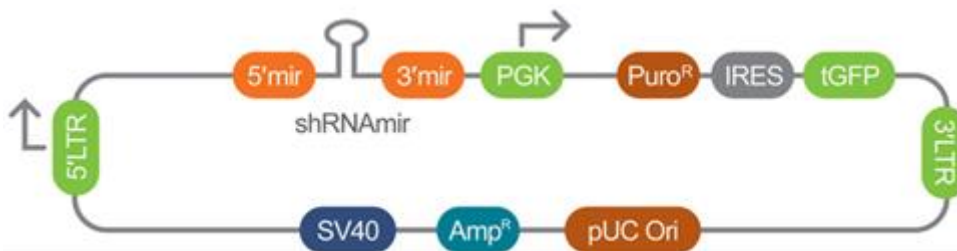


Figure 1: Diagrammatic representation of vector construct

a. The MLS vector contains modified MSCV 5' long terminal repeat (5'LTR) viral promoter which controls the expression of the selected shRNA sequence flanked by microRNA30 to allow processing through the endogenous microRNA pathway. The retroviral psi (Ψ) packaging element promotes viral genomic RNA packaging and delivery efficiency. The SV40 promoter drives the expression of the green fluorescent protein (GFP) which act as the selectable marker

for transduced cells. BglII, EcoR1 and XhoI are restriction site sequences flanking the shRNA insert.

- b. The MLP vector consists of a pUC Ori, the high copy origin of replication which is responsible for the propagation of the ampicillin resistance gene in *E.coli* and the SV40 promoter which drives the transcription of the Ampicillin resistant gene. The modified MSCV 5' long terminal repeat (5'LTR) viral promoter controls the expression of the selected shRNA sequence which is flanked by micro RNA to allow processing through the endogenous microRNA pathway. Additionally, a puromycin resistance gene sequence, the internal ribosome entry site (IRES) and a green fluorescent protein sequence (GFP) are under control of a phosphoglycerate kinase (PGK) promoter, followed by the 3'LTR transcriptional stop (modified from PLATINUM Select MLP Retroviral shRNA-mir Brochure).

4.1.6 Transformation of DH5- α competent *E.Coli*

DH5- α competent *E.coli* were thawed on ice and transformed with the ligation mix according to protocol. Bacteria were thawed on ice and 2 μ l ligated plasmid was added to 50 μ l competent cells and incubated for 20 minutes on ice. Cells were then heat shocked at 42°C for 2minutes, followed by 2 minutes' recovery on ice. 300 μ l fresh, pre-warmed lysogenic broth (LB) was added and cells were incubated at 37°C with slow shake of 100 RPM for 60 minutes. Next, 200 μ l of this mix was plated out on LB agar plates containing 100 μ g/ml ampicillin and incubated overnight at 37°C. Successfully transformed bacteria expressing ampicillin resistance grew and single bacterial clone from each plasmid was inoculated into 2ml LB medium containing 100 μ g/ml ampicillin and incubated at 37°C for 14hrs in a Multitron Pro incubator shaker.

4.1.7 DNA Sequencing

DNA was isolated from each culture using the Qiagen Midi Preparation kit and quantity as well as quality assessed by Nanodrop DNA measurement. Aliquots of Midi preparation DNA were sent to LGC (Berlin, Germany) for sequencing. Sanger sequencing was performed by sending 10 μ l reaction containing 100ng/ml isolated DNA, 4 μ l 5 μ M primer (MSCV5 primer) and DNase/RNase free H₂O. Sequencing data files were analyzed with the GENtle software (free software, Magnus Manske, University of Cologne). Subsequently, only plasmids containing the correct shRNA insert sequences were further amplified by inoculating 150ml LB medium containing 100ng/ml ampicillin and culturing it at 37°C for 14hrs in a Multitron Pro incubator shaker followed subsequently by Maxiprep according to manufacturer's instructions (Qiagen, Hilden, Germany).

4.1.8 Transfection of retroviral producing ecotropic phoenix cell line

To introduce gene targeted shRNA into the genome of MyD88 cells to mediate gene knockdown, the ecotropic retroviral packaging phoenix cell line was used to synthesize shRNA carrying viral particles which were subsequently used to infect MyD88 cells. Here, ecotropic phoenix cells were plated out one day prior to transfection at a density of 2.5×10^6 /ml in DMEM supplemented with 1% penicillin/streptomycin (P/S) and 10% fetal bovine serum (FBS) at 37°C, 5% CO₂, 95% humidity incubator to reattach and expand to reach ~80% confluency by the day of transfection. Calcium transfection (404, 405) was carried out by replacing complete DMEM with a substitute DMEM containing 1% P/S and only 2.5% FBS. Additionally, 25µM Chloroquine was added 5 minutes before addition of the transfection mixture to inhibit lysosomal degradation of plasmid DNA. A transfection mixture contained 18.5µg retroviral MLP vector with the respective shRNA sequence, 9.2µg Ψ-Plasmid which contains the retroviral packaging sequence necessary for infective virus production, 99µl of 2M CaCl₂ and filled up to 790µl with sterile H₂O. To this solution, 790µl of 2X HEPES buffered saline (HBS) was added drop-wise whilst bubbling with a pipette to create fine granular precipitates of DNA in uniform suspension. The mixture was then uniformly dispensed on the phoenix cells in the cell culture plate and gently mixed and incubated for 4h at 37°C. Next, the transfection medium was exchanged with fresh, normal culture medium as described above to reduce chloroquine induced toxicity. After 48h of incubation the virus containing medium was harvested and filtered through a 0.45µm syringe filter. If not used the same day virus was aliquoted and stored at -80°C.

4.1.9 Transduction of MyD88 cell line with viral supernatant

The MyD88 cells were transduced with the harvested viral supernatant by spin infection. 1×10^6 /ml MyD88 cells were plated out on a 12 well plate in a total volume of 1ml culture medium and 1ml of respective virus containing medium was added and centrifuged for 1hr at 400g. After that, 1ml of medium was taken off and replaced by 1ml of the respective virus containing medium and centrifuged again at 400g for 1hr. The plates were subsequently incubated for 48h at 37°C. Transduced cells were sub-cultured at a 1:5 ratio and antibiotic selection undertaken with 2µg/ml puromycin for at least one week.

4.1.10 Generation of cell lysates

A full 10cm cell culture plate of MyD88 KD cells after puromycin selection was used for each KD to generate cell lysates ($\sim 2 \times 10^7$ cells). Cells were harvested, centrifuged (300g, 10min, 4°C) and washed with 10ml ice cold PBS. After that, the cell pellet was resuspended in 20-150 μ l 1xRIPA buffer + protease inhibitor (Pi) + phosphatase inhibitor (Ps) depending on the pellet size. Cell lysis was performed for 30 min on ice before centrifugation at 16,000 rpm for 5min at 4°C. The supernatant containing the cellular proteins was collected and stored at -80°C.

4.1.11 Protein determination by Pierce Bicinchoninic acid (BCA) assay kit

The amount of protein per cell lysate was determined using Pierce BCA Protein Assay Kit according to the manufacturer's protocol (Thermo Fisher Scientific, Waltham, USA). One μ l of cell lysate was mixed with 99 μ l of RIPA buffer +Pi + Ps (1:100 dilution) and 12.5 μ l of this mixture was added to a 96 well plate in duplicates. Next, 100 μ l of freshly prepared BCA reagent was added and plates were incubated for 30min at 37°C before absorbance was measured at 450nm on a FluoSTAR Optima plate reader. BCA standards supplied with the kit were used to create a standard curve, from which the protein concentration of the MyD88 KDs were computed based on their blank corrected absorbance.

4.1.12 Sodium dodecyl sulphate polyacrylamide gel electrophoresis (SDS-PAGE)

Knockdown (KD) efficiency of MyD88 cells were validated on the protein level by means of SDS-PAGE electrophoresis. For this purpose, precast 4-20% gradient gels from BioRad, California, USA were purchased or self-made 12.5% gels were prepared according to recipe in [Table 1](#) for use. The precast gradient gels allowed for a resolution of a broader range of proteins permitting very high molecular weight and low molecular weight proteins to be resolved on the same gel. Protein lysates were mixed with 5X sample buffer, boiled at 95°C for 5 min to denature and cooled before 20 μ l was loaded onto the stacking gel. 5 μ l of pre-stained protein marker was loaded as a ladder (page ruler plus). The electrophoretic separation was carried out with a vertical Mini Protean Tetra Cell apparatus (BioRad) for 30min at 120V followed by 45min-1h at 180V in 1X running buffer depending on the size of the targeted protein.

Table 1: Recipe for preparation of stacking and separation gel

	12.5% separating gel	5% stacking gel
H ₂ O	1.4ml	1.75ml
Separating gel buffer	2.4ml	----
Stacking gel buffer	-----	0.31ml
30% PAA	2.7ml	0.42ml
10% APS	52.8 μ l	12.5 μ l
TEMED	5.28 μ l	2.5 μ l

4.1.13 Western blotting

At the end of the electrophoresis, separated proteins were blotted from the SDS-PAGE gel on to a nitrocellulose membrane using the BioRad semi-dry blot system. The blotting was performed in 1X blotting buffer for 1h at 360mA at 4°C and on ice. For proteins of large molecular weight such as: ATM (350kDa), DNA-PK (450kDa), ATR (300kDa) and ATX (410kDa) blotting time was increased to 2hrs. After blotting, the membranes were blocked with 5% Bovine serum albumin (BSA) or non-fat milk in tris-bufered saline (TBS) (according to manufacturer's recommendation for optimum resolution) for 1h at room temperature to prevent nonspecific binding of antibodies. Immunoblotting with primary antibody for the respective protein of interest was performed at 4°C overnight.

Following 3 washing steps with TBS-Tween and finally with TBS, the membrane was stained with secondary, fluorescent dye labeled antibodies for 1h, at room temperature, protected from light. The secondary antibodies were diluted 1:3000 in phosphate-bufere saline (PBS) with Odyssey blocking buffer (1:1 ratio). Secondary antibody dilution for staining housekeeping protein was done according to manufacturer's protocol. Protein bands were detected at 700 or 800nm using the LICOR Odyssey infrared imaging system after 3x washing each lasting for 5minutes with TBS-T.

4.2 Primary cells isolation

4.2.1 Isolation of primary thioglycollate induced murine macrophages

Wild type C57BL/6 J mice were used for isolation of all peritoneal macrophages. Mice were injected intra-peritoneal (i.p) with 1ml commercial thioglycollate and sacrificed after 4 days for peritoneal lavage. For this process, the peritoneum was washed with a total of 20ml Dulbecco's

Modified Eagle's Medium (DMEM) without supplements using a 24G cannula. This process involves filling the peritoneum up with DMEM, and siphoning back the media into a 50ml Falcon tube kept on ice. This process is repeated 4-5 times to optimally recover all elicited peritoneal macrophages. The cell suspension was centrifuged at 300g for 10min and the resulting cell pellet resuspended in 2-3ml ammonium-chloride-potassium (ACK) lysis buffer for 5 mins at room temperature to hemolyze all erythrocytes. Cells were subsequently washed by filling the tube up to 50ml with PBS and centrifuged for 10min at 300g. The cell pellet was resuspended in DMEM (+10% fetal bovine serum (FBS) and 1%P/S) depending on the pellet size and counted by flow cytometry. Cells were plated out at a concentration of 5×10^5 /ml and incubated to attach for a minimum of 24h. A small amount of cell suspension was used to determine the purity by flow cytometry. Lavaged cells were only used for cocultures when the purity of macrophages exceeded 75% as determined by double positive expression of F4-80 and CD11b staining and showed low expression of other immune cell type markers (see 4.2.2).

4.2.2 Purity check

The purity of isolated peritoneal macrophages was determined by antibody staining for cell surface markers followed by flow cytometry. Briefly, the cell suspension was centrifuged at 300g for 5min, resuspended and incubated in mouse FcR blocking reagent (Miltenyi Biotech, Berg. Gladbach, Germany) for 10min at 4°C to prevent nonspecific binding of antibodies. Extracellular surface markers were stained with fluorochrome conjugated antibodies specific to the surface antigens indicated in Table 2 below according to manufacturer's recommendations and incubated for 15min at 4°C. Cells were washed with 1ml cold PBS, followed by resuspension in 250µl PBS. Marker expressions were then analyzed by flow cytometry using a BD FACS Canto.

Table 2: Antibody panel for staining surface marker of murine macrophages for purity check

Purity check	Stain A	Stain B	Isotype
FITC	CD3		Rat IgG-1
PE	CD14	CD11c	Rat IgG2a
APC	F4-80	CD335	Rat IgG2a
Per CP	Ly6c		Mice IgG2a
APC-cy7	CD19		Mice IgG2a
PE-cy7	CD11b		Mice IgG-1

4.2.3 Isolation and differentiation of murine bone marrow derived macrophages

To obtain cells from the bone marrow, wild type C57B/16 J mice were sacrificed and femur and/or tibia were extracted removing all muscle and connective tissue from the bones. The bones were syringe through the heads at both ends to get the most cells out and minimize loss of cells as the majority of bone marrow cells resides in the femur/tibia head. Bones were flushed with 1.5ml DMEM/per bone using a 2ml syringe and a 0.4mm needle. Before cells were applied to a 0.45µm filter, they were dissociated by taking them up and down with the syringe. The Filter was washed with 8.5ml DMEM and cells were resuspended for 10min at 300g. Depending on the size of the pellet and the amount of erythrocytes the pellet was resuspended in 3-5ml ACK lysis buffer and incubated for 5min at room temperature. The cell suspension was filled to 50ml with PBS before an additional centrifugation step was performed. For long term storage the cells were frozen at -80°C in 1ml freezing medium per sample per bone. For direct use cells were resuspended thoroughly in 5ml DMEM (+FBS+P/S) and counted by Neubauer chamber. Cells were plated out on a 10cm cell culture plate at a concentration of 2.5×10^6 /ml for 24h in bone marrow differentiation medium. The supernatant was collected and the plate was washed twice with 3ml DMEM (+FBS+PS) to facilitate maximum recovery of none adhered cells. Next, the supernatant was centrifuged for 10min at 300g to pellet none adherent cells which were subsequently resuspended in differentiation medium, counted and plated out at 6×10^5 /ml to an uncoated bacterial dish and incubated for 48h. On the 3rd day, 4ml of differentiation medium was added and the cells were incubated for an additional 3 days. On the 6th day medium was removed and exchanged for normal DMEM (+FBS+PS) and incubated for another day before cells were detached by replacing DMEM (+FBS+PS) with cold PBS/2mM EDTA solution and putting the 10cm dish on ice and applying up and down pipetting to facilitate detachment of strongly adherent differentiated cells. For use in further experiments cells were counted by Casy cell counter and plated out at 5×10^5 /ml for 24hrs incubation. A small amount of

cell suspension was used for purity determination as indicated in 4.2.2. Resulting differentiated macrophages are described as M0 macrophages.

4.2.4 Macrophage phenotype staining and determination by flow cytometry

To ascertain whether different DDR gene KDs in tumor cells elicit differential phenotypic markers expression in macrophages upon contact in the coculture system, an extra- and intracellular macrophage marker panel was established to enumerate macrophage phenotypic marker expression following exposure to tumor cells harboring various DDR gene KDs observed to be associated with reduced phagocytosis in comparison to empty vector control. Macrophages were harvested from cell culture plates using cell scraper. After centrifugation for 5min at 300g, cells were transferred to FACS tubes and incubated at 4°C. Master mixes for the different stains were freshly prepared and extracellular markers were stained accordingly for 15min at 4°C in the dark.

Additional intracellular staining was performed for the panel where the phenotypic marker of interest was rather intracellularly expressed. Here, Fix & Perm Cell Permeabilization kit from Invitrogen was used to treat the cells according to manufacturer's instruction. Stained cells were washed with 1ml ice cold PBS, centrifuged and resuspended in 250µl PBS before analyzed on the Miltenyi MacsQuant VYB flow cytometer following an initial multi-color compensation-procedure.

Table 3: Extra-and Intracellular markers for murine macrophage phenotype determination

Laser	Channel (nm)	Colours	Macrophage Phenotypic Markers				Isotypes			
			1	2	3	4	1	2	3	4
405	450/50	Brilliant violet	CD80	PD-1		CCR7	Hamster IgG	Rat IgG2a		Rat IgG2a
488	525/50	FITC	MHCII	CD115	CD68	CD64	Rat IgG2b, κ	Rat IgG2a, κ	Rat IgG2a	Mouse IgG1, κ
	585/40	PE	CD206	CD200R	iNOS	CD86	Rat IgG2a	Rat IgG2a	Rat IgG2a	Rat IgG2b
	750LP	PE-Cy ⁷	CD38	PD-L1	1L-10	F4/80	Rat IgG2a, κ	Rat IgG2b	Rat IgG2b	Rec. Human IgG1
633	655-730	APC	CD16/32	TGF-β	Arg.1	EGR-2	Rat IgG2a, λ	Mouse IgG1	sheep IgG	Human IgG2a
		APC-Cy ⁷	CD11b	CD11b	CD11b	CD11b	Rat IgG2b, κ	Rat IgG2b, κ	Rat IgG2b, κ	Rat IgG2b, κ

4.2.5 Peripheral blood mononuclear cell isolation from Ghanaian CLL patients

Following an Ethical approval by the Committee on Human Research, Publications and Ethics of Kwame Nkrumah University of Science and Technology, a total of 50 CLL patients were recruited from the Haematology Malignancy Clinic of Komfo Anokye Teaching Hospital, Kumasi-Ghana following informed consent. Up to 15ml of whole blood was phlebotomized from each patient into EDTA anticoagulant monovett tubes. Peripheral blood mononuclear cells (PBMC) were subsequently isolated from each sample by density gradient centrifugation using Ficoll-Plaque Plus medium. Here, the hydrophilic high molecular weight polymers of sucrose and epichlorohydrin of this media forms a density gradient permitting separation of whole blood into fractions according to the cellular densities.

Whole blood was diluted 1:1 with PBS washing buffer and carefully overlaid on 15ml Ficoll-Paque medium held at an angle of 15-20°. Next, the sample was centrifuged at 1200g for 20mins without braking to enable different blood cells to separate out according to their densities. Granulocytes and erythrocytes migrate through the Ficoll-Paque to the bottom whereas lymphocytes, monocytes and platelets remain at the Ficoll-Paque interface forming the band of PBMC. Next, the PBMC layer is carefully recovered and washed twice in a balanced salt solution to remove remnant Ficoll contamination and platelets. Recovered cells were subsequently counted by Neubauer chamber and stored in liquid nitrogen tanks until shipment on dry-ice.

4.2.6 Phenotypic characterization of Ghanaian CLL patients

To phenotypically characterize the Ghanaian CLL patients, a panel of 30 antibodies (Table 4) against established diagnostic and prognostic markers was established. Antibody-conjugated flourophores selected were multi-color compensated on the Miltenyi MACSquant X (Miltenyi Biotec) flow cytometer prior to sample analysis.

Vials of PBMC samples were thawed rapidly at 37°C and washed in 10ml PBS to remove residual DMSO by centrifuging at 300×g for 5mins. The supernatant was removed completely and cells resuspended in PBS. Cell count and viability were enumerated on the CASY cell counter (Omni Life Sciences). Non-specific Fc receptors were blocked on cells by incubation of 1 x 10⁶ nucleated cells per 80µL of PBS buffer with 20µL of anti-human FcR blocking reagent and directly staining extracellular antigens with appropriate volumes of freshly prepared master-mix stain per tube. All isotype control tubes were similarly stained with isotype master-mix required for 15min at 4°C in the dark after which unbound antibodies were removed by washing with 1ml PBS at 300×g for

5mins. Cells were finally resuspended in 200ul of PBS and 1×10^3 events acquired on MACSquant X (Miltenyi biotec) flow cytometer. For cells in tubes where intracellular staining was required, an additional centrifugation step at $300 \times g$ for 5mins was carried out after extracellular antigen staining followed by treatment with fixation & Permeabilization and subsequent intracellular staining with the appropriate antibody according to manufacturer's instruction. Stained cells were washed with 1mL ice cold PBS, centrifuged and resuspended in 200 μ l PBS before cell acquisition by flow cytometer.

Table 4: Antibody panel for immunophenotyping of CLL cohort

	Panel of Phenotypic Markers						Isotypes					
	1	2	3	4	5	6	1	2	3	4	5	6
PE	CD20	IgK	CD25	CD56	CD200	CCR5 (CD195)	Mouse IgG1, κ	Mouse IgG1, κ	Mouse IgG1, κ	Mouse IgG1, κ	Mouse IgG1, κ	Rat IgG2a, κ
FIT-C		IgL	CD10	CD3	CD47	CCR7		Mouse IgG2a, κ	Mouse IgG1, κ	Mouse IgG2a, κ	Mouse IgG1, κ	Mouse IgG2a, κ
APC	CD79 b	IgM	CD11b	CD4	CD38	CD2	Mouse IgG1, κ	Mouse IgG1 κ	Mouse IgG1, κ	Mouse IgG1, κ	Mouse IgG1	Mouse IgG1
Per-CP Cy 5.5	CD23	IgD	CD14	CD8	PD-L1 (CD274)	CD16	Mouse IgG1, κ	Rat IgG2a, κ	Mouse IgG1, κ	Mouse IgG1, κ	Rat IgG2b, κ	Mouse IgG1, κ
PE-Cy7	CD19	CD19	CD19	CD19	CD19	CD19	Rat IgG2a, κ	Rat IgG2a, κ	Rat IgG2a, κ	Rat IgG2a, κ	Rat IgG2a, κ	Rat IgG2a, κ
Brilliant violet	CD22	ROR 1	ZAP-70		PD1	CCR2 (CD192)	Rec. Human IgG1	Mouse IgG1, κ	Mouse IgG1, κ		Mouse IgG1, κ	Mouse IgG2a, κ
APC-Cy7	CD5	CD5	CD5	CD5	CD5	CD5	Mouse IgG2a, κ	Mouse IgG2a, κ	Mouse IgG2a, κ	Mouse IgG2a, κ	Mouse IgG2a, κ	Mouse IgG2a, κ

4.3 Functional cell culture experiments

4.3.1 Cytotoxicity of MyD88 parental and KD cells to selected chemotherapeutic agents

Parental MyD88 and DDR knockdown cells generated from the parental Myd88 lymphoma cell line were tested for sensitivity to selected chemotherapeutic drugs including the current standard of treatment (R-CHOP) for diffuse large B-cell Lymphoma. Cells were suspended at 1×10^6 /ml in B cell medium and aliquoted 100 μ L/well on a 96 well plate. Selected chemotherapeutic agents, namely Mafosphamide, Doxorubicin, Etoposide and Cisplatin were diluted to a final concentration of 0 μ M, 2 μ M, 10 μ M, 20 μ M and 50 μ M. Cells were incubated for 48hrs and subsequently stained with Annexin V/ 7-AAD for 15min at room temperature in the dark. Stained samples were subsequently measured by flow cytometer (MACSquant VYB, Miltenyi Biotech) to determine viability in each concentration of chemotherapeutics. For all subsequent experiments where sub-lethal stressing of the tumor cells with genotoxic agents was required, an IC₂₀ concentration of genotoxic agent (concentration of the genotoxic agent that induces 20% of tumor cells death in 48hrs) was used.

4.3.2 Generation of cells' secretome/conditioned media (CM)

In order to generate cells secretome (conditioned media) for functional assays, tumor cells were sub-lethally treated *in vitro* with IC₂₀ concentration of Mafosphamide or vehicle control for 12hrs at 37°C. Afterwards, cells were washed three times to remove all traces of genotoxic substance and plated out at a concentration of 4×10^6 /ml in fresh culture medium for 24-30hrs. The resulting conditioned media was collected by taking the supernatant, centrifuging it for 10min at 2000rpm and filtering it out through a 0.45 μ m bore. The supernatant was aliquoted and stored at -80°C or used directly for functional experiments.

4.3.3 Genotoxic stressed tumor cells

In functional assays where genotoxic stressed tumor cells were required for co-culture, tumor cells were pretreated with IC₂₀ concentration of genotoxic substance determined from a 48hrs toxicity assay (see 4.3.1). Tumor cells were either treated with genotoxic substance or its vehicle control for 12hrs. The cells were then washed three times to remove remnant genotoxic substance before resuspended in fresh B-cell medium for co-culture experiments.

4.3.4 Antibody dependent cellular phagocytosis assay (ADCP)

Different macrophages were plated out at an optimized concentration determined for the respective type of macrophages (Table 5). Primary macrophages were incubated for 24hrs while cell line macrophages were incubated for 12h to allow reattachment. Afterwards, the leukemic target cells

were counted and added to the macrophages at an optimized concentration. As cells were plated out in 96 well plates a total volume of 100 μ l/cell type was used. To stimulate antibody dependent phagocytosis the mouse specific Cd20 monoclonal antibody, 18B12 was used and added to wells at a final concentration of 50 μ g/ml. The vehicle controls were filled up with the corresponding amount of cell culture medium. For each condition per experiment, 5 technical replicates were performed to capture assay variability (Figure 2A). The plates of effector cell co-cultured with tumor cells were incubated at 37°C for 16hrs after which remaining tumor cells per well were enumerated by flow cytometry using the MACSquant VYB. MyD88 cells were detected by gating first on size and granularity (FSC, SSC), followed by their GFP expression in the FITC channel as these tumor cells were transfected with GFP reporter gene. To assess antibody dependent phagocytosis, the amount of leukemic cells in the reactions with antibody was normalized to the amount of leukemic cells in the control reaction.

Table 5: Optimized concentrations for different cell types

Cell Type	Concentration	ADCP incubation time	Monoclonal antibody
MyD88 cell line	1.0*10 ⁶ /ml	16hrs	18B12
BMDM	5*10 ⁵ /ml	16hrs	18B12
Peritoneal Macrophage	5*10 ⁵ /ml	16hrs	18B12
J774A.1 Macrophage	1*10 ⁵ /ml	16hrs	18B12

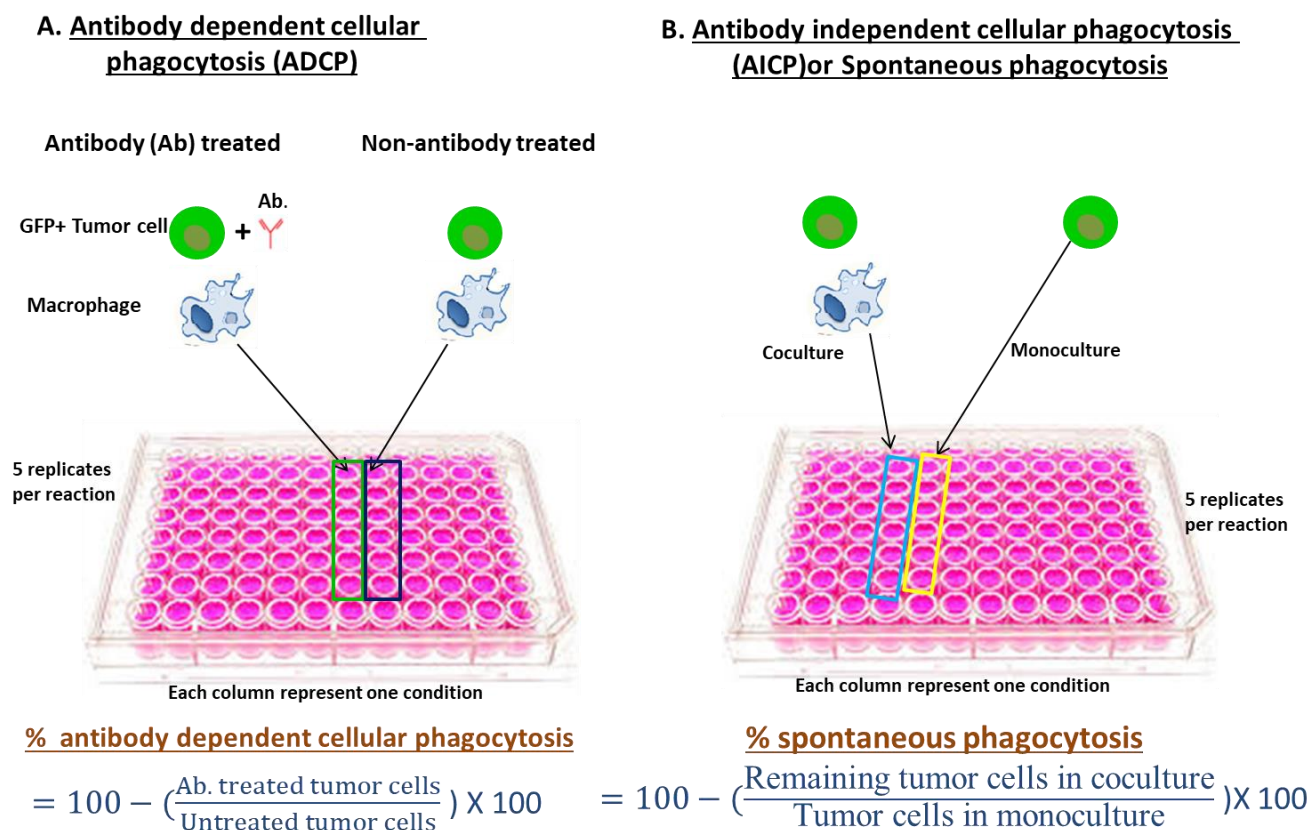


Figure 2: Diagrammatic depiction of ADCP and AICP experimental setup

A co-culture of macrophages and tumor cells was set up by plating out macrophages (blue) at a certain density indicated in table 5 and allowed to attach for a certain amount of time. Subsequently tumor cells (green) are added together with monoclonal antibody (red) which is defined as “positive” or medium only which is defined as “negative”. Five replicates of positive and negative reactions are set up respectively per condition to reduce intra-assay variability. The peripheral wells on each plate are filled with phosphate buffered saline to control evaporation. After an incubation time of 16hrs, remaining tumor cells per well is enumerated by flow cytometry.

4.3.5 Determination of non-opsionized phagocytosis (spontaneous phagocytosis)

Non-opsionized phagocytosis was determined without the addition of antibody by using the same cell concentrations indicated in Table 5 above. Depending on the origins of the macrophages, cells were plated out in a total volume of 100µl for 12-24hrs before the start of an experiment to permit attachment. Subsequently, 100µl of tumor cells were added in the respective concentrations. In addition to the macrophage-tumor cells co-culture, a monoculture of tumor cells of the same concentration and volume was included in the setup (Figure 2B). Cells were incubated for 16hrs at

37°C and remaining tumor cells enumerated by flow cytometry using the MACSquant VYB by gating on the GFP⁺ population. As tumor cells with DDR KDs showed different proliferation rates to empty vector control cells, the amount of tumor cells in the macrophage co-culture were normalized to their respective monoculture controls.

4.3.6 Effect of genotoxic stress and effector cell contact on immune checkpoint antigens

To determine the baseline immune antigen expression level on the MyD88 KD tumor cells and evaluate expression patterns upon genotoxic stress and combined effect of genotoxic stress and effector cell contact, 1.0×10^6 cells/ml were plated in a 12-well plate as untreated, treated with IC₂₀ concentration of mafosphamide or pretreated, washed three times with PBS and co-cultured with macrophages for 16hrs. Tumor cells were removed and washed three times at 350g for 5 mins each with ice cold PBS. Cells were subsequently blocked with anti-mouse FcR reagent and stained with a master-mix of an appropriate antigen specific antibody or their corresponding isotypes (Table 6) for 15 mins at 4°C. Cells were once more washed with 1ml ice cold PBS to remove all unbound antibodies and a final volume of 200µl suspension made. For each sample, 10,000 events were acquired from the GFP⁺ expressing population after exclusion of doublets using a multi-color compensation on the MACSquant X (Miltenyi Biotec) and MFI of the immune antigens per the acquired populations determined.

Table 6: Antibody panel for assessment of immune checkpoint antigens expression

Antigen	Antibody conjugate	Isotype
CD47	APC anti-CD47	Rat IgG2a, κ
CD200	PE- anti -CD200	Rat IgG2a, κ
PD1	Brilliant violet anti-PD1	Rat IgG2a, κ
PD-L1	PE-Cy ⁷ anti-PD-L1	Rat IgG2b, κ

4.3.7 Immune checkpoint antigen inhibition in co-culture of MyD88 cells

Having determined immune checkpoint antigen expression on the MyD88 cell line, the relevance of immune checkpoint inhibitors in the treatment of this phenotype was assessed through co-culture systems that employed addition of pre-determined optimal concentrations of the checkpoint inhibitor antibodies indicated in Table 7. The respective macrophages were plated overnight as previously outlined (Table 5) in a volume of 100µl/ well on a 96 – well plate. Myd88 empty vector cells or DDR genes KD generated from these cells were suspended at 1×10^6 /ml and 100µl/ added per well. Additionally, anti-Cd20 antibody was added to a final concentration of 50µg/ml and immune

checkpoint inhibitors to a final concentration indicated in Table 7 below were also added. The final volume per well of the co-culture was 225 μ l and all samples were incubated at 37°C for 16hrs. Remaining cells per well after 16hrs were enumerated by flow cytometry.

Table 7: Optimized concentration of immune checkpoint inhibitors

	Initial conc.	Final conc. in co-culture
α PD1	4.49 mg/ml	50 μ g/ml
Anti-PD-L1 (Atezolizumab)	60mg/ml	20 μ g/ml
Anti-CD47	8.89 mg/ml	15 μ g/ml

4.4 Total exosome isolation from cell culture media

The total exosome fraction from cell lines were isolated from cell culture media using the BLAH isolation kit (Invitrogen, Life Technologies). Empty vector control and p53 KD MyD88 cell lines were expanded in 150cm² culture plates to obtain a total of 500 x 10⁶/ml cells. Cells were then centrifuged at 1200 rpm for 5mins to remove supernatant and subsequently washed two times with PBS under the same conditions before they were cultured in FBS-free medium overnight to exclude any contaminating extracellular vesicles (EVs). Next, cells were centrifuged again at 1200 rpm for 5mins and the supernatant discarded. The cell pellet was resuspended in 30ml CD293 medium on a 150 cm² culture plates and incubated overnight at 37°C. Next, the cells were centrifuged at 1200rpm for 5mins and the cell-free supernatant transferred into a new 50ml falcon tube for an additional spin at 2900 rpm for 10mins. Once more, cell-free supernatant was transferred to a new 50ml falcon and centrifuged at 3500 rpm for 20mins. To further remove any contaminant, the cell-free supernatant was filtered through 0.2 μ m filter pore before 0.5 volumes of the total exosome isolation reagent for cell-free medium was added, vortexed well to mix and incubated at 4°C overnight. Next, the mixture was centrifuged at 10,000g for 60mins at 4°C to pellet down the EVs. The supernatant was carefully aspirated and discarded and the pellet resuspended with 1200 μ l of PBS and transferred into ultracentrifuge tubes for subsequent centrifugation at 110,000 rpm for 1hr, 15mins at 4°C. The supernatant was carefully aspirated and discarded and the EV pellet resuspended again in 1X PBS for immediate use or stored at -80 °C until needed.

4.4.1 Functional effect of exosomes on tumor cells- macrophages co-culture

Macrophages were plated overnight to attach at the indicated concentrations (Table 5). MyD88 empty vector cells were used as target cells at a suspension of 1×10^6 /ml. For each well, 100 μ l of tumor cells suspension were added to the macrophages.

Next, co-cultures were setup with addition of exosomes alone, anti-Cd20 antibody alone, exosomes/anti-Cd20 combination, exosomes/anti-Cd20/anti-Cd47 combinations, exosomes/ anti-Cd20/anti-PD-L1 combinations from empty vector control cells or p53 KD cells. Co-cultures were incubated for 16hrs and remaining cells/well enumerated by flow cytometry measurement. In all setup cases involving exosomes, 5 μ l of the respective exosome suspension was used or 5 μ l of 1X PBS (which is the diluents for the exosome) was used as control.

4.5 Statistical analysis and data illustration

All diagrams were generated using GraphPad Prism software and results are displayed as mean of technical replicates. If not indicated otherwise error bars represent standard error of the mean (SEM) and statistical differences were calculated by one-way Anova and Bonferroni post-test after confirming normality with Shapiro-Wilk normality test. Significance was indicated as * = $p < 0.05$, ** = $p < 0.01$, *** = $p < 0.001$. Non-significance was not displayed.

Quantification of western blot was calculated by determining the band intensity using Image Lite software (LICOR). Densitometry of each protein was normalized to housekeeping gene (β -actin or gapdh) and control loading and displayed as column diagram. No statistical testing was applied here as technical replication was inadequate within one experiment.

5 Results: The role of DNA damage response in the tumor-macrophage interaction

5.1 Functional impact of DNA damage response genes deregulation on phagocytosis and efficacy of immune checkpoint inhibitors in a murine model of ABC-like DLBCL

5.1.1 Introduction

The microenvironment in the bone marrow suppresses tumor cells killing by immunotherapy. Previous study using a humanized mouse model of double-hit lymphoma (406) in our group identified the bone marrow microenvironment as a source of treatment refractoriness to antibody targeted tumor cells killing (21). Tumor cells were effectively eliminated in the microenvironment of the spleen, liver, and peripheral blood by antibody-based therapy such as Alemtuzumab, but not from the bone marrow microenvironment. However, combination of cyclophosphamide and Alemtuzumab, effectively eliminated tumor cells from the protective bone marrow microenvironment, resulting in prolonged survival.

It was observed that, chemo-immunotherapy (CIT) induced an acute secretory activating phenotype (ASAP) of soluble factors which triggered profound effector cell-mediated tumor cell phagocytosis. Induction of ASAP through genotoxic stress thus highlights the importance of ASAP mechanistically to CIT regimens in cancer treatment and most importantly, reveals a critical role of the DNA damage response (DDR) in this synergistic interaction. Thus, to understand the biological mechanisms involved in cellular response to DNA damage in relation to macrophage mediated phagocytosis, there is the need to focus on the key members of the DDR pathway.

This thesis aims to elucidate the genetic drivers of the DDR pathway underlying immune-tumor cell interactions in the tumor microenvironment.

Using a murine model of ABC-subtype of DLBCL (MyD88 M552 cell line), this chapter aims to discuss the following:

1. Loss of DDR genes and its effect on phagocytosis of tumor cells
2. Effect of immune checkpoint inhibitors with chemoimmunotherapy on phagocytosis of tumor cells with deregulated DDR genes
3. Role of critical DDR genes on the constitution of extracellular vesicles cargo and phagocytosis

5.2 Characterization of the E μ -Myc and OSU-CLL cell lines for *in vitro* assessment of DDR on phagocytosis

E μ -Myc cell line derived from the E μ -Myc mouse model and OSU-CLL cell line generated by Epstein-Barr virus (EBV) transformation of B-cells from a CLL patient were used in in-vitro experiments using coculture system with different effector cells including J774.1A, murine thioglycollate induced peritoneal macrophages and feeder media differentiated bone marrow-derived macrophages. The E μ -Myc mouse model recapitulates Burkitt's lymphoma type of aggressive B-cell malignancy and was generated by placing c-myc transgene under control of IgH enhancer (E μ -myc) which drives development of lymphoblastic lymphomas of predominantly pre-B, mixed-B or B-cells (407). In the context of this work, the E μ -Myc model permits further validation of candidate DDR gene(s) from *in vitro* experiments in an *in vivo* setting under fully functional immunocompetent background where the complexities of cellular interaction from immune cells as well as stromal cells exist.

OSU-CLL cell line, on the other hand was generated by EBV transformation and recapitulates mutated IgHV subtype of chronic lymphocytic leukaemia (CLL) (408). Short hairpin ribonucleic acids (shRNA) mediated knock-down (KD) of DDR genes generated from the OSU-CLL Cell lines would provide insight into genetic drivers of DNA damage response pathway players with functional role in immune-tumor cells interaction under genotoxic stress within the tumor microenvironment in the matured B-cell setting.

5.2.1 OSU-CLL cells inappropriate for studying Fc-gamma-mediated phagocytosis due to inherent stickiness

Initially, E μ -Myc and OSU-CLL cell lines were screened for Cd20 antigen expression, which is required for the engagement of anti-Cd20 to recruit macrophages to the targeted tumor cells. Both cell lines showed over 90% positivity. However, OSU-CLL cells could not be further used due to their stickiness into clumps impeding accurate cell count on flow cytometer in the phagocytosis assay. Therefore, only E μ -Myc cells were further characterized by their sensitivity to selected chemotherapeutic substances including Mafosphamide, Doxorubicin, Cisplatin, and Etoposide. E μ -Myc cells were very sensitive to etoposide (IC₅₀: 0.37 μ M), doxorubicin (IC₅₀: 1.37 μ M) and mafosphamide (IC₅₀: 2.08 μ M) but showed less sensitivity towards Cisplatin (IC₅₀: 24.8 μ M) (Figure 3B). Subsequently, two genotoxic agents which induce DNA damage by different mechanisms; mafosphamide (an alkylating agent that induces double strand DNA breaks) and etoposide (a topoisomerase II inhibitor which induces DNA breaks through re-ligation inhibition), were selected and IC₂₀ concentration were determined and used for sub-lethal genotoxic stressing of cells for coculture experiments.

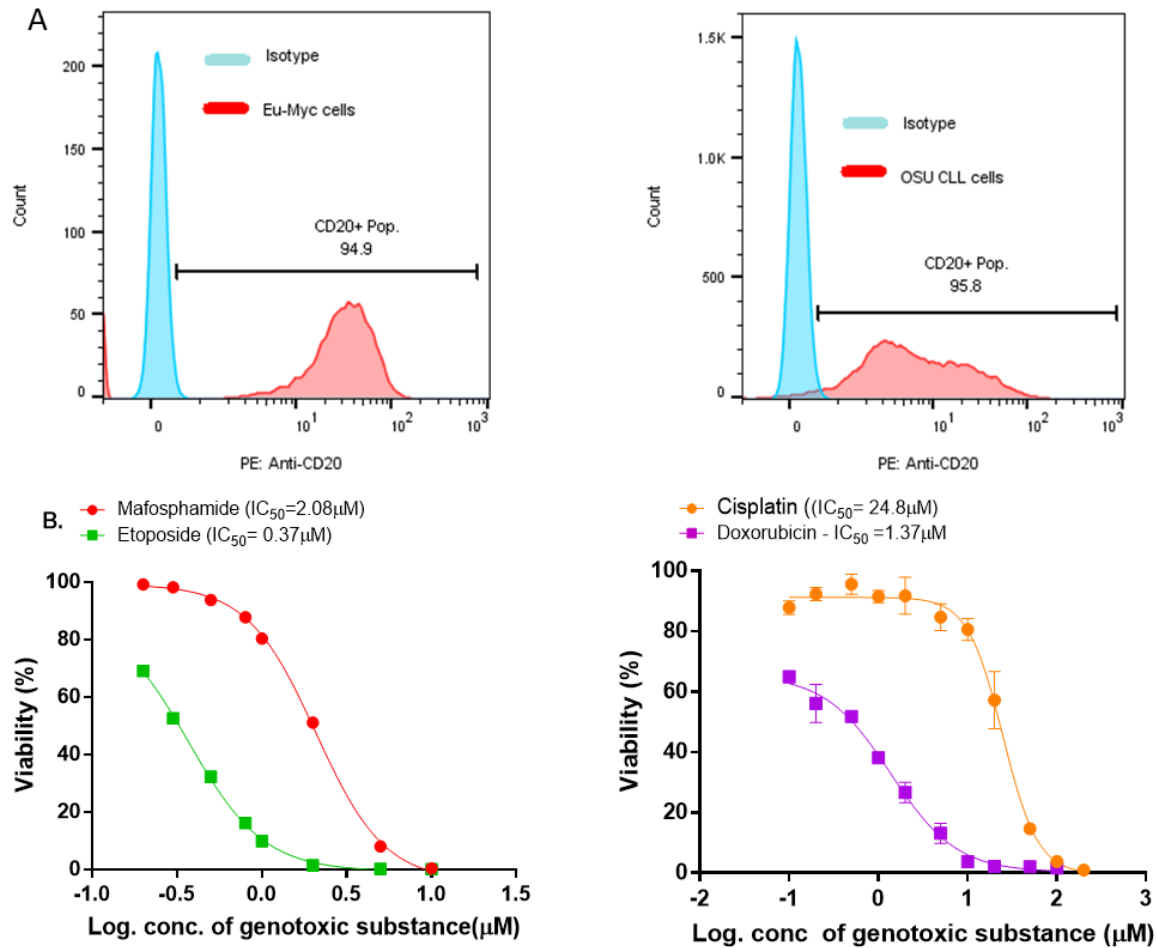


Figure 3: Characterization of E μ -Myc and OSU-CLL cell lines by CD20 antigen expression and sensitivity to genotoxic substances

- A. CD20 expression of E μ -Myc and OSU-CLL cell lines relative to their respective isotypes. Cells were stained with PE- anti-CD mAb and expression levels measured by flow cytometry.
- B. Sensitivity of E μ -Myc cell to selected genotoxic substances. Cells were seeded at 1×10^5 /well in triplicates and incubated with serial concentrations of genotoxic substance for 48hrs followed by AnnexinV/7-AAD staining and 10,000 events acquisition and enumeration by flow cytometry.

5.2.2 High Cd20 antigen expression of E μ -Myc cell is critical to genotoxic substance-induced ADCP

Following validation of CD20 antigen expression on E μ -Myc cells, a baseline antibody dependent cellular phagocytosis (ADCP) and antibody independent cellular phagocytosis (AICP) were performed with or without sub-lethal pretreatment of the cells with IC₂₀ concentration of mafosphamide or etoposide. In the absence of anti-CD20 antibody, the level of tumor cell phagocytosis was very similar in the untreated compared to genotoxic pretreated E μ -Myc cells (Figure 4, D) either when co-cultured with thioglycollate induced murine peritoneal macrophages (untreated vs mafosphamide pretreated; $p=0.137$, and untreated vs etoposide pretreated $p=0.179$), or J77.4A1 macrophage cell line (untreated vs mafosphamide pretreated; $p=0.145$, and untreated vs etoposide pretreated; $p=0.999$).

However, significant increases in the level of ADCP were observed in the presence of anti-CD20 antibody in genotoxic pretreated cells co-cultured with thioglycollate induced murine peritoneal macrophages ($p=0.016$ and $p=0.031$ for mafosphamide and etoposide pretreated cells respectively) (Figure 4A). Similarly, coculture experiments using J774.1A macrophage cell line as effector cells showed a significant ($p=0.010$) increase in ADCP of mafosphamide pretreated E μ -Myc cells compared to untreated cells (Figure 4C). Thus, the result in this E μ -Myc cells line model recapitulates similar results as reported in the Myc/BCL2 driven “double-hit” lymphoma hMB cell line model where it was shown that cyclophosphamide-Alemtuzumab combination lead to higher tumor cells phagocytosis (406).

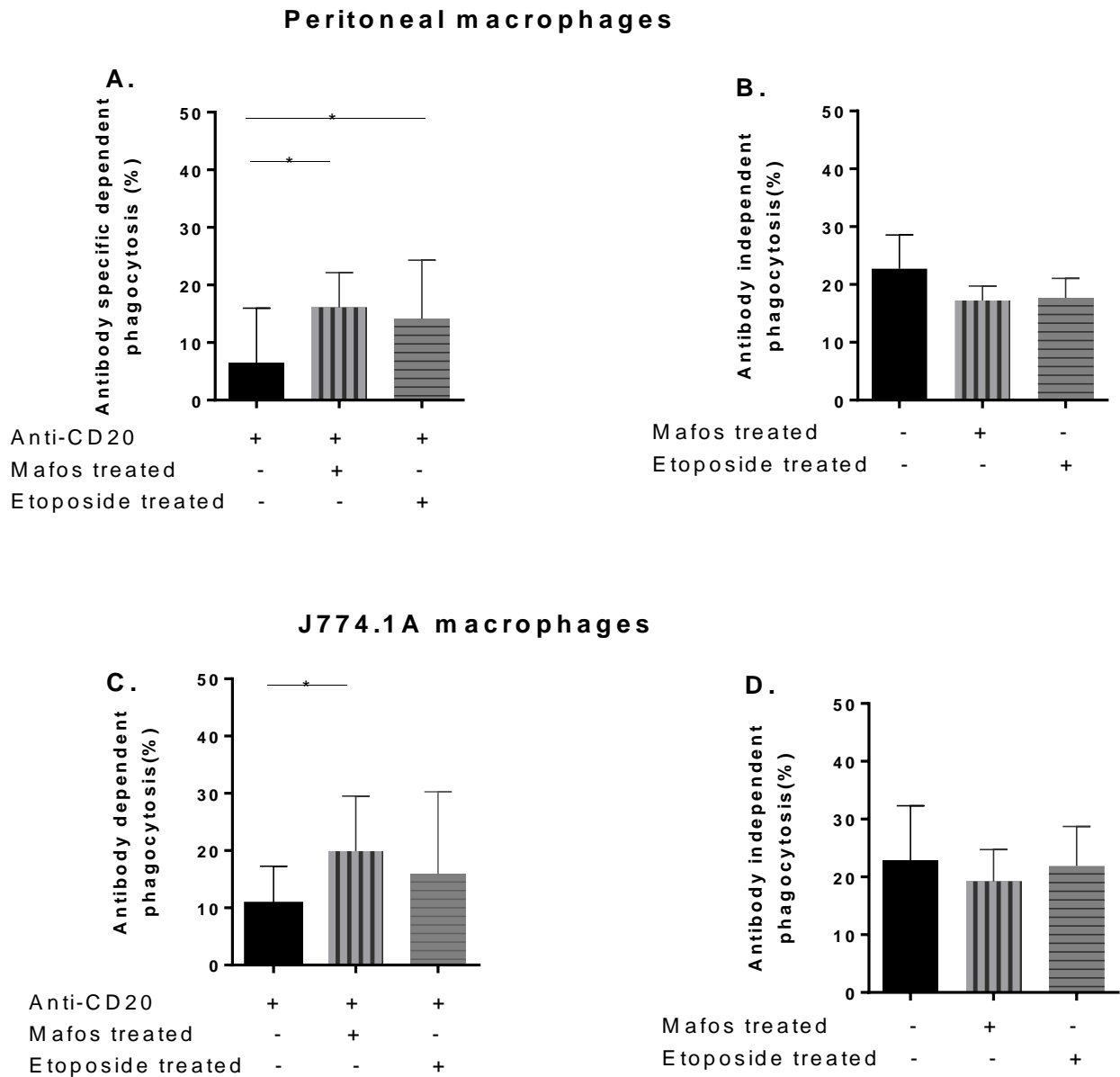


Figure 4: Genotoxic pretreatment of Eu-Myc cells induces a higher ADCP

A-D. Level of anti-CD20 mAb (18B12) mediated phagocytosis (A, C) and non-antibody mediated phagocytosis (B, D) of E μ -Myc cells cocultured with J774.1A and thioglycollate induced mouse peritoneal macrophages as effector cell. Anti-CD20 mAb (18B12) was used at optimal concentration of 10 μ g/ml. Remaining cells in antibody treated and untreated wells were enumerated by flow cytometry (n=3). (* = $p < 0.05$, ** = $p < 0.01$, *** = $p < 0.001$, **** = $p < 0.0001$).

5.2.3 E μ -Myc cells inappropriate for studying Fc-gamma-mediated phagocytosis due to in vitro loss of Cd20 expression

shRNA mediated-knockdowns (KD) of DNA damage response genes including p53, ATM, ATR, ATX, DNA-PK, p38, p21, CHK1, CHK2, MK2, Bim and Bak were generated in the E μ -Myc Burkitt's lymphoma cell line. The generated KD cells were used as a tool to elucidate the role of the DNA damage response genes in the interaction of tumor cells with macrophages in the tumor microenvironment. Following a series of coculture experiments to enumerate effects of KD genes under CIT including mono-treatment controls, a progressive loss of effect of anti-CD20 treatment was observed with the empty vector control cells. Irrespective of the effector cells used, the level of ADCP remained reduced in both untreated and mafosphamide pretreated E μ -Myc cells, abrogating the relevance of targeting CD20 antigen as a treatment option

(Figure 5A, B). This data shows that tumor cell killing by ADCP is ineffective when the antibody targeted molecule is under expressed.

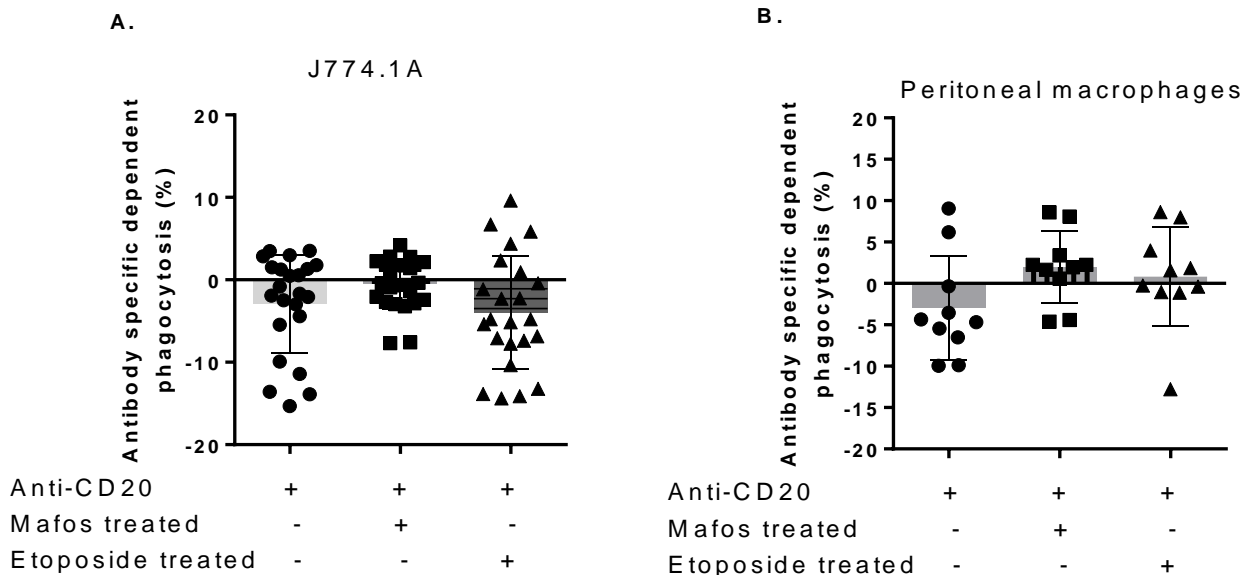


Figure 5: ADCP of Eu-Myc cells reduces in culture regardless of genotoxic pretreatment

A. Level of anti-CD20 mediated phagocytosis of E μ -Myc cells coculture with J774.1A macrophages. Anti-CD20 monoclonal antibody was used at final concentration of 10 μ g/ml in a 16hrs coculture system. Remaining cells in antibody treated and untreated wells were enumerated by flow cytometry (n=6).

- B. Level of anti-CD20 dependent phagocytosis of E μ -Myc cells coculture with thioglycollate derived peritoneal macrophages. Anti-CD20 monoclonal antibody was used at final concentration of 10 μ g/ml in a 16hrs coculture system. Remaining cells in antibody treated and untreated wells were enumerated by flow cytometry (n=3).

5.2.4 E μ -Myc cells show reduced Fc- γ mediated phagocytosis relative to other B-cells

Following loss of antibody-dependent phagocytosis of the E μ -Myc cells, the phagocytic ability of the effector cells were re-checked on the assumption that, intercellular engagement with tumor cells could induced effector cells exhaustion. Hence, CD19⁺ B cells were isolated from the spleens of C57BL/6J mouse (representing normal B-cells) and the T-cell leukemia-1 oncogene (TCL-1) transgenic mouse (representing B-CLL cells). J774.1A macrophages were cultured alone or in coculture with E μ -Myc cells, TCL-1 B-cells or normal CD19⁺ B-cells from C57BL/6J mouse for 16hrs. All B-cells were subsequently removed and effector J774.1A macrophages cocultured with Dyelight 488 fluorescent labeled beads for additional 16hrs and proportion of macrophages that have phagocytosed beads enumerated by flow cytometry.

Interestingly, the percentage of J774.1A macrophages that had phagocytosed Dyelight beads remained similar across all the pre-exposure conditions compared to J774.1A macrophages not pre-exposed to any B-cells (Figure 6A), suggesting J774.1A macrophages were not functionally exhausted to phagocytose despite exposures to different malignant B-cells and normal B-cells.

To assess whether J774.1A macrophages phagocytose the normal B-cells and different malignant B-cells to a similar extent through antibody dependent mechanism and non-antibody dependent /spontaneous mechanism, cocultures of J774.1A macrophages with E μ -Myc cells, TCL-1 cells or normal C57BL/6J mouse CD19⁺ B-cells were performed. The result revealed that, both malignant B-cells and normal B-cells were spontaneously/none Fc γ dependently phagocytosed to the same extent (Figure 6C). However, in the presence of anti-CD20 mAb, TCL-1 B-cells (p=0.0036) and CD19⁺ B-cells from normal C57BL/6J mouse (p=0.0004) were significantly phagocytosed by Fc γ dependent mechanism than E μ -Myc cells (Figure 6B).

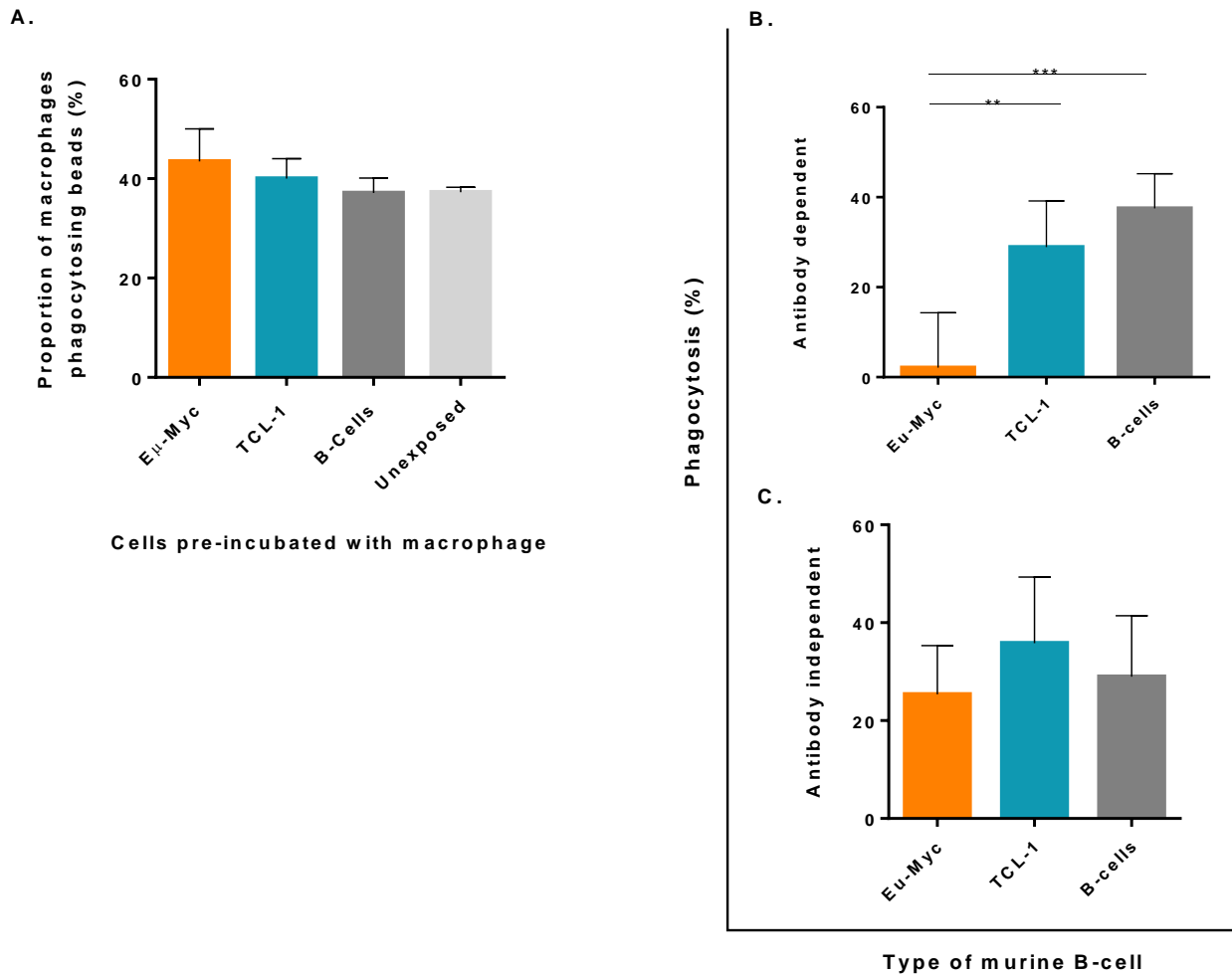


Figure 6: Eu-Myc cells show reduced Fc gamma mediated phagocytosis

- A. Proportion of J774.1A macrophages that had phagocytosed DyeLight beads. Macrophages were previously cocultured with either E μ -Myc cells, CD19⁺ splenic B-cells from TCL-1 mouse, CD19⁺ B-cells from normal C57BL/6J mouse or unexposed to any B-cells for 16hrs before coculture with beads (n=4).
- B. Level of anti-CD20 dependent phagocytosis of E μ -Myc cells, CD19⁺ splenic B-cells from TCL-1 mouse or normal C57BL/6J mouse coculture with J774.1A macrophages (n=2).
- C. Level of non-antibody dependent cellular phagocytosis (AICP) of E μ -Myc cells, CD19⁺ splenic B-cells from TCL-1 mouse or normal B-cells from C57BL/6J mouse coculture with J774.1A macrophages (n=2). (* = $p < 0.05$, ** = $p < 0.01$, *** = $p < 0.001$, **** = $p < 0.0001$).

5.2.5 E μ -Myc cells downregulate expression of CD20 antigens

In a treatment regimen approach that employs antigen specific targeting with a specific antibody, the expression levels and pattern of the antigen is critical to treatment outcomes. Hence, a direct re-assessment of CD20 expression of E μ -Myc empty vector cells in culture and a stored post-transduction aliquot were performed. Results revealed remarkable reduction of CD20 antigen expression from 73.4% (Figure 7A) post-transduction level to 13.2% (Figure 7B) of those in current culture. This was subsequently confirmed with Alexa Flour 488 conjugated Rat anti-murine mIgG2a antibody to opsonized anti-CD20 monoclonal antibody. Whereas splenic CD19+ B-cells of the TCL-1 mouse used as a positive control showed high levels of opsonized anti-CD20 antibody (Figure 7E), the E μ -Myc empty vector cells showed remarkably reduced opsonized anti-CD20 antibody (Figure 7D). Therefore the loss of opsonized anti-Cd20 mediated phagocytosis of tumor cells was as a result of loss of Cd20 antigen expression on tumor cells.

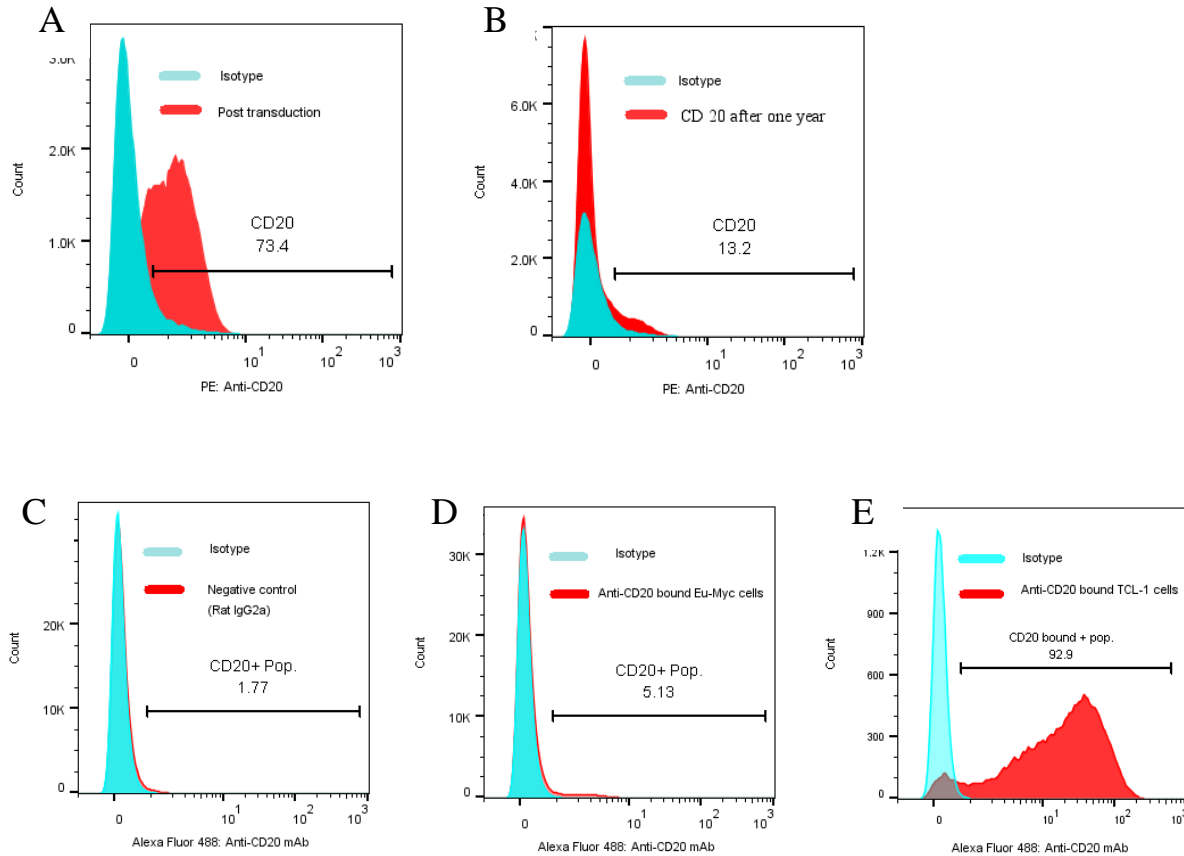


Figure 7: Suppressed Cd20 expression causes diminished anti-CD20 specific phagocytosis of $E\mu$ -Myc cells

- Level of CD20 antigen expression of $E\mu$ -Myc empty vector control cells in culture
- Level of CD20 antigen of post-transduction stored aliquot of $E\mu$ -Myc control cells
- Negative control showing background levels of $E\mu$ -Myc cells bound to Alexa-Fluor coupled rat anti-murine IgG2a antibody in the absence of anti-Cd20 antibody
- Proportion of $E\mu$ -Myc cells bound to anti-Cd20 antibody demonstrated by rat anti-murine IgG2a
- Proportion of CD19+ splenic B-cells from TCL-1 mouse bound to anti-Cd20 antibody demonstrated by rat anti-murine IgG2a antibody. Cell were pre-incubated with anti-CD20 mAb (IgG2a) for 3hrs, then unbound antibody washed completely before staining with Alexa-Fluor coupled rat anti-murine IgG2a antibody.

(* = $p < 0.05$, ** = $p < 0.01$, *** = $p < 0.001$, **** = $p < 0.0001$).

5.3 Characterization of Myloid Differentiation Primary Response Protein 88 (MyD88) cell line for functional genetic studies

Following loss of CD20 antigen expression that prevented further experiments with the Eu-Myc cell line, a search for a reliably robust replacement cell line model identified the MyD88 cell line as an alternative candidate. The MyD88 cell lines were derived from the MyD88 mouse model, generated by Cre-mediated recombinase conditional expression of MyD88p.L252P (the orthologous position of the human MYD88p.L265P mutation) in combination with conditional over-expression of BCL2 which drives clonal development of ABC-like subtype of diffuse large B-cells lymphoma(402). The MyD88 mouse model thus represents one of the few available models for studies of the highly aggressive, heterogeneous NHL sub-types with poor prognosis.

5.3.1 Baseline characteristics of Cd20 expression, genotoxic sensitivity, antibody dependent cellular phagocytosis (ADCP) and proliferation of MyD88 clones

Three of the five clones of cells generated from individual mouse of the Myd88 model (M191, M108 and M552) were screened for CD20 antigen expression (Figure 8A), baseline antibody depended cellular phagocytosis (ADCP) (Figure 8B), sensitivity to genotoxic substance (Figure 8C) and proliferation pattern over time (Figure 8D). Here, a greater percentage of cells of M552 clone expressed a higher level of Cd20 antigen (>90%) and proliferated at a double rate per hour compared to M191 sub-clone. However, M552 and M191 clones showed a marginal difference in ADCP, which does not pass statistical significance ($p=0.052$). Additionally, M552 sub-clone showed reduced sensitivity to mafosphamide ($IC_{50}=4.97\mu M$) compared to M191 ($IC_{50}=4.07\mu M$) and M108 ($IC_{50}=3.42\mu M$) sub-clones. Thus, among the three MyD88 cell line sub-clones assessed, M108 sub-clone was the least proliferative and most sensitive to mafosphamide. The level of baseline ADCP was significantly higher for both M191 ($p<0.0001$) and M552 ($p<0.0001$) compared to M108 sub-clone. Based on these initial results of this ABC-subtype model of diffuse large B-Cell lymphoma M552 sub-clone was selected for all further experiments.

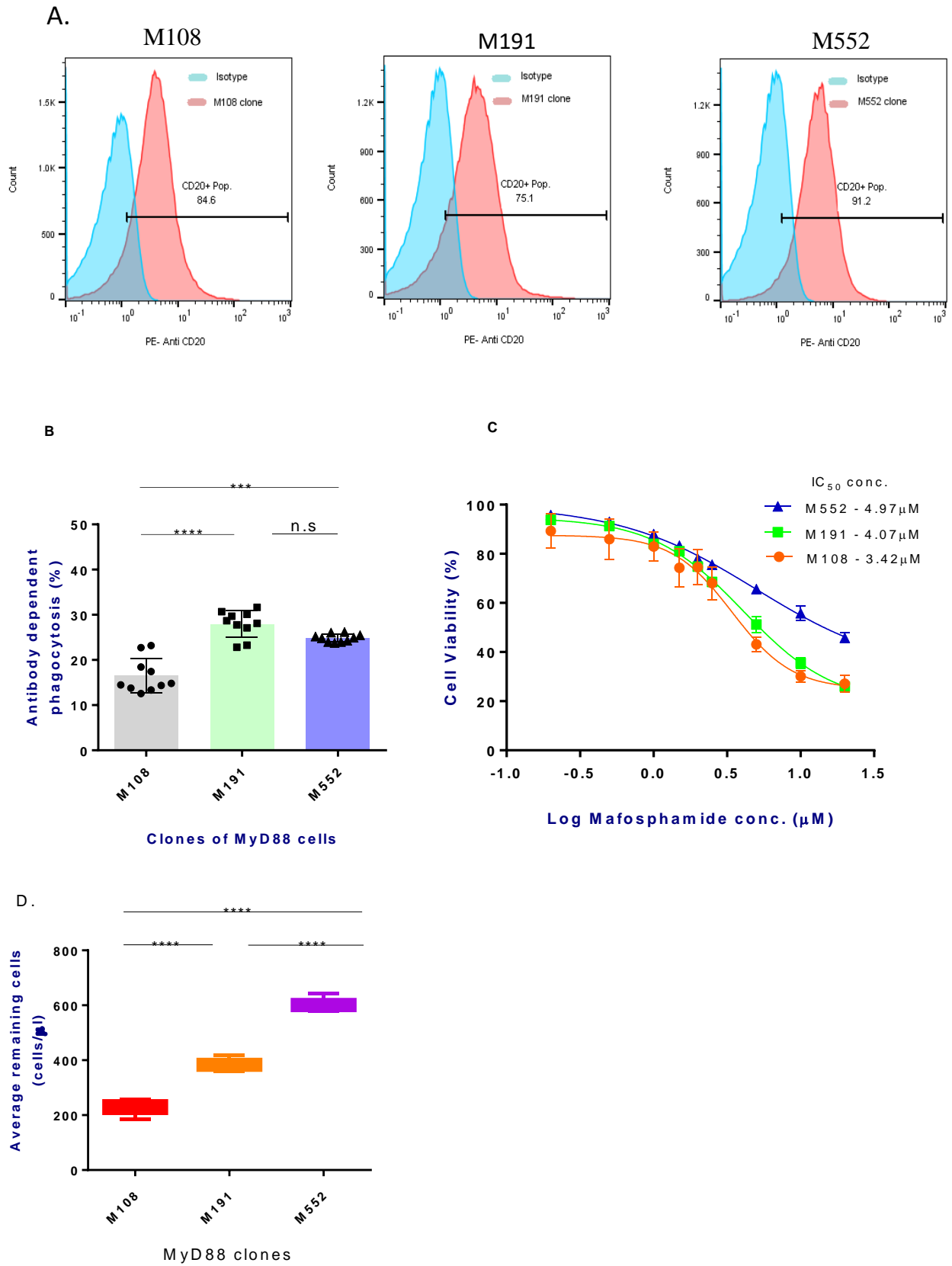


Figure 8: Baseline characterization of sub-clones of MyD88 cell line

- A. CD20 expression of MyD88 clones relative to respective isotypes. Cells were stained with PE-anti-CD20 mAb and expression levels measured by flow cytometry.
 - B. Level of anti-CD20 mAb (18B12) dependent phagocytosis of different MyD88 cell clones. Cells were cocultured at 37°C for 16hrs using J774.1A macrophages as effector cell with final optimum concentration of 18B12 monoclonal antibody of 50µg/ml for a final coculture volume of 225µl. Remaining cells in antibody treated and untreated wells were enumerated by flow cytometry (n=2).
 - C. Sensitivity of MyD88 clones to mafosphamide. Cells were seeded at 1×10^5 /well in triplicates and incubated with serial concentrations of mafosphamide for 48hrs followed by AnnexinV/7-AAD staining and 10,000 events acquisition and enumeration by flow cytometry.
 - D. Proliferation pattern of MyD88 clones. Cells were plated at 15×10^3 /100µl (i.e. 150 cells/ µl) and incubated at 37°C for 16hrs. Remaining cells were enumerated by flow cytometer (n=2)
- (* = $p < 0.05$, ** = $p < 0.01$, *** = $p < 0.001$, **** = $p < 0.0001$).

5.3.2 Genotoxic pretreatment increases phagocytosis of M552 cells under anti-CD20 treatment

To further characterize M552 clone of the MyD88 cell line, the sensitivity to the genotoxic component of the current front-line therapy, R-CHOP (Rituximab, cyclophosphamide, doxorubicin, vincristine and prednisone) and cisplatin was tested (Figure 9A). Tested as mono-genotoxic substances, mafosphamide exhibited the highest sensitivity to M552 cells ($IC_{50}= 4.25\mu M$). Doxorubicin, a DNA inter-calator that interrupt macromolecule biosynthesis by inhibition of topoisomerase II thereby inducing apoptosis exhibited low sensitivity ($IC_{50}= 9.21\mu M$) as well as etoposide $IC_{50}=14.84 \mu M$). On the other hand Cisplatin, a platinum-based anti-neoplastic agent which induces DNA damage through cross-linking by preferentially binding guanine residues showed very low sensitivity ($IC_{50}= 46.15\mu M$), whilst vincristine, an inhibitor of microtubule polymerization that interferes cell division at metaphase showed very poor sensitivity ($IC_{50}=$ never reached at $250 \mu M$).

In the Myd88 cell line model, the synergy of enhanced tumor cells phagocytosis following combined genotoxic substance/antibody treatment was recapitulated in cocultures with J774.1A macrophage, murine peritoneal macrophages and murine bone marrow derived macrophages (Figure 9B - D). In cocultures where J774.1A macrophages were used as effector cells, increased phagocytosis were observed with single agent treatments such as anti-CD20 mAb ($p=0.0001$), mafosphamide ($p=0.019$) compared to untreated. Mafosphamide pretreatment alone showed no significant advantage ($p=0.422$) over anti-CD20 monotreatment. However, combination of mafosphamide pretreatment with anti-CD20 mAb significantly increased tumor cell phagocytosis compared to anti-CD20 alone ($p=0.024$) and mafosphamide pretreatment alone ($p=0.0001$) (Figure 9B). In contrast to the result of J774.1A coculture, no significant change in tumor cell phagocytosis was observed in single treatment with anti-CD20 mAb ($p=0.884$) or mafosphamide pretreatment alone ($p>0.9999$) compared to untreated coculture when peritoneal macrophages were used as effector cells (Figure 9C). However, combined treatment with mafosphamide and anti-CD20 resulted in significant tumor cells phagocytosis compared to untreated ($p=0.0015$), anti-CD20 mAb alone ($p=0.0001$) and mafosphamide treatment alone ($p=0.0013$).

Similarly, in cocultures with feeder media differentiated mouse bone marrow derived macrophages, combination treatment of mafosphamide/anti-CD20 mAb induced significantly higher tumor cell phagocytosis ($p < 0.0001$ and $p = 0.0095$ respectively), compared to either anti-CD20 mono-treatment or mafosphamide mono-treatment. However, as observed in peritoneal macrophage cocultures, phagocytosis of tumor cells treated with single agents such as anti-CD20 ($p = 0.6070$) and mafosphamide alone ($p = 0.1781$) did not significantly differ from the untreated coculture (Figure 9D). This data show that genotoxic stress induces a synergy with anti-Cd20 antibody treatment to promote enhanced macrophage mediated tumor cells killing.

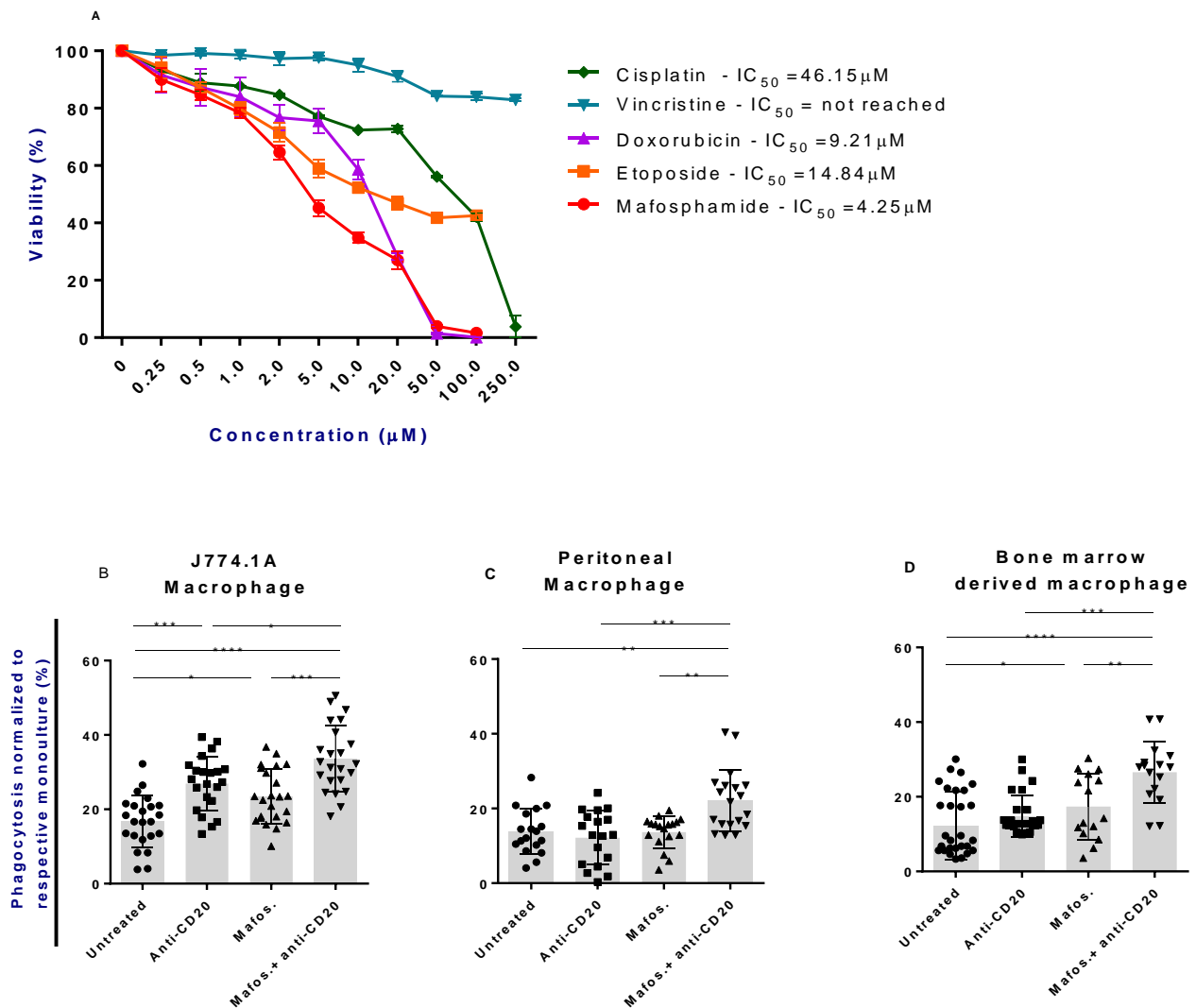


Figure 9: Characterization of M552 cell line by genotoxic agents and phagocytic patterns in coculture with different murine macrophages

- A. Toxicity assay of M552 clone of MyD88 cell line following treatment with serial dilutions of different genotoxic agents. Cells were plated at 1×10^5 /well in triplicates and incubated with serial concentrations of genotoxic agents for 48hrs followed by AnnexinV/7-AAD staining and 10,000 events acquisition and enumeration by flow cytometry.
- B-D. Phagocytosis of M552 cell line untreated or pretreated with different agents in coculture system with J774.1A cell line (n=5) (B), thioglycollate derived murine (n=4) (C) or feeder media differentiated bone marrow derived murine macrophages (n=4) (D). Cocultures were incubated at 37°C for 16hrs and remaining tumor cells enumerated by flow cytometry. Mafosphamide pretreatment of cells was carried out with IC₂₀ Concentration (1.64μM ie. determined from a 48hrs toxicity assay) for 12hrs while anti-CD20 antibody concentration of 50μg/ml was used. (* = $p < 0.05$, ** = $p < 0.01$, *** = $p < 0.001$, **** = $p < 0.0001$).

5.3.3 Generation and characterization of M552 cell line with knockdown of DNA damage response genes

Genotoxic substances function by inducing DNA damage which triggers the DNA damage response system (DDR). DDR comprises a complex network of DNA damage sensors and initiators that recruit repair machinery to damage site, halt the cell cycle by activating cell cycle checkpoint kinases, and initiate repair of damage DNA or commit cells to senescence or apoptosis when damage is irreparable in order to maintain genome stability.

Having observed that combination of genotoxic substance and anti-CD20 significantly increased macrophage phagocytosis of tumor cells, further work focused on the role of DNA damage response genes in the macrophages-tumor cells interactions in the tumor microenvironment and identify critical gene(s) in the DDR pathway which functionally mediate this interaction. Thus, shRNA mediated knockdowns (KD) of major DNA damage response genes, including p53, ATM, ATR, ATX, DNA-PK, p38, p21, CHK1, CHK2, MK2, Bim and Bak in M552 clone of MyD88 cell line was performed. The KD efficiency of the generated cell lines were assessed by western blot analysis (Figure 10). Subsequently, generated KD cell were further characterized (Figure 11- Figure 12).

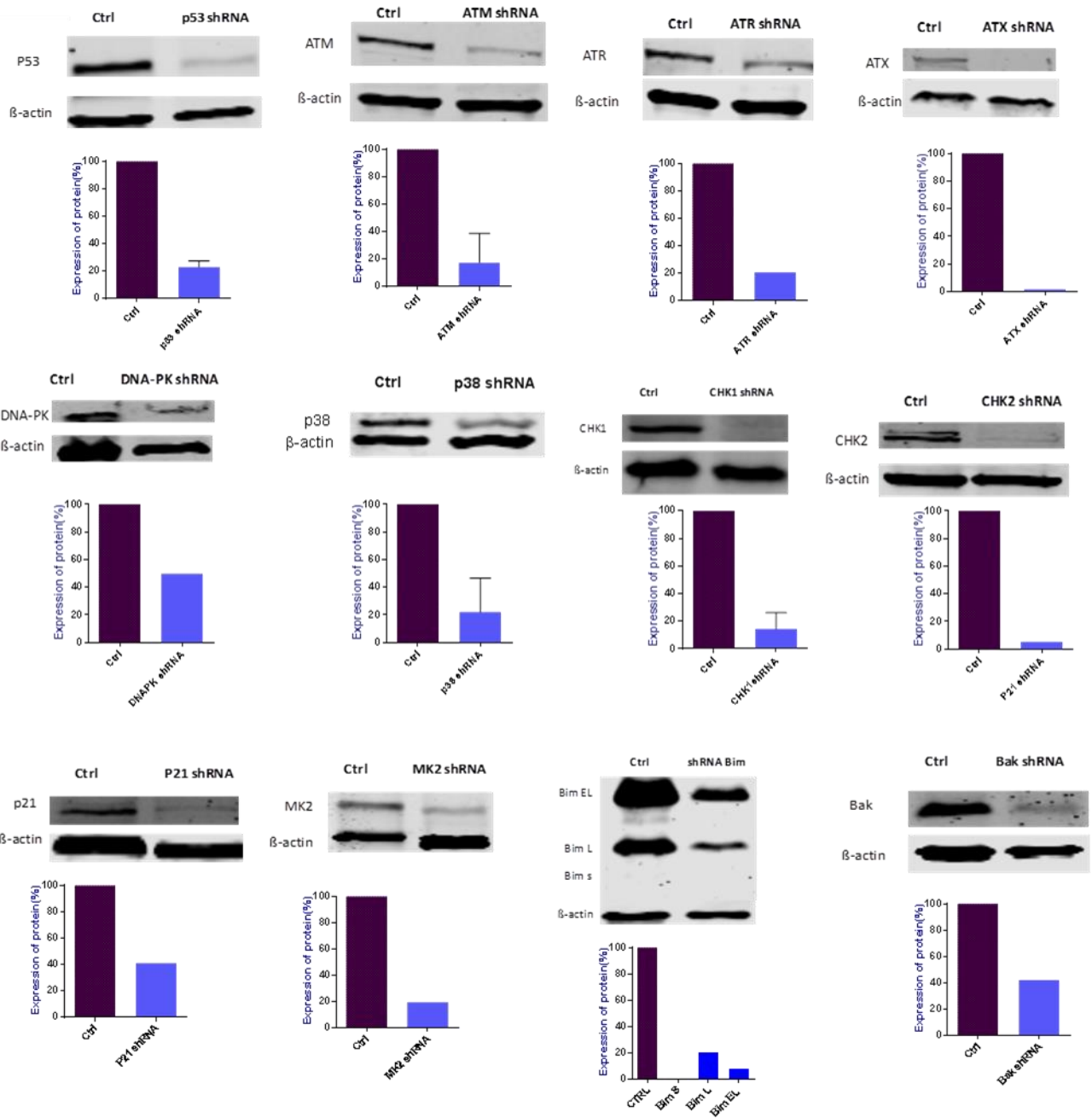


Figure 10: Efficiency of shRNA mediated knockdowns of DNA damage response genes in M552 clone cell

Assessment of knockdown efficiency of M552 lines by Western blot analysis. Protein expressions of KD genes are normalized to cellular β -actin and that of empty vector control (n=2-3). A representative blot of each protein is shown.

5.3.4 Knockdown of DNA damage response genes changes proliferation pattern of M552 cells

Generally, KD of DDR genes lead to changes in the proliferative rates of some KD cells. In the untreated state for instance, significantly high proliferation rates occur for DNA-PK ($p < 0.0001$) and CHK1 ($p < 0.0001$), whereas significantly low proliferation rates were observed with p38 ($p < 0.0001$), CHK2 ($p = 0.0342$), MK2 ($p = 0.0001$), Bim ($p < 0.0001$) and Bak ($p < 0.0001$) in comparison to the empty vector control (MLP). Genotoxic stress of M552 KD cells with mafosphamide influenced cellular proliferation for some KD genes. For instance, mafosphamide pretreated DNA-PK and CHK1 KD cells maintained significantly higher proliferation rates ($p = 0.0259$ and $p < 0.0001$ respectively) compared to pretreated empty vector cells whereas P38 ($p < 0.0001$) and MK2 ($p = 0.0169$) showed a reduced proliferation rate relative to the empty vector control (Figure 11A). In both untreated and genotoxic stressed states, DNA-PK and CHK1 KD cells showed the highest proliferative rates (Figure 11B). P38 and Bak KD cells were the least proliferative in the untreated state.

Mafosphamide pretreatment significantly reduced the proliferation rate of some KD cells such as empty vector control cells (MLP-Ctrl) ($p = 0.0003$), ATM ($p = 0.0002$), ATX ($p = 0.0012$), DNA-PK ($p < 0.0001$), CHK1 ($p < 0.0001$) and CHK2 ($p = 0.0332$) KD cells compared to their untreated counterparts. Expectedly, for p53, ATR, p38, p21, MK2, Bim and Bak KD cells, genotoxic pretreatment did not significantly alter their proliferation rate compared to their untreated cells. However, KD cells of CHK2, Bim and Bak that showed an initial low proliferation rate to the empty vector control subsequently attained similar proliferative rate as the control cells upon genotoxic treatment indicating a better survival of these cells harboring DDR KDs upon genotoxic agent mediated DNA damage compared to control cells with intact DDR mechanism. Together, this data shows that downregulation of some genes in the DDR pathway affects cellular proliferation.

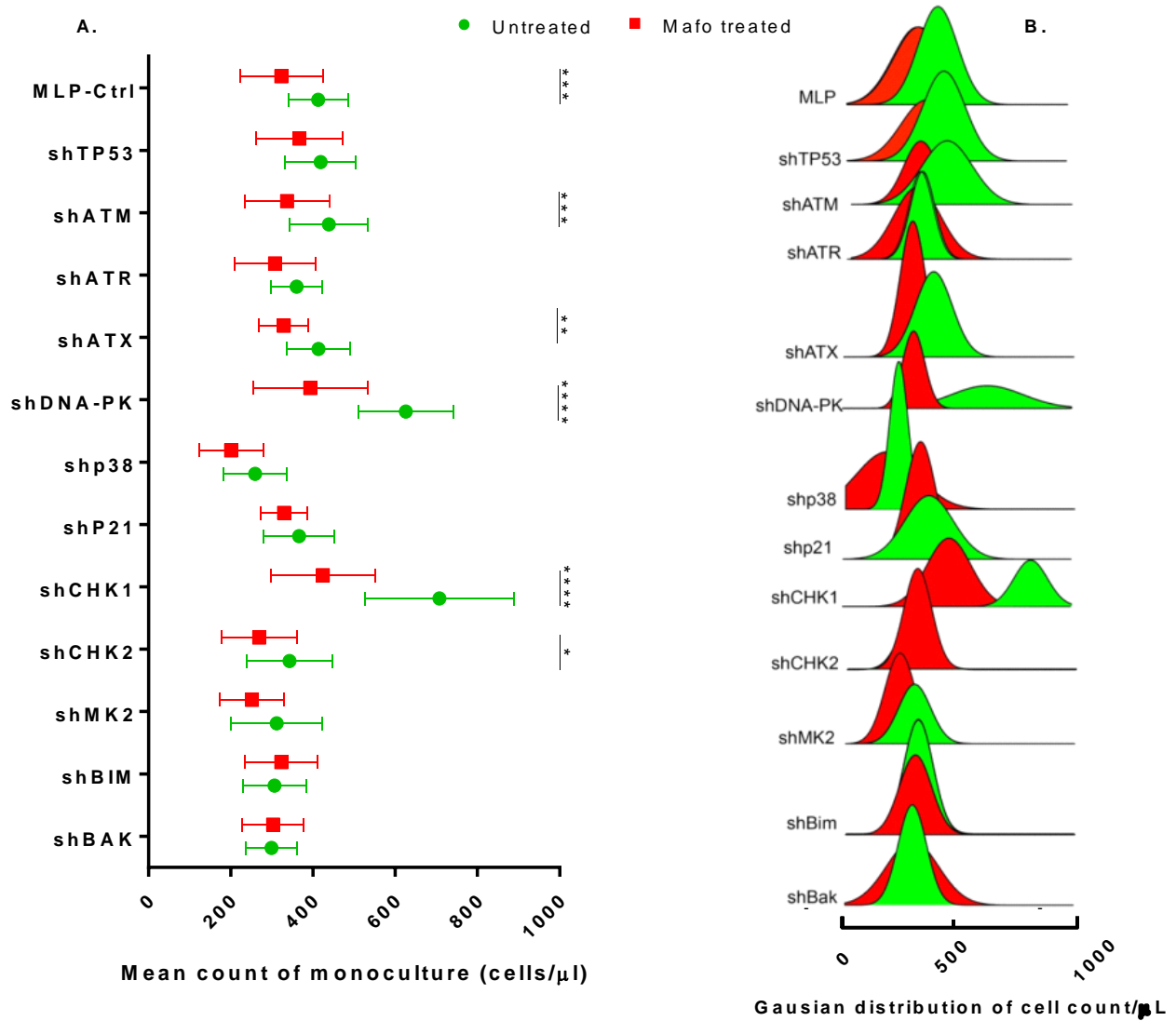


Figure 11: Proliferation pattern of untreated and mafosphamide pretreated M552 KD cells

A. Proliferation pattern of untreated (green) and mafosphamide pretreated (red) M552 KD cells. Sub-lethal pretreatment was induced with IC₂₀ concentration of mafosphamide for 12hrs followed by monoculture incubation for 16hrs. Remaining cells after incubation were enumerated by flow cytometry.

B. Gaussian distributed histogram generated by transformation of absolute cell counts (n=8).

(* = $p < 0.05$, ** = $p < 0.01$, *** = $p < 0.001$, **** = $p < 0.0001$).

5.3.5 Knockdown of DNA damage response genes alter sensitivity of M552 cells to genotoxic treatment

Previous experiments revealed that parental M552 cell line showed reduced sensitivity to a number of genotoxic substances tested from the current frontline combinatory treatment regimen (Figure 9A). Mafosphamide (cyclophosphamide) a component of the current frontline treatment regimen for DLBCL showed the strongest cytotoxicity to M552 cell line. Thus, we opted to test the chemo-sensitivity of generated M552 DDR genes KD cells with mafosphamide which is also the selected genotoxic agent to induce genotoxic stress in our subsequent experiments. Overall, KD of DDR genes resulted in considerable variations in the sensitivity of the generated KD cells to mafosphamide (Figure 12). Two main groups based on the chemo-sensitivity of the DDR gene KD cells were observed.

In the first group, KD of the particular DDR genes significantly increased chemo-resistance of the cells to mafosphamide-induced cytotoxicity compared to the empty vector control. This group include p53 ($IC_{50} = 12.51$, $p=0.0001$), ATM ($IC_{50} = 15.29$, $p<0.0001$), ATX ($IC_{50} = 8.66$, $p=0.0450$), p21 ($IC_{50} = 11.22$, $p=0.0006$), MK2 ($IC_{50} = 27.75$, $p<0.0001$) and Bim ($IC_{50} = 9.90$, $p=0.0051$).

In the second group which include ATR ($IC_{50} = 7.78$, $p=0.1963$), DNA-PK ($IC_{50} = 4.76$, $p=0.9968$), p38 ($IC_{50} = 7.0$, $p=0.5708$), CHK1 ($IC_{50} = 3.87$, $p=0.6899$), CHK2 ($IC_{50} = 4.88$, $p=0.9993$) and Bak ($IC_{50} = 7.86$, $p=0.1728$), gene KD did not significantly alter chemo-sensitivity of the KD cells to mafosphamide compared to the empty vector control cells.

Among the generated KD cells, CHK1, CHK2 and DNA-PK KD cells were the most sensitive to mafosphamide. Interestingly, of the six M552 KD cells associated with significantly increased resistance to mafosphamide induced cell death, four (p53, ATM, p21 and Bim) are involved in the major pathways mediating p53 transcriptional activity that culminates in cell cycle arrest and senescence induction or non-transcriptional activity that include mitochondria translocation and apoptotic induction through interaction with MCL-1, BCL-2 and Bcl-XL to free-up Bim for subsequent interaction with Bax/Bak.

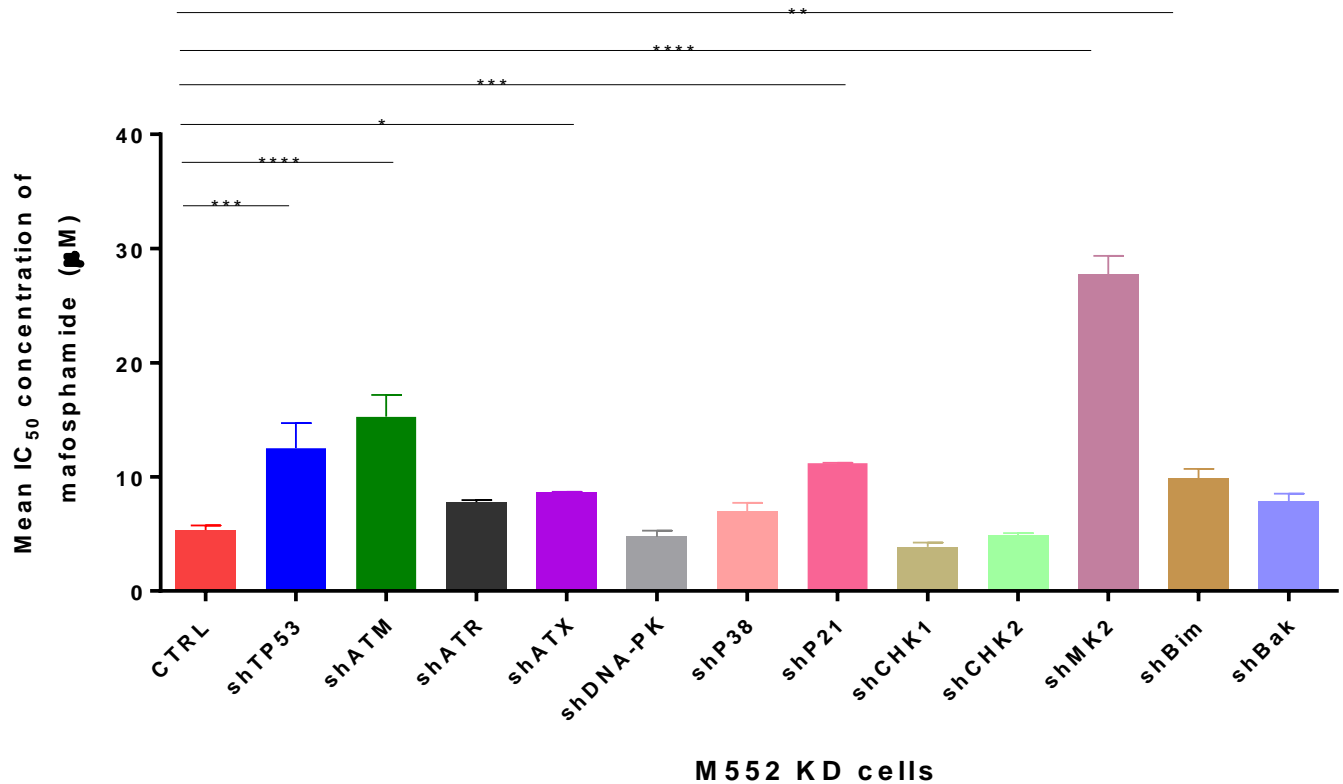


Figure 12: Sensitivity of M552 cell lines harboring DDR genes KD to mafosphamide

Sensitivity of generated DDR genes KD M552 cell lines to mafosphamide. Cells were plated at 1×10^5 /well in triplicates and incubated with serial concentrations of genotoxic agents for 48hrs followed by AnnexinV/7-AAD staining and 10,000 events acquisition and enumeration by flow cytometry. Result presented as mean IC₅₀ concentrations of replicate experiments (n=3)

(* = $p < 0.05$, ** = $p < 0.01$, *** = $p < 0.001$, **** = $p < 0.0001$).

5.4 Genes in DNA damage response pathway are crucial for effective tumor cell phagocytosis

To decipher the role of DDR genes in the context of tumor cell phagocytosis, the validated M552 KD lines were cocultured with thioglycollate induced murine peritoneal macrophages (Figure 13), murine bone marrow derived macrophages (BMDM) (Figure 14) and murine cell line J774.1A macrophage (Figure 34, Appendix). In all cases, phagocytosis was determined by normalizing remaining cells in the coculture to that of the respective corresponding monoculture after 16hrs of incubation. This was done to correct for the differences in proliferation rates between different KD cells and also to eliminate direct cytotoxic effect of mafosphamide in cocultures involving the use of sub-lethally stressed KD cells. The determined phagocytosis of the KD cells were then normalized to that of the empty vector control (shCtrl) to obtain the change in phagocytosis as a result of the effect of the KD gene.

5.4.1 Phagocytic function of peritoneal macrophage is impaired by knockdown of critical DNA damage response genes in tumor cells

Macrophages are professional phagocytes and express a plethora of receptors to engage phosphatidylserine and other “eat me” molecules either directly or through tethering molecules to mediate non-opsonized phagocytosis. Additionally, macrophages serve as one of the major effectors of antibody-mediated therapies due to their expression of all types of fragment crystallizable – gamma (Fc- γ) receptors whose engagement with Fc domain of an antibody, triggers phagocytosis of antibody opsonized cells (409). To understand the effect of DDR gene downregulation on phagocytosis in this disease model in the context of non-opsonized and antibody opsonized system, generated DDR KD tumor cells were cocultured with murine peritoneal macrophages with addition of anti-CD20 mAb (18B12). A heatmap overview (Figure 13A) shows two major clusters based on tumor cell treatment. Mafosphamide-stressed tumor cells cocultures, clustered (columns) away from treatment naive tumor cell cocultures. Thus suggesting that mafosphamide impacts the phagocytic process in the coculture. Untreated and anti-CD20 treated DDR gene knockdown tumor cells showed a general decline in phagocytosis albeit, not significantly different ($p>0.05$) from that of empty vector control cells (Figure 13B). However, KD of p38 gene substantially reduced

phagocytosis of untreated cells ($p=0.0009$, Figure 13D) and anti-CD20 mAb treated cells ($p<0.0001$, Figure 13E) compared to their respective empty vector controls. To understand the role of DDR genes in tumor cells phagocytosis upon genotoxic treatment, DDR genes KD cells were sub-lethally pretreated with mafosphamide, a precursor of activated cyclophosphamide - an alkylating agent that induces DNA damage.

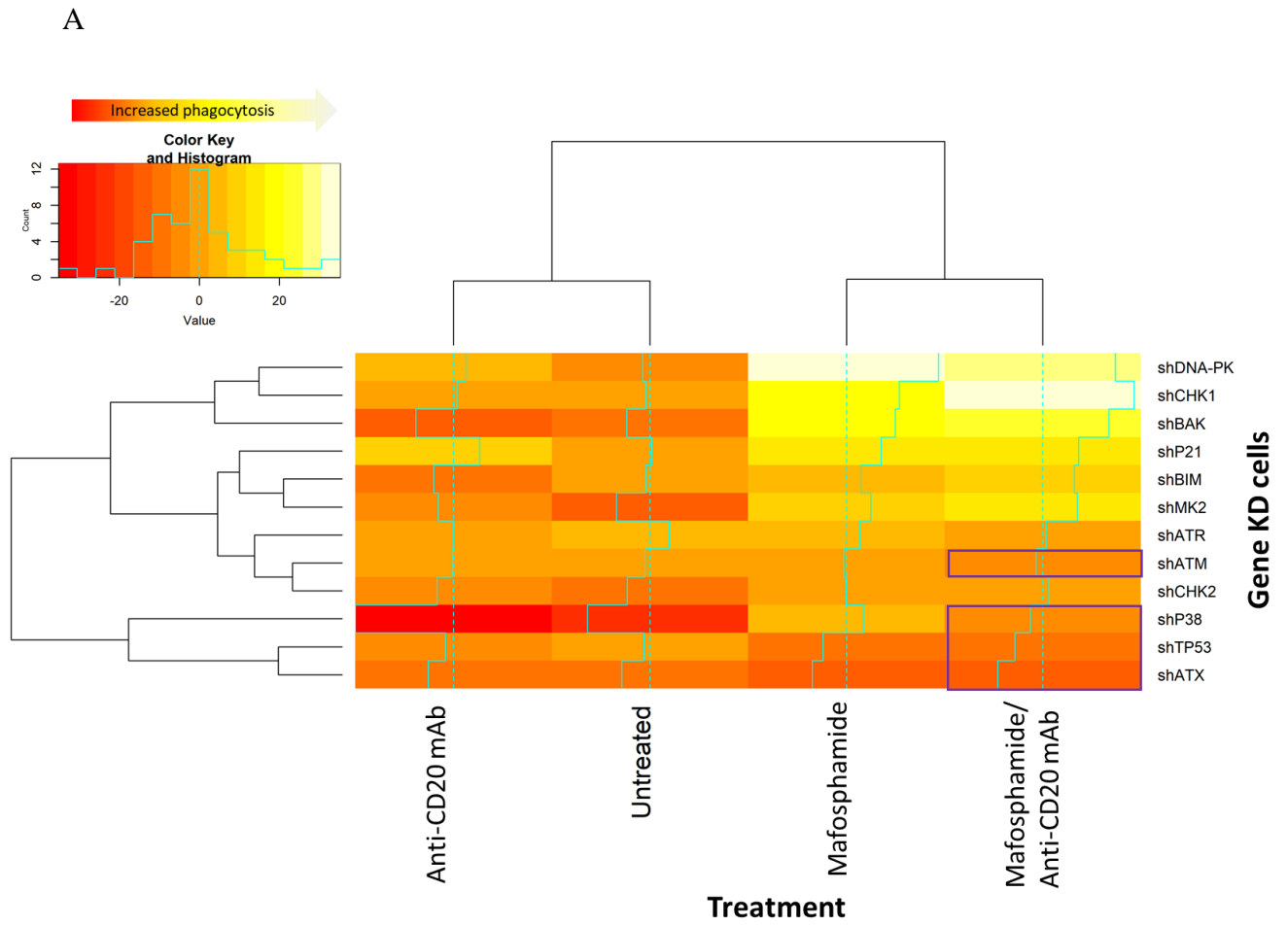
Here, a sharp dissipation of microenvironment support and an increase in phagocytosis for KD cells of p38 ($p=0.0061$), Bak ($p=0.0406$) and DNA-PK ($p<0.0001$) (Figure 13H) was observed compared to their respective treatment naive KD cells. However, only mafosphamide treated DNA-PK KD cells were significantly phagocytosed ($p=0.0034$) compared to mafosphamide treated control cells (Figure 13F).

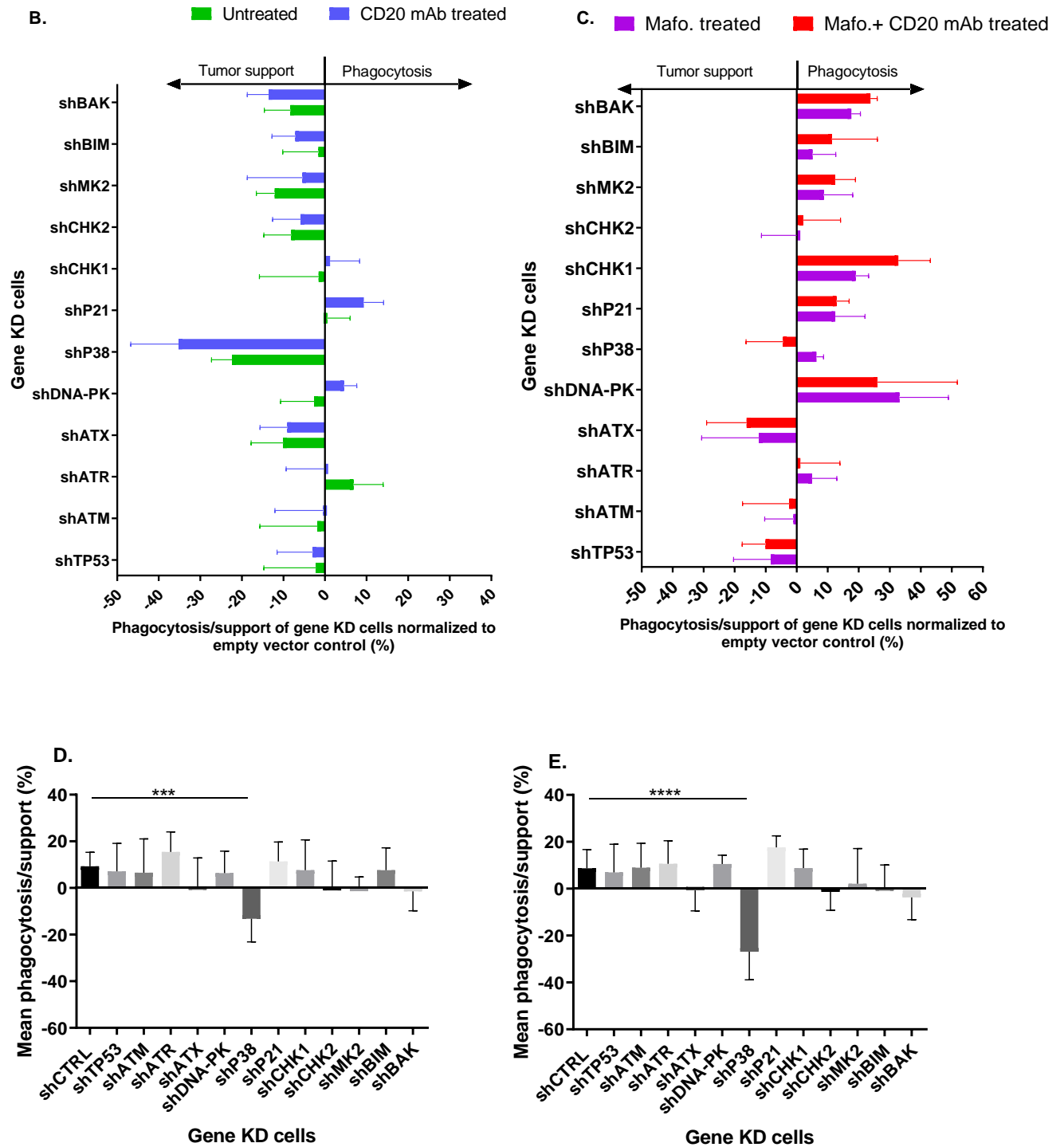
Interestingly, whilst mafosphamide treatment enhanced phagocytosis of most DDR gene KD tumor cells, phagocytosis of some KD cells such as ATX, p53 and ATM remained persistent low regardless of treatment (Figure 13C).

Having previously observed significantly increased phagocytosis of the empty vector cells upon treatment with mafosphamide-anti CD20 combination in coculture system involving peritoneal, bone marrow derived and J774.1A cell line macrophages (Figure 9B-D), we wondered whether chemo-immunotherapeutic (CIT) combination could circumvent the reduced phagocytosis observed with the aforementioned KD cells. Subsequently, DDR gene KD cells were sub-lethally treated with mafosphamide and cocultured with macrophages with addition of anti-mouse anti-CD20 mAb (18B12). Here, tumor cells' phagocytosis was significantly influenced by which DDR gene is knockeddown ($p<0.0001$) rather than mafosphamide pretreatment alone or in combination with anti-CD20 mAb ($p=0.4106$).

CIT-treated KD cells of p53 ($p=0.0168$) and ATX ($p=0.0276$) were significantly less phagocytosed than CIT-treated empty vector control cells (Figure 13G). On the other hand, whilst CIT-treatment further enhanced phagocytosis of Chk1 KD tumor cells ($p=0.0108$), a persistently reduced antibody dependent cellular phagocytosis trend was observed for p38 and ATM KD cells although, these were not statistically significant (Figure 13I).

Thus, downregulation of p53 and ATX genes in the M552 ABC- subtype of DLBCL impair efficient tumor cells' phagocytosis by macrophages regardless of treatment with mafosphamide and/or in combination with anti-CD20 monoclonal antibody.





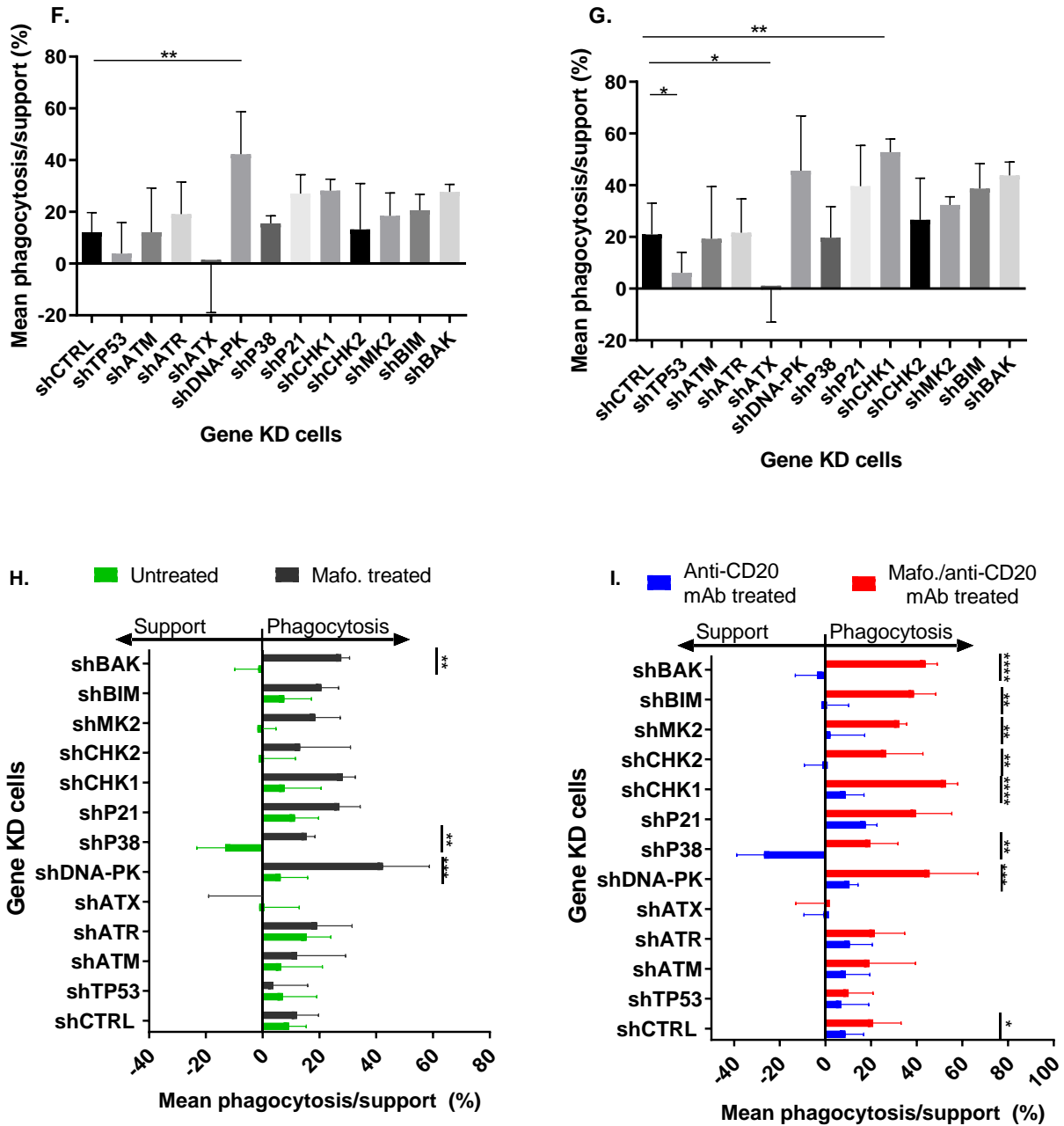


Figure 13: Critical genes in DDR regulate phagocytosis of tumor cells by peritoneal macrophages

A. Overview of phagocytosis pattern of M552 KD cells coculture with thioglycollate induced mouse peritoneal macrophages under different treatment conditions. Treatment conditions are presented in columns and KD genes are presented in rows on the heatmap. Color key depicts from the extreme left, reduced phagocytosis (deep red) to the opposite end increased phagocytosis (faded yellow). Broken green line represent empty vector control (shCTRL) cells

and the histogram indicate quantitatively, average percentage phagocytosis of all biological replicates of particular KD cell normalized to the empty vector control. The black box in the mafosphamide-anti-CD20 combination treatment highlights identified DDR genes mediating treatment resistance/refractory in this model (n=7).

- B-C. Detailed quantitative presentation of M552 KD cells coculture with thioglycollate induced peritoneal macrophages under different treatment conditions. Cocultures were performed without treatment (green), anti-CD20 monotherapy (blue), mafosphamide pretreatment of cells using IC₂₀ concentration (purple) and mafosphamide pretreatment in combination with anti-CD20 mAb (red). Phagocytosis of the KD cells in all conditions are normalized to the respective empty vector (shCTRL) control cells (n=7).
- D. Bar chart of average spontaneous phagocytosis of DDR gene KD cells coculture with mouse peritoneal macrophages (n=7)
- E. Bar chart of average antibody-dependent cellular phagocytosis of DDR gene KD cells coculture with mouse peritoneal macrophages (n=7)
- F. Bar chart of average spontaneous phagocytosis of mafosphamide treated DDR gene KD cells coculture with mouse peritoneal macrophages (n=7)
- G. Bar chart of average anti-CD20/mafospamide treated phagocytosis of DDR gene KD cells coculture with mouse peritoneal macrophages (n=7)
- H. Bar chart of average spontaneous phagocytosis of untreated and mafosphamide treated DDR gene KD cells coculture with mouse peritoneal macrophages (n=7)
- I. Bar chart of average antibody-dependent cellular phagocytosis of anti-CD20 treated verses mafosphamide/anti-CD20 combinaion treated DDR gene KD cells coculture with mouse peritoneal macrophages (n=7).

(* = $p < 0.05$, ** = $p < 0.01$, *** = $p < 0.001$, **** = $p < 0.0001$).

5.4.2 Similar DDR genes regulate tumor cells phagocytosis in primary macrophages from different anatomic compartments

Different anatomic compartments are known to present different challenges to the efficacy of therapeutic treatments in cancer. Again, due to differentiation procedures (in vivo for elicited peritoneal macrophages and ex vivo for bone marrow derived macrophages), macrophages from different anatomic niches may engage different genetic programs and respond differently to similar treatment conditions (410). It was therefore asked if the observed effect of identified KD genes is replicable in cocultures using different macrophages from different body compartment. Thus, similar coculture experiments of M552 KD cell lines with mouse bone marrow-derived macrophages (BMDM) were performed.

5.4.3 Knockdown of identified DDR genes impair phagocytic capacity of Bone Marrow-Derived Macrophages

Here, levels of non-opsonized tumor cell phagocytosis of untreated KD cells with BMDM (Figure 14) revealed a general reduction in phagocytosis of all KD cells compared to empty vector control (Ctrl) cells, except for ATM KD cells which were highly phagocytosed than the control ($p=0.0077$). Particularly, ATX ($p=0.0044$), Bim ($p<0.0001$) and Bak ($p<0.0001$) KD cells induced significant impairment in phagocytosis. BMDM remained significantly less phagocytic to anti-CD20 mAb treated KD cells including ATX ($p=0.0003$), Bak ($p<0.0001$) and ATR ($p=0.0412$) KD cells in comparison to the empty vector control cells with exception of ATM KD cells which were more phagocytosed than the anti-CD20 treated control cells ($p=0.0028$). Additionally, we compared the level of phagocytosis for each KD cells in the untreated state with its anti-CD20 treated cocultures to assess the impact of anti-CD20 monotherapy. Anti-CD20 induced increase in phagocytosis of Bim ($p<0.0001$), MK2 ($p=0.0047$), p38 ($p=0.0047$) and p53 ($p=0.0241$) KD cells however, the levels of phagocytosis were low compared to that of empty vector control cells (Figure 14A).

Mafosphamide stressed KD cells coculture with BMDM, showed a sharp increase of phagocytosis (Figure 14C) particularly for Bak, CHK2 and ATR KD cells although only CHK1 KD cells reach statistical significance compared to empty vector control ($p=0.0117$). Similar to the observation in cocultures with peritoneal macrophages, there was selective reduction of phagocytosis of certain DDR KD cells including p53, ATM, ATX, p38 and Bim under genotoxic treatment (Figure 14C) which persist under combined mafosphamide/anti-CD20 treatment with exception of ATM KD cells.

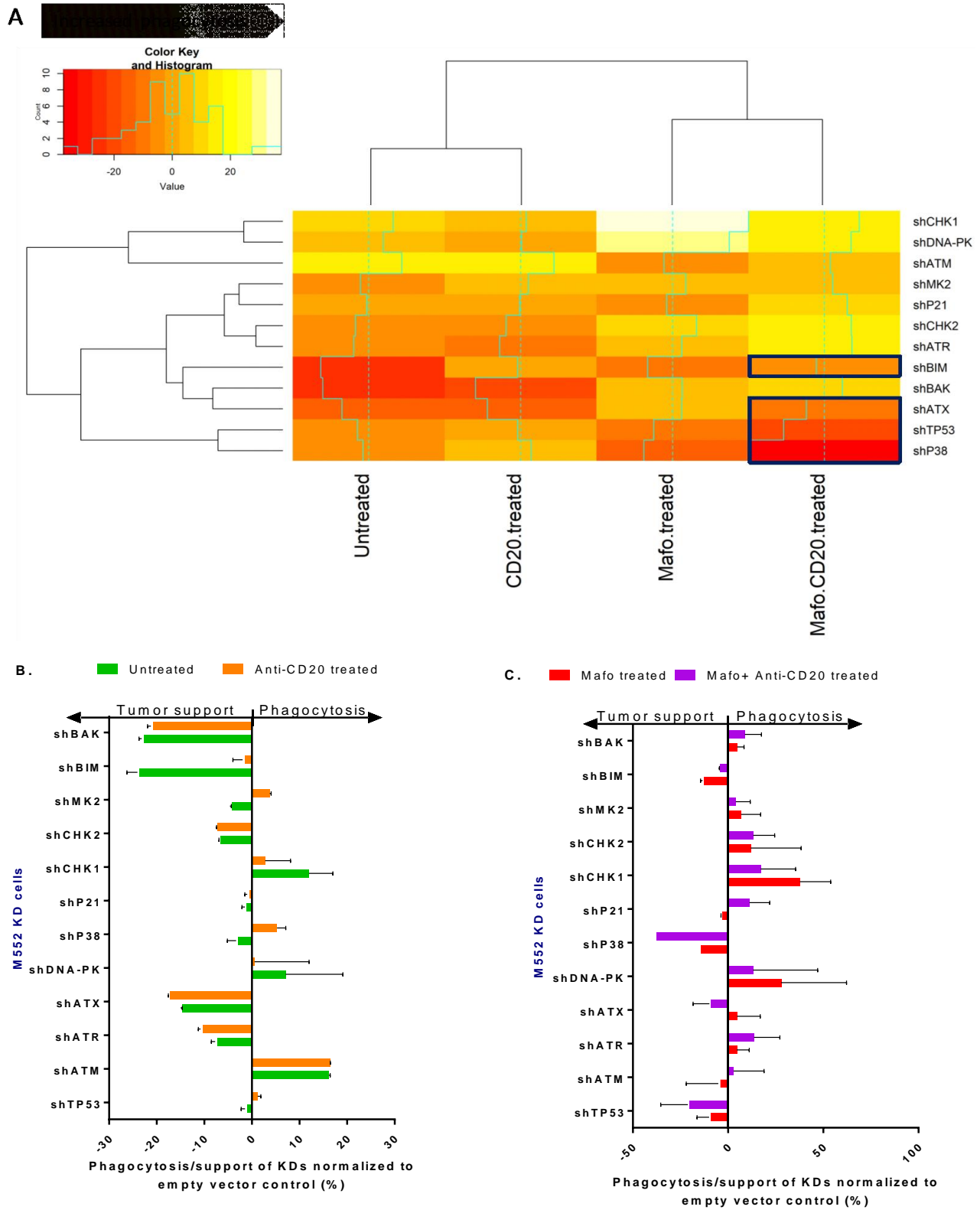


Figure 14: DDR genes regulation of tumor cells phagocytosis by DDR genes in coculture with by Bone marrow derived macrophages

- A. Overview of phagocytosis pattern of M552 KD cells coculture with feeder media differentiated mouse bone marrow macrophages under different treatment conditions. Treatment conditions are presented in columns and KD genes are presented in rows on the heatmap. Color key depicts from the extreme left, reduced phagocytosis (deep red) to the opposite end increased phagocytosis (faded yellow). Broken green line represent empty vector control (shCtrl) cells and the solid stepped lines indicate quantitatively, average phagocytosis of all biological replicates of particular KD cell normalized to the empty vector control. The black box in the mafosphamide-anti-CD20 combination treatment highlights identified DDR genes mediating treatment resistance/refractory in this model (n=3).
- B-C. Detailed quantitative presentation of M552 KD cells under different treatment conditions coculture with feeder media differentiated mouse bone marrow macrophages. Cocultures were performed without treatment (green), anti-CD20 monotherapy (yellow) (B), mafosphamide pretreatment of cells using IC₂₀ concentration (red) and combination of mafosphamide - anti-CD20 mAb (purple) (C). Phagocytosis of the KD cells in all conditions are normalized to the respective empty vector control cells (n=3).

5.4.4 Downregulation of DDR genes also influence phagocytic capacity of J774.1A macrophage cell line

In addition to the primary macrophages, cell line macrophages have proven useful in unraveling mechanisms in cancer biology despite inherent variations from primary cells (411). To ascertain if identified DDR genes KD cells show similar phagocytic pattern in coculture with J774.1A macrophage cell line, cocultures of J774.1A macrophage with M552 KD cells were carried-out. Non-opsonized phagocytosis of untreated DDR KD cells varied insignificantly from that of empty vector control. Similarly, phagocytosis of anti-Cd20 opsonized KD cells did not significantly differ from that of the empty vector. Thus, anti-CD20 alone did not significantly change the levels of phagocytosis of KD cells (Figure34B - Appendix). On the other hand, treatment with mafosphamide as a monotherapy or in combination with anti-CD20 resulted in modest increase in phagocytosis of ATM, DNA-PK, CHK1, Bim and Bak KD cells relative to that of anti-CD20 mono-treatment (Figure34C). Mafosphamide mono-treatment increased phagocytosis of some KD cells but failed to do same for ATX, p38, MK2, CHK2 and p53 KD cells where phagocytosis appeared markedly impaired. Amongst the impaired phagocytosed KD cells, p38 downregulation induced the strongest

impairment to mafosphamide mono-treatment ($p=0.0010$) and combined mafosphamide/anti-CD20 treatment ($p=0.0278$).

In brief, p38 and ATX downregulation in tumor cells impair phagocytosis of primary macrophages from the peritoneum and bone marrow. The observed effect is persist with and without chemotherapeutic or chemo-immunotherapeutic treatment of the tumor cells. Genotoxic treatment with mafosphamide or in combination with anti-Cd20 mAb promote phagocytosis of some tumor cells with knockdown of DDR genes but selectively favours survival of p53 and ATM KD cells which show impaired phagocytosis.

5.4.5 Peritoneal, bone marrow-derived and J774.1A macrophages show shared DDR genes dependencies in phagocytosis of tumor cells with downregulated DDR genes

Macrophages as tissue dwelling immune cells that differentiate from extravasated monocytes into different anatomical regions are influenced by the resident microenvironment milieu. Those such as BMDM which are differentiated outside their normal biologic environment may affect their sensitivity and responses. Although cell line macrophages are more homogenous, they always have a malignant background which presents experimental risk of significant bias.

To ascertain if any of the DDR genes knockdowns in tumor cells exert a common effect on phagocytosis despite the individual differences within macrophages, cocultures of different macrophages with M552 KDs under different treatment conditions were examined.

Cocultures of macrophages with unstressed KD cells showed that, 50% of the 12 KD genes were associated with reduced phagocytosis in peritoneal macrophages compared to 83% in J774.1A and 75% in Bone marrow derived macrophages. Stressing KD cells with sub-lethal mafosphamide pretreatment resulted in 41.7% being less phagocytosed by both peritoneal and BMDM macrophages and 33.3% less phagocytosed by J774.1A macrophages. In cocultures of unstressed KD cells, P38, MK2, ATX, CHK2 and Bak KD cells were less phagocytosed by all macrophages (Figure 15A) whereas p53 and p38 KD cells were less phagocytosed by all macrophages under genotoxic stress with sub-lethal mafosphamide pretreatment (Figure 15C). Also, unstressed p53 and Bim KD cells were less phagocytosed by BMDM and J774.1A macrophages but not peritoneal macrophages whereas unstressed p21 KD cells were less phagocytosed by the primary macrophages (peritoneal and BMDM) (Figure 15A).

Without genotoxic stress, ATM, DNA-PK and CHK1 KD cells were less phagocytosed by J774.1A macrophages only whereas, ATR KD cells were less phagocytosed by BMDM. Under genotoxic stress of sub-lethal mafosphamide, preferentially reduced phagocytosis of particular KD cells were observed for CHK2 KD in the case of peritoneal macrophages, MK2 for J774.1A macrophages and p21 and Bim in the case of BMDM. Under genotoxic stress, ATM KD reduced phagocytosis by both peritoneal and BMDM macrophages whereas ATX KD reduced phagocytosis of both peritoneal and J774.1A macrophages (Figure 15C). The trend suggests that upon genotoxic stress, two major functions of p53 play a role: trans-activation of the apoptotic machinery as well as its reciprocal interaction with p38 may be required for response to exogenous and endogenous stimuli / cytokine release and are centrally relevant for recognition and phagocytosis of tumor cells.

Anti-CD20 monotherapy alone was associated 75% reduction in phagocytosis of DDR KD cells by J774.1A macrophages (Figure 15B) compared to 33% when mafosphamide/anti-CD20 combination is used (Figure 15D). Furthermore, 50% of KD genes reduced phagocytosis of peritoneal macrophages compared to 33% with mafosphamide/anti-CD20 combination and 41.7% KD genes reduced phagocytosis of BMDM macrophages compared 33% with the combination. KD of ATX, CHK2 and Bak genes mediated reduced phagocytosis in all macrophage cocultures treated with anti-CD20 mAb alone whereas p38 and ATX reduced phagocytosis in all macrophages under combination treatment. As observed from coculture of unstressed KD cells with J774.1A macrophages (Figure 15A), ATM, DNA-PK and CHK1 KDs preferentially reduced anti-CD20 dependent cellular phagocytosis of J774.1A macrophages whereas MK2 and CHK2 showed similar effect under combination of genotoxic stress/anti-CD20. Under both anti-CD20 alone and combination with mafosphamide, Bim KD reduced phagocytosis of BMDM whereas p53 reduced phagocytosis in both BMDM and peritoneal macrophages.

Overall, these results show that phagocytic activity of macrophages are impaired when tumor cells harbor functional defective DNA damage response genes.

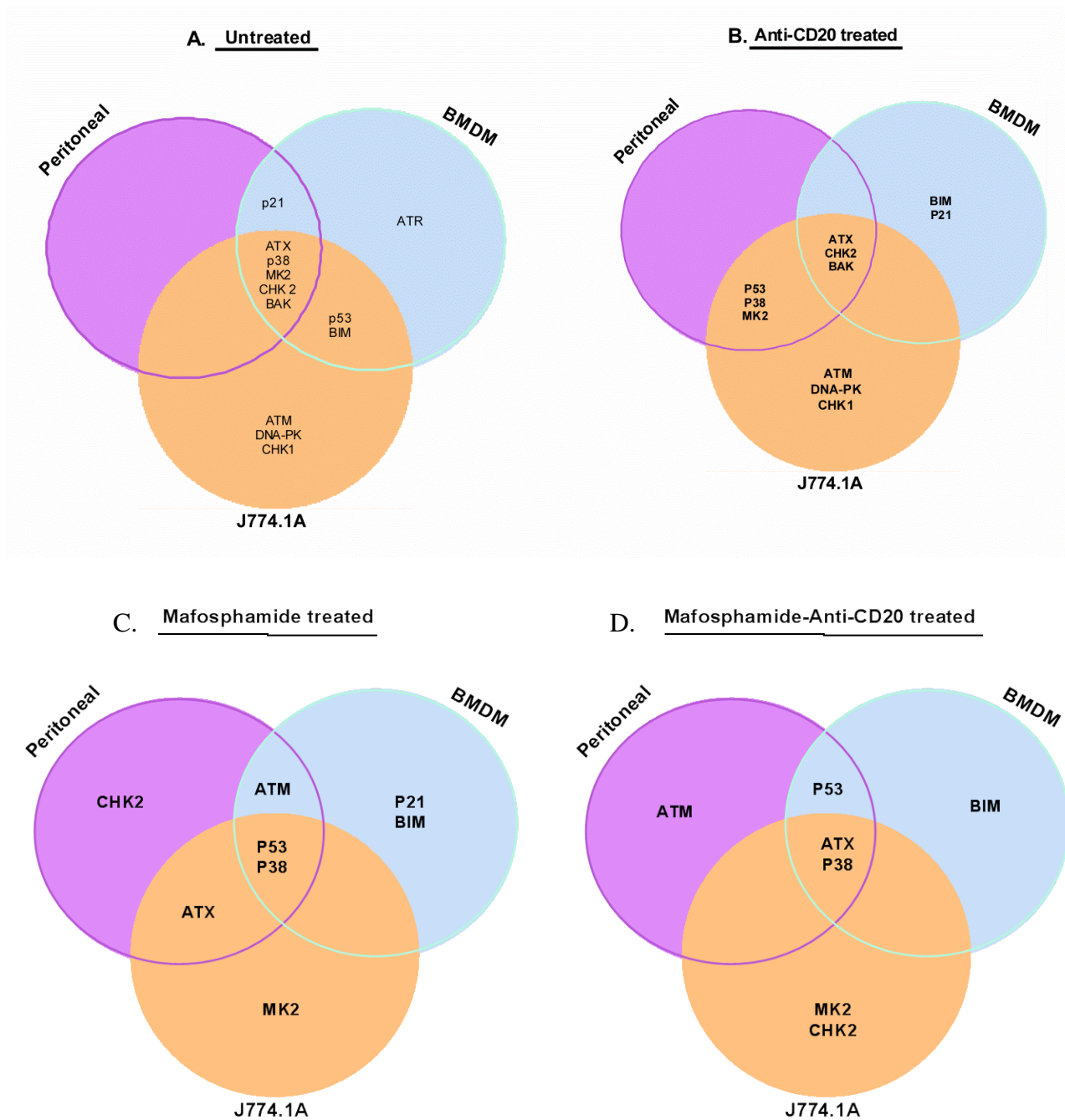


Figure 15: Pattern of phagocytosis of DDR KD M552 lymphoma cells of mouse peritoneal, bone marrow and J774.1A macrophages under different treatment condition.

- Distribution of untreated M552 KD cells less phagocytosed in cocultures with peritoneal, bone marrow derived and J774.1A macrophages.
- Distribution of M552 KD cells less phagocytosed in cocultures with peritoneal, bone marrow derived and J774.1A macrophages under anti-CD20 mAb treatment.

- C. Distribution of mafosphamide stressed M552 KD cells less phagocytosed in cocultures with peritoneal, bone marrow derived and J774.1A macrophages. Genotoxic stress was induced with sub-lethal pretreatment with IC₂₀ concentration of mafosphamide.
- D. Distribution of mafosphamide stressed M552 KD cells less phagocytosed in cocultures with peritoneal, bone marrow derived and J774.1A macrophages under anti-CD20 mAb treatment. Genotoxic stress was induced with sub-lethal pretreatment with IC₂₀ concentration of mafosphamide.

*Levels of phagocytosis of KD cells in each case are normalized to that of respective empty vector control cells.

5.4.6 Abrogation of critical DDR genes impair phagocytosis through changes in functional effects of cellular secretome (conditioned media)

Phagocytosis is a complex process influenced by the phenotype of both the target and the effector cells. Macrophages are critical innate sentinel cells crucial to phagocytosis. Macrophages express diverse receptors such as: the mannose receptor that recognizes conserved sequences on targets; complement receptors relevant for non-specific opsonized targets; and Fcγ - receptors that mediate specific immunoglobulin opsonized phagocytosis. On the other hand, whilst stressed target cells could induce their elimination by expression of phosphatidylserine (“eat me” signal, flips to the outer membrane and represents a marker for early apoptosis), tumor cells could mount resistance to immune phagocytic attack through expression of several immune checkpoint receptors such as, CD47 (don’t eat me signal), programmed cell death ligands 1 and 2 (PD-L1/2), CD200 and cytotoxic T lymphocyte antigen 4 (CTLA4). The complexities regarding phagocytosis are further compounded by secretion of a plethora of soluble factors by tumor cells capable of functionally modulating macrophages.

Considering the fact that heterogeneity exists in the treatment outcomes under the current R-CHOP frontline treatment for DLBCL, attention was focused on the KD genes identified to mediate impaired phagocytosis under anti-CD20/mafosphamide combination. Here, an understanding of the mechanisms through which some DDR KD genes impair phagocytosis was sought. Thus, the functional effect of the secretome of less phagocytosed KD cells in comparison to that of empty

vector control cells were investigated. DDR gene knockdown and control cells sub-lethally stressed with mafosphamid were cocultured with thioglycollate induced peritoneal macrophages in the secretome (generated from conditioned media [CM]) of mafosphamide stressed empty vector control cells with or without addition of anti-CD20 mAb antibody treatment.

Here, the secretome of mafosphamide stressed control cells restored phagocytosis of DDR gene KD cells and in some instances even induced significantly higher levels of anti-CD20-dependent phagocytosis of resistant KD cells such as p53 ($p=0.0345$), ATM ($p=0.0144$) and p38 ($p=0.0083$) compared to that of empty vector control cells (Figure 16A). Similarly, secretome of mafosphamide stressed empty vector control cells increased the level of phagocytosis in the absence of anti-CD20 treatment to levels, comparable to the empty vector control for p53 ($p=0.3778$), ATM ($p=0.2889$), ATX ($p=0.8474$) and p38 ($p=0.3321$) compared to the control cells (Figure 16B). Thus, contrary to impaired phagocytosis of the DDR genes KD cells in regular coculture media earlier observed (Figure 13C); the secretome of mafosphamide stressed control cells with intact DDR genes restores phagocytosis suggesting a critical role of the DNA damage response genes in phagocytosis through modulation of the composition of cellular secretome under genotoxic stress.

The observed tendency of secretome of control cells to rescue poorly phagocytosed DDR gene KD cells was confirmed. Here, mafosphamide-stressed empty vector control cells were cocultured with peritoneal macrophages in secretome of poorly phagocytosed KD cells. Whilst unstressed empty vector control cells were cocultured with macrophages in secretome of mafosphamide-stressed control cells. In this setup, two possible outcomes were anticipated. First, the secretome of poorly phagocytosed KD cells could inhibit phagocytosis of mafosphamide-stressed control cells or second, mafosphamide-stressed control cells would continually release secretome to induce phagocytosis, overriding any effects of the secretome from poorly-phagocytosed KD cells.

In line with the second expectation, mafosphamide stressed control cells showed similar anti-CD20 dependent phagocytosis levels in cocultures of secretome from poorly-phagocytosed DDR KD cells (p -values for P53= 0.0021, ATX = 0.1282, ATM =0.0553 and p38= 0.7835) compared to that of empty vector control cells (Figure 16C). Interestingly, the level of anti-CD20 dependent phagocytosis of control cells cocultured in secretome of mafosphamide stressed p53 KD cells were significantly higher ($p=0.0021$) than that in secretome of control cells. A similar trend of

phagocytosis was observed in the absence of anti-CD20 treatment (Figure 16D). Compared to earlier observation where identified DDR gene KD cells showed reduced phagocytosis in cocultures (Figure 13 and Figure 14), this series of experiments confirm that cellular secretome in the presence of intact DNA damage response system such as that of the control cells functionally differ from the secretome of poorly- DDR phagocytosed KD cells. Importantly, this observation suggests that DNA damage response mechanism mediates tumor cell phagocytosis by macrophages.

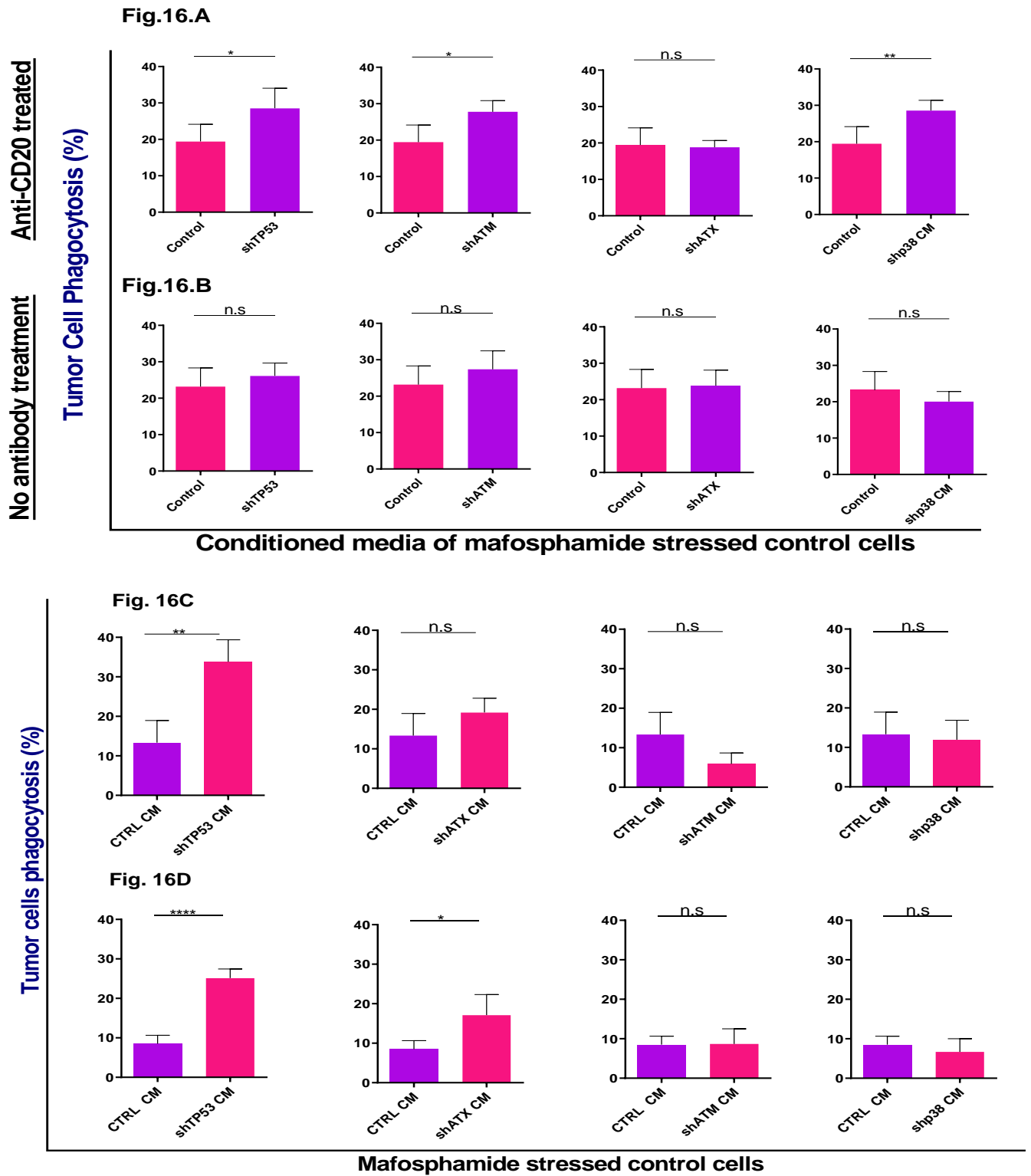


Figure 16: Secretome of control cells with functional DDR restores phagocytosis of DDR KD cells

-
- A. Level of antibody dependent cellular phagocytosis of mafosphamide-stressed DDR gene KD cells cocultured with peritoneal macrophages in secretome of mafosphamide-stressed empty vector control cells. Degree of phagocytosis of each KD cell is compared to that of control cells (n=3).
- B. Level of antibody independent cellular phagocytosis of mafosphamide-stressed DDR gene KD cells cocultured with peritoneal macrophages in secretome of mafosphamide-stressed empty vector control cells. Degree of phagocytosis of each KD cell is compared to that of control cells (n=3).
- C. Level of antibody dependent cellular phagocytosis of mafosphamide-stressed empty vector control cells cocultured with peritoneal macrophages in secretome of identified KD cells (n=2).
- D. Level of antibody independent cellular phagocytosis of mafosphamide pretreated empty vector control cells cocultured with peritoneal macrophages in secretome of identified KD cells (n=2).
- (* = $p < 0.05$, ** = $p < 0.01$, *** = $p < 0.001$, **** = $p < 0.0001$, n.s = not significant).

5.4.7 Genotoxic stress orchestrates DNA damage response gene-mediated secretory phenotype in tumor cells

Results from the preceding experiments suggest that, in the presence of a functional DDR, the secretory phenotype is orchestrated upon genotoxic stress. To validate this assumption, empty vector control cells (CTRL) were used as target cells in phagocytosis assay where they were split into two groups. One group remained untreated whilst the other was sub-lethally pretreated (stressed) with mafosphamide. The control cells were subsequently cocultured with peritoneal macrophages in the secretome of mafosphamide-stressed poorly-phagocytosed KD cells. In such an experimental setup, it was expected that genotoxic stressed control cells would progressively release secretome that would bolster phagocytosis compared to the untreated control cells despite the effect of the secretome from the DDR gene KD cells.

Expectedly, mafosphamide-stressed control cells showed significantly higher anti-CD20 dependent cellular phagocytosis compared to their untreated counterparts when cocultured in CM of control cells ($p = 0.0004$), CM of p53 KD cells ($p = 0.0008$), CM of ATM KD cells ($p = 0.0003$), CM of ATX KD cells ($p < 0.0001$) and CM of p38 KD cells ($p = 0.0007$) (Figure 17C).

Furthermore, unstressed CTRL cells were significantly phagocytosed when cocultured in CM of p53 KD cells ($p=0.0149$) and p38 KD cells ($p=0.0002$) compared to CM of CTRL cells. Contrarily, CM of ATX KD cells significantly inhibited phagocytosis of unstressed CTRL cells ($p<0.0001$) whereas CM of ATM KD cells showed similar effect on phagocytosis as CM of unstressed CTRL cells ($p=0.6948$) (Figure 17A). However, upon genotoxic stress of CTRL cells with mafosphamide, a similar increased levels of phagocytosis was observed in CM of p53 ($p=0.9294$), ATM ($p=0.1011$), ATX ($p=0.1174$) and significantly higher even in p38 ($p<0.0001$) compared to CM of mafosphamide stressed CTRL cells (Figure 17B).

Taken together, these results suggest three functional effects of the secretome of identified DDR KD genes. CM of p53 and p38 KD cells promotes phagocytosis of tumor cells with functionally intact DDR, whilst CM of ATX KD cells inhibits phagocytosis of tumor cells with functionally intact DNA damage response. CM of ATM KD cells show similar effect on phagocytosis as CM of CTRL cells. Under mafosphamide treatment of CTRL cells, however, CM of p53, ATX and ATM induce antibody dependent cellular killing of CTRL cells with functionally intact DNA damage response to the same extent as the CM of control cells. A significantly higher level of antibody dependent cellular phagocytosis of CTRL cells was however induced by CM of p38 KD cells.

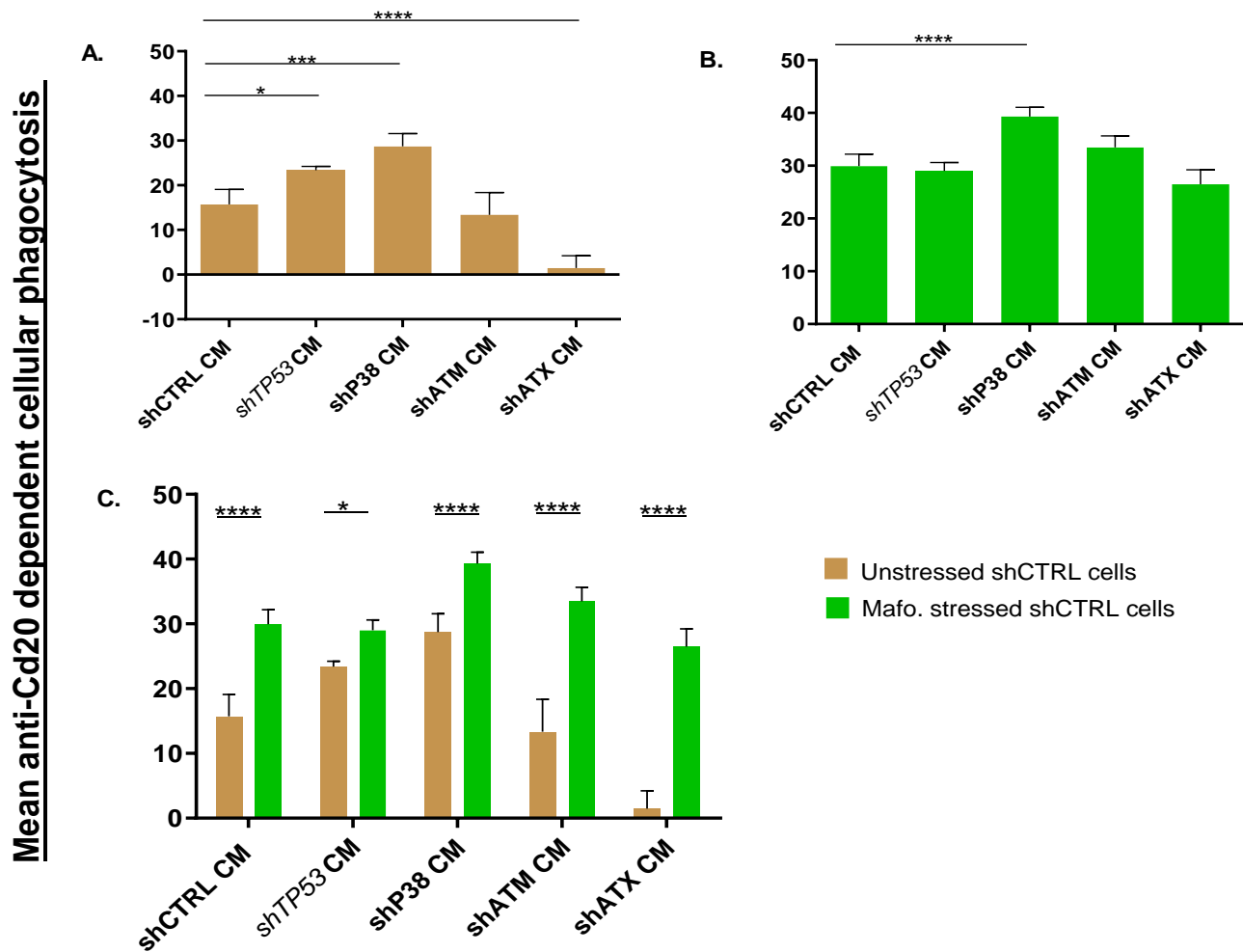


Figure 17: Impact of genotoxic stress on phagocytosis of empty vector control cells (shCTRL) cocultured in CM of DDR KD cells

- A. Level of antibody dependent cellular phagocytosis of untreated empty vector cells (shCTRL) cocultured with peritoneal macrophages in CM of DDR genes KD tumor cells.
- B. Level of antibody dependent cellular phagocytosis of mafosphamide stressed empty vector cells (shCTRL) cocultured with peritoneal macrophages in CM of DDR genes KD tumor cells
- C. Comparison of phagocytosis levels of unstressed and mafosphamide stressed empty vector cells cocultured with peritoneal macrophages in CM of DDR KD cells. A single representative result is shown (n=2). (* = $p < 0.05$, ** = $p < 0.01$, *** = $p < 0.001$, **** = $p < 0.0001$).

5.5 M552 lymphoma cell model of ABC-subtype DLBCL express high levels of immune checkpoint antigens

Immune responses are regulated by a collection of molecules which orchestrate a balance between co-stimulatory and inhibitory signals collectively called immune checkpoints (412, 413). Immune checkpoints thus regulate immune activation to moderate immune homeostasis and prevent auto-immunity. In most cancers however, immune checkpoints are often upregulated on tumor cells to suppress the response of immune cells - a well-known mechanism of tumor immune evasion. To determine the expression levels of major immune checkpoint antigens in the pathogenesis of the ABC-like DLBCL disease model, the MyD88 cell line M552 was assessed by flow cytometry (Figure 18A-E). Nascent M552 cells expressed significantly high levels of PD-L1 antigen ($p < 0.0001$) compared to PD1, CD47 and CD200 antigens. M552 cells also expressed high levels of CD47 antigen ($p = 0.0027$) compared to CD200 although a higher level of variability was observed between experimental replicates of CD47 expression over time compared to that of CD200 which was very stable throughout different time points measured. Additionally, M552 cells were genotoxically stressed by sub-lethal treatment with mafosphamide for 12hrs and re-assessed for expression of immune checkpoint antigens. Similar to the results of the unstressed cells, PD-L1 remained significantly highly expressed ($p < 0.0001$) compared to CD47, PD1 and CD200 antigens. Additionally, CD47 antigen was also expressed significantly ($p = 0.0102$) in comparison to CD200. Interestingly, stressing M552 cells with sub-lethal mafosphamide did not significantly alter the levels of immune checkpoint antigens (p -values for PD-L1, PD1, CD47 and CD200 were 0.7651, 0.9999, 0.8772 and 0.9997 respectively) compared to corresponding unstressed cells. This observation suggests that mafosphamide as a genotoxic substance does not affect the levels of immune checkpoint antigen expression, thus combinatory treatment with immune checkpoint inhibitors may be relevant to optimize treatment outcomes in this model.

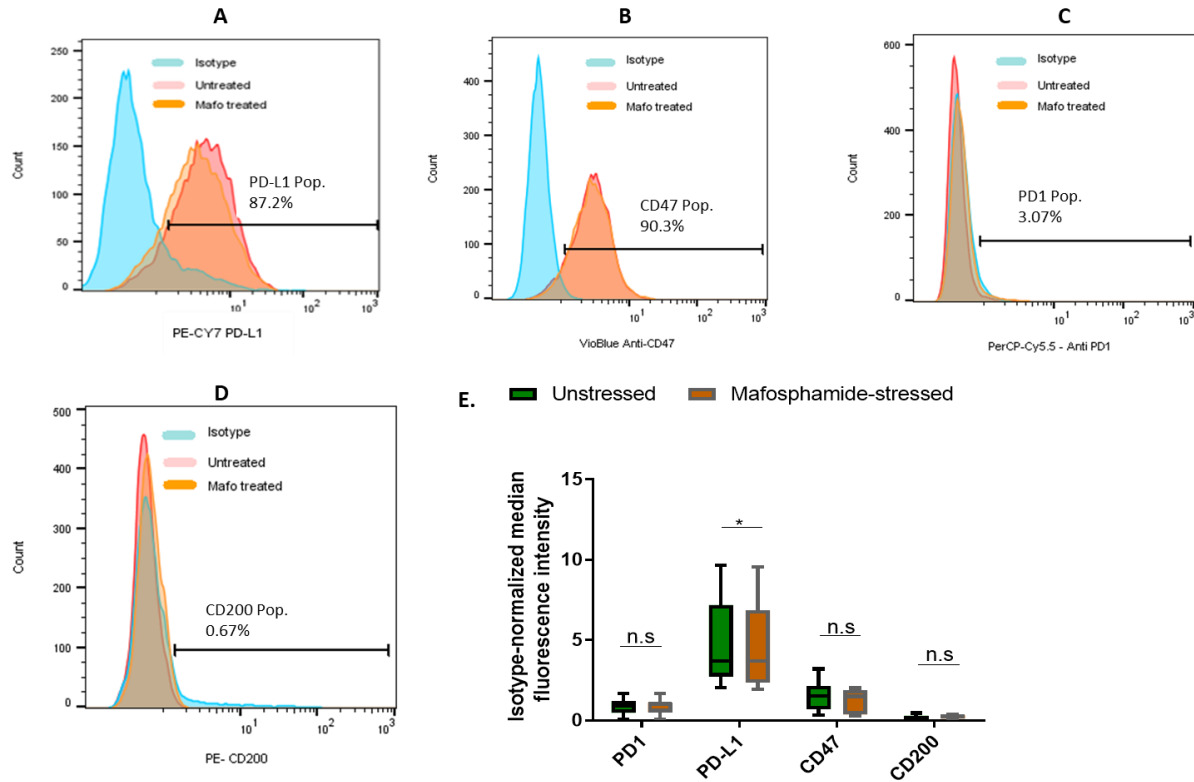


Figure 18: Expression patterns of immune checkpoint antigens of MyD88 cells unstressed and sub-lethally stressed with mafosphamide

- A. A representative histogram of PD-L1 antigen expression of untreated (red) and mafosphamide stressed (yellow) MyD88 cell line shown relative to isotype control (green).
- B. A representative histogram of CD47 antigen expression of untreated (red) and mafosphamide stressed (yellow) MyD88 cell line shown relative to isotype control (green).
- C. A representative histogram of PD1 antigen expression of untreated (red) and mafosphamide stressed (yellow) MyD88 cell line shown relative to isotype control (green).
- D. A representative histogram of CD200 antigen expression of untreated (red) and mafosphamide stressed (yellow) MyD88 cell line shown relative to isotype control (green).
- E. Summary of median fluorescence intensities (MFI) of immune checkpoint antigen expression of PD1, PD-L1, CD47 and CD200 of MyD88 lymphoma cells normalized to respective isotypes. MyD88 cells were either treatment naïve (green) or pre-stressed with sub-lethal concentration of mafosphamide (yellow) before assessment (n=7).

(* = $p < 0.05$, ** = $p < 0.01$, *** = $p < 0.001$, **** = $p < 0.0001$).

5.6 Immune checkpoint inhibitors further enhance phagocytosis of anti-CD20/mafosphamide treated tumor cells

Immune checkpoint inhibitors have become the cornerstone of durable tumor treatment responses in a variety of cancers including melanoma (414), lung (415), pancreatic tumors and breast cancers (416). Although checkpoint inhibitors such as ipilimumab has been suggested to have antitumor effect in DLBCL, other immune checkpoint inhibitors such as anti-PD-I ultimately fail despite an initial short period of response in DLBCL (417, 418).

Thus, for a heterogeneous disease as DLBCL where the ABC-like subtype presents a worse prognosis, exploration of the benefit of combinatory treatment of immuno-chemotherapy with immune checkpoint inhibitors may prove to be effective treatment strategy. Here, concentrations of immune checkpoint inhibitors including anti-PD-L1 (Atezolizumab), anti-PD-1 (α -PD1) and anti-CD47 inhibitor (MIAP301) were optimized for efficacy in *in vitro* application (Figure 35 A-C, Appendix). The optimum concentrations (highlighted by block pattern) chosen from the optimization experiments were 20 μ g/ml for PD-L1 inhibitor (Atezolizumab), 50 μ g/ml for PD1 inhibitor (α -PD1) and 15 μ g/ml of anti-CD47 inhibitor (MIAP301).

In coculture of M552 cells with J774.1A macrophages, significant spontaneous phagocytosis were observed with immune checkpoint inhibitors/genotoxic combination for anti-PD-1 ($p=0.0034$), anti-PD-L1 ($p<0.0001$) but not anti-CD47 ($p=0.3089$). Also, cocultures of immune checkpoint inhibitors with anti-CD20 mAb/mafosphamide combination showed significant increase of antibody dependent cellular phagocytosis for anti-PD-1 ($p<0.0001$), anti-PD-L1 ($p<0.0001$) and anti-CD47 ($p<0.0001$) (Figure 19A). This suggests checkpoint inhibitors are more efficacious when combined with genotoxic treatment. Without genotoxic treatment anti-CD47 was the only immune checkpoint inhibitor that induced significant ($p<0.0001$) tumor cell phagocytosis as a monotherapy compared to PD-L1 and PD1 inhibitors.

The significantly high level of phagocytosis induced by blocking CD47-signal-regulatory protein alpha (Sirp- α) axis in both treatment naïve and mafosphamide pretreated tumor cells raised the question whether phagocytosis could be further enhanced with treatment regimen utilizing combinations of immune checkpoint inhibitors. Thus, M552 – J774.1A cocultures were treated with

different combinations of checkpoint inhibitors. Without genotoxic treatment, anti-CD47 monotreatment induced significantly high antibody dependent cellular phagocytosis ($p=0.0007$) such that double checkpoint inhibitors combinations of anti-CD47 and anti-PD-L1 ($p = 0.8853$) and triple combinations of anti-CD47, anti-PD-L1 and anti-PD-1 ($p = 0.9711$) resulted in no further change in antibody dependent cellular phagocytosis (Figure 19B).

Similarly, using genotoxic stressed M552 cells for cocultures, monotreatment with anti-CD47 induced such a high level of phagocytosis ($p=0.0010$) such that double checkpoint combination of anti-CD47 and PD-L1 did not further alter the level of phagocytosis ($p= 0.9967$) compared to that of anti-CD47 alone.

Contrarily to effect of triple immune checkpoint treatment on ADCP using treatment naïve M552 cells, triple checkpoint treatment of genotoxic stressed tumor cells with anti-CD47, anti-PD-L1 and anti-PD-1 resulted in significant ($p=0.0415$) impaired phagocytosis compared to mono treatment with anti-CD47 alone or double treatment with anti-CD47 and anti-PD-L1 (Figure 19B).

In all effective combinations, tumor cell phagocytosis saturated between 50-60% both in treatment naïve and mafosphamide pretreated cells beyond which no further increase is observed irrespective of treatment combinations.

The impact of anti-CD47 on phagocytosis was recapitulated with primary macrophages as effector cells. Treatment naïve and genotoxic stressed M552 tumor cells were cocultured with thioglycollate induced mouse peritoneal macrophages and treated with anti-CD47 antibody.

Here, increased level of antibody dependent cellular phagocytosis ($p < 0.0001$) was observed in both treatment naïve and mafosphamide stressed cells. However, genotoxic stress with a sub-lethal concentration of mafosphamide in combination with anti-CD47 resulted in the highest level of tumor cells phagocytosis ($p < 0.0001$) compared to that observed with J774.1A macrophages as effector cells.

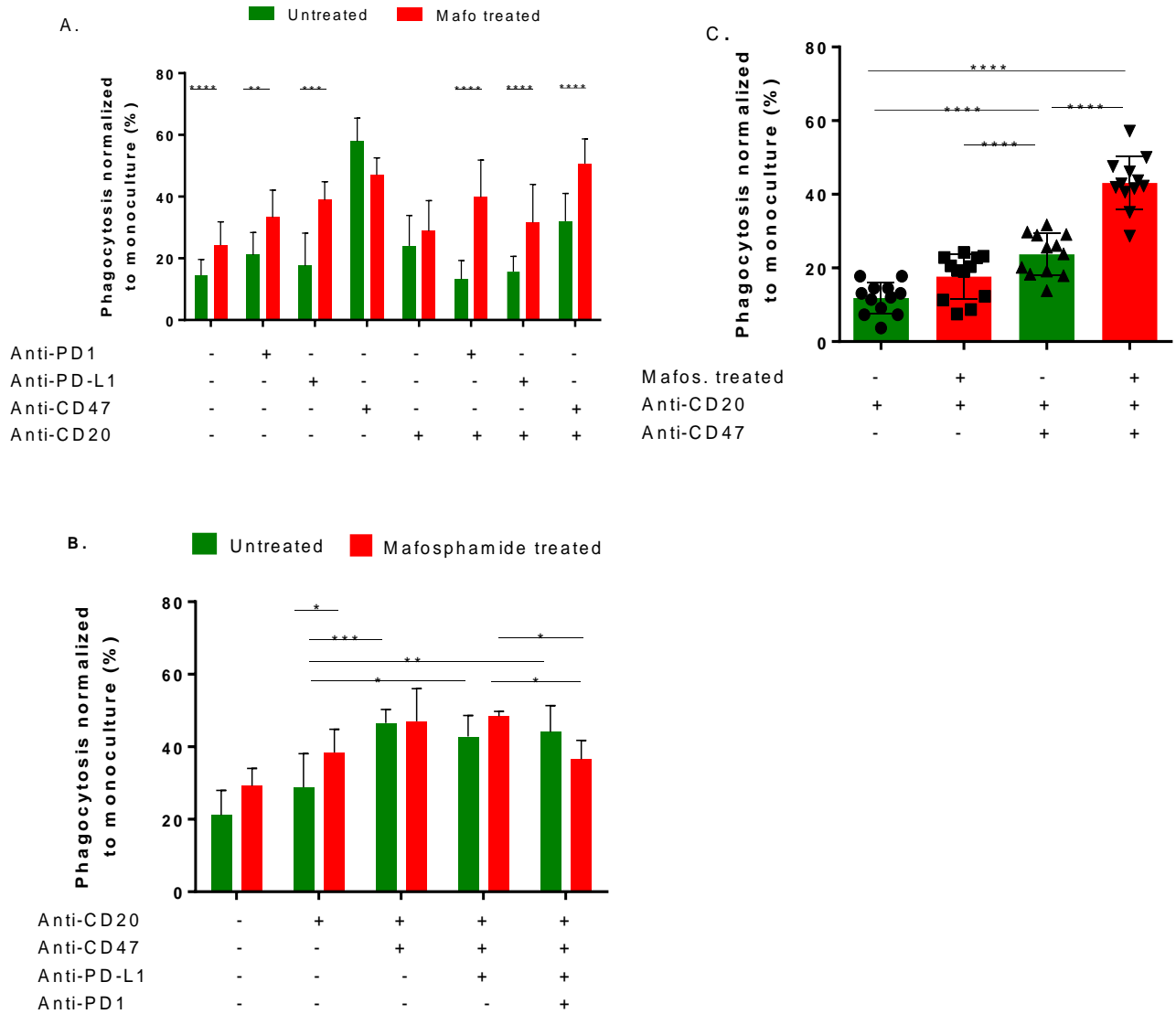


Figure 19: Levels of phagocytosis of M552 cells cocultured with effector macrophages under immune checkpoint inhibitors combinatory treatment.

A. Level of phagocytosis of M552 cells cocultured with J774.1A macrophages, treated with monotherapy of immune checkpoint inhibitors (n=4).

B. Level of phagocytosis of M552 cells cocultured with J774.1A macrophages, treated with combinations of immune checkpoint inhibitors (n=2)

C. Level of phagocytosis of M552 cells cocultured with thioglycollate induced peritoneal macrophages and treated with anti-CD47 checkpoint inhibitor (n=3). Genotoxic stress of M552 cells was induced with sub-lethal concentration of mafosphamide (IC₂₀ concentration).

(* = p < 0.05, ** = p < 0.01, *** = p < 0.001, **** = p < 0.0001).

5.6.1 Anti-CD47 promotes phagocytosis predominantly through interruption of CD47/Sirp- α interaction

CD47/signal regulatory protein alpha (Sirp- α) is one of the major immune cell checkpoint axis hijacked by tumor cells to silence phagocytic machinery of myeloid cells. A number of anti-CD47 antibodies are in clinical trials and laboratory use as they have demonstrated potent efficacy. However, it is argued that anti-CD47 demonstrates optimal efficacy through both Fc-Fc γ interaction and CD47/Sirp- α engagement (384, 419). To clarify the mechanism of anti-CD47 efficacy observed in the coculture of Myd88 M552 cell line model, full length rat anti-CD47 IgG mAb was enzymatically digested with pepsin and separated by affinity chromatography using Pierce F(ab)₂ preparation kit (Thermo Scientific) (Figure 36, Appendix). Subsequently, coculture of M552 cell line with J774.1A macrophages were treated with anti-CD20 mAb and serial dilutions of full length anti-CD47 or divalent fragment antigen binding (F(ab)₂) portion of anti-CD47. Compared to baseline anti-CD20 dependent phagocytosis, a minimum of 5 μ g/ml of full length anti-CD47 induced significant phagocytosis ($p < 0.0001$) whilst a minimum of 10 μ g/ml of F(ab)₂ was required to achieve significant phagocytosis ($p < 0.0001$). At the minimum concentration of both full length anti-CD47 and F(ab)₂ portion of anti-CD47, the levels of phagocytosis induced reached a saturation such that further increase in concentrations of both full length anti-CD47 and F(ab)₂ portions resulted in no further increase in levels of tumor cell phagocytosis (Figure 20). The findings suggest that F(ab)₂ portion of anti-CD47 mAb at the optimal concentration effectively blocks CD47/Sirp- α axis to promote anti-CD20 dependent cellular phagocytosis and that full length anti-CD47 could predominantly induce significant tumor cells phagocytosis by blocking CD47/Sirp- α interactions.

Next, we asked if F(ab)₂ portion of anti-CD47 could potentiate antibody dependent cellular phagocytosis of genotoxic stressed and unstressed M552 cells in a manner similar to that of full length anti-CD47 and whether it could synergize with other immune checkpoint inhibitors in coculture with J774.1A macrophages. Thus, cocultures of M552 cells with J774.1A macrophages and anti-CD20 mAb were treated with combinations of F(ab)₂ fragment of anti-CD47, anti-PD-L1 and anti-PD-1. Expectedly, inhibition of CD47/Sirp- α with F(ab)₂ fragments resulted in significantly higher levels ($p = 0.0009$) of ADCP in genotoxic stressed M552 cells compared to that of unstressed cells (Figure 20B). Furthermore, addition of anti-PD-L1 could further increase the

ADCP of unstressed M552 cells ($p=0.0032$) (Figure 20C) but not mafosphamide stressed cells ($p=0.6957$) (Figure 20D). Triple combination of F(ab)₂ fragments, anti-PD-L1 and PD-1 did not significantly affect phagocytosis of unstressed M552 cells compared to double combination of F(ab)₂ fragments and anti-PD-L1 or mono treatment with F(ab)₂ fragments. However, in mafosphamide stressed M552 cells, triple combination of F(ab)₂ fragments, anti-PD-L1 and PD-1 significantly impaired tumor cell phagocytosis ($p=0.0236$) compared to mono treatment with F(ab)₂ fragments. These findings suggest that in ABC-like subtype of DLBCL treated with chemo immunotherapy in combination with anti-CD47 immune checkpoint inhibitor, further combination with checkpoint inhibitors such as PD-L1 or PD-1 offers no additional benefits.

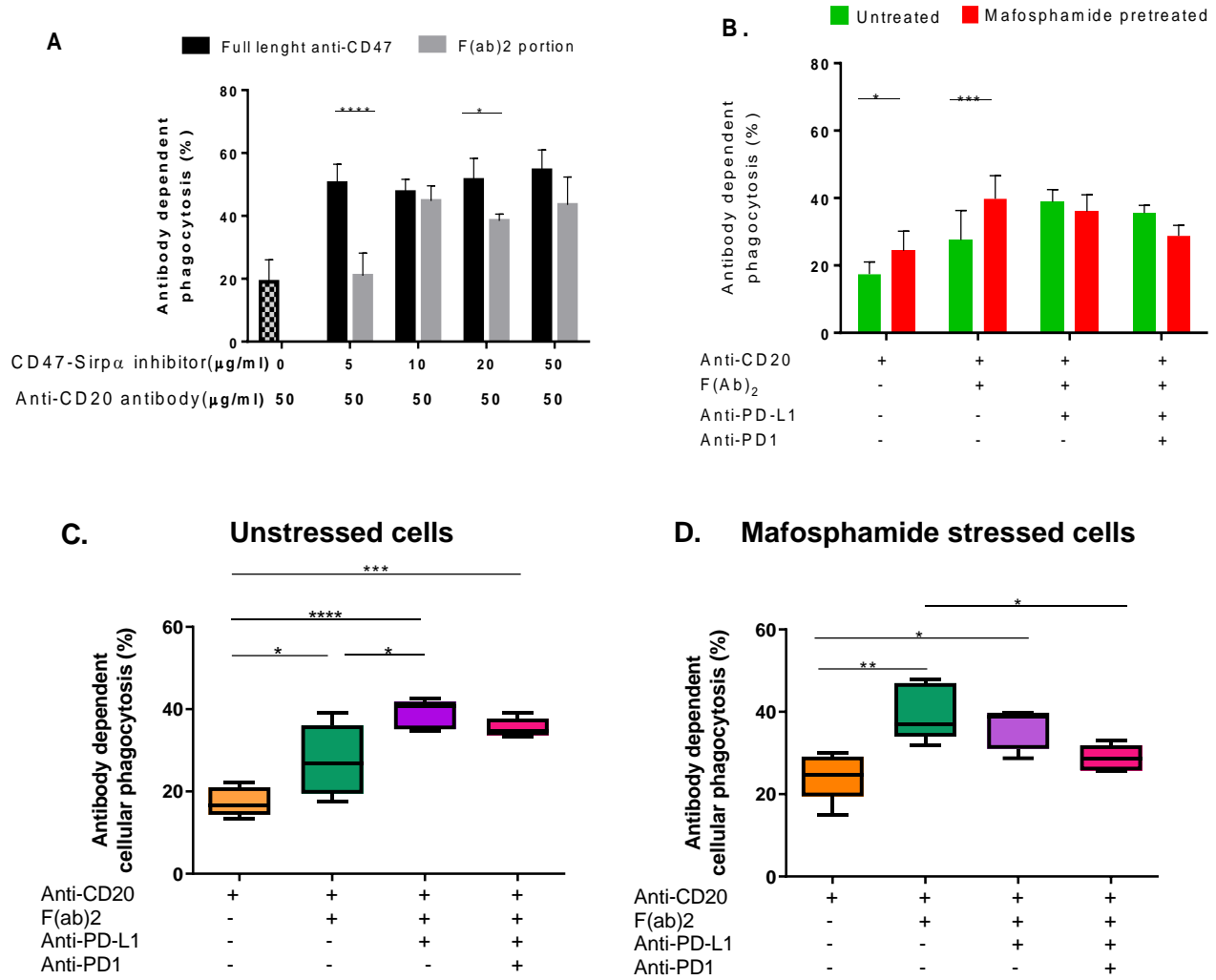


Figure 20: *F(ab)₂ fragment of anti-CD47 effectively induces higher ADCP through blockade of CD47-Sirp- α*

- A. Levels of antibody mediated phagocytosis following treatment with CD47-Sirp- α inhibitor using full length anti-CD47 or F(ab)2 fragment of anti-CD47 antibody. M552 cell lines were used as target cells and J774.1A macrophages as effector cells (n=2).
- B. Level of phagocytosis of genotoxic stressed and unstressed M552 tumor cells cocultured with J774.1A macrophages using F(ab)2 portion of anti-CD47 in combinations with anti-PD-L1 and anti-PD-1. A representative result is shown (n=2)

- C. Level of phagocytosis of unstressed M552 tumor cells cocultured with J774.1A macrophages using F(ab)₂ portion of anti-CD47 in combinations with anti-PD-L1 and anti-PD-1. A representative result is shown (n=2)
- D. Level of phagocytosis of mafosphamide stressed M552 tumor cells cocultured with J774.1A macrophages using F(ab)₂ portion of anti-CD47 in combinations with anti-PD-L1 and anti-PD-1. A representative result is shown (n=2)
- (* = $p < 0.05$, ** = $p < 0.01$, *** = $p < 0.001$, **** = $p < 0.0001$).

5.6.2 Treatment refractory DDR gene KD cells differ in immune checkpoint expressions

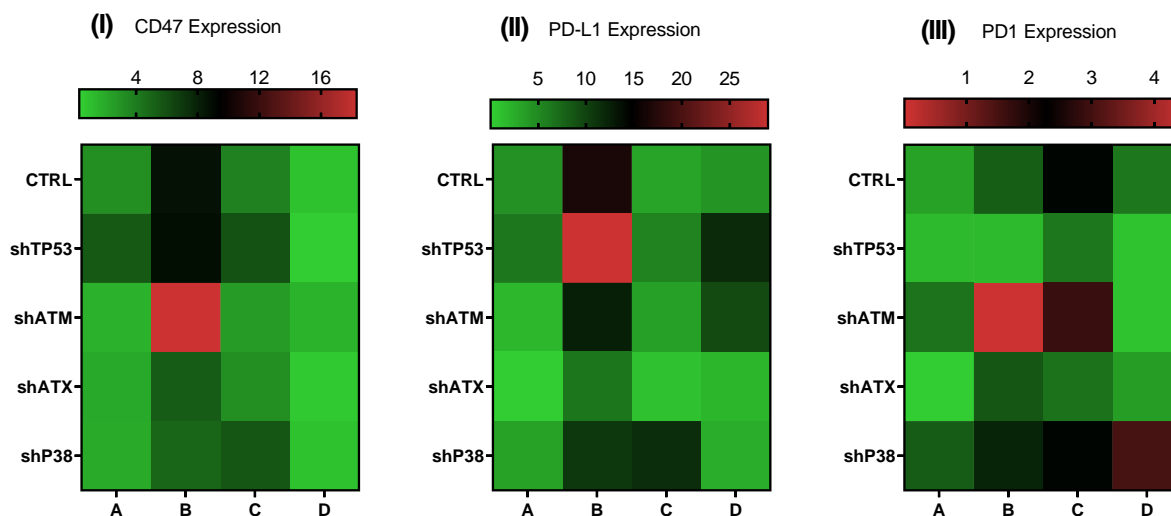
Immune checkpoint inhibitors (iCP) have shown tremendous improvement in cancer treatment by blocking receptors and ligands that antagonize effector cells functions. Despite this era of major breakthroughs in cancer therapy, responses to checkpoint inhibitors have not been universal. Genomic and immune features in pre-tumor biopsies have shown strong correlation to treatment outcomes and offered a glimpse as to mechanisms of treatment failures (420). Thus, focus was placed on determining the expression levels of immune checkpoint antigens and to ascertain the dynamics of checkpoint antigen expression under different treatment conditions. Hence, immune checkpoint antigens of untreated KD cells were determined as well as that of treatment naïve KD cells cocultured with mouse peritoneal macrophages. Additionally, expression of checkpoint antigens of mafosphamide stressed KD cells and mafosphamide stressed KD cells cocultured with mouse peritoneal macrophages were determined.

CD47 expression did not differ significantly between unstressed monoculture cells of empty vector control and selected KD cells (p53 ($p=0.9842$), ATM ($p=0.8318$), ATX ($p=0.9547$), and p38 ($p=0.9959$)). However, genotoxic stress with mafosphamide induced variable insignificant increases in all cells with the greatest change in median fluorescence intensity (MFI) seen in ATM KD and the lowest in p38 KD cells. Interestingly, contact of KD tumor cells with effector macrophages generally down-regulated CD47 expression particularly of genotoxic stressed KD cells and control (Figure 21(I)).

Baseline MFI of PD-L1 antigen expression remained variably insignificant between KDs cells and empty vector control cell. ATX KD cells expressed the least level of PD-L1. Mafosphamide

pretreatment, drove high levels of PD-L1 antigen expression in both selected KD cells and controls however, these differences remain statistically insignificant except for p53 ($p=0.0338$) which expressed the highest level of PD-L1 antigen under genotoxic stress relative to ATX which expressed the least amount of PD-L1 antigen.

Contact of unstressed KD cells with peritoneal macrophages in the coculture system reduces PD-L1 expression on most KD cell as well as control except for p38 KD cells which maintains insignificantly higher expression levels of MFI than baseline and mafosphamide stressed. Contact of genotoxic stressed KD with peritoneal macrophages reveal an increased tendency of PD-L1 expression in P53 and ATM KD cells compared to the control although none of these differences reached statistical significance (Figure 21(II)). The level of PD-1 expression by both DDR KD cells and empty vector control was very low at baseline and continue to be relatively low irrespective of treatment conditions of the cells (Figure 21(III)).



Shaded columns

A = Unstressed tumor cells

B = Mafosphamide stressed tumor cells

C = Unstressed tumor cells pre-exposed to murine thioglycollate induced peritoneal macrophages

D = Mafosphamide stressed tumor cells pre-exposed to murine thioglycollate induced peritoneal macrophages

*CTRL – Control tumor cells (empty vector)

*sh – Gene knockdown tumor cells

Figure 21: Immune checkpoint expression of DDR genes KD cells exposed to varied treatment

(I) Heatmap of median fluorescent intensities (MFI) of CD47 antigen of DDR genes KD M552 cells, unstressed (A), mafosphamide stressed (B), unstressed in coculture contact with peritoneal macrophages (C) or mafosphamide stressed in coculture contact with peritoneal macrophages(D) (n=4)

(II) Heatmap of median fluorescent intensities (MFI) of PD-L1 antigen of DDR KD M552 cells, unstressed (A), mafosphamide stressed (B), unstressed in coculture contact with peritoneal macrophages (C) or mafosphamide stressed in coculture contact with peritoneal macrophages(D) (n=4)

(III) Heatmap of median fluorescent intensities (MFI) of PD-1 antigen of DDR KD M552 cells, unstressed (A), mafosphamide stressed (B), unstressed in coculture contact with peritoneal macrophages (C) or mafosphamide stressed in coculture contact with peritoneal macrophages(D) (n=4). *Cells were stressed by pretreatment with IC₂₀ concentration of mafosphamide.

5.6.3 Immune checkpoint inhibitors overcome impaired phagocytosis of DDR genes KD cells

Following enhanced phagocytosis of M552 cells with functionally intact DDR genes under chemoimmunotherapy/immune-checkpoint inhibitors combination, we further investigated the effect of the combined therapy on M552 cells with knockdown DDR genes. Thus, both empty vector M552 cells with functional DDR and DDR KD M552 cells (p53, ATM, ATX, p38) were stressed by sub-lethal treatment with mafosphamide and cocultured with thioglycollate induced mouse primary peritoneal macrophages.

Cocultures were concurrently treated with anti-CD20/anti-CD47 or anti-CD20/anti-PD1 or anti-CD20/anti-PD-L1 combinations. The level of phagocytosis of empty vector control cells was not significantly altered when treated with combination of anti-CD20/anti-PD-L1 ($p=0.1749$) or anti-CD20/anti-PD-1 ($p=0.4342$). However, anti-CD20/anti-CD47 combination significantly ($p=0.0004$) increased the level of phagocytosis relative to anti-CD20 treatment alone. On the other hand, treatment of genotoxic stressed p53 KD cells with anti-PD-L1 ($p=0.0423$) or PD-1 ($p=0.0184$) or anti-CD47 ($p<0.0001$) in combination with anti-CD20 resulted in significantly higher phagocytosis of p53 KD cells compared to anti-CD20 alone without checkpoint inhibitor. p53 KD cells treated with the immune-checkpoint inhibitors thus attained similar levels of phagocytosis as the empty vector control in the case of anti-PD-L1 (0.2350), anti-PD-1 (0.8090) and anti-CD47 (0.1529) (Figure 22A).

Treatment of genotoxic stressed ATM KD cells with anti-PD-L1 ($p=0.0066$), PD-1 ($p=0.0142$) or anti-CD47 ($p<0.0001$) in combination with anti-CD20 resulted in significant increase in phagocytosis of ATM KD cells compared to ATM KD treated with anti-CD20 alone. Combined anti-CD20/CD47 induced a higher level of phagocytosis than anti-CD20/anti-PD-L1 ($p=0.0004$) or anti-CD20/anti-PD-1 ($p=0.0002$) combinations. However, contrary to the observation in p53 KD cells, ATM KD cells treated with immune-checkpoint inhibitors remained significantly less phagocytosed compared to empty vector control under similar combinations of treatments for anti-PD-L1 ($p=0.0005$), anti-PD-1 ($p=0.0014$) and anti-CD47 ($p=0.0376$) (Figure 22B).

In the case of ATX KD cells, with the exception of anti-CD20/anti-CD47 ($p < 0.0027$) which induced significant increase in phagocytosis of genotoxic stressed ATX KD cells, treatment with anti-CD20/anti-PD-L1 ($p = 0.9364$), anti-CD20/anti-PD-1 ($p = 0.7115$) failed to increase phagocytosis of ATX KD cells compared to anti-CD20 treatment alone. Thus similar to observation of ATM KD cells, ATX KD cells treated with immune-checkpoint inhibitors remained significantly less phagocytosed compared to empty vector control under similar treatments for anti-PD-L1 ($p < 0.0001$), anti-PD-1 ($p = 0.0198$) and anti-CD47 ($p = 0.0003$) (Figure 22C). Treatment of genotoxic stressed p38 KD cells with anti-PD-L1, PD-1 and CD47 in combination with anti-CD20 resulted in significant increase in phagocytosis ($p < 0.0001$) compared to p38 KD cells treated with anti-CD20 alone. Combined anti-CD20/CD47 induced in a higher level of phagocytosis than anti-CD20/PDL1 ($p = 0.0013$) or anti-CD20/PD1 ($p = 0.0003$) combinations. However, contrary to observation of ATM, p53 and ATX KD cells, immune-checkpoint inhibitor treated p38 KD cells were significantly phagocytosed compared to empty vector control under similar treatments for anti-PD-L1 ($p = 0.0253$), anti-PD-1 ($p = 0.0207$) and anti-CD47 ($p = 0.0012$) (Figure 22D).

In brief, depending on the mutated gene in the DDR, the impact of treatment on phagocytosis is qualitatively and quantitatively different but can be classified into three groups: ATM and ATX KD cells remain resistant; p53 resistance can be reversed, whilst loss of p38 leads to higher levels of phagocytosis than previously seen in the empty vector control. Anti-CD47 in particular induced an increased tumor cells phagocytosis irrespective of genomic alteration underlying DDR dysfunction.

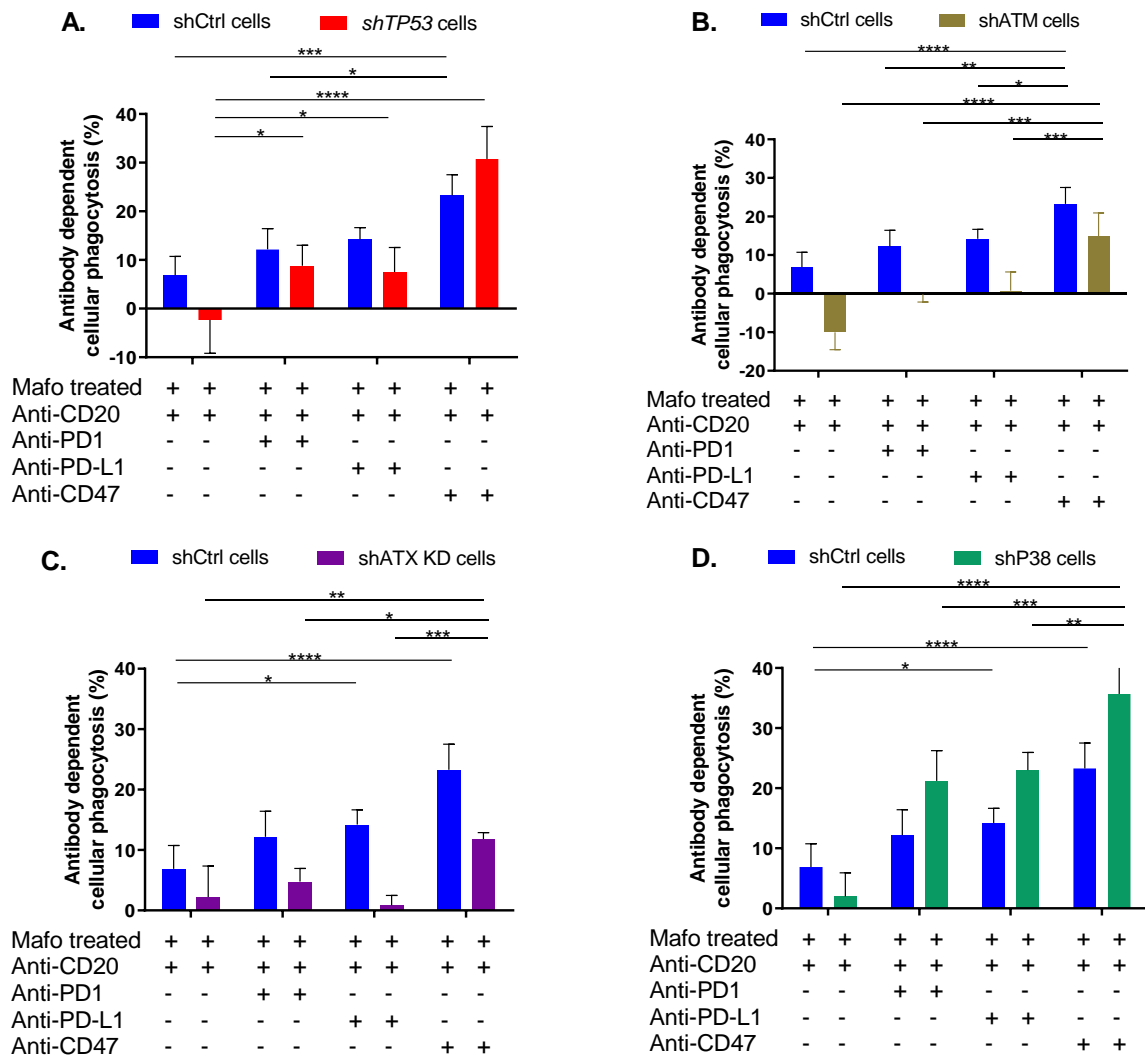


Figure 22: Levels of phagocytosis of genotoxic stressed empty vector control and DDR KD cells of M552 coculture with primary murine peritoneal macrophages. Cocultures were treated with anti-CD20 mAb and immune checkpoint inhibitors.

A–D. Levels of antibody dependent cellular phagocytosis of M552 empty vector control (shCTRL) compared to p53 KD(A), ATM KD(B), ATX KD(C) and p38 KD(D) cells cocultured with thioglycollate-induced mouse peritoneal macrophages. KD cells were stressed with mafosphamide and cocultures were simultaneously treated with anti-CD20 and either anti-CD47 or anti-PD-L1 or anti-PD1 for 16hrs. Level of phagocytosis of KD cells are displayed alongside that of empty vector control cells (n=3). (* = $p < 0.05$, ** = $p < 0.01$, *** = $p < 0.001$, **** = $p < 0.0001$).

5.6.4 Immune Checkpoint inhibitors bolster phagocytosis of other effector cells

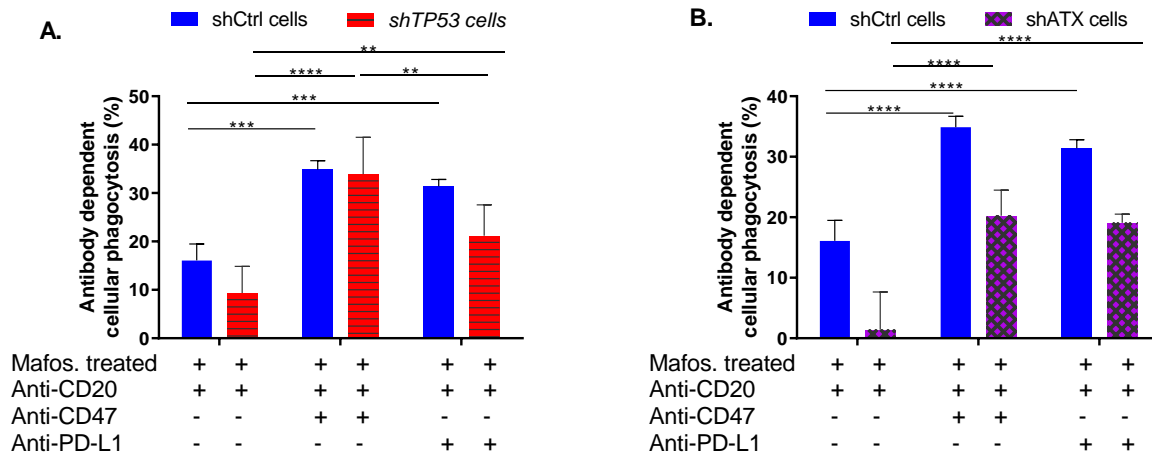
Macrophages from different anatomic niches show varied phagocytic capacity when exposed to tumor cells with DDR gene KD (Figure 15). To verify whether immune checkpoint inhibitors could circumvent impaired phagocytosis encountered by effectors cells, feeder media differentiated primary bone marrow derived macrophages (BMDM) and J774.1A cell line macrophages were cocultured with both empty vector M552 cells with functional DDR and DDR genes KD M552 cells identified to mediate impaired phagocytosis on combined chemo-immunotherapeutic treatment. Selected gene KD cells were sub-lethally stressed with mafosphamide before used in cocultures. Additionally, cocultures were concurrently treated with anti-CD20 mAb and combinations of immune-checkpoint inhibitors including anti-CD47, anti-PD1 and anti-PD-L1.

Combination of anti-CD47 ($p=0.0001$) and anti-PD-L1 ($p=0.001$) significantly increased the levels of phagocytosis of control cells compared to anti-CD20 treatment without checkpoint inhibitor. The level of phagocytosis of control cells treated with anti-CD47 was similar to that of anti-PD-L1 ($p=0.5895$). Following DDR genes KD, anti-CD47 ($p<0.0001$) and anti-PD-L1 ($p=0.0085$) significantly increased the levels of phagocytosis of genotoxic stressed p53 KD cells. Anti-CD47 induced significantly higher phagocytic effect ($p=0.0049$) than PD-L1 blockade (Figure 23A). Similarly, both anti-CD47 and anti-PD-L1 significantly ($p<0.0001$) increased the levels of phagocytosis of genotoxic stressed ATX KD cells (Figure 23B). Interestingly, a higher level of phagocytosis was observed with PD-L1/PD-1 axis blockade in ATX KD cells coculture with BMDM than with peritoneal macrophages.

Using J774.1A as effector cells in similar coculture setups, we observed significant induction of phagocytosis of genotoxic stressed control cells when treated with combination of anti-CD47 ($p<0.0001$) and anti-PD-L1 ($p=0.0285$) compared to anti-CD20 monotherapy. Anti-CD47 combination yielded significantly higher levels of control cells phagocytosis than anti-PD-L1 ($p=0.0001$) and anti-PD-1 ($p<0.0001$). However, in coculture with genotoxic stressed ATX KD cells, only anti-CD47 treatment induced significant phagocytosis ($p<0.0001$) with both anti-PD-L1 ($p=0.6692$) and anti-PD-1 ($p=0.0596$) failing to augment the level of phagocytosis achieved under anti-CD20 mono treatment (Figure 23C). Also coculture with p38 KD cells showed similar pattern of high phagocytosis with anti-CD47 ($p<0.0001$) and anti-PD-1 ($p=0.0012$) but not anti-PD-L1

(0.8258) contrary to observation in coculture with peritoneal macrophages. Again, a higher level of phagocytosis was induced through CD47/Sirp- α blockade ($p < 0.0001$) than PD-L1/PD-1 blockade (Figure 23D). Functioning directly downstream of p38, combination of immune checkpoint inhibitors with chemotherapy resulted in increased MK2 KD cells phagocytosis under anti-CD47 ($p < 0.0001$), PD-L1 ($p = 0.0018$) and PD-1 ($p = 0.0001$).

In brief, blockade of CD47/Sirp- α axis reduces tumor burden by increasing antibody dependent cellular phagocytosis with different macrophages as effector cells. Blockade of PD-L1/PD-1 axis only promotes phagocytosis of ATX KD cells by BMDM but not peritoneal or J774.1A macrophages.



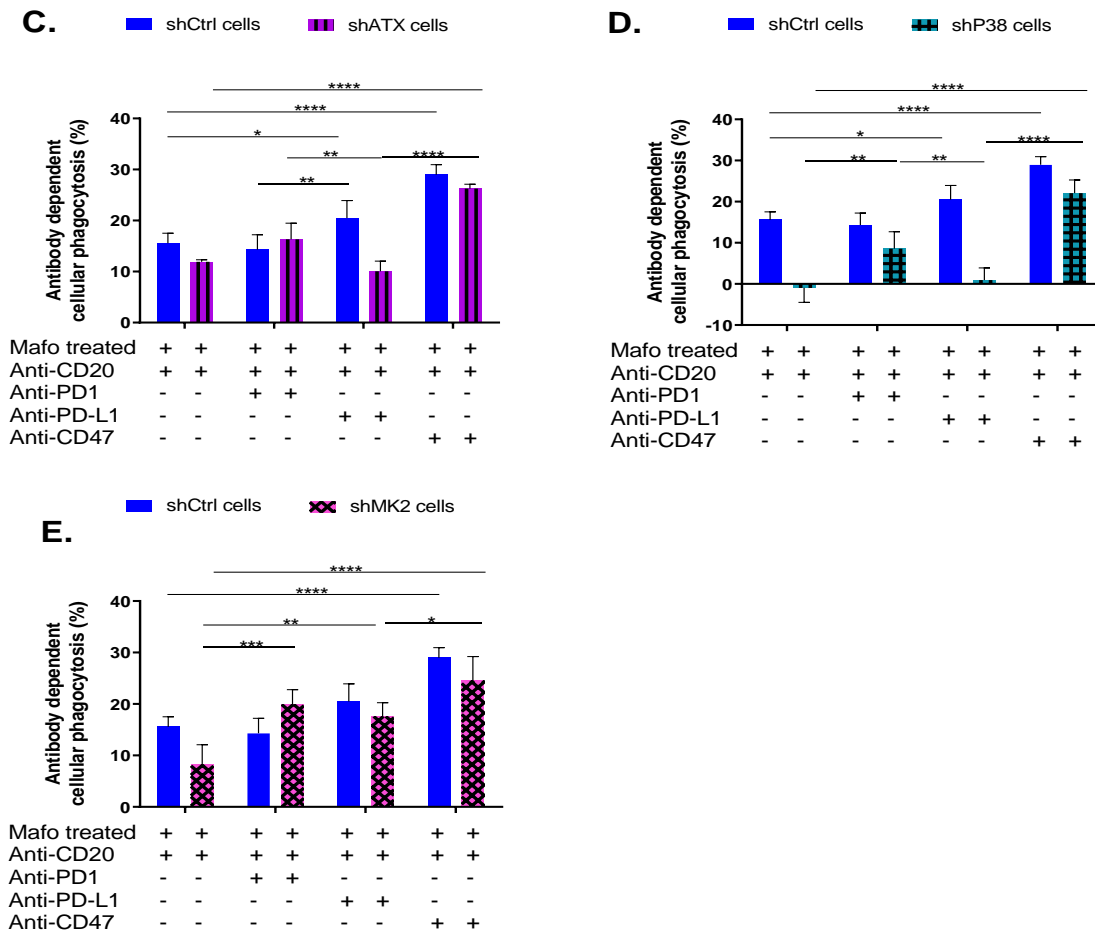


Figure 23: Levels of phagocytosis of genotoxic stressed empty vector control and DDR KD cells of M552 coculture with primary murine bone marrow macrophages and J774.1A macrophages. Cocultures were treated with anti-CD20 mAb and immune checkpoint inhibitors

A–B. Level of antibody dependent cellular phagocytosis of *shTP53* (A) and *shATX* (B) cells cocultured with murine bone marrow-derived macrophages. KD cells were sub-lethally pretreated with mafosphamide and cocultures were simultaneously treated with anti-CD20 mAb and either anti-CD47 or anti-PD-L1 or anti-PD1 for 16hrs. Level of phagocytosis of KD cells are displayed alongside that of empty vector control cells (shCtrl) (n=2)

C– E. Level of antibody dependent cellular phagocytosis of *shP38* (C), *shATX* (D) and *shMK2* (E) M552 cells cocultured with J774.1A macrophage. KD cells were sub-lethally pretreated with mafosphamide and cocultures treated with anti-CD20 mAb and either anti-CD47, anti-PD-L1 or anti-PD1 for 16hrs. Level of phagocytosis of KD cells are displayed alongside that of empty vector control cells (n=2). (* = $p < 0.05$, ** = $p < 0.01$, *** = $p < 0.001$, **** = $p < 0.0001$).

5.7 Tumors with downregulated DDR genes influence phenotypic characteristics of macrophages

Macrophages are critical innate immune cells involved in immune surveillance, organ development, tissue turnover and regeneration (421). These functions demand recognition of a wide spectrum of stimuli from infectious organism, immune complexes, apoptotic and necrotic cells. In response to these stimuli, macrophages are activated to orchestrate diverse functional roles. Generally, exposure to lipopolysaccharides (LPS), interferon gamma (IFN- γ), granulocytes-macrophage colony-stimulating factor (G-MCSF) induces transcriptional and phenotypic characteristics in macrophages described as classically activated or M1 which induces a pro-inflammatory posture (422). At the other extreme, exposure to a plethora of agents including fungal cells, parasites, immune complexes, complements, apoptotic cells, macrophage colony stimulating factor (M-CSF), interleukin-4 (IL-4), IL-13, IL-10, vitamin D₃ and tumor growth factor beta (TGF- β) induce anti-inflammatory, pro-tissue remodeling functions in macrophages termed M2 or alternatively activated (423, 424). However, a large continuum of activation characteristic such as manifested by tumor-associated macrophages (TAM) and macrophages expressing T-cell receptor and CD169; highlighting the limitations of the rigid bi-functional states of M1, M2 macrophages.

Since the strongest effect on the tumor cells were observed upon genotoxic stress, attention was focused to understand the interaction of the poorly phagocytosed KD cells on macrophages within the coculture system. Here, thioglycollate-induced mouse peritoneal macrophages were cocultured with sub-lethal mafosphamide pre-treated KD cells for 16hrs and the macrophages were immediately phenotyped with an antibody panel for polarization markers (Table 3). In comparison to macrophages exposed to the empty vector control cells (shCtrl), macrophages exposed to *shTP53*, *shATM*, *shATX* and *shp38* cells showed profound differences in phenotypic markers (Figure 24). Macrophages exposed to *shTP53* cells reduced expression of both M1 (pro-inflammatory) and M2 (anti-inflammatory) markers. For instance, TGF- β expression reduced by about 2-fold whilst its targets, IL10 and CD206 expression reduced by about 52% and 15% respectively. On the other hand, inducible nitric oxide synthase (iNOS), a critical enzyme required for nitric oxide generation in pro-inflammatory response reduced by about 40% whilst CD38 and CD80 expressions reduced by about 50% (Figure 25). Exposure to *shTP53* tumor cells also reduced expression of FcR of macrophages. CD64 (a critical Fc-gamma receptor required for antibody mediated phagocytosis) reduced by 32% whilst CD16/32 reduced marginally by 4%. However,

expression of CD80, a critical co-stimulatory receptor required for T-cell activation reduced by 50% upon exposure to p53 KD tumor cells.

Peritoneal macrophages exposed to ATM KD tumor cells strikingly increased TGF- β by approximately 3 fold change, PD-L1 by 82% and PD1 by 76% expression compared to exposure to control cells. Additionally, downregulation iNOS by approximately 50%, CD68 by 20% and CD80 by 17% tilted their polarization towards M2 phenotype of macrophages. However, there was also about 40% selective up regulation of surface chemotactic receptor type 7 (CCR7), the chemotactic receptor for chemokine ligands CCL19/CCL21 which mediate chemotaxis of M1 macrophages and CD38 a marker associated with M1 activated macrophages. Unlike exposure of macrophages to *shTP53* tumor cell, exposure to *shATM* cells increased expression of FcR of macrophages by 20% of CD16/32 and 7% of CD64 compared to exposure to control cells.

Exposure of mouse peritoneal macrophages to *shATX* tumor cells resulted in reduced expression of M1 markers including 70% reduction in CD80, 20% reduction in major histocompatibility complex II (MHC II), 21% reduction in CCR7, 29% reduction in CD38 and about 9% reduction in iNOS expression. However, expression of CD86 and CD68 markers increased by 38% and 30% respectively. Of the M2 macrophage polarization markers, TGF- β , IL-10 and PD-L1 expression decreased by 31%, 24% and 67% respectively compared to exposure to control cells. However, increases in M2 macrophage polarization markers including CD115 (21%), CD206 (35%), Arginase-1 (16%) and Early Growth Response Gene-2 (EGR-2) (15%) were observed upon exposure of macrophages to *shATX* tumor cells. Additionally, levels of expression of FcR including CD16/32 (28%) and CD64 (48%) decreased following exposure of macrophages to *shATX* tumor cells.

Exposure of *shp38* tumor cells to peritoneal macrophages in coculture also resulted in unique phenotypic expression pattern of M1, M2 and FcR markers. Expression of several markers associated with M1 polarisation state such as CD68, iNOS, CD86, CCR7 and MHC II increased in proportion of 93%, 66%, 56%, 81%, and 16% respectively above levels observed upon exposure of control cells to peritoneal macrophages. However, expression of other classically activated macrophage markers such as CD80 and CD38 reduced in proportion of 38% and 42% respectively compared to levels of expression observed with exposure to control cells. Similarly, exposure of peritoneal macrophages to *shp38* tumor cells resulted in elevation of some markers associated with

M2 polarisation states. For instance, there was a two-fold increase in expression of TGF- β , about 64% increase in CD206, 20% increase in EGR-2, 16% in CD200R, 11% in CD115 and 6% increase in arginase -1 levels upon exposure to p38 KD tumor cells compared to exposure to control cells. Contrarily, exposure to p38KD tumor cells induced reduced expression of PD-L1 (56%), PD-1 (44%) and IL-10 (17%) in peritoneal macrophages. But strikingly, expression of Fc-gamma receptors including CD16/32 and CD64 critical for antibody-mediated phagocytosis reduced averagely by 34% and 43% respectively upon macrophage exposure to p38 KD tumor cells.

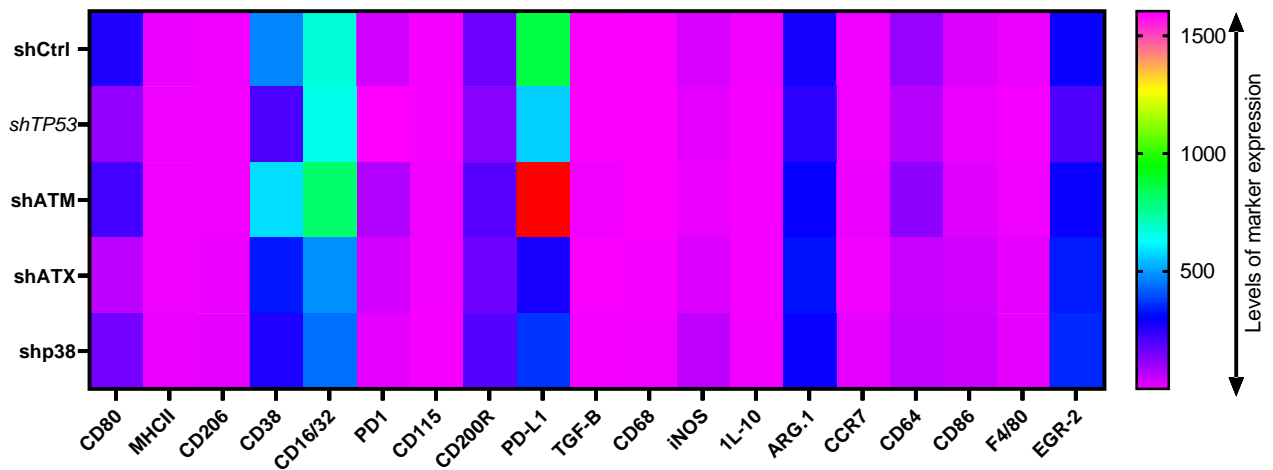


Figure 24: Expression pattern of activation markers in peritoneal macrophages following exposure to DDR gene KD tumor cells

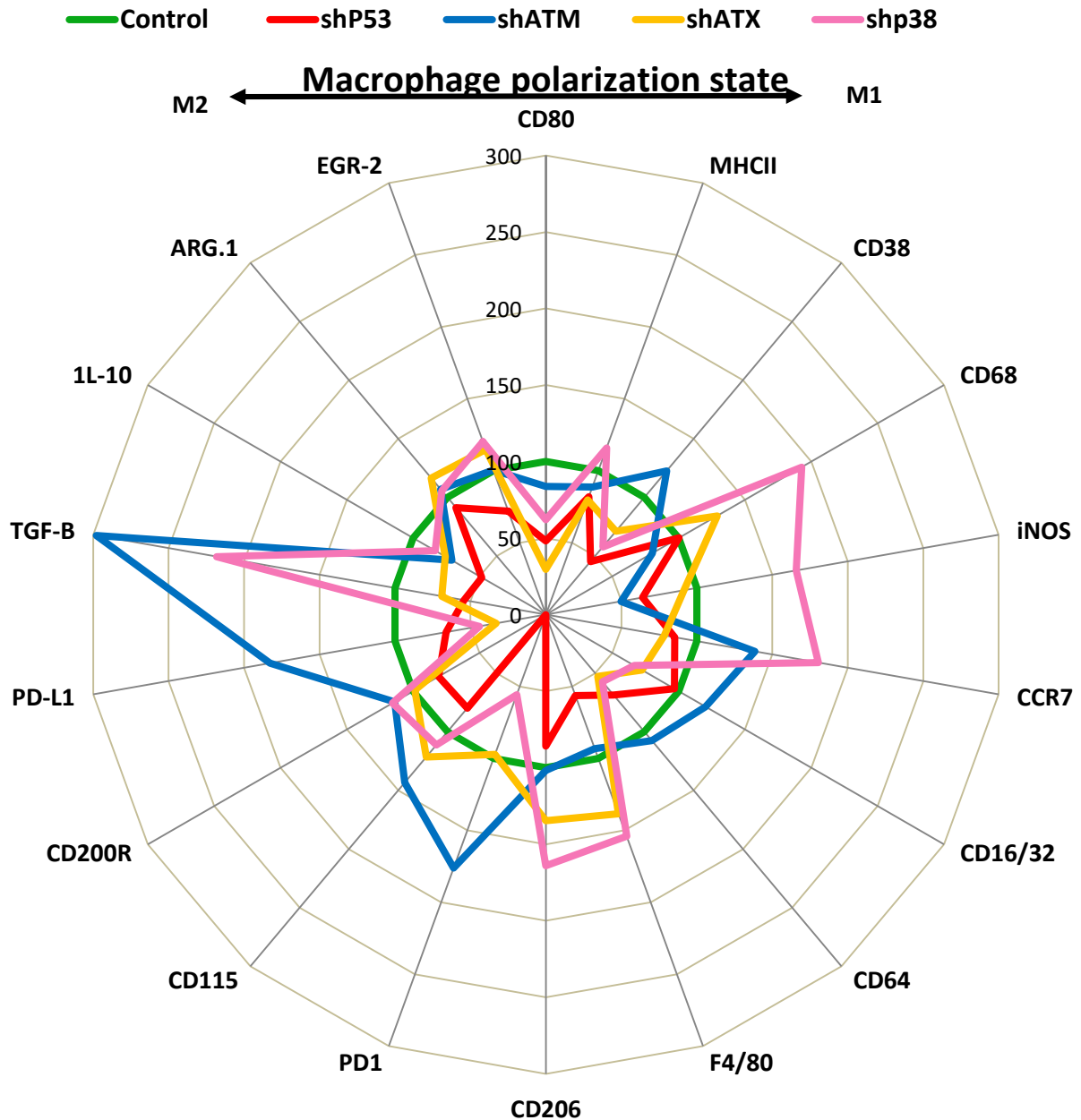


Figure 25: Phenotypic characteristics of mouse peritoneal macrophages cocultured with poorly phagocytosed tumor cells harboring KD of DNA damage response genes.

Phenotypic characteristics of thioglycollate induced mouse peritoneal macrophages exposed to mafosphamide stressed poorly phagocytosed tumor cells with DDR KD genes in a coculture setup. Isotype normalized median fluorescent intensities (MFI) of antigens are expressed as a percentage

relative to control (macrophage exposed to empty vector control cells) where for all antigens, expression of control is set to 100% on the radar plot. (**Green**=Macrophages exposed to empty vector control tumor cells, **red** =macrophages exposed to sh*TP53* tumor cells, **Blue** = macrophages exposed to shATM cells, **Yellow** = macrophages exposed to shATX cells, **Pink**=Macrophages exposed to shP38 cells) (n=2).

5.8 *TP53* is required for functional extracellular vesicles composition and optimum outcome of immune checkpoint inhibitors

In health, cells release secretomes consisting of growth factors, cytokines, chemokines, extracellular vesicles (EVs) and microRNAs to mediate inter-cellular communications. Secretion alterations thus reflect presence of atypical cellular phenotypes indicative of diseases. In cancer, tumor cells and associated stromal cells communicate directly via cell-cell contact and through a variety of molecules discharged as cellular secretome (425). Analysis of cellular secretome reveal differences in composition of tumor secretome compared to healthy cells from which the tumor arises. Thus a cell's secretome could reveals biomarkers of the disease and offer understanding of molecular mechanisms involved in its pathophysiology. Furthermore, it provides room for discovery of novel treatment strategies (426).

To further evaluate the functional differences observed between the secretomes of control cells and the DDR genes KD tumor cells, EVs were isolated from controls and *TP53* KD cells for functional antibody independent cellular phagocytosis (AICP) and antibody dependent cellular phagocytosis (ADCP) assays. Treatment of monocultures of target cells with exosomes from control and *TP53* KD cells showed no direct toxicity to target cells according to Annexin-V/7-Aminoactinomycin D (7-AAD) staining (Figure 37, Appendix). Using empty vector control cells as target and J774.1A macrophages as effectors, EVs of *TP53* KD tumor cells significantly ($p=0.0021$) reduced the level of antibody independent cellular phagocytosis (Figure 26A).

However, in the presence of anti-CD20 mAb, EVs of *TP53*KD cells induced a lesser antibody dependent cellular phagocytosis compared to the control although the decrease did not reach statistical significant ($p=0.5632$) (Figure 25B). Addition of anti-CD47 mAb significantly ($p<0.0001$) increased the level of ADCP of target cells (Figure 26C) and the level of phagocytosis could further be increased with EVs of control cells ($p=0.0009$) but not that of *TP53* KD cells ($p=0.8806$). This suggests that following CD47/SIRP- γ blockade with anti-CD47, EVs of cells with

functional DDR genes such as the control cells could trigger enhanced tumor cells phagocytosis by macrophages, a function which is lost in the presence of *TP53* gene KD.

Similar to the effect observed with anti-CD47, blocking PD-L1/PD-1 axis with Atesolizumab (anti-PD-L1), significantly increased ADCP ($p < 0.0001$) compared to anti-CD20 alone. Again, the level of ADCP achieved with anti-PD-L1 blockade could further be increased with EVs of control cells ($p = 0.0008$) but not that of *TP53* KD cells (Figure 26D). This highlights the importance of *TP53* gene to the functional constitution of the EVs cargo and suggests a fundamental role of *TP53* in EV's processes.

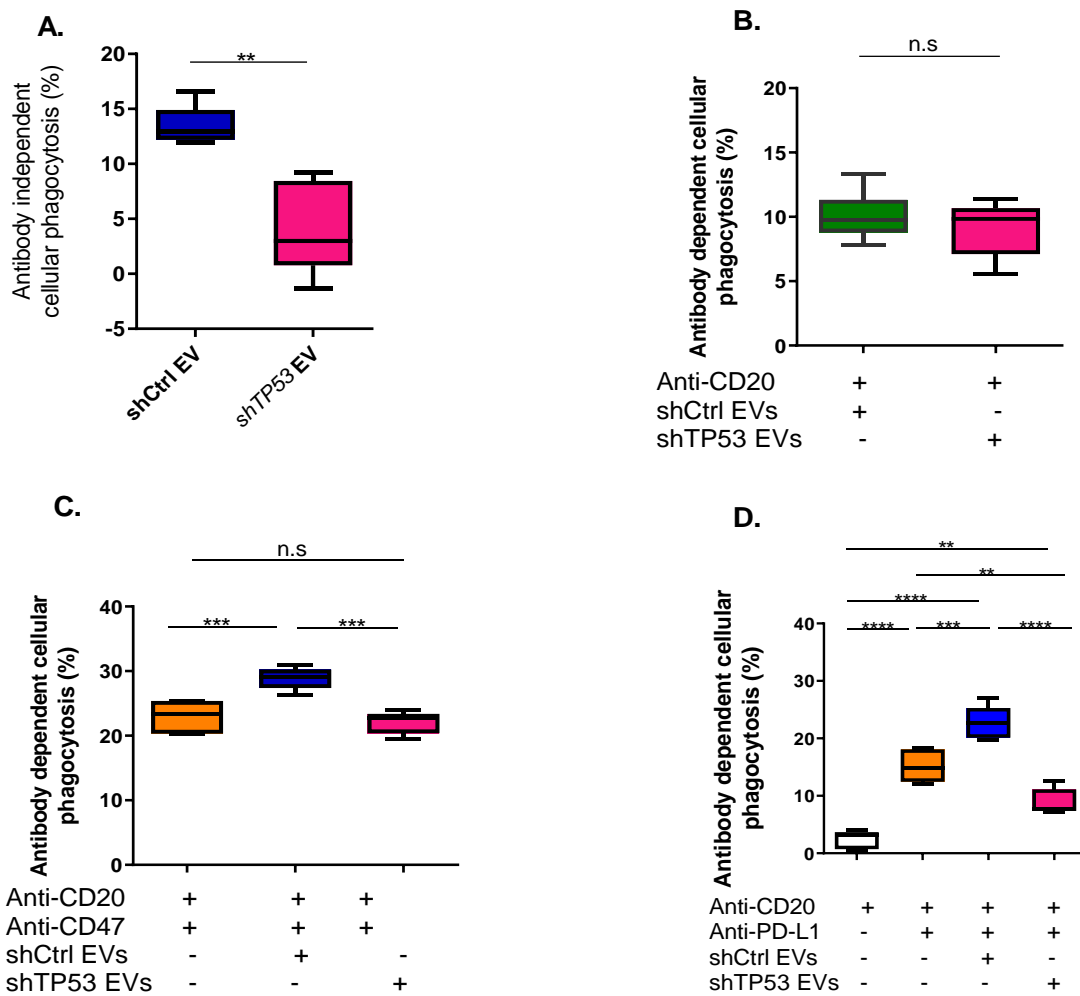


Figure 26: *TP53* KD changes the functional effect of the exosomal response to immune checkpoint antibody combinations

-
- A. Level of antibody independent cellular phagocytosis of target cells coculture with J774.1A macrophages. Cocultures were supplemented with 5µl of EVs from shCtrl or shTP53 KD cells.
 - B. Level of antibody dependent cellular phagocytosis of target cells with J774.1A macrophages. Cocultures were treated with anti-CD20 and 5µl of EVs from shCtrl or *shTP53* cells.
 - C. Level of antibody dependent cellular phagocytosis of target cells coculture with J774.1A macrophages. Cocultures were treated with combination of anti-CD20 mAb and anti-CD47 antibody or with addition of 5µl EVs from shCtrl or *shTP53* cells.
 - D. Level of antibody dependent cellular phagocytosis of target cells coculture with J774.1A macrophages. Cocultures were treated with combination of anti-CD20 mAb and anti-PD-L1 antibody or with addition of 5µl EVs from shCtrl or *shTP53* cells. All cocultures were incubated for 16hrs. (* = $p < 0.05$, ** = $p < 0.01$, *** = $p < 0.001$, **** = $p < 0.0001$).

5.9 Unraveling the Molecular Signature of “Tropical” African Chronic Lymphocytic Leukaemia (CLL) – The Ghanaian Cohort

5.9.1 General introduction and objectives

In the developed countries such as the United States and Western Europe, CLL is the commonest adult leukemia with a median age of incidence of 71yrs and a preferential male predominance of disease cases (427, 428). Recognized as a heterogeneous disease of variable clinical course, CLL presents with variable pathogenetic etiologies with demonstrable genetic lesions including chromosomal deletions, trisomy and translocations (65). Despite the clinical heterogeneity in CLL presentation, the B-cell immunoglobulin receptor mutational status distinctly separates CLL into two subtypes of different progression outcomes. CLL that expresses B-cell immunoglobulin receptor showing $\geq 98\%$ homology to the germline sequences are described as unmutated, is associated with poor disease prognosis (68) whereas CLL that expresses $< 98\%$ homology to germline receptor is described as mutated and associated with good disease prognosis (429).

Additionally, high expression of surrogate markers including zeta-associated protein of size 70 kDa (ZAP-70) and CD38 are characteristics of unmutated CLL subtype associated with poor prognosis (430-432). ZAP-70 is a cytoplasmic protein tyrosine kinase usually associated with T-cell receptor but could be found in a subset of CLL patients where it participate in B-cell receptor (BCR) signaling due to its resemblance to the spleen tyrosine kinase (Syk) whilst CD38 is a multi-

functional cyclic adenosine diphosphate ribose (cADP) hydrolase enzyme. In Western countries, 40-50% of CLL patients present with unmutated immunoglobulin heavy variable (IgHV) gene whilst 50-60% present with somatically mutated IgHV.

Differences have been reported in incidence, epidemiology and clinical features of CLL among different racial groups and geographical settings. This may reflect unique features due to different genetic and environmental factors. In tropical Africa, CLL is diagnosed in an increasingly youthful population with 50% of participants in one study being less than 45 years reported (433), a rate far higher than 11% <55yrs from the Surveillance, Epidemiology, and End Results (SEER) study (427) and 7-20% from other studies from Europe. Again, contrary to the male predominance incidence of 2:1 in the USA and Western Europe, a female predominant incidence of 3:1 (434) and 2:1 (435) is observed in tropical African countries.

Basic data on molecular signatures of CLL, characterizing the phenotypic expressions of the malignant B-cells, their IgHV mutational status or established prognostic surrogates' patterns are scanty in the literatures on CLL patients in sub-Saharan Africa (433, 434, 436, 437).

Thus this work aims to establish phenotypic characteristics of a cohort of Ghanaian CLL patients by determining phenotypic expression of diagnostic as well as prognostic markers and explore any existing inter-relationships.

5.9.2 Demographic characteristics of recruited CLL patients

A total of fifty (50) informed and consented suspected CLL patients were recruited from the Oncology Department of Komfo Anokye Teaching Hospital, Kumasi – Ghana. All recruited participants were out-patients and convenient sampling was applied until the 50 recruitment target was reached. Peripheral blood mononuclear cells (PBMC) were separated by density gradient centrifugation on Ficoll-Paque medium for onward shipment to CECAD, University of Cologne, Germany where analysis were performed. Of the 50 recruited patients, 45 (90%) were immunophenotypically confirmed as CLL based on peripheral blood lymphocytosis ≥ 5000 cell/ul and co-expression of CD19+ CD5+ and CD23+ on the malignant B-cells by an independent Hematologist. The remaining 5 (10%) had other blood malignancies. Of the confirmed CLL patients, females formed the majority with a representation of 51.1% (n=23) whereas males constituted the remaining 48.9% (n=22). The median age of patients were 56yrs for males (range,

22-78) and 59yrs for females (range, 17-84). At recruitment, 28.9% (n=13) of the patients presented with organomegaly including lymphadenopathy of cervical, axillary, inguinal which were local or multi-nodular sites. Similarly, patients also presented with splenomegaly (28.9%, n=13) which was massive in size (>6cm below the costal margin) in 15.6 % (n=7) and hepatomegaly (17.8%, n=8). Eleven (24.4%) of the recruit at the time of enrolment had started combinatorial chemotherapy treatment including agents such as cyclophosphamide, doxorubicin, chlorambucil, mephalan, vincristine, dexamethosone and prednisolone as shown in Table 8.

Table 8: Basic demographics of recruited patients

	Total n (%)	Male n (%)	Female n (%)
Study Participants	50(100%)	25(50%)	25(50%)
Confirmed CLL	45(90.0%)	22(44.0%)	23(46.0%)
Non-CLL Diseases	5(10%)	3(6.0%)	2(4.0%)
Confirmed CLL Patients			
Median Age(yrs)	59(17-84yrs)	56(22-78)	59(17-84)
≥55yrs	26(57.8%)	11(24.4)	15(33.3)
<55yrs	19(42.2%)	11(24.4%)	8(17.8%)
Organomegaly			
Lymphadenopathy	13(28.9%)	8(17.8%)	5(11.1%)
Splenomegaly	13(28.9%)	8(17.8%)	5(11.1%)
Hepatomegaly	8(17.8%)	3(6.7%)	5(11.1%)
On Treatment			
On Treatment	11(24.4%)	5(11.1%)	6(13.3%)

5.9.3 Hematological profile of CLL patients

Consented CLL patients were evaluated for complete blood count using Sysmex KX 4000i hematology analyzer (Sysmex Corporation, Kobe, Japan) upon enrolment to determine total white blood cell (WBC) count, red blood cell (RBC) counts, platelets counts, hemoglobin concentration determination together with the red blood cells indices. The different blood cells parameters between male and female CLL patients were then compared using Mann-Whitney test for non-parametric variables to compute significant differences between genders. Stratification of hematological parameters of CLL cohort using the normal reference ranges applicable for age and gender established for the geographical jurisdiction of the patients (438) revealed that >95% of CLL patients presented with leukocytosis (Table 9).

This was reflected in the median leukocyte counts obtained in both sexes ($63.6 \times 10^9/L$ (range, 5.8-579.4) and $60.46 \times 10^9/L$ (range, 7.7- 609.2)) in males and females respectively (Figure 27B)

compared to 5.47 and 5.62 ($\times 10^9/L$) established for the corresponding gender of the healthy population (438).

Total WBC count in the CLL cohort was comparably similar between the male and female patients ($p=0.5142$). Flow cytometer assessment of leukaemic CD19+CD5+ double positive B-cells (Figure 27C) showed that marked leukocytosis were due to lymphocytosis CD19+CD5+ expressing malignant B-cells whose count did not differ between male and female patients ($p=0.8835$).

Platelet counts is another critical variable in CLL as together with hemoglobin and organomegaly influences the staging of the disease and to a large extent initiation of treatment intervention. Platelet counts were reduced in half of our CLL patients at enrolment (Table 9).

Platelets count did not significantly differ between male and female patients ($p=0.572$) (Figure 27D) however, compared to healthy adult within the geographical jurisdiction (median platelets, male = $186 \times 10^9/l$, female = $214 \times 10^9/l$) platelets counts in the CLL group was remarkably reduced (median platelets count, male = $95.0 \times 10^9/l$ (range, 6.0 - 411.0); female = $109.0 \times 10^9/l$ (range, 24.0 - 299.0)).

Assessment of anaemia using hemoglobin concentration showed that 68.2% ($n=15$) of the male CLL patients had reduced hemoglobin levels compared to 26% ($n=6$) of the females when patients are stratified using reference ranges established for the geographical location (Table 9).

The fewer number of female CLL patients with anemia is as a result of a lower limit of the established hemoglobin reference range in the geographical area of the study (males = 10.69 - 18.76g/dL and females = 8.19 - 16.17g/dL) compared to (13.0-18.0g/dl for males and 11.5 - 16.5g/dl for females) in the developed world. Thus, if the hemoglobin reference applicable to most Western countries are used, 81.8% ($n=18$) of the male and 91.3% ($n=21$) of the females in this study would have reduced hemoglobin (Hb) levels, signifying anemia. Expectedly, the median hemoglobin levels (Male, Hb=8.85g/dl (range, 5.5-13.8); female, Hb=8.70g/dl (range, 5.6-11.9)) (Figure 27E) and red blood cells (RBC) count (Male, RBC= $3.06 \times 10^{12}/l$ (range, 1.70- 4.74); female, $3.09 \times 10^{12}/l$ (range, 1.18-4.72)) (Figure 27F) in the CLL patients group was found to be low compared to (Male, Hb=15.2g/dl; female, Hb=12.50g/dl) and red blood cells (RBC) count (Male, RBC = $5.19 \times 10^{12}/l$; female, RBC= $4.38 \times 10^{12}/l$) of the adults in the geographical region (438). However, both hemoglobin levels ($p=0.788$) and RBC counts ($p=0.996$) did not significantly differ between the male and female CLL patients.

Table 9: Stratification of full blood count of CLL patients by the normal reference ranges

Parameter	Male	Reference ranges	Female	Reference ranges
WBC count				
Increased	21 (95.5%)	(3.28 - 11.23)x 10⁹/L	22 (95.7%)	(3.25 - 10.64)x 10⁹/L
Normal	1 (4.5%)		1 (4.3%)	
RBC count				
Normal	8 (36.4%)	(3.61 - 6.97)x 10¹²/L	13 (56.5%)	(3.08 - 5.88)x 10¹²/L
Low	14 (63.6%)		10 (43.5%)	
Hemoglobin				
Normal	7 (31.8%)	(10.69 - 18.76)g/dL	17 (74.0%)	(8.19 - 16.17)g/dL
Low	15 (68.2%)		6 (26.0%)	
Platelets count				
Increased	1 (4.5%)	(85.93 - 348.2)x 10⁹/L	0	(110.95 - 416.3)x 10⁹/L
Normal	10 (45.5%)		10 (43.5%)	
Low	11 (50%)		13 (56.5%)	

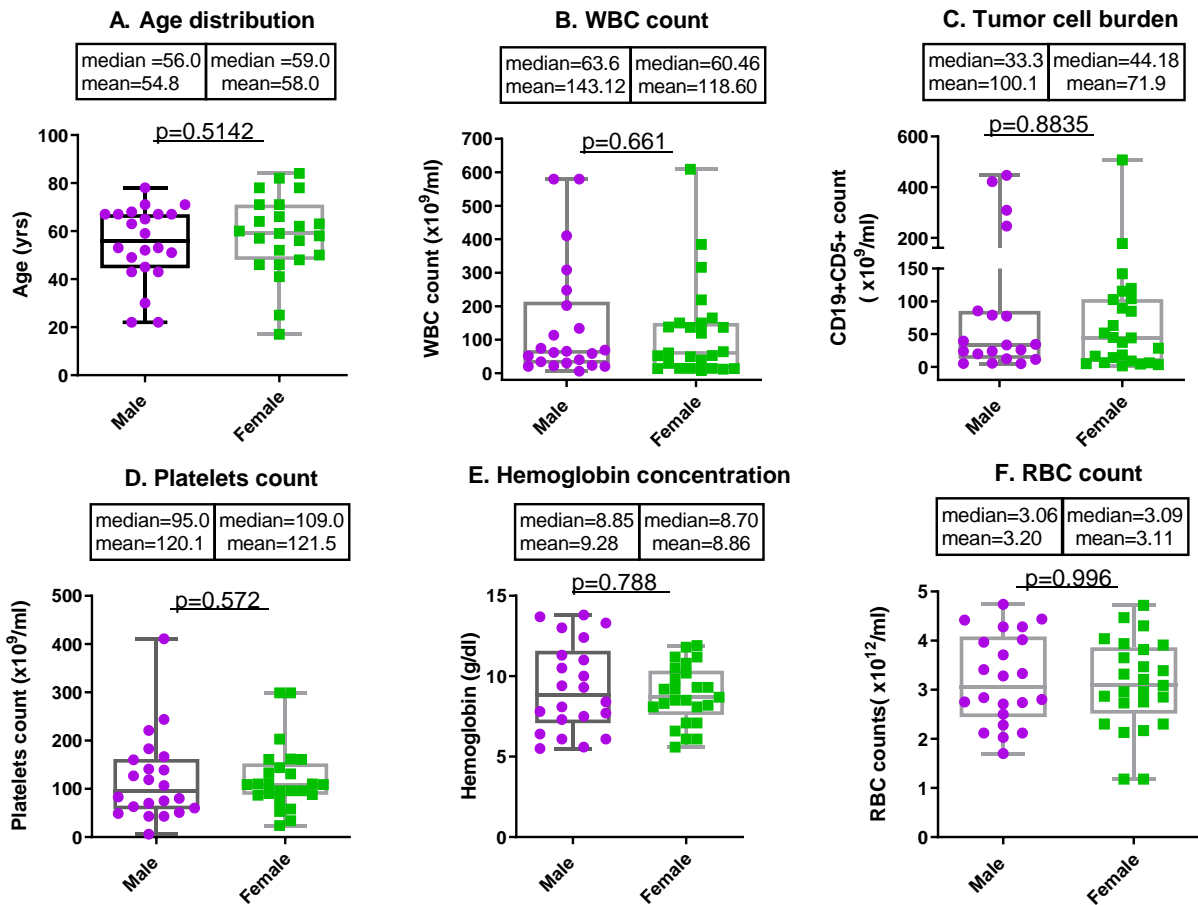


Figure 27: Complete blood count profile of CLL patients

- A. Age distribution of CLL study participants
- B. Distribution of Total white blood cells count according to gender of study participants.
- C. Distribution of CLL B-lymphocytes co-expressing C19+/CD5+ among study participants
- D. Distribution of Platelets count among study participants
- E. Hemoglobin concentration distribution among study participants
- F. Red blood cells distribution of study participants

*All variable were analyzed using Mann-Whitney test for non-parametric variables. P-value $p < 0.05$ was deemed significance. Results are presented as scatter plots showing range values, median (line at the middle of the box) and 25th and 75th quartile ranges.

5.9.4 Ghanaian CLL patients present with advance clinical stages of the disease at diagnosis

CLL remains currently an incurable disease with conventional chemotherapy or chemo-immunotherapy as available management options and possibility of cure only achievable through allogeneic stem cell transplantation (439). As a heterogeneous disease in clinical course, some patients may never need an intervention whereas in others, the disease rapidly transform into an aggressive DLBCL-like disease termed Richter's Transformation, with fatal outcome within a year. Staging of CLL patients thus enables earlier intervention for patients who may benefit from treatment. Rai (440) and Binet (441) staging system are the two of the most clinically accepted options of CLL staging.

In this study, patients were staged according to the Binet criteria (Figure 28A). Of the total CLL patients, 13.6% (n=6) presented at Binet stage A (Figure 28B), 50% (n=22) at stage B and the remaining 38.4% (n=18) at stage C. In comparison to a single center study in Europe (Lublin-Poland) where Binet clinical staging criteria was used to stratify 112 CLL patients, 37% were at Binet stage A, 47% at stage B and 18% at stage C (442) This support the notion that a greater percentage of the Ghanaian CLL patient present with advance clinical stages than is seen elsewhere.

Binet Stage	Definition
A	<ul style="list-style-type: none"> • Haemoglobin $\geq 10\text{g/dl}$ • Platelets $\geq 100,000/\mu\text{l}$ • < 3 affected regions² (LN¹, liver or spleen)
B	<ul style="list-style-type: none"> • Haemoglobin $\geq 10\text{g/dl}$ • Platelets $\geq 100,000/\mu\text{l}$ • ≥ 3 affected regions² (LN¹, liver or spleen)
C	<ul style="list-style-type: none"> • Haemoglobin $< 10\text{g/dl}$ • Platelets $< 100,000/\mu\text{l}$

Legend

¹ LN – Lymph nodes

² The Regions (n=5), include cervical, axillary, inguinal lymph nodes enlargement (unilateral or bilateral), liver and spleen enlargement (detection only upon physical examination)

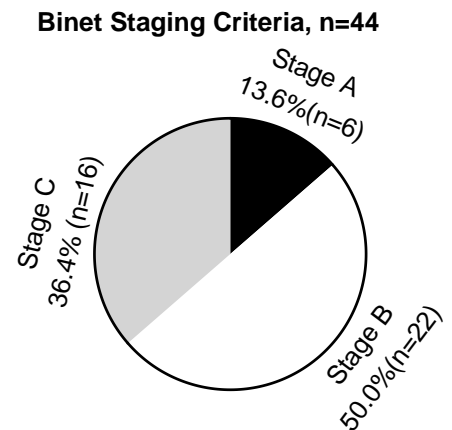


Figure 28: Binet staging criteria and stratification of Ghanaian CLL patients

5.9.5 Challenges of geographic specific hematology reference ranges and Binet staging system

Binet stage C is considered a trigger criteria for treatment intervention; however in our study only 25% (n=11) patients were on chemotherapy treatment (Table 8).

The large number of Ghanaian CLL patients who present at stage B and C relative to few on treatment could also be as a result of existing geographic specific established hematological reference ranges which were lower compared to reference ranges applicable to those in the Western countries. The lower hemoglobin and platelets reference level observed among the dissidents of this geographic region (438) forces a lower score on the Binet system in this patients group.

5.9.6 Expression of surface immunoglobulin IgM and IgD in CLL

5.9.6.1 General introduction

The ultimate aim of B-cell ontogeny is the production of a flexible immune cell repertoire that is capable of recognizing and eliminating a huge array of antigens confronted by the immune system. Additionally, BCR expression is essential for the survival of mature B-cells (443). Generation of B-cell receptor diversity is thus critical to permit immunological capability to respond to vast antigens routinely confronted. The BCR complex is composed of two major components: the recognition portion constituted by surface membrane-bound immunoglobulin (sIg) and the transmission portion

composed of co-receptors such as CD79a and CD79b. The sIg is a heterodimer of two (2) heavy chains (IGH) and 2 light chains (Ig Kappa or Ig Lambda) linked by disulfide bonds. Each immunoglobulin chain consists of N-terminal variable (V) domain which binds the antigen, and the C-terminal constant (C) domain responsible for membrane insertion and various effector functions (444). The C-domain determines the type of immunoglobulin isotype of the BCR. Five (5) different isotypes of immunoglobulin exist: IgM, IgG, IgA, IgE and IgD. At each developmental stage of the B-cell, different isotype of immunoglobulin is produced through alternative splicing of common IgM and IgD mRNA transcript and Class Switch Recombination. Thus differential splicing of long primary mRNA transcripts is the main mechanism of simultaneous expression of IgM and IgD B-cell repertoire.

In CLL, dim expression of surface IgM (sIgM) and IgD (sIgD) are reported although the exact proportion and combination varies (445). Thus in this group of African CLL patients, we aimed to determine the pattern of expression of IgM and IgD B-cell receptor isotypes in peripheral blood and explore its relationship to established prognostic and biologic variables to determine possible effect on the biology of CLL.

5.9.6.2 Threshold for immunoglobulin positivity and statistical analysis

To categorize CLL cells on the positivity of expression of Ig isotype, a threshold of $\geq 30\%$ of CD19+CD5+ cells expressing a particular surface immunoglobulin was deemed as positive whilst for an immunoglobulin light chains (kappa and Lambda) the expression $<5\%$ of CD19+CD5+ cells was classified as negative .

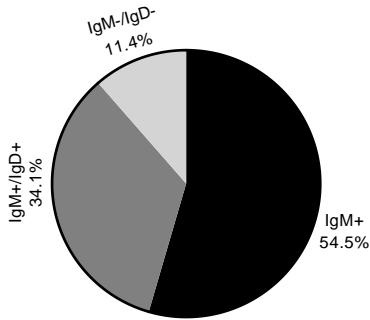
Proportion of patients expressing immunoglobulin isotypes were presented as percentages and expression of sIgM and IgD in a patient was compared by Wilcoxon paired sign ranked test. Correlation of IgM and IgD expression was determined by Spearman rank test and expression effect of sIgM on sIgD was assessed by linear regression. P-value < 0.05 was deemed significant in all computations.

5.9.6.3 Surface IgM and kappa light chains are dominant isotypes of immunoglobulin in CLL patients

More than half of CLL patients (54.5%) in our study expressed monotypic sIgM isotype whereas one-third (34.1%) expressed both IgM and IgD isotypes. None of the CLL patients in our study expressed only IgD isotype however, for 11.4% of our patients; dual IgM/IgD expression fell short

of threshold for positivity (Figure 29A). The presence of other BCR isotypes such as IgA, IgG and IgE were not tested for in this study. When the expression of sIgM is compared to IgD, sIgM is significantly highly expressed than IgD (median 90.72% , range, 0.4900- 99.94 vs median 10.22, range , 0.0300- 97.67, $p < 0.0001$) (Figure 29B). By plotting expression of sIgM against sIgD, it can be seen that there is a moderate positive correlation between IgM and IgD expression ($n=44$, $r=0.388$, $p= 0.0092$) (Figure 29C) however, a linear regression of $r^2 = 0.1399$ indicates a very weak relationship which may not be biologically significant. The lack of strong correlation of IgM vs IgD expression within patients may suggest that expression levels of IgM and IgD may be independently regulated which may explain their differential responses to antigen although it's expected that the clonality of IgM and IgD should lead to recognition of the same antigen. Fifty – seven percent (57%) of the CLL patients showed monotypic restriction of immunoglobulin light chain expression. Of these patients, 31.8% ($n=14$) showed Ig kappa (IgK) restriction and 25% ($n=11$) showed Ig lambda (λ) restriction. Eight patients (18.2%) expressed both IgK and Ig λ whereas the remaining 25% ($n=11$) were classified as double negative for IgK/Ig λ expression for having $<5\%$ of CD19+CD5+ cells expressing Ig light chains (Figure 29D). Surface IgM expression of CD19+CD5+ cells among different clinical stages (Binet criteria) of CLL showed similar levels of expression (Figure 29E₁) with all patients at stage A being positive for IgM expression, 81.8% ($n=18$) of patients in stage B and 93.8% of patients in stage C expressing IgM positivity (Figure 29E₂). Similarly, sIgD expression level did not significantly differ with clinical stage of CLL (Figure 29F₁), however, proportion of patients positive for IgD expression increased with increasing clinical stage from clinical stage A (16.6%), stage B (30.4%) to stage C (43.8%) (Figure 29F₂).

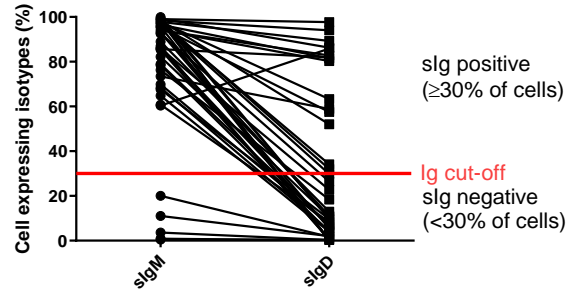
A. Surface IgM and IgD expression of CLL patients, n=44



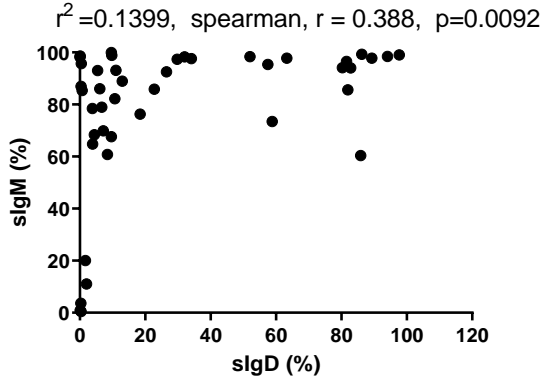
B. IgM vs IgD expression, n=44

Median =90.72% Mean=78.83%	Median=10.22% Mean=29.34%
-------------------------------	------------------------------

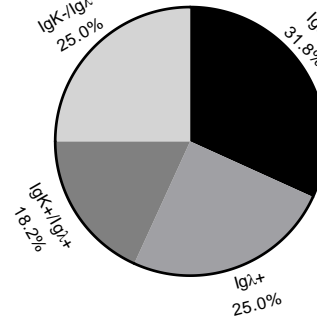
Wilcoxon paired signed rank $p < 0.0001$



C. Expression of IgM vs IgD for 44 CLL patients



D. Ig light chains expression, n=44



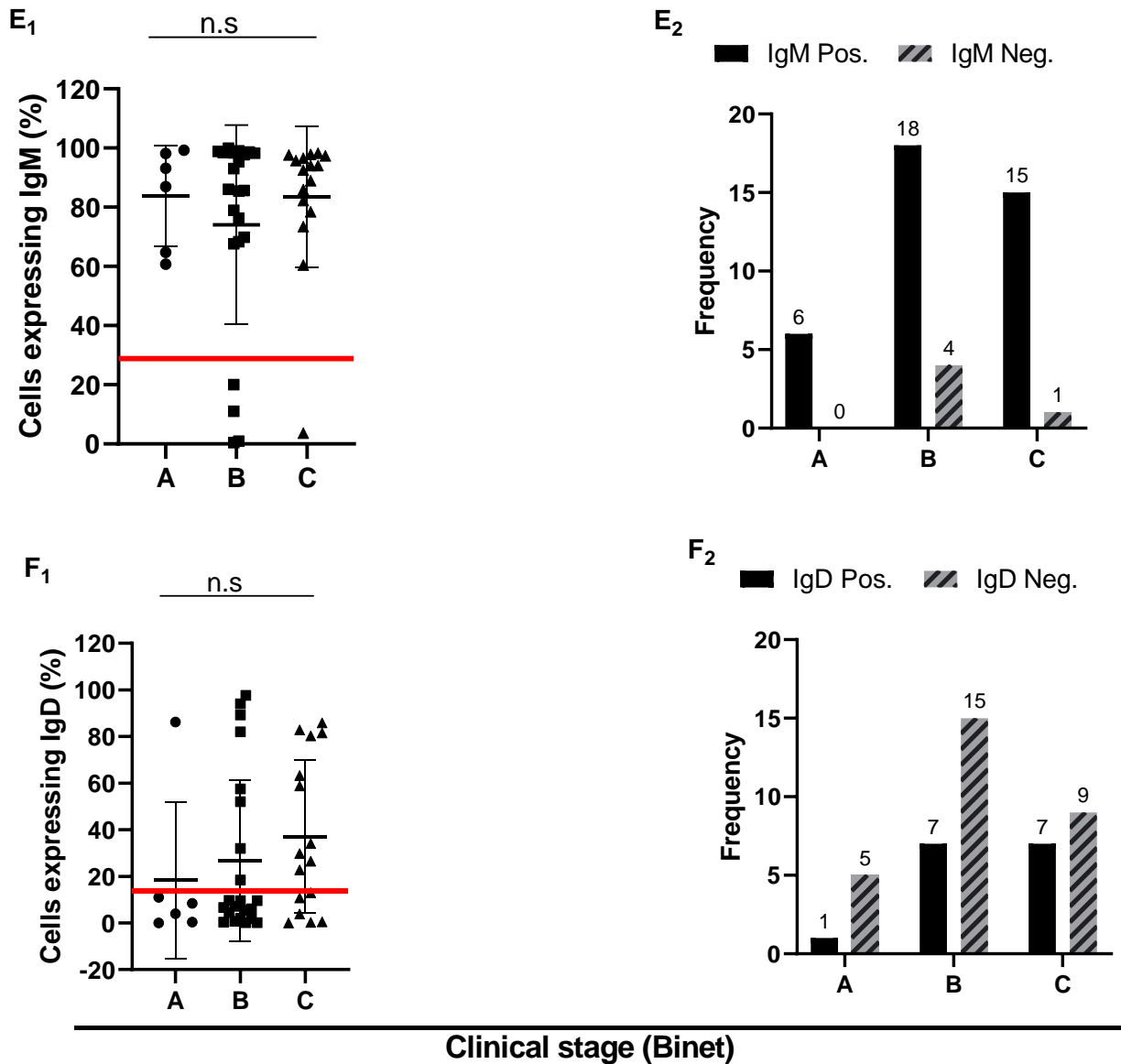


Figure 29: Surface immunoglobulin expression pattern in CLL patients

- A. Percentage expression pattern of surface IgM and IgD immunoglobulin in CLL patients. sIg were gated on CD19+CD5+ cell population and a cut-off of $\geq 30\%$ of total cells expressing sIg was deemed positive for sIg expression.
- B. Scatter plot of sIgM vs IgD expression of CLL patients. Red line indicates $\geq 30\%$ expression threshold to determine positivity of Ig expression.
- C. Scatter plot showing Spearman correlation of sIgM to sIgD in CLL patients.

- D. Percentage expression pattern of surface Ig light chains Ig kappa (IgK) and Ig lambda (λ) in CLL patients. Light chains expression $\geq 5\%$ of gated on CD19+CD5+ cell were deemed positive for expression.
- E. Comparison of surface IgM expression with clinical stage of disease (E_1) and frequency distribution (E_2)
- F. Comparison of surface IgM expression with clinical stage of disease (F_1) and frequency distribution (F_2)

5.9.7 ZAP-70 and CD38 expression in CLL patients

5.9.7.1 General introduction and aim

Normal B-cells present a B-cell receptor (BCR) which comprises of surface immunoglobulin coupled to signal transduction subunit of CD79A and CD79B. Antigen encounter and BCR clustering promotes phosphorylation of the immuno-receptor tyrosine-based activating motif (ITAM) by Src-family kinases including Lck/Yes novel tyrosine kinase (Lyn), Fyn and B-lymphocyte kinase (Blk). Phosphorylated immuno-receptor tyrosine kinase activation motif (ITAM) then recruit spleen tyrosine kinase (Syk), Bruton tyrosine kinase (BTK) and phosphatidylinositol-kinase subunit delta (PI3K δ) to engage pathways including nuclear factor kappa beta (NF-KB), rat sarcoma (RAS) and mitogen-activated protein kinases (MAPK) to effect B-cells proliferation and survival.

In CLL high expression of, ZAP-70 is found to be associated with the BCR in a sub-group of patients who present with worse prognosis (431, 446). Here, ZAP-70 couples to the BCR and up-regulate Syk phosphorylation and activation as well as downstream signaling events (447). However, recent observation of similar levels of Syk kinase expression in both ZAP-70+ and ZAP-70- patients led to a confirmation that ZAP-70 could induce BCR signaling independent of its kinase activity (448). The mutational status of the BCR could predict the course of the disease (68). CLL with unmutated IgHV is associated with poor prognosis, whilst that with mutated IgVH Gshows good prognosis(68). Gene expression profiling has revealed that, ZAP-70 expression is specifically associated with CLL with BCR immunoglobulin heavy chain showing > 98% homology to the germline Ig sequence (431). Thus, ZAP-70 expression in CLL B-cells was established as a prognostic indicator which can be used to stratify CLL into two subtypes of good

prognosis or worse prognosis. ZAP-70 has been shown to be remarkably stable and a threshold of $\geq 20\%$ of CD19+CD5+ cells is recommended as the threshold for positivity (449).

CD38 is a transmembrane glycoprotein expressed in high amount on the surface of some leukemic cells. It functions as both a cell surface enzyme and a surface receptor, was one of the earlier factors found to correlate to IgHV mutational status. CD38 expression on CLL cells was shown to have prognostic value (450, 451). As more light was shed on CD38 expression, controversies arose about its use as prognostic factor as other researcher failed to recapitulate the published results (452, 453) while other identified variations in CD38 expression over time (454). Additionally, the threshold to ascribe CD38 positivity had remained very controversial with different cut-off such as 7%, 20%, and 30% of CD19 + CD5+ expression having been used by different researchers (455, 456).

To ascertain the prognosis of the CLL cohort, assessment of the expression levels of ZAP-70 and CD38 on gated CD19+CD5+ double positive cells were carried out by flow cytometry. Additionally, prognostic factors were correlated to Ig isotypes expression and other biologic variables to decipher any biologic influence on the disease pathology. In all cases, threshold of $\geq 20\%$ of CD19+CD5+ cells was considered positive for ZAP-70 expression whilst a threshold of $\geq 30\%$ of CD19+CD5+ cells was considered positive for CD38.

5.9.7.2 Prognostic factors

Using ZAP-70 expression to infer prognosis, 20.5% (n=9) of the CLL patients in the study show poor prognosis (Figure 30A). This was found to be very similar to prognostic evaluation using CD38 expression where 18.2% (n=8) patients have poor prognosis (Figure 30B).

Thus about 80% of CLL patients assessed at recruitment have a favourable course of the disease.

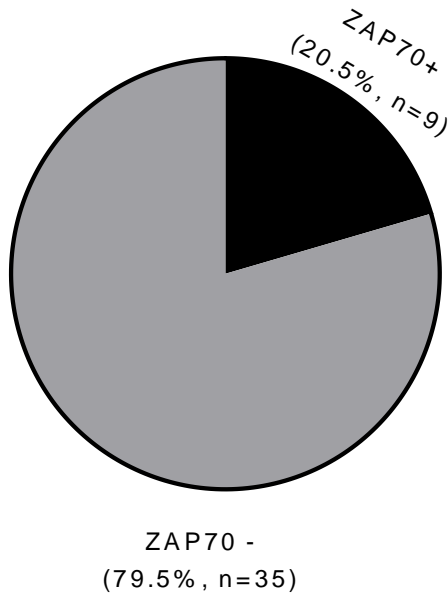
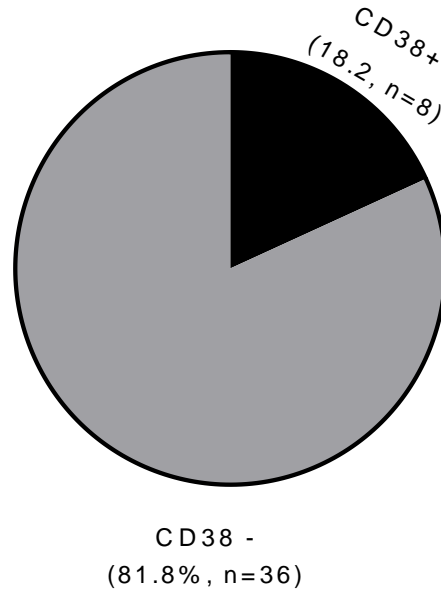
A. ZAP-70 expression**B. CD38 expression**

Figure 30: Prognostic assessment of CLL patients using ZAP-70 and CD38 expression

- A. Percentage distribution of ZAP-70 expression of CLL patients. Patient was deemed ZAP-70+ if $\geq 20\%$ of CD19+CD5+ cells express ZAP-70 by flow cytometry
- B. Percentage distribution of CD38 expression of CLL patients. Patient was deemed CD38+ if $\geq 30\%$ of CD19+CD5+ cells expresses CD38 by flow cytometry.

5.9.7.3 Relation of prognostic markers to sIg isotypes and other biologic variables

The association of surface immunoglobulin with prognostic markers such as ZAP-70 and CD38 expression was explored using Mann-Whitney test. Here, expression levels of sIgM (Figure 31 A) and sIgD (Figure 31B) were stratified by ZAP-70 positivity or otherwise. Interestingly, sIg expression between ZAP-70 positive and negative CD19+CD5+ CLL cells did not vary significantly ($p=0.55$ and 0.455 respectively) suggesting that sIgM and IgD expressions have no effect on prognostic stratification of CLL. Also, CD38- CLL patients significantly expressed higher levels of sIgM ($p=0.022$) than CD38+ patients (Figure 31C). However, IgD isotype expression was relatively similar ($p=0.182$) regardless of CD38 positivity or otherwise (Figure 31D). Receptor

tyrosine kinase – like orphan receptor 1 (ROR1) act as a receptor for Wnt5a to form a complex with TCL-1 to promotes CLL survival and proliferation through AKT activation (457, 458). Additionally, the binding of ROR1 to cortactin recruits RhoA to mediate actin polymerization which enhance migration of tumor cells (459). Thus, although ROR1 expression is variable in CLL patients (460) contrary to earlier perception (461), its high expression is associated with unfavorable prognosis in CLL (462).

Here, evaluation of ROR1 expression in CLL patients relative to sIgM and IgD showed no significant difference ($p=0.2136$ and 0.5690 respectively, Figure 31E and F).

Similarly, expression of ROR1 by malignant B-cells did not significantly differ with ZAP-70 ($p=0.927$) and CD38 statuses ($p=0.7153$) (Figure 31G-H).

Taken together, these results suggest that the expression levels of BCR in peripheral blood of CLL have very little effect on the disease biology. It is suggestive that since proliferation of CLL cells occur in the microenvironment of the lymph nodes and bone marrow; perhaps the emigrated tumor cells in the peripheral blood do not reflect events within the tumor microenvironment.

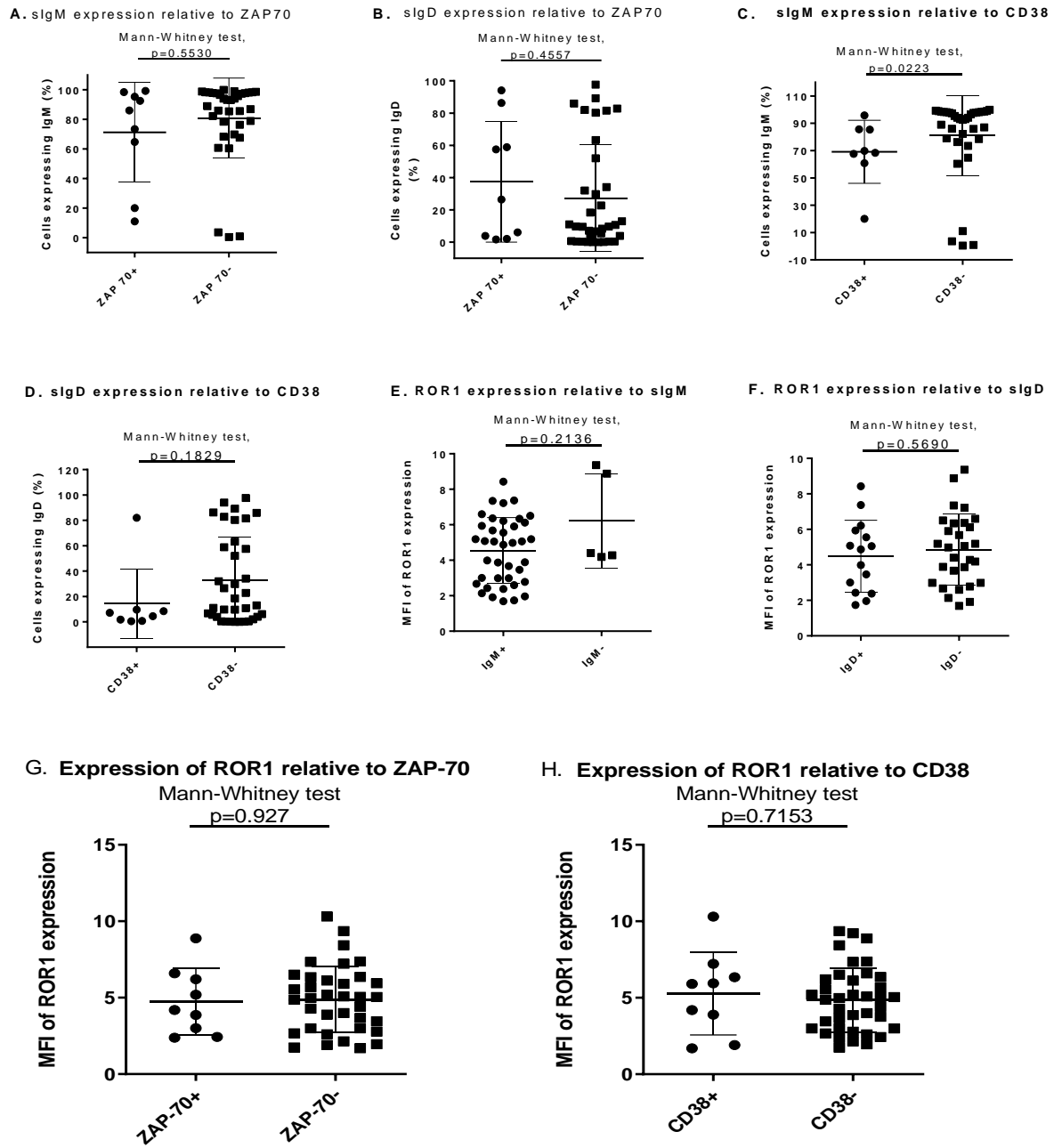


Figure 31: The expression levels of surface immunoglobulin in various groups defined by published prognostic factors

5.9.8 Expression of immune checkpoint antigens on peripheral CD19+CD5+ CLL cells

5.9.8.1 General introduction and aims

The tumor microenvironment is often infiltrated by different types of innate and adaptive immune cells whose immune surveillance roles may be hindered by many mechanisms (463). Immune checkpoints are a group of receptor-based signal cascade molecules which function as part of the immune system and regulate homeostasis of immune response to prevent inflammatory tissue damage, auto-immunity (336, 464) and ensure self-tolerance (465). In a variety of human cancers, immune checkpoint antigens are elevated particularly within the tumor microenvironment to enable immune surveillance evasion and gain immune tolerance (466). Beyond the initial discovery of cytotoxic T-lymphocyte-associated protein 4 (CTLA-4) (467) and programmed cell death protein 1 (PD-1) and its ligand (PD-L1 and PD-L2) (468), several other immune checkpoint molecules including lymphocyte-activation gene 3 (LAG-3) (469), T-cell immunoglobulin and mucin-domain containing-3 (TIM-3) (470) and, CD47-Sirp- α , CD200, have been reported.

The development of several checkpoint inhibitor antibodies have demonstrated remarkable effectiveness against immune checkpoint antigens in specific lymphoma subtypes, including classical Hodgkin lymphoma and primary mediastinal B-cell lymphoma (336).

Recent immunogenomic data suggest linkage between tumor mutational burden, prevalence of neo-antigens and tumor-associated antigens with efficacy of immune checkpoint inhibitors (471, 472).

Thus expression levels of some immune checkpoint proteins of the CLL cohort were determined and their correlations with prognostic markers were explored. Higher levels of CD47 proteins were expressed on peripheral CD19+CD5+ tumor cells compared to CD200 ($p < 0.0001$), PD-1 ($p < 0.0001$), and PD-L1 ($p < 0.0001$). By categorizing expression of prognostic factor, ZAP-70 into positive and negative sub-groups according to published criteria (449), differential expression of the immune checkpoint proteins between the sub-groups using Mann-Whitney test were explored. Here, CD47 expression was relatively lower in ZAP-70 negative CLL patients compared to ZAP-70 positive, however, the difference does not reach statistical significance ($p = 0.2047$). Similarly, expression differences of PD-1 ($p = 0.3855$) and PD-L1 ($p = 0.4325$) among ZAP-70 positive and negative sub-groups were insignificant. (Figure 32, B, D, and E respectively). However, expression of CD200 was significantly reduced in ZAP-70 negative patients compared to ZAP-70 positive counterparts ($p = 0.0433$). In brief, immune checkpoint expression of CD47, PD-1 and PD-L1 is not

affected by prognostic status of ZAP-70. However, high expression of CD200 in ZAP-70 positive CLL patients may provide a potential target for immunotherapeutic combination treatment in this CLL sub-group. Interestingly, bimodal distribution of PD-L1 expression in ZAP-70 negative group (Figure 32E) prompted a further probe using PD-L1 MFI cutoff ≥ 6 to distinguish high PD-L1 expression (n=18) from MFI <6 of low PD-L1 expression (n=17).

Using this cut-off, a subgroup with good prognosis according to ZAP-70 score but significantly ($p < 0.0001$) high expression of PD-L1 antigen was identified (Figure 32G). The result could have implication for a minority of CLL patients described as “discordant” by prognostic stratification who could benefit from anti-PD-L1 treatment strategy (473).

Comparison of immune checkpoint antigen expression of patients CLL cells based on median fluorescent intensities of CD47 ($p=0.6252$), CD200 ($p=0.9002$), PD-1 ($p=0.8732$) and PD-L1 (0.7030) among CD38 positive and negative sub-groups on the other hand showed no significant differences. This suggests that although the immune checkpoint antigens influence immunological crosstalk within the tumor microenvironment, they do not necessarily impact prognostication of the disease.

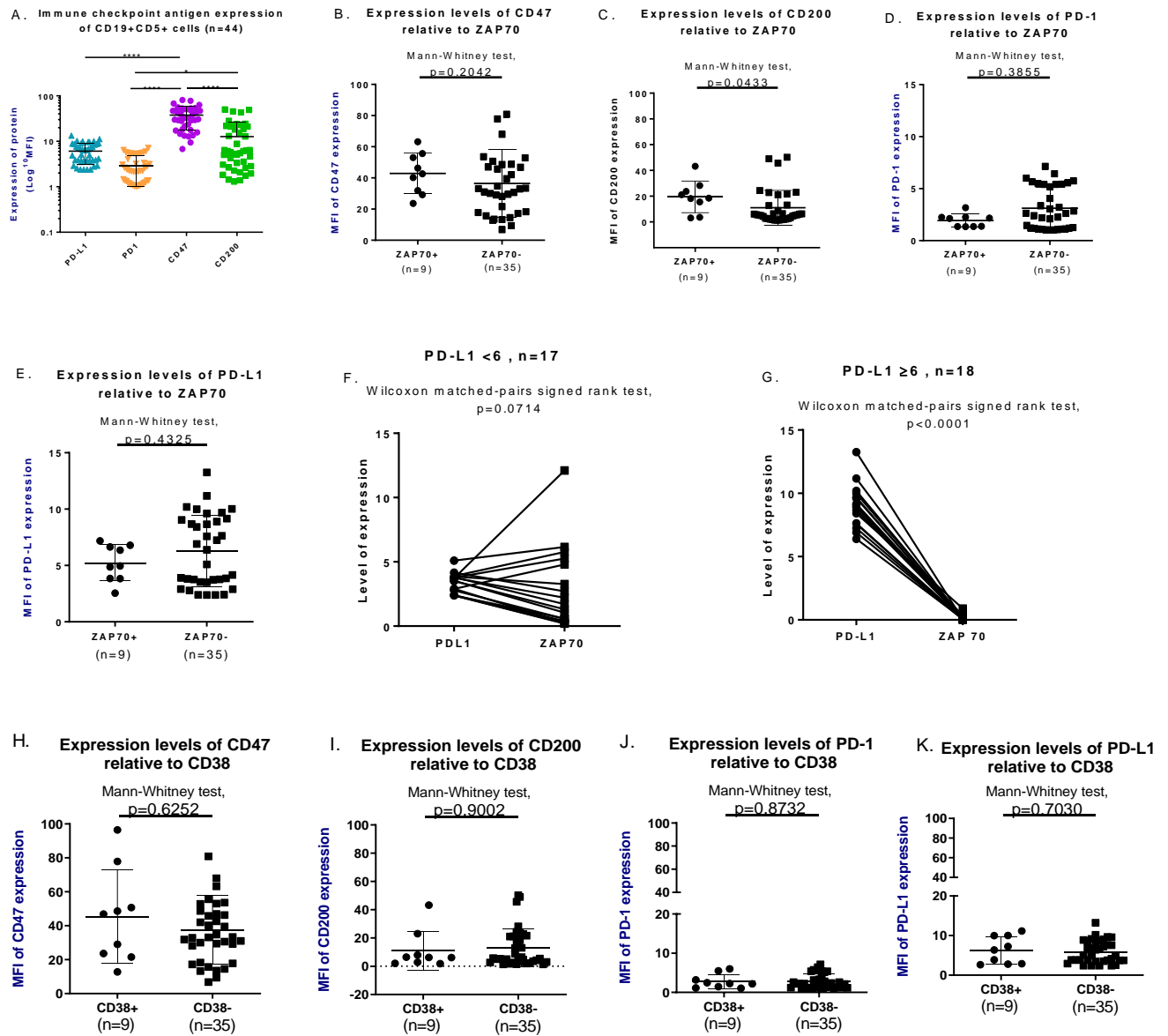


Figure 32: Comparative analysis of immune checkpoint proteins expression with published prognostic factors in CLL

- A. Pattern of expression levels of immune checkpoint proteins determined by flow cytometer in CLL patients. Median fluorescence intensities (MFI) are compared.
- B. Stratification of CD47 antigen expression by ZAP-70 sub-grouping
- C. Stratification of CD200 antigen expression by ZAP-70 sub-grouping.
- D. Stratification of PD-1 antigen expression by ZAP-70 sub-grouping.
- E. Stratification of PD-L1 antigen expression by ZAP-70 sub-grouping.

- F. Sub-classification of ZAP-70 negative patients according to their PD-L1 expression <6
- G. Sub-classification of ZAP-70 negative patients according to their PD-L1 expression ≥ 6
- H. Stratification of CD47 antigen expression by CD38 sub-grouping.
- I. Stratification of CD200 antigen expression by CD38 sub-grouping.
- J. Stratification of PD-1 antigen expression by CD38 sub-grouping.
- K. Stratification of PD-L1 antigen expression by CD38 sub-grouping.

5.9.9 Clinical stage in CLL is independent of immune checkpoint and prognostic parameters

Prognostic parameters and immune checkpoint expression were stratified by clinical staging (Binet criteria) of CLL in this cohort and compared by ANOVA for trends in the progression of the disease. Here, differences in expression of PD-L1, PD-1, CD47 and CD200 (Figure 33A-D) across Binet clinical stages A, B and C did not attain statistical significance. Also, ZAP-70, CD38 and ROR1 expression across the Binet clinical stages showed no significant differences between stages A, B and C (Figure 33E-G). However, among the number of CLL patients positive for CD38 expression (n=8), 75% were in clinical stage B while 12.5% each were in clinical stages A and C respectively. Also in the ZAP-70 positive patients, 55.6% were in Binet stage B and 22.2% each in Binet stages A and C respectively. These results thus indicate that in this cohort of CLL patients, immune checkpoint expression and ZAP-70 and CD38 prognostic markers are independent of the clinical stages of the CLL disease. Nonetheless, a greater majority of patients (>77%) with poor prognostic indicators fall in the advanced clinical stages (B and C) of the disease.

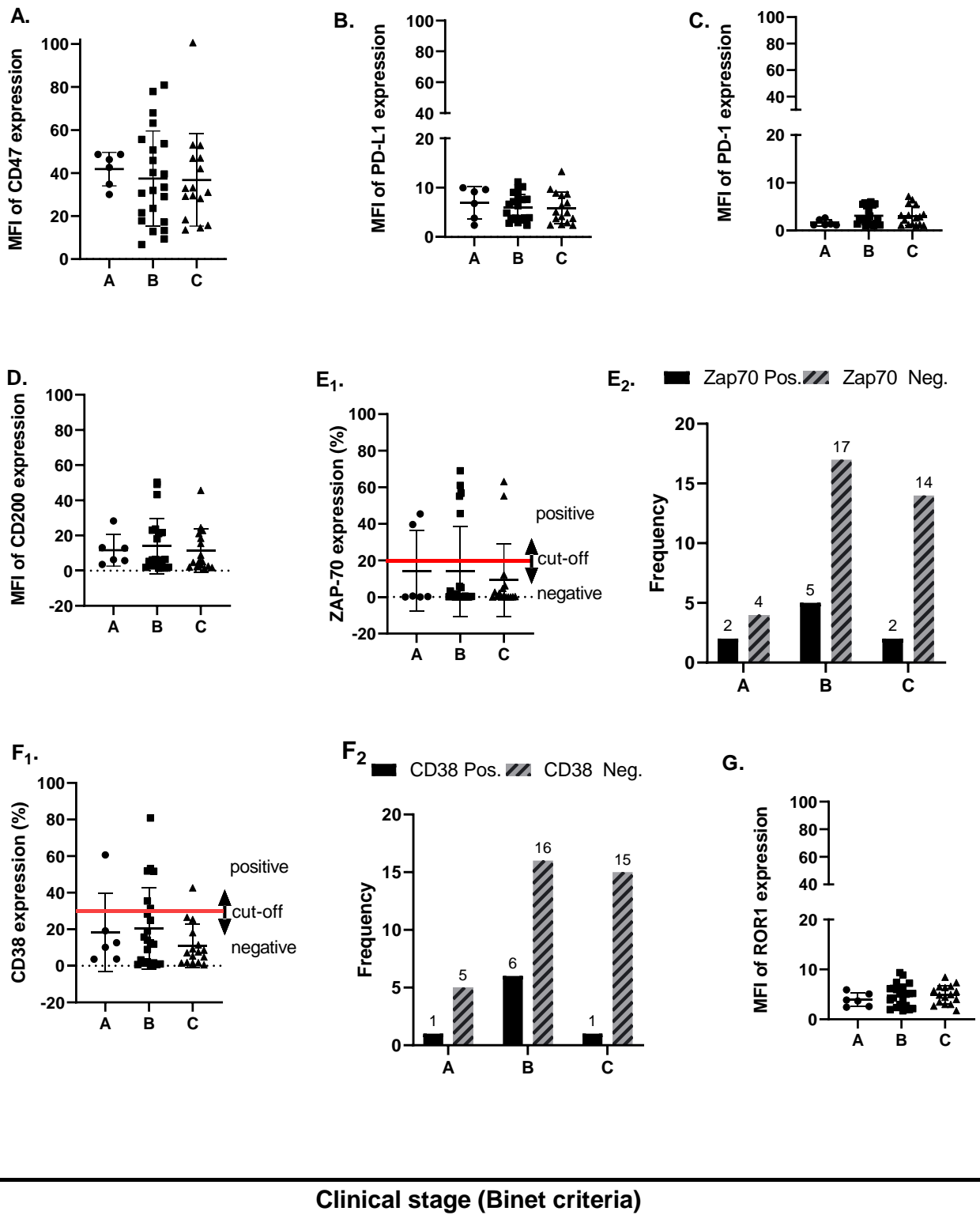


Figure 33: Clinical stage in CLL is independent of immune checkpoints and prognostic markers

- A. Stratification of CD47 expression by Binet staging criteria in CLL patients
- B. Stratification of PD-L1 expression by Binet staging criteria in CLL patients
- C. Stratification of PD-1 expression by Binet staging criteria in CLL patients
- D. Stratification of CD200 expression by Binet staging criteria in CLL patients
- E. Stratification of ZAP-70 expression by clinical stage of CLL (E₁) and frequency distribution (E₂). Red line indicate $\geq 20\%$ positivity of tumor cells used as cut-off to determine positivity
- F. Stratification of CD38 expression by clinical stage of CLL (F₁) and frequency distribution (F₂). Red line indicate $\geq 30\%$ positivity of tumor cells used as cut-off to determine positivity
- G. Stratification of ROR-1 expression by Binet staging criteria in CLL patients

6 Discussion

6.1 Functional impact of DNA damage response genes deregulation on phagocytosis and efficacy of immune checkpoint inhibitors in a murine model of ABC-like diffuse large B-cell lymphoma (DLBCL)

6.1.1 Introduction

Tumor supportive microenvironments remain a critical barrier toward effective cancer cells elimination. In a previous study of humanized mouse model of treatment refractory B-cell leukaemia (406), the bone marrow microenvironment was identified as an essential barrier to treatment success. Importantly, genotoxic treatment with chemotherapy induced an acute secretory activating phenotype (ASAP) of soluble factors which synergized with antibody treatment to induce profound effector cell mediated antibody dependent tumor cells phagocytosis (21). Induction of enhanced reactivation of effector cells functions circumvented the therapy-resistant microenvironment of the bone marrow.

However, since ASAP induction requires genotoxic damage of tumor DNA, this reveals a critical role of the DNA damage response (DDR) system in the interactions of tumors with immune effector cells within the tumor microenvironment.

The current study thus, aims to elucidate the genetic drivers of DDR pathway which mediate tumor – effector cells interactions and the biological mechanisms employed in tumor cells phagocytosis within the microenvironment.

6.1.2 E μ -Myc cells downregulate Cd20 expression precluding use for DNA damage response genes functional assays utilizing anti-Cd20 mediated phagocytosis

Cd20 is a phosphorylated protein which forms part of the integral structure of the B-cells membranes where it regulates transmembrane calcium flux (474). In most chemo-immunotherapeutic (CIT) regimen for NHL, targeting Cd20 antigen has been an attractive option because the molecule is not expressed on hematopoietic stem cells and plasma cells but adequately expressed on a number of B-cell tumors, it is not normally shed from B-cell surface

and it is not internalized by the cells upon antibody binding (475, 476). Additionally, Cd20 interact with multiple other surface proteins on B cells such as CD40, MHC II, CD53, CD81, CD82, and C-terminal src kinase-binding protein (CBP) and its molecular function has been linked with the signaling propensity of the B-cell receptor (BCR) following observation that inhibitors of BCR also decrease surface expression of Cd20 (477).

The E μ -Myc mouse model recapitulates Burkitt's lymphoma type of aggressive B-cell malignancy (478, 479) and has been used in a number of studies to elucidate different biological mechanisms (480-482). In this study, an initial high level of Cd20 antigen expression pre and post retroviral mediated shRNA transduction resulted in significantly high antibody dependent cellular phagocytosis (ADCP) of tumor cells in anti-CD20 based chemo-immunotherapy. Unfortunately, subsequent decline in levels of ADCP was shown to be caused by reduced surface expression of Cd20 antigen of E μ -Myc cells. Downregulation of Cd20 expression ultimately led to remarkable impairment of anti-Cd20 dependent tumor cell killing, abrogating the initial efficacy of chemotherapy/anti-Cd20 combination previously observed with this cell line. This confirms the finding that Cd20 surface expression is a determinant of innate anti-CD20 antibody sensitivity (483) notwithstanding the argument based on longitudinal sampling transcriptomic approach that sensitivity to CD20 immunotherapy is not regulated by differences in CD20 expression but rather galectin-1 expression (484). Although the cause of Cd20 loss was not further explored in this work, its incidence has been observed and reported in other cell lines and in patients with B-cell malignancies at the clinics (485-487) where reduced Cd20 expression is associated with anti-Cd20 treatment resistance and inferior patients survival (488, 489). Among the possible causes of Cd20 antigen loss include cell autonomous mechanisms which results in Cd20 mRNA splice variants translated into truncated protein lacking the anti-Cd20 binding epitope (490), mutations in Membrane Spanning 4-domains A1 (*MS4A1*; CD20) gene (491) and Cd20 antigen internalization by the malignant B-cell (492). Alternatively, anti-Cd20 bound antigen could be removed from cell surface by Fc- γ expressing phagocytic cells in a process called trogocytosis resulting in lack of Cd20 antigen (493-495). Additionally, histone deacetylation (496) and notch-1 mutation (497) are identified epigenetic mechanisms that suppress surface Cd20 antigen expression on B-cells.

6.2 Evaluation of MyD88 cell line for functional assays elucidating DNA damage response genes regulation of macrophage phagocytic functions under chemo-immunotherapy

MyD88 cell lines were derived from the MyD88 mouse model, generated by Cre-mediated recombinase conditional expression of Myd88p.L252P (the orthologous position of the human MYD88p.L265P mutation) in combination with conditional over-expression of BCL2 which drives clonal development of activated B-cell (ABC) like subtype of diffuse large B-cells lymphoma(402). The MyD88 mouse model thus represents one of the few available models for studies of the highly aggressive, heterogeneous NHL sub-types with poor prognosis.

In the evaluation assessment of three of the five clones of MyD88 cell lines received for this work, the M552 clone was selected based on a high CD20 (>90%) expression, a high proliferative rate compared to the other clones, a high baseline level of anti-CD20 dependent cell-mediated phagocytosis and the least sensitive to mafosphamide based on their respective IC₅₀ concentrations.

However, further genotoxic evaluation on M552 cell line against single agents of the current frontline R-CHOP therapy showed appreciable sensitivity to mafosphamide (derivative of cyclophosphamide) but resistant to the remaining single agents including vincristine, etoposide and doxorubicin. These are consistent attributes of the post germinal center ABC-subtype of DLBCL which presents clinically with poorer prognosis with frontline R-CHOP treatment compared to the germinal center B-cell like (GCB) subtype (80).

Also, mafosphamide treatment of M552 cell lines induced significantly enhanced anti-CD20 dependent phagocytosis. This finding recapitulate the synergy of acute secretory associated phenotype-chemoimmunotherapy reported in the humanized mouse model of double-hit lymphoma (hmB) (21) thus giving credence to the role genes in the DNA damage response pathway play to modulate tumor-effector cells interactions in the tumor microenvironment.

6.2.1 Downregulation of DNA damage response genes influence proliferation of M552 KD cells

Functional DNA damage response is required to maintain genome integrity and fidelity of genetic material transfer to off-springs (87). Defect in the DNA repair may lead to genomic instability, tumor development, treatment relapse and cell death (498, 499). In the ABC sub-type of MyD88 lymphoma model, shRNA were used to suppress protein expressions of critical DDR genes and their impact on proliferation and chemo-sensitivity examined. shRNA suppression of mRNA of DDR genes resulted in different levels of KD efficiencies. However, >60% reduction of target protein expression were achieved with the shRNA in all cases. MyD88 KD cells showed three different trends of proliferation following shRNA KDs of DDR genes. In all instances, proliferation was determined by absolute count of remaining cells in culture after 16hrs of seeding specific number of cells.

In the first group of genes, a significantly high cellular proliferation was observed with down-regulation of DNA-PK and CHK1 proteins compared to that of empty vector control. However, when KD cells were stressed with sub-lethal concentration of genotoxic agent, a decline in proliferation of DNA-PK and CHK1 KD cells was observed compared to their unstressed counterpart but both nonetheless remained more proliferative than the empty vector control.

In the life of a cell, a number of exogenous and endogenous factors such as ionizing radiation, genotoxic substance or metabolic products such as free radicals could cause DNA damage. DNA double strand break (DSB) is one of the most harmful damages resolved by non-homologous end joining (NHEJ) (134) or homologous recombination (HR) repair mechanisms (114). The catalytic sub-unit of DNA-PK, Ku70/80 directly mediates double strand break repairs in mammalian cells (500). DNA-PK functions in multiple cellular processes including regulation of transcription, progression of the cell cycle (501) and maintenance of telomeres lengths (502). Down-regulation of DNA-PK thus resulted in increased proliferation of cells relative to controls with intact DNA damage response.

Chk1 is largely activated by ATR in response to DNA stalled replication fork where it mediates phosphorylation and proteosomal degradation of Cdc25A phosphatase (503). Thus activity of Cdk2/cyclin E or Cdk2/cyclin A complex is reduced leading to blockage of cell cycle through the S-phase (504, 505). Similarly, Chk1 also halt the cell cycle at G₂/M transition by phosphorylation of Wee-1-kinase that inhibits cyclin-dependent kinase 1 (Cdk1) activity and also activate Cell Division Cycle 25C (Cdc25C) phosphatase to de-phosphorylate Cdk1 to limit activity of Cdk1/cyclin B1 leading to the slowing or stalling of DNA replication. Thus, Chk1 blocks/slows DNA synthesis in the S-phase to facilitate repair of damaged genomes of cells already committed to S phase and blocks G₂/M to prevent cells with damaged chromosomes from entering mitosis, providing time for repair while simultaneously preventing immediate mitotic catastrophe. Hence, downregulation of Chk1 abrogates these checkpoints in cell cycle driving uncontrolled cellular proliferation.

Contrary to the trend observed in this set of DDR genes, the second group of genes including p38, MK2, CHK2, Bim and Bak showed significantly reduced proliferation compared to the empty vector control when gene expression were reduced with shRNA. However, when stressed with sub-lethal concentration of genotoxic agent, proliferation of CHK2, Bim and Bak KD cells remained unaffected whereas that of p38 and its downstream substrate MK2 decreased relative to that of stressed empty vector control. A number of studies had reported increased resistance of CHK2 KD to ionizing radiation and apoptosis (506, 507) however, slow proliferation rate following knockout of CHK2 was also observed in mouse fibroblast cells similar to observation in the MyD88 cell line.

Finally, down-regulation of DDR genes of p53, .ATM, ATR, ATX and p21 increased proliferation of some KD cells albeit not significantly different from that of empty vector control cells. However, relative to the control cells, sub-lethal genotoxic stress showed no inhibitory effect on proliferation of these KD cells.

6.2.2 Downregulation of DNA damage response genes alter sensitivity of M552 cells to genotoxic treatment

Conventional genotoxic drugs acts by inducing DNA damage or targeting cell division mechanism such as DNA replication and chromosome segregation (508, 509). In the process, complex cellular mechanisms involving kinase mediated cell cycle checkpoints, DNA repairs, cellular senescence and apoptosis when repairs fail are orchestrated to resolve genomic damage and prevent premature entry into mitotic phase thereby forestalling cell dead by mitotic catastrophe.

M552 cell lines with DDR genes downregulated show different sensitivities to mafosphamide treatment. For instance, downregulation of genes including p53, ATM, ATX, p21, MK2 and Bim reduced sensitivity of KD cells to mafosphamide compared to the empty vector control cells. Such genes associated with reduced chemo-sensitivity in the M552 cells could functionally be grouped into three pathways in cell cycle regulation.

For instance, p53, a gene described as the guardian of the genome due to its essential role to maintain genome integrity is activated by multiple DNA damage sensor kinases including ATM, ATR and DNA-PK in response to genotoxic stress (510). Activated p53 mediate both G1 and G2 cell cycle arrest to permit DNA repairs. At the G1phase, p53 transcriptionally induces expression of p21 which binds and further inhibits cyclins A/Cdk2 and E/Cdk2 complexes to enforce the halt of cell cycle at G1 phase (511) in tandem with ATM activated CHK2 kinase which initiate checkpoint mediated G1 cell cycle arrest by inhibitory phosphorylation of Cdc25A (512). Although the G2/M phase arrest is accomplished through combined effect of multiple pathways, p53 is again pivotal in cell cycle arrest. Here, p53 induces transcriptional repression of both cdc25C and cyclin B (513), induces expression of protein 14-3-3 sigma to sequestrate cyclin B1–cdc2 complexes in the cytoplasm (514) as well as Growth Arrest and DNA Damage-inducible 45 (GADD45) to inhibit cyclin B-Cdc2 complexes to abolish transition from G2-M phase of the cell cycle (513, 514). Importantly, p53 can also transactivates several components of the apoptotic effector machinery including apoptotic peptiase activating factor 1 (Apaf-1) (515), Bcl-2 Associated X-protein (Bax) (516), BH3 only proteins such as Puma (517), Noxa (518) and BH3

interacting-domain death agonist (Bid) to induce apoptosis in cases of failed DNA damage repairs. Thus the magnitude of p53 mediated cellular processes to ensure genome integrity guarantees that downregulation of its expression hinders regulatory mechanisms of the cycle and leads to chemo-resistance. The result on p53 is concordance to the report regarding resistance to apoptosis in p53^{-/-} lymphoblast expressing BCL-2 (519). The importance of p53 to genome integrity is further highlighted by its mutation in over 50% of human cancers.

In M552 cell lines, downregulation mitogen-activated protein kinase-activated protein kinase 2 (MAPKAPK2 or MK2) reduced chemo-sensitivity to mafosphamide. This is surprisingly contrary to that reported on head and neck squamous cell carcinoma where RNA interference (siRNA) or pharmacological inhibition of MK2 reduced tumor burden and increased survival (520). A similar benefit of MK2 KD has been reported in multiple myeloma patients where there is over expression or chromosomal gain of MK2 gene locus (521). However, p38/MK2 have been observed to function as global response mechanism to activate both G1/S intra-S and G2/M cell cycle checkpoints in cells with weak expression of p21 due to reduced activation of p53 (522).

Here, MK2 phosphorylates heterogenous nuclear ribonucleoprotein A0 (hnRNPA0) to stabilize Gadd45 α mRNA Poly(A)-specific ribonuclease (PARN) to block Gadd45 α mRNA decay. Gadd45 α through a positive feedback loop sustains MK2-dependent cytoplasmic sequestration of Cdc25B/C to block mitotic entry in the presence of unrepaired DNA damage (523). Since MK2 mediated G2/M checkpoint is active in p53 defective background however in the ABC-subtype MyD88 cell line model with constitutively active NK-F β and gain of BCL2 gene, the chemo-resistance effect of MK2 downregulation could be as a result of opposing effect of NK-F β on p53 function (524, 525).

Despite its well-known function in responding to errors in mRNA splicing (526), ATX (SMG-1) has also been shown to activates p53 in response to DNA double strand breaks by phosphorylating serine 15(527). P53 phosphorylation on serine 15 is of particular importance for cell cycle arrest, apoptosis and senescence. Activated p53 in turn stimulates p21 and executes

the G1/S checkpoint however, stability of p21 has been shown to depend on ATX and ATM through p53 dependent synthesis and p53-independent proteolysis of p21(528). Thus relative to controls cells with full complement of functional DDR, downregulation of ATX significantly increases the chemo-resistance of ATX KD MyD88 cells. This result confirms the finding that ATX depleted cells show prolonged Cdc25A stability and fail to inactivate CDK2 in response to radiation, thus resulting in CDK2-mediated tumor cell proliferation (529). This result thus lend credence to the recent role of ATX as a tumor suppressor (530, 531).

Another interesting gene whose down-regulation induced significant chemo-resistant in M552 cells was Bim. Bim is one of the BH3 only proteins alongside Puma, Noxa, Bid and Bik in the BCL-2 family which induce apoptosis by antagonizing anti-apoptotic members of the BCL-2 family such as BCL2, BCL-xL, BCL-w, MCL-1 thereby unleashing the pro-apoptotic executioners of the BCL-2 family such as Bax and Bak (532). The pro-apoptotic proteins alter mitochondria membrane permeability to promote cytochrome-C escape to activate caspase mediated cell death. In the MyD88 ABC-sub-type model of DLBCL where acquired BCL-2 copy number gain exists, it was expected that Bim-mediated apoptosis provocation would be countered by high levels of pro-survival BCL-2 protein. However, our results reveal significant chemo-resistance upon mafosphamide treatment of Bim KD cells suggesting that, the ability to engage all BCL-2 anti-apoptotic members and direct activation of BCL-2 pro-apoptotic members such as Bax and Bak, makes Bim a potent apoptosis inducer in this model (533, 534).

Unlike other DDR genes KD cells, DNA-PK KD cells showed mafosphamide sensitivity which was not significant from that of empty vector control cells. This is in stark contrast to report of enhanced radio-sensitivity following pharmacological inhibition or siRNA downregulation of DNA-PK expression in some human cell lines exposed to radiation damage (535). However, others contend that kinase inactivated DNA-PK mutants, make DNA-PK deficient cells highly radiosensitive but have no effect on transformed DNA-PK deficient cells(536). Nonetheless, mafosphamide treatment reduced proliferation of DNA-PK KD cell. DNA-PK phosphorylates a number of downstream targets including replication protein A (RPA), Chk2, and Chk1 in

response to DNA damage. Phosphorylation of RPA enables broken ends of DSB to be repaired by the catalytic sub-unit Ku70/80 whereas CHK2 and CHK1 activation through phosphorylation, optimize enforcement of S, G2/M cell cycle arrest (537).

Lack of chemoresistance observed with downregulation of DNA-PK, a critical kinase of the non-homologous end-joining (NHEJ) pathway, could be due to overlapping roles in activating downstream effector kinases by other phosphoinositide 3-kinase related kinases (PIKKs) such as ATM and ATR. The result aligns with report that DNA double strand break repair can proceed independent of DNA-PK (538). DNAPK also partake in optimal activation of p53 in response to DNA damage by phosphorylating MDM2, an ubiquitin ligase which inhibits p53 activation (539). Thus phosphorylation of MDM2 detaches it from p53 leading to accumulation and activation of p53. The complex redundancy nature of p53 activation by several DNA damage sensor kinases for instance by ATM on serine 15, ATR on 15 and 37, DNA-PK on 15 and 37 explains the reason while shRNA mediated downregulation of some individual genes in the DDR has little effect on chemo-sensitivity of the KD cells.

Similar to DNA-PK, p38 and ATR, KD of CHK1 and CHK2 genes resulted in varied but not significant differences in cell sensitivity to mafosphamide compared to the empty vector control. CHK1 as a genome integrity checkpoint kinase is activated by ATR in response to single-strand DNA breaks, replication errors at the S-phase and stalled replication forks (540). Activated CHK1 reduce DNA synthesis at the S-phase by inactivating CDK2/Cdc25A complex through degradation of Cdc25A (541). Again, CHK1 could block entry into mitosis at G2 phase by activation of Wee1 kinase and inhibition of Cdc25A phosphatase to allow time for DNA repairs (542). However, notwithstanding these critical roles of CHK1 in DDR, loss of CHK1 function has been shown to have different outcomes in different cells (543-545). On one hand, chemical inhibition or downregulation of CHK1 expression increases chemosensitivity of fast replicating tumor cells such as those driven by MYC over expression where higher levels of CHK1 expression is critical to balance replication stress-associated DNA damage (546-548). The dependence vulnerability of these tumors on CHK1 expression has been shown to be clinically relevant in a number of clinical trials (547, 549). On the other hand, tumors overexpressing BCL2 are protected from intrinsic

apoptosis induced by downregulation of CHK1 (550). Thus contrarily to effectiveness of CHK1 inhibitors in the GC-subtype of DLBCL (551) where myc over expression is a common phenomenon (552), the ABC-subtype of DLBCL recapitulated by M552 cell line express constitutive active NK-FB and BCL-2 copy number gain (553) which accord protection against apoptosis.

Similar to effect of CHK1 gene KD on chemosensitivity to mafosphamide, CHK2 gene KD in M552 cells did not potentiate chemosensitivity or resistance to mafosphamide treatment in comparison to that of empty vector control cells. The CHK2 kinase contrarily to CHK1 mediates G1 cell cycle arrest following activation by ATM in response to DNA damage (512). Here, CHK2 inhibits Cdc25A, a phosphatase that removes inhibitory phosphorylation of cyclin A/Cyclin-dependent kinase (Cdk) 2 and cyclin E/Cdk2 complexes to prevent cells from proceeding into S-phase (175). However, the G1 cell cycle checkpoint also critically relies on p53 upon ATM activation which provides an alternative if not complementary pathway to G1 cell cycle arrest. Here, p53 transcriptionally induce production of p21 which directly bind to inhibit Cdk2 complexes to induce G1 arrest (511). In fact, the binding of p21 to Cdk2 complexes is sufficient to induce G1 cell cycle arrest (554). Thus the lack of impact of CHK2 KD on genotoxicity following mafosphamide treatment could be due to the effect of complementary pathways of cell cycle arrest in the BCL-2 over expressing M552 cell line.

6.3 Tumor cells phagocytosis is influenced by DDR genes downregulation

Following shRNA-mediated downregulation of DDR genes, levels of baseline antibody independent cellular phagocytosis (AICP) of KD cells were similar to that of empty vector control except for p38 KD cells which were significantly less phagocytosed by peritoneal macrophages. Similarly, induction of anti-CD20 dependent cellular phagocytosis (ADCP) showed significantly reduced phagocytosis of p38 KD cells but similar levels of phagocytosis of the remaining DDR KD cells compared to the empty vector control cells. For both AICP and ADCP, consistently reduced phagocytosis of ATX, MK2, CHK2 and Bak KD cells relative to the control were observed although

the levels of reduction did not attain statistical significance. Apoptotic cell recognition by macrophages is crucial to the phagocytic process. Heterogeneous expression of chemo-attractants (find me signal) including Fractalkine (i.e., CXC3CL1), adenosine triphosphate (ATP), uridine triphosphate (UTP) nucleotides and sphingosine – 1- phosphate (S1P) mediate phagocytes direction to the location of apoptotic cells. Then, exposure of “eat me” signals such as enrichment of phosphatidylserine residues on outer leaflet of cell membrane, exposure of calreticulin and annexin 1, intercellular adhesion molecule 3 (ICAM 3) and changes in surface proteins glycosylation are required for apoptotic-bound cells identification whereas display of “don’t eat me” molecules such as CD47, CD31, CD300a etc facilitates distinction of dead-bound cells from live cell. The ABC-subtype of MyD88 cell lines model expresses constitutively active NF- κ B and copy number gain of BCL-2 which induce proliferation and antagonize cellular apoptosis. The observed similarity of level of phagocytosis of KD cells and controls thus could be due to the underlying genetic aberration in pathways that already favor parental cell survival in this disease.

Numerous scavenger receptors such as T-cell immunoglobulin and mucin domain containing 4 (TIM-4) (555) and CD300f, the G protein-couple receptor (GPCR) brain-specific angiogenesis inhibitor 1 (BAI1) (556), α v β 3/5 integrin (557), Mer and Axl receptor tyrosine kinases (394, 558, 559) are employed in non-opsonized phagocytosis to recognize and bind exposed phosphatidylserine (PS) and other so-called ‘eat-me’ signal molecules enriched on the surface of apoptotic cells(560). Contrarily, in antibody opsonized phagocytosis of viable cells, Fc region of antibodies ligated to target cells are bound by Fc γ R of macrophages to induce membrane receptor clustering and phosphorylation of the cytoplasmic tail of Fc γ R activating immunoreceptor tyrosine-based activation motifs (ITAM) in the process.

The concerted engulfment signaling following PS binding and Fc–Fc γ R engagement ultimately converge on guanine triphosphatases (GTPase) enzyme Ras-related C3 botulinum toxin substrate 1 (Rac), a member of the Rho family of enzymes which regulate intracellular actin dynamics and target cell internalization. Here, actin polymerization extends pseudopods of phagocytes in a zippering manner to engulf the target cell into phagosome and ultimately phagolysosome where cellular degradation occurs. The trend of consistent reduction in phagocytosis of p38 KD cells in

our study suggests p38 gene is crucial for modulation of a critical target(s) common to both opsonized and non-opsonized phagocytosis.

Additionally, target cell recognition, rather than effector cell potency, limits phagocytosis in that a constant proportion of available target cells are killed regardless of the macrophage: target cell ratio (561). Our data indicate that p38 mitogen activated protein kinase pathway (MAPK) deregulation in tumor cells, influence proportion of tumor cells phagocytosed by macrophages.

Interestingly, whilst we observed increase in phagocytosis of all other DDR KD cells upon genotoxic stress with mafosphamide alone or in combination with anti-CD20 mAb, a resilient impairment in both spontaneous and anti-CD20 dependent cellular phagocytosis of p53 and ATX KD cells and to a lesser extent ATM and p38 were observed. Recounting that, these same KD genes mediated tumor cells apoptosis resistance under genotoxic treatment in our cytotoxicity assays, it could be inferred that downregulation of p53 and ATX do not only trigger failure of cell cycle arrest, DNA repairs, and apoptosis induction but also affect recognition and phagocytosis of tumor cells through cell-cell contact with macrophages. This could be due to the fact that, recognition of phosphatidylserine enriched on outer membrane of apoptotic cells is central to effective non-opsonized phagocytosis (562). A low exposure of PS driven by high survival advantage of combined BCL-2 over-expression and constitutively active NF- κ B leveraged by specific genetic advantage of downregulated DDR genes promote survival rather than inducement of apoptosis. Considering the fact that antibody dependent cellular phagocytosis mainly relies on Fc portion of opsonizing antibody engagement with Fc γ R_s of macrophages whereas non-opsonized phagocytosis employs a plethora of macrophage receptors such as TIM 1, 3,4, stabilin 1/2, or BAI-1 that recognize PS directly or Tyro 3/Axl Mer kinases, CD300f, scavenger receptor class f1 (SCARF), advanced glycation end products (RAGE) and CD91 that recognize PS indirectly through binding to cognate tethering molecules such as growth arrest specific 6 protein (Gas-6), protein S, milk fat globule- epidermal growth factor 8 (MFG-E8), complement component 1q (C1q), calreticulin, dead domain 1 α – ligand or scavenger and mannose receptors which recognize other “eat me” molecules such as glycosylated proteins and oxidized low density lipoprotein (oxLDL), it is tempting to suggest that observed impaired phagocytosis could have a common mediating entity

to both opsonized and non-opsonized cellular phagocytosis. One interesting possibility is the control of post-apoptotic phagocytic event by p53 beyond its conventional role in suppressing tumor and inducing apoptosis. Here, p53 regulate phagocytosis through transcriptional trans-activation of dead domain 1 α (DD1- α) gene. DD1- α function as an engulfment ligand that engages in intermolecular interaction at intercellular junctions of apoptotic cells and macrophages to promote phagocytosis (563). Impairment of p53 through mutation or indirectly through any of its activators such as ATM (564), ATX (529) thus hinders efficient phagocytosis.

Another possibility is dysregulated balance in activation of Rac/Cdc42 GTPases and other Rho GTPases such as Ras homolog family member A (RhoA) and its downstream effector Rho kinase. A crosstalk between Rac/Cdc42 GTPases which control actin polymerization and membrane protrusion formation (565) and RhoA which controls cell membrane contraction (566) regulates the phagocytic process in macrophages during non-opsonized and Fc-dependent cellular phagocytosis. Here, specific signaling pathways activated by individual PS receptors and Fc – Fc γ R engagement ultimately converge on GTPase Rac/Cdc42 activation. Since RhoA and it downstream effector Rho kinase antagonizes Rac/Cdc42 activity deregulation promoting RhoA activity, ultimately inhibits phagocytosis.

Another possibility if not parallel or complementary is pathway of apoptosis LC3 (microtubule-associated protein 1A/1B-light chain 3)-associated phagocytosis (LAP) is triggered in circumstances where engagement of cellular targets through both PS and Fc receptors by macrophage triggers the autophagy machinery with subsequent recruitment of LC3 into the cargo-containing phagosome formed.

6.3.1 Abrogation of critical DDR genes impact phagocytosis through changes in functional effects of cellular secretome

Phagocytosis is a complex process which relies on multi-dimensional cross-talk between the target and the effector cell. Beyond direct cell-to-cell contact, communication through the cellular secretome is another mechanism by which tumor cells influence their surrounding stroma (567). The cells secretome consist of soluble proteins, lipids and vesicles secreted to the extracellular

space to mediate diverse cellular processes (425). The richness and functional relevance of cellular secretome is underscored by its use in other disease models such as ischemic heart function where the use of single cytokines alone failed to yield result (568, 569). Tumor cells display secretome with altered composition to the normal tissues from which they were derived. Using an *in-vitro* coculture experimental approach that mimic the current frontline treatment regimen for DLBCL, R-CHOP, critical DDR genes (p53 and ATX) which mediate impaired phagocytosis under immuno-chemotherapeutic treatment (figure 11, 12) were identified. To explore the mechanisms through which identified DDR KD genes affect phagocytosis, the functional effects of the secretome of identified KD cells in comparison to that of control cells were investigated.

Coculture of mafosphamide stressed KD cells with peritoneal macrophages in conditioned media of genotoxic stressed control cells, rescued impaired phagocytosis of KD cells by restoration of phagocytosis (fig 14). This suggests that, CM of control cells functionally differ from that of the conditioned media (CM) of KD cells. Additionally, the results imply that identified DDR KD genes potentially play a role in the composition/secretory mechanisms of the cell's secretome.

Interestingly, the effect of CM of control cells directly influenced the phagocytic activity of the macrophages as observed increase in phagocytosis of KD cells occurred in both antibody-mediated and non-antibody mediated cocultures. Considering that, therapeutic antibodies eliminate living cells through Fc - Fc γ receptor engagement (570), whilst non-antibody mediated phagocytosis relies on PS and other soluble cell-bound proteins, lipids and metabolites that forms the molecular code for apoptotic cells removal to eliminate dying cells (571, 572), this result suggest a direct effect of CM of control cells on the macrophages.

Additionally, the functional ability of CM of genotoxic stressed control cells to complement the deficit in the secretome of KD cells, were validated. Mafosphamide stressed control cells were cocultured with peritoneal macrophages in the secretome of identified DDR genes KD cells. Here, mafosphamide stressed control cells were expected to continuously discharge secretome which would compensate for the lack in the CM of DDR KD cells. Expectedly, a similar high levels of phagocytosis of genotoxic stressed control cells in the CM of DDR KD cells compared to the control cells, suggest that, soluble factors released from control cells could replenish deficit in CM

of KD cells. The question however remains whether this phenomenon occurs only under duress of genotoxic stress. Thus, validation of role of genotoxic stress through a coculture of unstressed (untreated) and mafosphamide stressed control cells with peritoneal macrophages showed significantly higher levels of phagocytosis of mafosphamide stressed control cells compared to unstressed cells (Fig.15). This result agrees with the finding that, genotoxic stress-induced acute secretory phenotype that bolsters antibody-dependent cellular phagocytosis of tumor cells (21). Major genes in the DDR including TP53, ATM, ATX and p38 have been reported to be associated with secretion of the cellular secretome (573). Focusing on the role of wt-p53 in cell secretome, it was demonstrated that, of 111 secreted proteins observed in LN-Z308 glioma cell line, 39 were expression-wise upregulated whilst 21 were downregulated by wt-p53. Subsequently, wt-p53 was shown to affect protein secretion and modulate immune signaling through recruitment of M1-polarized macrophages to eliminate hematopoietic stem cells in senescence (574, 575). Agreeable to earlier reports, gene ontology studies identified over-expression of genes involved in exocytosis and vesicle-mediated protein transport suggesting that wt-p53 mediated cellular protein secretion into CM predominantly through non-classical cellular secretory pathway (574). P53 activation in HSCs shifts their secretory profile from supporting M2 to M1 polarization of macrophages through secretion of IFN- γ and IL-6. Consistent with this observation, the induction of enhanced phagocytosis by CM of control cells compared to that of gene KD cells could be attributed to possible presence of M1 – polarizing cytokines secreted in the presence of functional p53 gene.

ATX (SMG1) gene functions in the mRNA surveillance and genotoxic stress response pathway. As a central player in mRNA surveillance, ATX mediates nonsense-mediated decay (NMD) of mRNAs containing premature stop codons by phosphorylating Up-frameshift protein 1/Regulator of nonsense transcript 1 (UPF1/RENT1) (576) in order to prevent accumulation of truncated proteins (530). However as a serine/threonine kinase, ATX shares overlapping roles with ATM and it's required for optimum activation of p53 following cellular exposure to genotoxic stress (529). Beyond these roles, SMG1 has been suggested to be a tumor suppressor whose expression and function could be downregulated in a number of cancers through promoter region hypermethylation (577). Mammalian target of rapamycin (mTOR) signaling pathway regulates cell growth and proliferation and is essential for the process of protein synthesis. SMG1, has been demonstrated to

antagonize the function of mTOR (531). Thus shRNA-mediated KD of SMG1 could potentially affect directly cellular protein synthesis and secretion into CM or indirectly influence the cellular secretome through lack of optimum activation of p53 functions.

p38 is a stress-activated protein kinase recognized as the 3rd major signaling pathway of mitogen-activated protein kinase (MAPK). It is activated by environmental stresses and inflammatory cytokines upon which it regulates cell cycle, differentiation, apoptosis and production of pro-inflammatory cytokines (IL-1 β , TNF- α and IL-6) release.

NF- κ B is a transcription factor which binds specific DNA element sequences of target genes to drive expression of pro-inflammatory cytokines such as IL-1, TNF- α , IL-6 that regulate multiple aspects of innate and adaptive immune functions (578). However, NF- κ B is transcriptionally regulated by ATM kinase under genotoxic stress (579).

In non-malignant cells, a finely tuned cellular secretome is essential to maintain physiological homeostasis, however in cancer, changes in the abundance of components of cellular secretome have been observed (321, 580, 581). Generally, the tumor cell secretome is shown to confer resistance to cell death, whilst secretome of tumor cells undergoing chemotherapy is reported to enable cancer cell survival and expansion of cancer stem cells resulting in treatment refractoriness and tumor relapse (582). Interestingly, it was observed in this study that the secretome of sub-lethal mafosfamide stressed tumor cells with intact DNA damage response system induced enhanced tumor cell phagocytosis. Additionally, such secretome was sufficient to induce phagocytosis of DDR genes KD tumor cells. In a previous work in our lab using a double hit-lymphoma cell line -HmB, the existence of an acute secretory activating phenotype (ASAP) was established. Such secretion was induced in tumor cells upon sub-lethal treatment with genotoxic agent and exhibited a rapid functional effect within 24hrs that led to enhanced tumor cell phagocytosis. This function of ASAP is thus at variance with that of senescence activating secretory phenotype (SASP) orchestrated by metabolically active cells under growth arrest which requires up to 5 days to establish. Tumor cells utilize cellular secretome to influence the function of cells within the TME as well as prime distant pre-metastatic niches.

6.3.2 Importance of KD cells to cellular secretome composition

Beyond its conventional role as a tumor suppressor to safe-guard the genome integrity, p53 as a transcription factor, has been reported to control other target genes which encode secreted proteins, soluble factors and extracellular vesicles such as exosomes (583, 584).

Mutant p53 functions as an aberrant transcription factor that can interact with other transcription factors to reprogram the cellular transcriptome of cancer cells aberrant secretion of extracellular proteins

6.3.3 Expression of high levels of immune checkpoint antigens promote tumor cell phagocytosis with checkpoint inhibitors-based chemo-immunotherapy

Immune checkpoints are molecules present on immune cells whose engagements regulate immune activation. Checkpoint molecules function to activate either immune stimulatory or immune inhibitory pathways to ensure immune homeostasis by controlling cellular tolerance and prevent tissue damage. Tumors cells can evade the host immune system by usurping immune checkpoint pathways, such as the cytotoxic T-lymphocyte associated protein 4 (CTLA-4)-CD80/86, CD47-SIRP- α and PD-1-PD-L1/2 pathways. The advent of immune checkpoint inhibitors in 2010 heralded the beginning of a new era where repressive immune checkpoint pathways could be successfully manipulated to promote tumor cells recognition and elimination by the immune cells. Despite 60% cure rate achievable with standard anti-CD20 based chemotherapy in DLBCL, 30-40% of patients relapse on or refractory to treatment (585). This has triggered a number of clinical trials aimed to explore efficacy of combinatory treatment with immune checkpoint inhibitor to meet the urgent treatment requirement of this patient's subset (418, 586). Here, significantly high levels of expression of immune checkpoint antigens including PD-L1, CD47 and PD-1 were expressed by MyD88 ABC-subtype of DLBCL cell line. Agreeably, earlier reports (587, 588) had identified high expression of PD-L1 in DLBCL to correlate with poor prognosis setting the tone for the use of anti-PD-1/anti-PD-L1 as part of treatment strategy in this patient group. However, a number of genotoxic drugs have been reported to induce PD-L1 expression on diverse tumor cells thus limiting their potential benefit in manipulating the immune dynamics of the tumor microenvironment on the side of treatment (589, 590). Contrarily to reported up regulation of PD-L1 by exogenous stress

including alkylating agents (591), treatment of MyD88 cell line with mafosphamide in this study did not significantly increase cell surface expression of any of the immune checkpoint antigens tested (fig. 16E). This theoretically suggest that combinatory treatment of chemotherapy with anti-PD-L1 or anti-PD-1 could enhance tumor cells elimination as high expression of PD-L1 is a critical biomarker of therapeutic efficacy (592, 593). A higher level of tumor cells phagocytosis were observed for combinations of anti-PD-1 or anti-PD-L1 with mafosphamide in both anti-CD20 dependent cellular phagocytosis and non-antibody dependent cellular phagocytosis compared to mafosphamide treatment alone. This observation agrees with numerous reports highlighting the superior advantage of combined anti-PD-1/PD-L1-chemotherapy over chemotherapy alone (353, 594-596). The remarkable efficacy of anti-PD-1/PD-L1 combination with conventional chemotherapy is attributed to two main reasons.

First, anti-PD-1/PD-L1 antibodies inhibit interactions between PD-1 and PD-L1 thus interrupting negative signal suppression of T-cell activation and effector functions to restore antitumor immunity (597). Second, PD-L1 treatment is reported to upregulated multiple inflammatory pathways in macrophages which result in increased tumor infiltration with activated macrophages promoting tumor cells elimination (598).

Despite the increase in phagocytosis induced by anti-PD-1/PD-L1 combination with genotoxic treatment, blockade of CD47-Signal regulatory protein- α (SIRP- α) with anti-CD47 resulted in the highest level of tumor cells phagocytosis (fig 17B). Here, contrarily to observation of PD-1/PD-L1 blockade, anti-CD47 induced significantly high non-opsonized phagocytosis as well as anti-CD20 dependent cellular phagocytosis of tumor cell with or without genotoxic treatment. This could be attributed to blockade of “marker of self-antigen”, CD47 thus facilitating recognition of tumor cells for phagocytosis. In the event of anti-CD20 mediated cellular phagocytosis, additional activation of macrophages through FcR- γ engagement of opsonized tumor cells, signal via kinases leading to downstream accumulation of focal adhesion proteins such as phospho-paxillin and talin to promote phagocytosis of opsonized live tumor cells (599). The pathways utilized by immune checkpoint proteins are unique and have been shown to be non-redundant (600) providing the rationale for combination of different checkpoint inhibitors in treatment strategies. In the MyD88 cell line model, combination of anti-CD47 with anti-PD-L1/ PD-1 induced no further increase of

phagocytosis as anti-CD47 treatment alone increased phagocytosis to a saturating limit (fig 17B). In the context of J774.1A and murine peritoneal macrophages as effector cells, the synergy of mafosphamide treatment with anti-CD47 induced the highest level of anti-CD20 dependent cell-mediated phagocytosis. This result is consistent with findings of a clinical study that evaluated rituximab-anti-CD47 (Hu5F9-G4) combination in relapse/refractory DLBCL and follicular lymphoma patients where the combination induced durable response (601). Beyond blood cancers, the efficacy of anti-CD47 combination with conventional chemo-immunotherapy has also been reported in solid cancers such as endometrial and breast cancer where CD47-SIRP α blockade induced macrophage infiltration to orchestrate enhanced antibody dependent cellular phagocytosis (602, 603).

6.3.4 Anti-CD47 promotes phagocytosis through CD47-Sirp- α disruption

Most human cancer cells over-express the CD47 integrin associate protein to repress engulfment by phagocytes such as macrophages, dendritic cell, Natural Kill cells (NK cells), granulocytes and monocytes (604). Following the high level of tumor cells killing efficiency demonstrated by anti-CD47 antibodies, both in-vitro and clinical trials studies (383), increasing attention is focused on the mechanisms of action of these antibodies. This is of urgent importance due to reported risk of hemolytic anaemia and thrombocytopenia due to destruction of other CD47- bearing cells such as erythrocytes and thrombocytes (605, 606). Controversially, anti-CD47 antibodies have been reported for CD47- SIRP- α blockade (419) and Fc γ R-Fc fragment interaction (384), implying that the antibody could potentially mediate effector cells killing of all body cells bearing the CD47 antigen.

Using F(ab)₂ fragments of anti-CD47 mAb in an in-vitro coculture a significantly high level of tumor cells phagocytosis was achieved at 10 μ g/ml compared to 5 μ g/ml of full length anti-CD47mAb. Subsequent F(ab)₂ fragment concentrations tested yielded similar levels of phagocytosis at same concentrations as full length anti-CD47 antibody. F(ab)₂ fragment of anti-CD47 lacks Fc domain as such blocks only CD47- SIRP α interaction without Fc γ R engagement hence, does not induce antibody-dependent cellular phagocytosis (ADCP) or antibody-dependent cellular cytotoxicity (ADCC). This data suggests that F(ab)₂ fragments of anti-CD47 mAb

(MIAP301) suppress phagocytic inhibitory signals that emanate from CD47-SIRP α pathway activation and synergize with anti-CD20 antibody to enhance tumor cells phagocytosis.

This results is in concordance with others where either CD47 knockdown or anti-CD47 or anti-Sirp- α or in-vivo setting using mice lacking Sirp- α cytoplasmic tail resulted in significantly enhanced antibody dependent cellular phagocytosis(419). Additionally, combination of mafosphamide, anti-Cd20 mAb and F(ab)₂ portion of anti-CD47 induced significantly superior level of phagocytosis compared to anti-Cd20 mAb and F(ab)₂ portion without chemotherapy (Figure 18B). Again, similar to earlier observation with full length anti-CD47 antibody, combination treatment with mafosphamide, anti-Cd20 mAb and F(ab)₂ leads to a level of phagocytic saturation where combination of additional immune checkpoint inhibitors such as anti-PD-L or/and α -PD-1 do not further increase phagocytosis.

6.3.5 Poorly phagocytosed DDR KD cells show different immune checkpoint antigen expression upon genotoxic treatment

Immune checkpoint molecules are over-expressed in a variety of tumors and various authors have reported induction of higher expression of immune checkpoint molecules such as PD-L1 by exogenous stress from chemotherapy and radiotherapy. Prevailing evidence indicate that PD-L1 levels in tumors is an important factor which influence therapeutic efficacy (607, 608). This assertion is collaborated by evidence of elevated PD-L1 levels in high responders of immuno-chemotherapeutic based treatments (593). This forms the bases to assess surface expression of immune checkpoint molecules including PD-L1, PD-1, CD47 and CD200 on poorly phagocytosed DDR KD M552 – DLBCL cells.

Genotoxic stress induced variable level of immune checkpoint antigens expression of monoculture cells of tumor with significant increase of PD-L1 in p53 KD cells (Figure 19II) and CD47 in ATM KD cells (Figure 19I). The data suggest possible functional roles of p53 and ATM genes in the regulation of PD-L1 and CD47 expression respectively. *TP53* has been linked to PD-L1 modulation via its effect on miR-34 where p53 directly binds the 3' untranslated region of PD-L1 to suppress its expression (609). Thus, wild-type p53 suppress expression of PD-L1 whereas p53 mutants, deletion or knockdown were associated with high levels of PD-L1 expression and low levels of miR-34.

Also, significant over-expression of CD47 in ATM KD cells under genotoxic stress suggests a functional role of ATM regulation of CD47 expression in DNA damage. CD47 binds to SIRP- α to trigger inhibitory signaling that prevents macrophage phagocytosis of normal and cancerous cells (610). Additionally, thrombospondin-1 can competitively bind to CD47 to induce cellular proliferation, differentiation and recovery from genotoxic stress. Thus, regulation of CD47 expression by ATM could be a mechanism to prevent survival of cells with damaged DNA induced by genotoxic stress.

6.3.6 Immune checkpoint inhibitors circumvent impaired phagocytosis of DDR genes KD cells

DLCBL is a heterogeneous disease and the ABC-subtype has been shown to have the worse prognosis. Treatment intensification and addition of targeted therapies have both failed to improve outcomes with Rituximab-based cyclophosphamide, doxorubicin, vincristine, prednisone combination (R-CHOP) in clinical trials (611, 612). Also, PD-L1 expression in DLBCL is associated with inferior response to R-CHOP and non-germinal center immunophenotype (587, 613). Although monotherapy treatment with anti-PD-1 in relapse/refractory DLBCL was disappointing (418, 614), addition of PD-1/PD-L1 blockade to R-CHOP, reverses treatment outcomes such that high expression of PD-L1 then correlated with increased response to combination therapy (615). Genomic alterations that affect critical pathways such as *TP53* mutation is common in cancers and adversely affects treatment outcomes (616). Thus, assessment of immune checkpoint inhibitors in combination with mafosphamide for the treatment poorly phagocytosed M552 cell lines with downregulated DDR genes was undertaken. Here, blockade of PD-1/PD-L1 axis with α -PD1 or atesolizumab significantly increased the levels of tumor cells phagocytosis of *TP53*, ATM, and P38 KD cells but not of ATX KD cells. A possible reason for poor effect of anti-PD-1/PD-L1 on phagocytosis of ATX KD cells is the very low expression of the antigens associated with ATX downregulation. This is consistent with the finding that, PD-L1/PD-1 blockade in a mouse model of ABC-subtype DLBCL enhanced anti-CD20 dependent cellular cytotoxicity (617). Interestingly, CD47-Sirp- α blockade with anti-CD47mAb increased significantly the level of tumor cell phagocytosis irrespective of the DDR gene knockdown, suggesting that anti-CD47 combinatorial treatment with R-CHOP could potentially enhance outcomes in relapse/refractory

ABC-subtype DLBCL. Our results agree with similar reports among ABC-subtype DLBCL patients and cell lines where CD47 blockade enhanced efficacy of R-CHOP regimen (385).

6.3.7 Tumors with downregulated DDR genes influence phenotypic characteristics of macrophages in vitro

Macrophages are heterogeneous group of cells with enormous plasticity in providing innate immune responses through phagocytosis, antigen processing and presentation and cytokines secretion. Diverse microenvironmental signals encountered by macrophages alter their transcriptional program and functional roles (618). Typically, the state of polarization of macrophage is influenced by specific cytokine stimulation which drives different intrinsic transcription factors, metabolism, surface receptor expression and secretory molecules. Classical macrophage activation, M1 promotes pro-inflammatory responses whereas alternative macrophage activation, M2 stimulates anti-inflammatory responses (619). However, between the two extreme polarization states is a wide continuum of activation states (M2a, M2b, M2c, M2d, TAM and T cell receptor and CD169 macrophages) (620). It is believed that, the crosstalk between tumor cells and macrophages drives the phenotypic and functional changes in both M1 and M2 subtypes. However, as executioners of the innate immune system with efficiently unique ability to phagocytose a variety of targets, macrophages often fail to perceive and attack tumor cells despite the alterations in tumor genome. The effect of cytokines on macrophage polarization status is known, however the question of how different mutational status of tumor cells influence polarization states of macrophages remains unanswered. Thus, here, a direct exposure of murine peritoneal macrophages to poorly phagocytosed tumor cells harboring KDs of DDR genes in a coculture system was performed to study phenotypic adaptations of macrophages to tumor cells within the tumor microenvironment.

Strikingly, exposure of peritoneal macrophages to *TP53* KD tumor cells resulted in significant reduction in expression of transforming growth factor beta (TGF- β), a potent immunosuppressive agent which promotes anti-inflammatory responses (621). Additionally, expression of IL-10 and CD206 – known markers of M2 polarized state and iNOS, a marker of M1 polarized state required for nitric oxide production and pro-inflammatory response reduced relative to that of control cells.

Again, macrophages exposed to *TP53* KD tumor cells also reduced expression of CD64 –an Fc- γ receptor relevant for antibody engagement and CD80 a co-stimulatory factor critical for T-cell activation. Thus, increased expression of TGF- β polarize macrophages into TAM-like (M2-like) phenotype with up-regulation of anti-inflammatory cytokine IL-10 and suppression of pro-inflammatory cytokines TNF- α and IL-12 (284). Our data demonstrates the reverse where reduced expression of TGF- β due to exposure to *TP53* KD tumor cells leave the macrophage in an anergy state.

Peritoneal macrophages exposed to ATM KD tumor cells on the other hand showed polarization toward an M2-like phenotype with markedly increased expression of markers such as TGF- β and decreased expression of inducible nitric oxide synthase (iNOS). Additionally, these macrophages increased expression of surface chemotactic receptor, CCR7 which is less externally expressed in the alternative activated state than classically activated macrophages (622). Also, relative to the phenotype of control macrophages, those exposed to ATM KD tumor cells increased expression of both PD-1 and PD-L1. High PD-1 expression of macrophages have been shown to correlate with poor phagocytic ability of tumor cells (623). Additionally, tumor cells could induce PD-L1 expression in macrophages by altering prostaglandin E₂ (PGE₂) metabolism (624). High expression of PD-1 makes macrophages susceptible to immune manipulation by tumor cells whilst induce PD-L1 expression suppresses and inactivates effector T-cells functions leading to tumor progression. However expression of these immune checkpoint antigens provide avenue to increase the efficacy of combinatory treatment with PD-1/PD-L1 blockade antibodies.

Similar to effect of *TP53* KD tumor cells, macrophage exposed to ATX KD cells reduced expression of M2 markers such as TGF- β , IL-10, CD115 and CD206. Additionally, Fc- γ receptors including CD64, CD32/16 were downregulated, indicating a potential impairment of capacity to effect antibody dependent cellular phagocytosis. Also, CD80 a critical molecule for co-stimulatory signal by antigen presenting cells required for T-cells clonal expansion and optimal cytokine production (625) was relatively reduced in macrophages exposed to ATX KD cells compared to controls. High CD38 expression on macrophage in hepatocellular carcinoma, has been correlated to good prognosis (626) whiles, presence of CD68⁺ macrophages in breast cancer predicts worse

prognosis (627-629). Macrophages exposed to ATX KD tumor cells expressed increased CD68 levels and decreased CD38 levels suggesting that downregulation of ATX primes macrophages to support a worse disease course with inferior outcomes.

Contrary to the phenotypic expression of macrophages exposed to ATX KD, macrophages exposed to p38 KD cells showed increased expression of alternative activated M2-like markers of TGF- β and the mannose receptor CD206. Although these macrophages also downregulated Fc- γ receptors such as CD64 and CD34/16, they maintained a high expression of some pro-inflammatory M1- like molecules including iNOS, CD68 and chemotactic ligand CCL19 and CCL21 receptor CCR7. Additional, PD-1 expression was suppressed and PD-L1 expression induction on macrophages by tumor cells was not observed.

6.3.8 *TP53* is required for packaging extracellular vesicles and optimum outcome of immune checkpoint inhibitors

Antibody independent cellular phagocytosis (spontaneous phagocytosis) serves as a mechanism of eliminating apoptotic cells to ensure tissue homeostasis (630) and surface expression of phosphatidylserine (PS) is critical to apoptotic cell recognition and phagocytosis. Extracellular vesicles (EVs) comprising of exosomes, microvesicles and apoptotic bodies routinely shed by cells have been identified as PS enriched-cargo that mediate intercellular communication upon uptake (631, 632). P.S of apoptotic cells upon phagocytosis induced macrophages to release immune regulatory cytokines including high levels of TGF- β 1 which induce M2-like anti-inflammatory phenotype in macrophages with higher phagocytic capacity (620, 633).

In macrophages-target cells coculture treated with EVs, significantly higher levels of non-antibody dependent cellular phagocytosis was induced by EVs of empty vector control cells than that of *TP53* KD cells. Also, whilst EVs of control cells could significantly further enhances the level of ADCP in immune checkpoint treated cocultures (anti-CD47 or anti-PD-L1), EVs of *TP53* KD cells fails to induce any further increase of ADCP. These results point to functional differences of EVs with downregulation of *TP53* and confirm the role of TP53 in extracellular vesicles processing. Our results affirm the report that TP53 controls protein secretion into cellular secretome and EVs through direct transcriptional regulation of tumor suppressor-activated pathway 6 (TSAP6), a gene

which mediates protein selection or loading into secretome and EVs (634). Thus downregulation of *TP53* potentially affects critical elements that mediate tumor cells phagocytosis. It is reported that apoptosis increases release of PS into cargos of extracellular vesicles which subsequently impact on macrophage phagocytic function upon internalization (635). As a major inducer of cellular apoptotic machinery (636), downregulation of *TP53* results in reduced apoptosis and thus reduced level of non-opsonized phagocytosis.

This result suggests that functional *TP53* is required for optimum effectiveness of chemo-immunotherapy involving anti-CD47 and anti-PD-L1 therapy in the ABC-subtype of DLBCL.

6.4 Demographic of CLL cohort and Presentation at Diagnosis

CLL is the commonest adult leukaemia in the United States of America (USA) and Europe, accounting for 30% of all blood cancer (637, 638). Across different geographical settings and racial groups, differences in CLL incidence, epidemiology and clinical features have been reported which may reflect unique biology of the disease due to different genetic and environmental settings. Unlike in US and Europe, the incidence of CLL is reported to be very low in Africa, Asia and the Far East.

Research from tropical Africa, indicate that CLL occurs predominantly in youthful population with female predominance and differences of tumor cell morphology (427, 433, 434, 639). Among diaspora African-American CLL patients, higher percentage of unmutated IgVH genes (65% versus 47%) and deletion of chromosome 17p13 and 11q22.3 associated with poor prognosis and survival outcome has been reported (640). Interestingly, Coombs et al found that people of African descent had a lower frequency (10 out of 15) risk alleles of single nucleotide polymorphisms (SNPs) known to confer risk of developing CLL, yet the overall clinical outcome of CLL was inferior in African patients (641). These highlights germline genetic predisposition difference and potential differences in CLL biology between Western and African populations.

This study investigated the molecular signature of “tropical” CLL by measuring informative molecular markers relevant for tumor phenotyping, prognostic and immune interactions in CLL patients recruited from the Oncology Department of Komfo Anokye Teaching Hospital in Ghana, West Africa.

Within the period of the study, fifty (50) consecutive informed and consented patients with presumptive diagnosis of CLL were recruited for the study. All patients were from the out-patient unit of the Oncology Department and females form the majority (51.1%) of the participants. Whilst the proportion of male to female ratio deviate from 1:2 reported among CLL patients in the Western developed countries such as USA and EU (642), it is in agreement with 1:1 overall ratio earlier reported by Fleming within the African sub-region (639).

The median age at diagnosis was 59yrs in this cohort, sharply contrast 72yr reported in EU (643, 644), 70yrs in the USA (645) and 74yrs in UK. (646) but is very comparable to 61yrs in Senegal (437), 59yrs in Nigeria(647) both in West Africa and 55yrs in Ethiopia (648) in the East Africa. Agreeably, a larger majority of CLL patients (57.8%) were over 55yrs at diagnosis however, a sizable portion of patients (42.2%) were below 55yrs at diagnosis compared to 10% of cases reported in Europe (643).

Compared to earlier report by Fleming (433) in which 50% of study participants were below 45yrs at a center in the neighboring country, Nigeria, the increase in the age at diagnosis could reflect the increase in the general life expectancy observed over the years.

6.4.1 Ghanaian CLL patients present with advanced diseases at diagnosis

In a large majority of CLL patients (>95%), significant leukocytosis due to accumulation of CD19+/CD5+ tumor cells was the most presenting finding at diagnosis. The level of tumor cells burden was not significantly different across gender. Additionally, high prevalence of anemia (86.7%) was the next striking hematological feature of the disease and males were more likely to be anemic (68%) than females (26%). The lower incidence of anemia in females is as a result of a lower limit of the established hemoglobin reference range in the geographical area of the study (males =10.69 - 18.76g/dL and females = 8.19 - 16.17g/dL) (438) compared to (13.0-18.0g/dl for males and 11.5 – 16.5g/dl for females) reference ranges applicable to the Western world but often adapted for use as default range in a number of laboratories. Thus, if default adapted hemoglobin reference ranges are used, then a higher incidence of anemia, predominant in females (91.3%) than males (81.8%) is observed in this CLL cohort. The prevalence of anemia is higher than that reported by the neighboring countries such as Nigeria (78%) (647) and Senegal (62.5%) (437).

Similar sub-regional trends is also observed with platelets counts where thrombocytopenia was present in 53.3% of patients at diagnosis in this cohort which is similar to 52.5% reported from Senegal but both are higher than 39.1% reported in Sudan. Clinical staging of the CLL cohort to predict the outcome of the patients at the time of initial diagnosis was carried out using the criteria proposed by Binet (441). Only a small portion of 13.6% of patients presented at Binet stage A, the remaining majority presented at stage B (50%) and stage C (36.4%). The high proportion of patients

presenting with Binet stages B and C in this study reflects delayed report to the hospitals with sickness as has been observed in other cases of cancers (649) where previous medical consultations, ignorance, resort to herbal treatment, seeking spiritual intervention, and financial incapability were identified as major causes of the delay. Additionally, there is the possibility of auto-immune cytopenia driving higher incidence of anemia and thrombocytopenia (650) thus affecting the clinical staging in this cohort but evidence of this was not explored in this study. Across the sub-Saharan African, similar trends in staging of CLL has been reported including Nigeria (Binet stages A=5.2%, B=11.3% and C=54.6%) (647), Senegal (Binet stages A=7.0%, B=22.5% and C=62.5%) (437) and Sudan (Binet stages A=9.1%, B=41.8% and C=49.1%) (651). Interestingly, in the developed World, CLL patients at diagnosis present with a predominant lower clinical stage of the diseases. This has been reported in the USA (Binet stages A=52.3%, B=31.4% and C=16.0%) (65) and also estimated for the European union countries (Binet stages A=60.0%, B=30.0% and C=10.0%) (652). Beyond the estimation of clinical stage of the disease, empirical data from Italy (Binet stages A=79.0%, B=12.2% and C=8.8%) (653) and Germany (Binet stages A=68.0%, B=26.0% and C=16.0%) (654) also confirm the low proportion of late stage CLL patients.

Also in part of Asia, low prevalence of late stage CLL clinical prevalence than that observed in Africa is reported by South Korea (Binet stages A=60.0%, B=10.0% and C=30.0%) (655), China (Binet stages A=56.1%, B=21.7% and C=22.2%) (656) and India (Binet stages, A=11, B=52, C=37) (657). Survival of CLL patients is affected by the clinical stage and progression of the disease (652). Thus, the high aggressive form of CLL observed in tropical Africa (640, 658) could be as a result of the late diagnosis where substantial damage is already caused to the bone marrow and resulting hematopoietic failure weaken the immune system to ward of infections.

6.4.2 Good prognosis of CLL cohort thwarted by late poor clinical stage at diagnosis

CLL follows a highly variable clinical course where the disease remains indolent in some patients' whiles taking an aggressive course of progression in others (68). Patients presenting at early stage remains a heterogeneous group with 30-50% developing progressive disease within a short period of time. Identified prognostic markers such as mutational status of IgVH region, deletions of chromosomes 11q23, 17p13, ZAP-70, CD38 positivity and serum markers including thymidine

kinase, and β -2 macroglobulin (429, 453) serve as the means to identify asymptomatic patients with low tumor burden whose disease are more likely to progress. Such asymptomatic patients could benefit from early treatment modalities aimed to induce complete remission (659).

Among the cohort of CLL patients, using a cut-off $\geq 20\%$ for ZAP-70 and $\geq 30\%$ for CD38 positivity, 20.5% of patients according to ZAP-70 and 18.2% of patients according to CD38 positivity showed poor prognosis and risk an aggressive clinical course of the disease at diagnosis. The high concordance of agreement between ZAP-70 and CD38 positivity underline the report that these markers are functionally linked and that CD38 ligation leads to phosphorylation of ZAP-70 (450). Also, ZAP-70 status was not influenced by surface immunoglobulin (sIgM and IgD), suggesting that disease prognosis is independent of surface immunoglobulin expression. Additionally, in this cohort, receptor tyrosine kinase like orphan receptor 1 (ROR1) expression did not differ with surface immunoglobulin, ZAP-70 and CD38 expression.

Surprisingly whilst majority of the study participants presented with late stage clinical condition (86.4%, Binet stage B and C) at diagnosis, prognostic assessment by ZAP-70 (20.5% positive) and CD38 (18.2% positive) rather suggested a favourable disease progression in majority of the participants. This trend has also been reported in other countries in the Sub-Saharan Africa where ZAP-70 and CD38 assessment had been performed for CLL patients. For instance in Sudan, 32.7% CLL patients were positive for ZAP-70 and 37.3% were positive for CD38 however 90.9% presented at diagnosis with advanced clinical stages of the disease (651). Whilst proportion of CLL patients presenting at diagnosis with late stage Binet criteria was also observed (85.0%) in Senegal (437), the proportion of patients positive for CD38 was also equally high (70%) in contrast to our result, that reported in Sudan and among African-Americans in the USA (640).

These results are in stark contrast with that reported in the Western developed countries where a greater proportion of CLL patients are diagnosed at early clinical stage (Binet stage A). For instance, A late stage prevalence of 42% (Binet stages B+C) at diagnosis among a Germany cohort where 46.8% were positive for Zap-70 and 29.0% were positive for CD38 is reported (654). Similarly, in USA, an advanced Binet stage of 10% at diagnosis among Caucasian American CLL patients who showed Zap-70 positivity of 47% against CD38 positivity of 30% is reported (640).

The high disparities in proportion of CLL patients presenting at late disease stage at diagnosis between African CLL cohorts and the Western cohorts are not self-understood however the probable reasons may be due to late attendance to the hospitals due to initial quest for alternative traditional treatment, a practice quite prevalent in most African countries. Additionally, health awareness and policy that permit regular health checkups as practiced in most developed world is virtually non-existing in most Africa countries. As such while a substantial portion of patients are diagnosed accidentally through a routine full blood count in developed countries, most patients diagnosed in Africa actually report to the hospitals due to conditions associated with CLL advancement. In the Ghanaian CLL cohort, a major clinical contributor to advance Binet stage was low hemoglobin concentration and platelet counts. It is also established that the lower limit of hemoglobin reference range for the geographical jurisdiction among female healthy population is lower compared to ranges applicable in the Western developed countries (438). This coupled with low socio-economic status could drive a higher incidence of anemia and for that matter late clinical stage according to Binet criteria in CLL patients in Africa. Finally, a high incidence of parasitic infections including malaria in Africa are associated with red cells destruction, hemoglobin and platelets reduction and organomegaly which could complicate the clinical assessment and staging of CLL disease in African patients (660).

6.4.3 Surface immunoglobulin (sIg) pattern and their correlation to other biologic variables

In CLL, expression of sIg with restriction of light chains is part of the diagnostic criteria. Both IgM and IgD isotypes of immunoglobulins utilize identical antigen binding regions, however IgD is believed to complement the function of IgM by promoting inflammation and linking adaptive and innate immune systems as its receptors are expressed by both CD4+ and CD8+ T-cells.

Surface immunoglobulin (Ig) expression of 44 CLL patients showed, 88.6% (n=39) sIgM isotype of which 54.5% (n=24) expressed only sIgM whilst the rest, 15 (34.1%) co-expressed IgM/IgD. Five patients (11.4%) expressed no detectable sIgM or IgD. The reports of surface immunoglobulin expression trend have been variable according to the findings of different research groups. Generally, a dominant co-expression of IgM+/IgD+ , followed by IgM+/IgD- has been reported as the trend in studies where larger number of CLL patients had been recruited (661-664). Similar

trends of sIg expression patterns despite recruiting a smaller CLL groups of 66 and 76 patients respectively have been observed (665). Although type of anti-immunoglobulin (polyclonal vs monoclonal), time/period of sIg determination and other factors could affect the result of immunoglobulin determination, however, one major problem as a cause of variability is different cut-off values used to determine positivity of sIg among different research groups.

Contrary to the dominant trend of IgM+/IgD+ co-expression observed in the aforementioned studies, the Ghanaian CLL cohort showed predominant IgM+/IgD- phenotype with a higher proportion of kappa light chain restriction (31.8%) compared to lambda (25.0%) which is consistent with the findings of Rudders et al (666) in 26 CLL patients where the authors observed 85% of IgM expression compared to 15% of IgM+/IgD+ co-expression. Similar trend was observed among 60 CLL patients where sIgM was predominantly expressed in 47% of cases compared to 15% of IgM+/IgD+ co-expression (667).

For 11.4% of patients in this study, sIgM/IgD could not be detected. The expression of others isotypes of immunoglobulins such as IgG or IgA isotypes have been reported in CLL in place of or alongside IgM or IgD (661, 662, 666). However, since regulation of IgM and IgD expression is post-transcriptional (668), class switching recombination will result in deletion of μ and δ chains required for IgM and IgD formation to permit replacement by γ , α or ϵ chains for IgG, IgA or IgE formation. The possibility of expression of other immunoglobulin isotypes such as IgG, IgA and IgE could account for the cases where sIgM and sIgD failed to reach positivity threshold or were not detected, however the presence of these other immunoglobulin isotypes were not tested for in this study. Additionally, CLL is reported to show low or dim immunoglobulin intensity on flow cytometer because of impair transport of synthesized Ig to cell surface membranes lead to accumulation of Ig in the cytoplasm (669). However, in this study, only surface immunoglobulins were tested.

Among the CLL cohort, IgM was significantly more expressed and showed poor correlation to IgD suggesting the expression of the two isotypes are independently regulated despite the fact that both isotypes express same variable regions with similar antigenic epitope specificity (670, 671). Higher

sIgM expression has been reported to be associated with unmutated IgVH genes, late stage (Binet stage C) presentation and shorter treatment free survival (672, 673).

Additional, whilst IgM, IgD, and ROR1 expression did not differ by ZAP-70 prognostication, CLL patients showing good prognosis according to CD38 expressed significantly higher IgM but similar IgD and ROR1 as those with poor prognosis. The B-cell receptor is central to the pathogenesis of CLL, thus the lack of effect of expression levels of BCR immunoglobulins on CLL prognosis does not negate the role of BCR in the disease biology; rather it could be suggestive that peripheral B-CLL cells may not reflect events within the microenvironments which serve as the protective and proliferative centers of the B-cells.

6.4.4 Expression of Immune checkpoint and their correlation to prognostic factors

As a critical moderator of immune homeostasis, immune checkpoints are co-opted by CLL B-cells to avert killing action of immune surveillance cells. In this CLL cohort, high expression of several immune checkpoint antigens including PD-L1, PD-1, CD47 and CD200 were detected on peripheral CLL cells. Expression of different checkpoint antigens imply that tumor cells utilize different non-overlapping pathways to evade immune destruction (674). However tumor cells expression of PD-L1, PD-1, CD47 and CD200 were found to be independent of ZAP-70 and CD38 expression suggesting that, these immune checkpoints antigens do not influence disease prognosis. Similarly, the lack of prognostic impact of PD-L1 on ZAP-70 and CD38 status has also been reported among 112 Polish CLL patients. Here, although quantitative RT-PCR was used to measure gene expression levels of PD-L1, the same conclusion was arrived at compared to flow cytometric measurement in our case (442). Another reason accounting for lack of effect of immune checkpoint antigens on prognosis is that, other mechanisms such as secretion of IL-10 by CLL cells downregulates T-cells effector functions through a signaling pathway non-redundant to PD1/PD-L1.

Interestingly among the favourable prognosis patients in the Ghanaian CLL cohort, a subgroup was identified that expressed significantly high levels of PD-L1 despite being ZAP-70 negative. This further highlights heterogeneity within the favourable prognostic group and identifies a subgroup which could potentially benefit from PD-L1/PD-1 blockade.

Furthermore, our results confirms that of others who reported that, expression of immune checkpoint antigens and prognostic factor (ZAP-70, CD38) did not differ significantly between different clinical stages determined by Binet criteria (442).

7 Conclusion

The main conclusions derived from this thesis are as follows:

7.1 Elucidation of the role of DNA-damage response in the tumor microenvironment interaction

- Functional *TPP53* and *ATX* (SMG-1) genes of DNA damage response pathway are essential for phagocytosis of ABC-subtype DLBCL cells. Loss of *TP53* and *ATX* in DLBCL induces resistance towards chemoimmunotherapy (CIT) by inhibition of macrophage effector functions.
- Secretome of genotoxic stressed control cells with functional DDR genes restore impaired phagocytosis of KD cells, suggesting cellular secretome as a major conduit for intercellular crosstalk and reveals a critical role for *TP53* and *ATX* genes in formation/secretion of the cellular secretome.
- High expression of immune checkpoint antigen on ABC-subtype DLBCL, promotes enhanced antibody dependent cellular phagocytosis with chemoimmunotherapeutic combination with immune checkpoint inhibitors such as anti-CD47, anti-PD-L1, anti-PD1.
- Blockade of CD47/Sirp- α interaction circumvent impaired ADCP due to *TP53*, *ATX*, KD providing the rational for incorporation of checkpoint inhibitors into current R-CHOP treatment regimen for *TP53*, *ATX* mutated, resistant/refractory ABC-subtype of DLBCL.

7.2 Molecular characterization of a “Tropical” Chronic Lymphocytic Leukemia cohort

- Ghanaian chronic lymphocytic leukaemia (CLL) patient have lower median age at diagnosis and a higher proportion of youth population and female predominance compared to CLL patients from the developed world such as Europe and the USA.
- A substantial number of Ghanaian CLL patients (86.4%) present with late clinical disease stage at diagnosis despite a higher proportion showing good prognosis (80%) by ZAP-70

and CD38 status which is contrary to reported pattern of CLL patients in the developed countries but consistent with that observed on the African continent.

- CLL in Ghanaian patients expressed predominant sIgM+ and kappa light chain restriction not correlated to prognostication of ZAP-70 and CD38 status. Contrarily, IgM+/IgD+ co-expression is the predominant phenotype reported among CLL patients in USA and Western Europe.

8 Outlook

The tumor microenvironment has other immune cells whose functional roles may influence overall outcome of tumor cells elimination. There is thus the need to evaluate the functional role of DDR genes identified to mediate impaired phagocytosis in an *in vivo* setting that offers immunocompetent background. For this purpose, the MyD88 mouse model can be reconstituted with specific DDR gene KD cell by tail injection for engraftment and treatment combinations including immune checkpoint inhibitors administered and evaluated.

Identified DDR genes may participate in a common or different pathways to influence macrophage activation. There is the need to evaluate the secretome of each KD gene in comparison to control by comprehensive cytokine profiling and proteomics to clarify the specific molecules involved in the cellular crosstalk. This could provide an opportunity to supplement or augment current treatment regimen to achieve a better outcome.

The phenomenon recapitulated the acute secretory activating phenotype (ASAP) reported in an aggressive “double-hit” lymphoma model of Myc-BCL2 suggesting possible broad-base nature of the phenomenon and its potential application in the TME as a therapeutic strategy.

9 References

1. Wang M, Zhao J, Zhang L, Wei F, Lian Y, Wu Y, et al. Role of tumor microenvironment in tumorigenesis. *Journal of Cancer*. 2017;8(5):761-73. PubMed PMID: 28382138. Pubmed Central PMCID: PMC5381164. Epub 2017/04/07.
2. Nazemi M, Rainero E. Cross-Talk Between the Tumor Microenvironment, Extracellular Matrix, and Cell Metabolism in Cancer. *Frontiers in Oncology*. 2020;10:239. PubMed PMID: 32175281. Pubmed Central PMCID: 7054479.
3. Ma XJ, Dahiya S, Richardson E, Erlander M, Sgroi DC. Gene expression profiling of the tumor microenvironment during breast cancer progression. *Breast Cancer Research : BCR*. 2009;11(1):R7. PubMed PMID: 19187537. Pubmed Central PMCID: 2687710.
4. Oczko-Wojciechowska M, Pfeifer A, Jarzab M, Swierniak M, Rusinek D, Tyszkiewicz T, et al. Impact of the Tumor Microenvironment on the Gene Expression Profile in Papillary Thyroid Cancer. *Pathobiology*. 2020;87(2):143-54. PubMed PMID: 32320975.
5. Menter T, Tzankov A. Mechanisms of Immune Evasion and Immune Modulation by Lymphoma Cells. *Frontiers in Oncology*. 2018;8:54. PubMed PMID: 29564225. Pubmed Central PMCID: 5845888.
6. de Charette M, Houot R. Hide or defend, the two strategies of lymphoma immune evasion: potential implications for immunotherapy. *Haematologica*. 2018 Aug;103(8):1256-68. PubMed PMID: 30006449. Pubmed Central PMCID: 6068015.
7. Qian BZ, Pollard JW. Macrophage diversity enhances tumor progression and metastasis. *Cell*. 2010 Apr 2;141(1):39-51. PubMed PMID: 20371344. Pubmed Central PMCID: 4994190.
8. Tille JC, Vieira AF, Saint-Martin C, Djerroudi L, Fuhmann L, Bidard FC, et al. Tumor-infiltrating lymphocytes are associated with poor prognosis in invasive lobular breast carcinoma. *Modern Pathology : an official journal of the United States and Canadian Academy of Pathology, Inc*. 2020 Nov;33(11):2198-207. PubMed PMID: 32404955.
9. Zhang J, Yan Y, Yang Y, Wang L, Li M, Wang J, et al. High Infiltration of Tumor-Associated Macrophages Influences Poor Prognosis in Human Gastric Cancer Patients, Associates With the Phenomenon of EMT. *Medicine (Baltimore)*. 2016 Feb;95(6):e2636. PubMed PMID: 26871785. Pubmed Central PMCID: 4753880.

10. Tadeo I, Berbegall AP, Navarro S, Castel V, Noguera R. A stiff extracellular matrix is associated with malignancy in peripheral neuroblastic tumors. *Pediatr Blood Cancer*. 2017 Sep;64(9). PubMed PMID: 28121069.
11. Xiong G-F, Xu R. Function of cancer cell-derived extracellular matrix in tumor progression. *Journal of Cancer Metastasis and Treatment*. 2016;2(9):357.
12. Walker C, Mojares E, Del Rio Hernandez A. Role of Extracellular Matrix in Development and Cancer Progression. *Int J Mol Sci*. 2018 Oct 4;19(10). PubMed PMID: 30287763. Pubmed Central PMCID: 6213383.
13. Takeshima H, Ushijima T. Accumulation of genetic and epigenetic alterations in normal cells and cancer risk. *NPJ Precis Oncol*. 2019;3:7. PubMed PMID: 30854468. Pubmed Central PMCID: 6403339
14. Torgovnick A, Schumacher B. DNA repair mechanisms in cancer development and therapy. *Frontiers in Genetics*. 2015;6:157. PubMed PMID: 25954303. Pubmed Central PMCID: 4407582.
15. Peller S, Rotter V. TP53 in hematological cancer: low incidence of mutations with significant clinical relevance. *Hum Mutat*. 2003 Mar;21(3):277-84. PubMed PMID: 12619113.
16. Poulogiannis G, Frayling IM, Arends MJ. DNA mismatch repair deficiency in sporadic colorectal cancer and Lynch syndrome. *Histopathology*. 2010 Jan;56(2):167-79. PubMed PMID: 20102395.
17. Rovira J, Valera A, Colomo L, Setoain X, Rodriguez S, Martinez-Trillos A, et al. Prognosis of patients with diffuse large B cell lymphoma not reaching complete response or relapsing after frontline chemotherapy or immunochemotherapy. *Ann Hematol*. 2015 May;94(5):803-12. PubMed PMID: 25501975. Pubmed Central PMCID: 4374121.
18. Agbay RL, Jain N, Loghavi S, Medeiros LJ, Khoury JD. Histologic transformation of chronic lymphocytic leukemia/small lymphocytic lymphoma. *Am J Hematol*. 2016 Oct;91(10):1036-43. PubMed PMID: 27414262.
19. Wang Y, Tschautscher MA, Rabe KG, Call TG, Leis JF, Kenderian SS, et al. Clinical characteristics and outcomes of Richter transformation: experience of 204 patients from a single center. *Haematologica*. 2020 Mar;105(3):765-73. PubMed PMID: 31197071. Pubmed Central PMCID: 7049354.
20. Nakad R, Schumacher B. DNA Damage Response and Immune Defense: Links and Mechanisms. *Frontiers in Genetics*. 2016;7:147. PubMed PMID: 27555866. Pubmed Central PMCID: 4977279.

21. Pallasch CP, Leskov I, Braun CJ, Vorholt D, Drake A, Soto-Feliciano YM, et al. Sensitizing protective tumor microenvironments to antibody-mediated therapy. *Cell*. 2014 Jan 30;156(3):590-602. PubMed PMID: 24485462. Pubmed Central PMCID: 3975171.
22. Bray F, Ferlay J, Soerjomataram I, Siegel RL, Torre LA, Jemal A. Global cancer statistics 2018: GLOBOCAN estimates of incidence and mortality worldwide for 36 cancers in 185 countries. *CA: A Cancer Journal for Clinicians*. 2018 Nov;68(6):394-424. PubMed PMID: 30207593.
23. Sung H, Ferlay J, Siegel RL, Laversanne M, Soerjomataram I, Jemal A, et al. Global Cancer Statistics 2020: GLOBOCAN Estimates of Incidence and Mortality Worldwide for 36 Cancers in 185 Countries. *CA: A Cancer Journal for Clinicians*. 2021 May;71(3):209-49. PubMed PMID: 33538338.
24. Rowley JD. Letter: A new consistent chromosomal abnormality in chronic myelogenous leukaemia identified by quinacrine fluorescence and Giemsa staining. *Nature*. 1973 Jun 1;243(5405):290-3. PubMed PMID: 4126434.
25. Anandakrishnan R, Varghese RT, Kinney NA, Garner HR. Estimating the number of genetic mutations (hits) required for carcinogenesis based on the distribution of somatic mutations. *PLoS Comput Biol*. 2019 Mar;15(3):e1006881. PubMed PMID: 30845172. Pubmed Central PMCID: 6424461.
26. Fabbri G, Rasi S, Rossi D, Trifonov V, Khiabani H, Ma J, et al. Analysis of the chronic lymphocytic leukemia coding genome: role of NOTCH1 mutational activation. *The Journal of Experimental Medicine*. 2011 Jul 4;208(7):1389-401. PubMed PMID: 21670202. Pubmed Central PMCID: 3135373.
27. Fridman JS, Lowe SW. Control of apoptosis by p53. *Oncogene*. 2003 Dec 8;22(56):9030-40. PubMed PMID: 14663481.
28. Tomasz Skorski AB, Margaret Nieborowska-Skorska, Miroslaw Majewski, Robert Martinez, John K.Choi, Rossana Trotta, Pawel Wlodarski, Danilo Perrotti, Tung O.Chan, Mariusz A.Wasik, Philip N.Tsichlis and Bruno Calabretta Transformation of hematopoietic cells by BCR/ABL requires activation of a PI-3k/Akt-dependent pathway. *The EMBO Journal* 1997;16 (20):6151-61.
29. Quail DF, Bowman RL, Akkari L, Quick ML, Schuhmacher AJ, Huse JT, et al. The tumor microenvironment underlies acquired resistance to CSF-1R inhibition in gliomas. *Science*. 2016 May 20;352(6288):aad3018. PubMed PMID: 27199435.
30. Joyce JA, Pollard JW. Microenvironmental regulation of metastasis. *Nat Rev Cancer*. 2009 Apr;9(4):239-52. PubMed PMID: 19279573. Pubmed Central PMCID: 3251309.

31. Walser T, Cui X, Yanagawa J, Lee JM, Heinrich E, Lee G, et al. Smoking and lung cancer: the role of inflammation. *Proceedings of the American Thoracic Society*. 2008 Dec 1;5(8):811-5. PubMed PMID: 19017734. Pubmed Central PMCID: 4080902.
32. Teras LR, Patel AV. The Epidemiology of Obesity and Hematologic Malignancies. In: Mittelman SD, Berger NA, editors. *Energy Balance and Hematologic Malignancies*. Boston, MA, Springer US; 2012. p. 1-30.
33. Matos A, Marinho-Dias J, Ramalheira S, Oliveira MJ, Bicho M, Ribeiro R. Mechanisms underlying the association between obesity and Hodgkin lymphoma. *Tumour biology : The Journal of the International Society for Oncodevelopmental Biology and Medicine*. 2016 Oct;37(10):13005-16. PubMed PMID: 27465553.
34. Perez-Hernandez AI, Catalan V, Gomez-Ambrosi J, Rodriguez A, Fruhbeck G. Mechanisms linking excess adiposity and carcinogenesis promotion. *Front Endocrinol (Lausanne)*. 2014;5:65. PubMed PMID: 24829560. Pubmed Central PMCID: 4013474.
35. Bhaskaran K, Douglas I, Forbes H, dos-Santos-Silva I, Leon DA, Smeeth L. Body-mass index and risk of 22 specific cancers: a population-based cohort study of 5.24 million UK adults. *Lancet*. 2014 Aug 30;384(9945):755-65. PubMed PMID: 25129328. Pubmed Central PMCID: PMC4151483. Epub 2014/08/19.
36. Strnad M. Salt and cancer. *Acta Medica Croatica : casopis Hrvatske Akademije Medicinskih Znanosti*. 2010 May;64(2):159-61. PubMed PMID: 20649083. Epub 2010/07/24.
37. Rowe M, Fitzsimmons L, Bell AI. Epstein-Barr virus and Burkitt lymphoma. *Chinese Journal of Cancer*. 2014 Dec;33(12):609-19. PubMed PMID: 25418195. Pubmed Central PMCID: 4308657.
38. Zhang LL, Wei JY, Wang L, Huang SL, Chen JL. Human T-cell lymphotropic virus type 1 and its oncogenesis. *Acta Pharmacol Sin*. 2017 Aug;38(8):1093-103. PubMed PMID: 28392570. Pubmed Central PMCID: 5547553.
39. Ng J, Wu J. Hepatitis B- and hepatitis C-related hepatocellular carcinomas in the United States: similarities and differences. *Hepat Mon*. 2012 Oct;12(10 HCC):e7635. PubMed PMID: 23233865. Pubmed Central PMCID: 3517810. Epub 2012/12/13.
40. Crosbie EJ, Einstein MH, Franceschi S, Kitchener HC. Human papillomavirus and cervical cancer. *Lancet*. 2013 Sep 7;382(9895):889-99. PubMed PMID: 23618600.
41. Inaba T. Radiation-induced and therapy-related AML/MDS. *Japanese Journal of Clinical Medicine*. 2009;67(10):1880-3. Pubmed Central PMCID: 19860183.

42. Ghasvand R, Robsahm TE, Green AC, Rueegg CS, Weiderpass E, Lund E, et al. Association of Phenotypic Characteristics and UV Radiation Exposure With Risk of Melanoma on Different Body Sites. *JAMA Dermatology*. 2019 Jan 1;155(1):39-49. PubMed PMID: 30477003. Pubmed Central PMCID: 6439571.
43. Moan J, Grigalavicius M, Baturaite Z, Dahlback A, Juzeniene A. The relationship between UV exposure and incidence of skin cancer. *Photodermatology, Photoimmunology & Photomedicine*. 2015 Jan;31(1):26-35. PubMed PMID: 25213656.
44. Yoshida M, Seiki M, Yamaguchi K, Takatsuki K. Monoclonal integration of human T-cell leukemia provirus in all primary tumors of adult T-cell leukemia suggests causative role of human T-cell leukemia virus in the disease. *Proc Natl Acad Sci U S A*. 1984 Apr;81(8):2534-7. PubMed PMID: 6326131. Pubmed Central PMCID: 345097.
45. Gao X, Cui X, Zhang X, Zhao C, Zhang N, Zhao Y, et al. Differential genetic mutations of ectoderm, mesoderm, and endoderm-derived tumors in TCGA database. *Cancer Cell International*. 2020 Dec 11;20(1):595. PubMed PMID: 33308219. Pubmed Central PMCID: 7730784.
46. Harris NL, Jaffe ES, Stein H, Banks PM, Chan JK, Cleary ML, et al. A revised European-American classification of lymphoid neoplasms: a proposal from the International Lymphoma Study Group. *Blood*. 1994 Sep 1;84(5):1361-92. PubMed PMID: 8068936.
47. Jaffe ES. *Pathology and genetics of tumours of haematopoietic and lymphoid tissues*. Lyon: IARC Press; 2001.
48. Arber DA, Orazi A, Hasserjian R, Thiele J, Borowitz MJ, Le Beau MM, et al. The 2016 revision to the World Health Organization classification of myeloid neoplasms and acute leukemia. *Blood*. 2016 May 19;127(20):2391-405. PubMed PMID: 27069254.
49. Swerdlow SH, Campo E, Pileri SA, Harris NL, Stein H, Siebert R, et al. The 2016 revision of the World Health Organization classification of lymphoid neoplasms. *Blood*. 2016 May 19;127(20):2375-90. PubMed PMID: 26980727. Pubmed Central PMCID: 4874220.
50. Nakao M, Yokota S, Iwai T, Kaneko H, Horiike S, Kashima K, et al. Internal tandem duplication of the *flt3* gene found in acute myeloid leukemia. *Leukemia*. 1996;10(12):1911-8. PubMed PMID: 8946930.
51. Noguera NI, Breccia M, Divona M, Diverio D, Costa V, De Santis S, et al. Alterations of the *FLT3* gene in acute promyelocytic leukemia: association with diagnostic characteristics and analysis of clinical outcome in patients treated with the Italian AIDA protocol. *Leukemia*. 2002 Nov;16(11):2185-9. PubMed PMID: 12399960.

52. Stirewalt DL, Radich JP. The role of FLT3 in haematopoietic malignancies. *Nat Rev Cancer*. 2003 Sep;3(9):650-65. PubMed PMID: 12951584.
53. Xu W, Yang H, Liu Y, Yang Y, Wang P, Kim SH, et al. Oncometabolite 2-hydroxyglutarate is a competitive inhibitor of alpha-ketoglutarate-dependent dioxygenases. *Cancer Cell*. 2011 Jan 18;19(1):17-30. PubMed PMID: 21251613. Pubmed Central PMCID: 3229304.
54. Nowell P, Hungerford D. *A minute chromosome in human chronic granulocytic leukemia*. 1st edition . Oxford: Oxford University Press; 2004.
55. Skorski T, Bellacosa A, Nieborowska-Skorska M, Majewski M, Martinez R, Choi JK, et al. Transformation of hematopoietic cells by BCR/ABL requires activation of a PI-3k/Akt-dependent pathway. *EMBO J*. 1997 Oct 15;16(20):6151-61. PubMed PMID: 9321394. Pubmed Central PMCID: 1326299.
56. Melo JV, Barnes DJ. Chronic myeloid leukaemia as a model of disease evolution in human cancer. *Nat Rev Cancer*. 2007 Jun;7(6):441-53. PubMed PMID: 17522713.
57. Batista DA, Hawkins A, Murphy KM, Griffin CA. BCR/ABL rearrangement in two cases of Philadelphia chromosome negative chronic myeloid leukemia: deletion on the derivative chromosome 9 may or not be present. *Cancer Genetics and Cytogenetics*. 2005 Dec;163(2):164-7. PubMed PMID: 16337861.
58. Virgili A, Brazma D, Reid AG, Howard-Reeves J, Valganon M, Chanalaris A, et al. FISH mapping of Philadelphia negative BCR/ABL1 positive CML. *Molecular Cytogenetics*. 2008 Jul 18;1:14. PubMed PMID: 18638369. Pubmed Central PMCID: 2500019.
59. Moorman AV, Ensor HM, Richards SM, Chilton L, Schwab C, Kinsey SE, et al. Prognostic effect of chromosomal abnormalities in childhood B-cell precursor acute lymphoblastic leukaemia: results from the UK Medical Research Council ALL97/99 randomised trial. *The Lancet Oncology*. 2010 May;11(5):429-38. PubMed PMID: 20409752.
60. Lo Nigro L. Biology of childhood acute lymphoblastic leukemia. *J Pediatr Hematol Oncol*. 2013 May;35(4):245-52. PubMed PMID: 23612374. Pubmed Central PMCID: 23612374.
61. Caligaris-Cappio F, Hamblin TJ. B-cell chronic lymphocytic leukemia: a bird of a different feather. *J Clin Oncol*. 1999 Jan;17(1):399-408. PubMed PMID: 10458259.

62. Hallek M, Cheson BD, Catovsky D, Caligaris-Cappio F, Dighiero G, Dohner H, et al. Guidelines for the diagnosis and treatment of chronic lymphocytic leukemia: a report from the International Workshop on Chronic Lymphocytic Leukemia updating the National Cancer Institute-Working Group 1996 guidelines. *Blood*. 2008 Jun 15;111(12):5446-56. PubMed PMID: 18216293. Pubmed Central PMCID: 2972576.
63. Cramer P, Hallek M. Prognostic factors in chronic lymphocytic leukemia-what do we need to know? *Nature reviews Clinical Oncology*. 2011 Jan;8(1):38-47. PubMed PMID: 20956983.
64. Ansell SM, Li CY, Lloyd RV, Phyllyk RL. Epstein-Barr virus infection in Richter's transformation. *Am J Hematol*. 1999 Feb;60(2):99-104. PubMed PMID: 9929100. Epub 1999/02/03.
65. Dohner H, Stilgenbauer S, Benner A, Leupolt E, Krober A, Bullinger L, et al. Genomic aberrations and survival in chronic lymphocytic leukemia. *N Engl J Med*. 2000 Dec 28;343(26):1910-6. PubMed PMID: 11136261.
66. Friedman DR, Lucas JE, Weinberg JB. Clinical and biological relevance of genomic heterogeneity in chronic lymphocytic leukemia. *PloS One*. 2013;8(2):e57356. PubMed PMID: 23468975. Pubmed Central PMCID: 3585365.
67. Ten Hacken E, Burger JA. Microenvironment interactions and B-cell receptor signaling in Chronic Lymphocytic Leukemia: Implications for disease pathogenesis and treatment. *Biochimica et Biophysica Acta*. 2016 Mar;1863(3):401-13. PubMed PMID: 26193078. Pubmed Central PMCID: 4715999.
68. Hamblin TJ, Davis Z, Gardiner A, Oscier DG, Stevenson FK. Unmutated Ig VH genes are associated with a more aggressive form of chronic lymphocytic leukemia. *Blood* 1999; 94(6):1848-54.
69. Hus I, Podhorecka M, Bojarska-Junak A, Rolinski J, Schmitt M, Sieklucka M, et al. The clinical significance of ZAP-70 and CD38 expression in B-cell chronic lymphocytic leukaemia. *Annals of Oncology : official journal of the European Society for Medical Oncology / ESMO*. 2006 Apr;17(4):683-90. PubMed PMID: 16524977.
70. Thomas RK, Re D, Wolf J, Diehl V. Part I: Hodgkin's lymphoma--molecular biology of Hodgkin and Reed-Sternberg cells. *The Lancet Oncology*. 2004 Jan;5(1):11-8. PubMed PMID: 14700604.
71. Clodi K, Younes A. Reed-Sternberg cells and the TNF family of receptors/ligands. *Leuk Lymphoma*. 1997 Oct;27(3-4):195-205. PubMed PMID: 9402319.
72. Horie R, Higashihara M, Watanabe T. Hodgkin's lymphoma and CD30 signal transduction. *Int J Hematol*. 2003 Jan;77(1):37-47. PubMed PMID: 12568298.

73. Cheng P, Zlobin A, Volgina V, Gottipati S, Osborne B, Simel EJ, et al. Notch-1 regulates NF-kappaB activity in hemopoietic progenitor cells. *Journal of Immunology*. 2001 Oct 15;167(8):4458-67. PubMed PMID: 11591772.
74. van den Berg A, Visser L, Poppema S. High expression of the CC chemokine TARC in Reed-Sternberg cells. A possible explanation for the characteristic T-cell infiltrate in Hodgkin's lymphoma. *Am J Pathol*. 1999 Jun;154(6):1685-91. PubMed PMID: 10362793. Pubmed Central PMCID: 1876772.
75. Amini RM, Enblad G. Relationship between Hodgkin's and non-Hodgkin's lymphomas. *Med Oncol*. 2003;20(3):211-20. PubMed PMID: 14514970.
76. Re D, Kuppers R, Diehl V. Molecular pathogenesis of Hodgkin's lymphoma. *J Clin Oncol*. 2005 Sep 10;23(26):6379-86. PubMed PMID: 16155023.
77. Perry AM, Diebold J, Nathwani BN, MacLennan KA, Muller-Hermelink HK, Bast M, et al. Non-Hodgkin lymphoma in the developing world: review of 4539 cases from the International Non-Hodgkin Lymphoma Classification Project. *Haematologica*. 2016 Oct;101(10):1244-50. PubMed PMID: 27354024. Pubmed Central PMCID: 5046654.
78. Teras LR, DeSantis CE, Cerhan JR, Morton LM, Jemal A, Flowers CR. 2016 US lymphoid malignancy statistics by World Health Organization subtypes. *CA: A Cancer Journal for Clinicians*. 2016 Nov 12;66(6):443-59. PubMed PMID: 27618563.
79. Alizadeh AA, Eisen MB, Davis RE, Ma C, Lossos IS, Rosenwald A, et al. Distinct types of diffuse large B-cell lymphoma identified by gene expression profiling. *Nature*. 2000 Feb 3;403(6769):503-11. PubMed PMID: 10676951.
80. Rosenwald A, Wright G, Chan WC, Connors JM, Campo E, Fisher RI, et al. The use of molecular profiling to predict survival after chemotherapy for diffuse large-B-cell lymphoma. *N Engl J Med*. 2002 Jun 20;346(25):1937-47. PubMed PMID: 12075054.
81. Karube K, Enjuanes A, Dlouhy I, Jares P, Martin-Garcia D, Nadeu F, et al. Integrating genomic alterations in diffuse large B-cell lymphoma identifies new relevant pathways and potential therapeutic targets. *Leukemia*. 2018 Mar;32(3):675-84. PubMed PMID: 28804123. Pubmed Central PMCID: 5843901.
82. Kramer MH, Hermans J, Wijburg E, Philippo K, Geelen E, van Krieken JH, et al. Clinical relevance of BCL2, BCL6, and MYC rearrangements in diffuse large B-cell lymphoma. *Blood*. 1998 Nov 1;92(9):3152-62. PubMed PMID: 9787151.

83. Barrans S, Crouch S, Smith A, Turner K, Owen R, Patmore R, et al. Rearrangement of MYC is associated with poor prognosis in patients with diffuse large B-cell lymphoma treated in the era of rituximab. *J Clin Oncol*. 2010 Jul 10;28(20):3360-5. PubMed PMID: 20498406.
84. Offit K, Lo Coco F, Louie DC, Parsa NZ, Leung D, Portlock C, et al. Rearrangement of the bcl-6 gene as a prognostic marker in diffuse large-cell lymphoma. *N Engl J Med*. 1994 Jul 14;331(2):74-80. PubMed PMID: 8208268.
85. Alberts B. DNA replication and recombination. *Nature*. 2003 Jan 23;421(6921):431-5. PubMed PMID: 12540917.
86. Hanahan D, Weinberg RA. Hallmarks of cancer: the next generation. *Cell*. 2011 Mar 4;144(5):646-74. PubMed PMID: 21376230.
87. Jackson SP, Bartek J. The DNA-damage response in human biology and disease. *Nature*. 2009 Oct 22;461(7267):1071-8. PubMed PMID: 19847258. Pubmed Central PMCID: 2906700.
88. Lindahl T, Barnes DE. Repair of endogenous DNA damage. *Cold Spring Harbor Symposia on Quantitative Biology*. 2000;65:127-33. PubMed PMID: 12760027.
89. Guengerich FP. Interactions of carcinogen-bound DNA with individual DNA polymerases. *Chem Rev*. 2006 Feb;106(2):420-52. PubMed PMID: 16464013.
90. Schroeder GK, Lad C, Wyman P, Williams NH, Wolfenden R. The time required for water attack at the phosphorus atom of simple phosphodiester and of DNA. *Proc Natl Acad Sci U S A*. 2006 Mar 14;103(11):4052-5. PubMed PMID: 16537483. Pubmed Central PMCID: 1449644.
91. Lindahl T, Karlstrom O. Heat-induced depyrimidination of deoxyribonucleic acid in neutral solution. *Biochemistry*. 1973 Dec 4;12(25):5151-4. PubMed PMID: 4600811.
92. Lindahl T, Nyberg B. Rate of depurination of native deoxyribonucleic acid. *Biochemistry*. 1972 Sep 12;11(19):3610-8. PubMed PMID: 4626532.
93. Beranek DT. Distribution of methyl and ethyl adducts following alkylation with monofunctional alkylating agents. *Mutation Research*. 1990 Jul;231(1):11-30. PubMed PMID: 2195323. Pubmed Central PMCID: 2195323.
94. Rajski SR, Williams RM. DNA Cross-Linking Agents as Antitumor Drugs. *Chem Rev*. 1998 Dec 17;98(8):2723-96. PubMed PMID: 11848977.

95. Sonntag C. Free Radical-Induced DNA Damage and Its Repair. 1st edition. Heidelberg: Springer Berlin; 2006.
96. Breen AP, Murphy JA. Reactions of oxyl radicals with DNA. *Free Radical Biology & Medicine*. 1995 Jun;18(6):1033-77. PubMed PMID: 7628729.
97. Goodman MF, Woodgate R. Translesion DNA polymerases. *Cold Spring Harbor Perspectives in Biology*. 2013 Oct 1;5(10):a010363. PubMed PMID: 23838442. Pubmed Central PMCID: 3783050.
98. Clausen AR, Zhang S, Burgers PM, Lee MY, Kunkel TA. Ribonucleotide incorporation, proofreading and bypass by human DNA polymerase delta. *DNA Repair (Amst)*. 2013 Feb 1;12(2):121-7. PubMed PMID: 23245697. Pubmed Central PMCID: 3552135.
99. Jinks-Robertson S, Bhagwat AS. Transcription-associated mutagenesis. *Annu Rev Genet*. 2014;48:341-59. PubMed PMID: 25251854. Pubmed Central PMCID: 9464043.
100. Dahm R. Friedrich Miescher and the discovery of DNA. *Developmental Biology*. 2005;278(2):274-88.
101. Watson JD, Crick FH. Molecular structure of nucleic acids; a structure for deoxyribose nucleic acid. *Nature*. 1953 Apr 25;171(4356):737-8. PubMed PMID: 13054692.
102. Friedberg E. A brief history of the DNA repair field. *Cell Research*. 2008;18:3-7.
103. Ward JF. DNA damage produced by ionizing radiation in mammalian cells: identities, mechanisms of formation, and reparability. *Progress in Nucleic Acid Research and Molecular Biology*. 1988;35:95-125.
104. Douki T. The variety of UV-induced pyrimidine dimeric photoproducts in DNA as shown by chromatographic quantification methods. *Photochemical & Photobiological Sciences*. 2013 (12):1286-302.
105. Valko M, Rhodes CJ, Moncol J, Izakovic M, Mazur M. Free radicals, metals and antioxidants in oxidative stress-induced cancer. *Chemico-biological Interactions*. 2006 Mar 10;160(1):1-40. PubMed PMID: 16430879.
106. Dizdaroglu M, Jaruga P. Mechanisms of free radical-induced damage to DNA. *Free Radic Res*. 2012 Apr;46(4):382-419. PubMed PMID: 22276778.
107. Chaney SG, Sancar A. DNA repair: enzymatic mechanisms and relevance to drug response. *Journal of the National Cancer Institute*. 1996 Oct 2;88(19):1346-60. PubMed PMID: 8827012.

108. Roos WP, Nikolova T, Quiros S, Naumann SC, Kiedron O, Zdzienicka MZ, et al. Brca2/Xrcc2 dependent HR, but not NHEJ, is required for protection against O(6)-methylguanine triggered apoptosis, DSBs and chromosomal aberrations by a process leading to SCEs. *DNA Repair (Amst)*. 2009 Jan 1;8(1):72-86. PubMed PMID: 18840549.
109. Peto R. The Causes of Cancer: Quantitative Estimates of Avoidable Risks of Cancer in the United States Today. In: Castellani A, editor. *The Use of Human Cells for the Evaluation of Risk from Physical and Chemical Agents*. Boston, MA: Springer; 1983. p. 587–93.
110. Wogan GN, Hecht SS, Felton JS, Conney AH, Loeb LA. Environmental and chemical carcinogenesis. *Seminars in Cancer Biology*. 2004 Dec;14(6):473-86. PubMed PMID: 15489140.
111. Melendez-Colon VJ, Luch A, Seidel A, Baird WM. Cancer initiation by polycyclic aromatic hydrocarbons results from formation of stable DNA adducts rather than apurinic sites. *Carcinogenesis*. 1999 Oct;20(10):1885-91. PubMed PMID: 10506100.
112. Ciccia A, Elledge SJ. The DNA damage response: making it safe to play with knives. *Mol Cell*. 2010 Oct 22;40(2):179-204. PubMed PMID: 20965415. Pubmed Central PMCID: 2988877.
113. Fugmann SD, Lee AI, Shockett PE, Villey IJ, Schatz DG. The RAG proteins and V(D)J recombination: complexes, ends, and transposition. *Annu Rev Immunol*. 2000;18:495-527. PubMed PMID: 10837067.
114. Li X, Heyer WD. Homologous recombination in DNA repair and DNA damage tolerance. *Cell Res*. 2008 Jan;18(1):99-113. PubMed PMID: 18166982. Pubmed Central PMCID: 3087377.
115. Chang HHY, Pannunzio NR, Adachi N, Lieber MR. Non-homologous DNA end joining and alternative pathways to double-strand break repair. *Nature reviews Molecular Cell Biology*. 2017 Aug;18(8):495-506. PubMed PMID: 28512351. Pubmed Central PMCID: 7062608.
116. Symington LS. Mechanism and regulation of DNA end resection in eukaryotes. *Crit Rev Biochem Mol Biol*. 2016 May-Jun;51(3):195-212. PubMed PMID: 27098756. Pubmed Central PMCID: 4957645.
117. Shibata A, Moiani D, Arvai AS, Perry J, Harding SM, Genois MM, et al. DNA double-strand break repair pathway choice is directed by distinct MRE11 nuclease activities. *Mol Cell*. 2014 Jan 9;53(1):7-18. PubMed PMID: 24316220. Pubmed Central PMCID: 3909494.
118. Wang W, Daley JM, Kwon Y, Krasner DS, Sung P. Plasticity of the Mre11–Rad50–Xrs2–Sae2 nuclease ensemble in the processing of DNA-bound obstacles. *Genes & Development*. 2018;31(23-24):2331-2336.

119. Reginato G, Cannavo E, Cejka P. Physiological protein blocks direct the Mre11-Rad50-Xrs2 and Sae2 nuclease complex to initiate DNA end resection. *Genes Dev.* 2017 Dec 1;31(23-24):2325-30. PubMed PMID: 29321179. Pubmed Central PMCID: 5795779.
120. Hurley PJ, Bunz F. ATM and ATR: components of an integrated circuit. *Cell Cycle.* 2007 Feb 15;6(4):414-7. PubMed PMID: 17312392.
121. Kinner A, Wu W, Staudt C, Iliakis G. Gamma-H2AX in recognition and signaling of DNA double-strand breaks in the context of chromatin. *Nucleic Acids Res.* 2008 Oct;36(17):5678-94. PubMed PMID: 18772227. Pubmed Central PMCID: 2553572.
122. Stiff T, O'Driscoll M, Rief N, Iwabuchi K, Lobrich M, Jeggo PA. ATM and DNA-PK function redundantly to phosphorylate H2AX after exposure to ionizing radiation. *Cancer Res.* 2004 Apr 1;64(7):2390-6. PubMed PMID: 15059890.
123. Rogakou EP, Pilch DR, Orr AH, Ivanova VS, Bonner WM. DNA double-stranded breaks induce histone H2AX phosphorylation on serine 139. *J Biol Chem.* 1998 Mar 6;273(10):5858-68. PubMed PMID: 9488723.
124. Chen HT, Bhandoola A, Difilippantonio MJ, Zhu J, Brown MJ, Tai X, et al. Response to RAG-mediated VDJ cleavage by NBS1 and gamma-H2AX. *Science.* 2000 Dec 8;290(5498):1962-5. PubMed PMID: 11110662. Pubmed Central PMCID: 4721589.
125. de Jager M, van Noort J, van Gent DC, Dekker C, Kanaar R, Wyman C. Human Rad50/Mre11 is a flexible complex that can tether DNA ends. *Mol Cell.* 2001 Nov;8(5):1129-35. PubMed PMID: 11741547.
126. Huertas P, Jackson SP. Human CtIP mediates cell cycle control of DNA end resection and double strand break repair. *J Biol Chem.* 2009 Apr 3;284(14):9558-65. PubMed PMID: 19202191. Pubmed Central PMCID: 2666608.
127. Huertas P, Cortes-Ledesma F, Sartori AA, Aguilera A, Jackson SP. CDK targets Sae2 to control DNA-end resection and homologous recombination. *Nature.* 2008 Oct 2;455(7213):689-92. PubMed PMID: 18716619. Pubmed Central PMCID: 2635538.
128. Mochan TA, Venere M, DiTullio RA, Jr., Halazonetis TD. 53BP1 and NFB1/MDC1-Nbs1 function in parallel interacting pathways activating ataxia-telangiectasia mutated (ATM) in response to DNA damage. *Cancer Res.* 2003 Dec 15;63(24):8586-91. PubMed PMID: 14695167.
129. Stewart GS, Wang B, Bignell CR, Taylor AM, Elledge SJ. MDC1 is a mediator of the mammalian DNA damage checkpoint. *Nature.* 2003 Feb 27;421(6926):961-6. PubMed PMID: 12607005.

130. Andegeko Y, Moyal L, Mittelman L, Tsarfaty I, Shiloh Y, Rotman G. Nuclear retention of ATM at sites of DNA double strand breaks. *J Biol Chem*. 2001 Oct 12;276(41):38224-30. PubMed PMID: 11454856.
131. Kozlov SV, Graham ME, Jakob B, Tobias F, Kijas AW, Tanuji M, et al. Autophosphorylation and ATM activation: additional sites add to the complexity. *J Biol Chem*. 2011 Mar 18;286(11):9107-19. PubMed PMID: 21149446. Pubmed Central PMCID: 3059052.
132. Setiাপutra D, Durocher D. Shieldin - the protector of DNA ends. *EMBO Rep*. 2019 May;20(5). PubMed PMID: 30948458. Pubmed Central PMCID: 6501030.
133. Hartlerode AJ, Morgan MJ, Wu Y, Buis J, Ferguson DO. Recruitment and activation of the ATM kinase in the absence of DNA-damage sensors. *Nature Structural & Molecular Biology*. 2015 Sep;22(9):736-43. PubMed PMID: 26280532. Pubmed Central PMCID: 4560612.
134. Lieber MR. The mechanism of double-strand DNA break repair by the nonhomologous DNA end-joining pathway. *Annu Rev Biochem*. 2010;79(1):181-211. PubMed PMID: 20192759. Pubmed Central PMCID: 3079308.
135. Loblrich M, Jeggo P. A Process of Resection-Dependent Nonhomologous End Joining Involving the Goddess Artemis. *Trends Biochem Sci*. 2017 Sep;42(9):690-701. PubMed PMID: 28739276. Pubmed Central PMCID: 5604544.
136. Frit P, Ropars V, Modesti M, Charbonnier JB, Calsou P. Plugged into the Ku-DNA hub: The NHEJ network. *Prog Biophys Mol Biol*. 2019 Oct;147:62-76. PubMed PMID: 30851288.
137. Grawunder U, Zimmer D, Fugmann S, Schwarz K, Lieber MR. DNA ligase IV is essential for V(D)J recombination and DNA double-strand break repair in human precursor lymphocytes. *Mol Cell*. 1998 Oct;2(4):477-84. PubMed PMID: 9809069.
138. West RB, Yaneva M, Lieber MR. Productive and nonproductive complexes of Ku and DNA-dependent protein kinase at DNA termini. *Mol Cell Biol*. 1998 Oct;18(10):5908-20. PubMed PMID: 9742108. Pubmed Central PMCID: 109177.
139. Walker JR, Corpina RA, Goldberg J. Structure of the Ku heterodimer bound to DNA and its implications for double-strand break repair. *Nature*. 2001 Aug 9;412(6847):607-14. PubMed PMID: 11493912.
140. Gottlieb TM, Jackson SP. The DNA-dependent protein kinase: requirement for DNA ends and association with Ku antigen. *Cell*. 1993 Jan 15;72(1):131-42. PubMed PMID: 8422676.

141. Chanut P, Britton S, Coates J, Jackson SP, Calsou P. Coordinated nuclease activities counteract Ku at single-ended DNA double-strand breaks. *Nature Communications*. 2016 Sep 19;7:12889. PubMed PMID: 27641979. Pubmed Central PMCID: 5031800.
142. Daley JM, Laan RL, Suresh A, Wilson TE. DNA joint dependence of pol X family polymerase action in nonhomologous end joining. *J Biol Chem*. 2005 Aug 12;280(32):29030-7. PubMed PMID: 15964833.
143. Li Z, Otevrel T, Gao Y, Cheng HL, Seed B, Stamato TD, et al. The XRCC4 gene encodes a novel protein involved in DNA double-strand break repair and V(D)J recombination. *Cell*. 1995 Dec 29;83(7):1079-89. PubMed PMID: 8548796.
144. Critchlow SE, Bowater RP, Jackson SP. Mammalian DNA double-strand break repair protein XRCC4 interacts with DNA ligase IV. *Current Biology : CB*. 1997 Aug 1;7(8):588-98. PubMed PMID: 9259561.
145. Lindahl T. Instability and decay of the primary structure of DNA. *Nature*. 1993 Apr 22;362(6422):709-15. PubMed PMID: 8469282.
146. Wallace SS, Murphy DL, Sweasy JB. Base excision repair and cancer. *Cancer Lett*. 2012 Dec 31;327(1-2):73-89. PubMed PMID: 22252118. Pubmed Central PMCID: 3361536.
147. Jeppesen DK, Bohr VA, Stevnsner T. DNA repair deficiency in neurodegeneration. *Prog Neurobiol*. 2011 Jul;94(2):166-200. PubMed PMID: 21550379. Pubmed Central PMCID: 3123739.
148. Gillet LCJ, Schärer OD. Molecular mechanisms of mammalian global genome nucleotide excision repair. *Chemical Reviews*. 2006.
149. Sugasawa K, Ng JM, Masutani C, Iwai S, van der Spek PJ, Eker AP, et al. Xeroderma pigmentosum group C protein complex is the initiator of global genome nucleotide excision repair. *Mol Cell*. 1998 Aug;2(2):223-32. PubMed PMID: 9734359.
150. Volker M, Mone MJ, Karmakar P, van Hoffen A, Schul W, Vermeulen W, et al. Sequential assembly of the nucleotide excision repair factors in vivo. *Mol Cell*. 2001 Jul;8(1):213-24. PubMed PMID: 11511374.
151. Ljungman M, Lane DP. Transcription - guarding the genome by sensing DNA damage. *Nat Rev Cancer*. 2004 Sep;4(9):727-37. PubMed PMID: 15343279.
152. Mellon I, Spivak G, Hanawalt PC. Selective removal of transcription-blocking DNA damage from the transcribed strand of the mammalian DHFR gene. *Cell*. 1987 Oct 23;51(2):241-9. PubMed PMID: 3664636.

153. Cleaver JE. Defective repair replication of DNA in xeroderma pigmentosum. *Nature*. 1968 May 18;218(5142):652-6. PubMed PMID: 5655953.
154. Lehmann AR. DNA repair-deficient diseases, xeroderma pigmentosum, Cockayne syndrome and trichothiodystrophy. *Biochimie*. 2003 Nov;85(11):1101-11. PubMed PMID: 14726016.
155. Friedberg EC, Walker GC, Siede W, Wood RD. *DNA Repair and Mutagenesis*. 2 ed. Washington, DC: ASM PRESS; 2005.
156. Kunkel TA, Erie DA. DNA mismatch repair. *Annu Rev Biochem*. 2005;74:681-710. PubMed PMID: 15952900.
157. Hong Z, Jiang J, Hashiguchi K, Hoshi M, Lan L, Yasui A. Recruitment of mismatch repair proteins to the site of DNA damage in human cells. *Journal of Cell Science*. 2008 Oct 1;121(Pt 19):3146-54. PubMed PMID: 18765568.
158. Lopez de Saro FJ. Regulation of interactions with sliding clamps during DNA replication and repair. *Curr Genomics*. 2009 May;10(3):206-15. PubMed PMID: 19881914. Pubmed Central PMCID: 2705854.
159. Junop MS, Obmolova G, Rausch K, Hsieh P, Yang W. Composite active site of an ABC ATPase: MutS uses ATP to verify mismatch recognition and authorize DNA repair. *Mol Cell*. 2001 Jan;7(1):1-12. PubMed PMID: 11172706.
160. Geng H, Sakato M, DeRocco V, Yamane K, Du C, Erie DA, et al. Biochemical analysis of the human mismatch repair proteins hMutSalph α MSH2(G674A)-MSH6 and MSH2-MSH6(T1219D). *J Biol Chem*. 2012 Mar 23;287(13):9777-91. PubMed PMID: 22277660. Pubmed Central PMCID: 3323011.
161. Constantin N, Dzantiev L, Kadyrov FA, Modrich P. Human mismatch repair: reconstitution of a nick-directed bidirectional reaction. *J Biol Chem*. 2005 Dec 2;280(48):39752-61. PubMed PMID: 16188885. Pubmed Central PMCID: 1435381.
162. Dzantiev L, Constantin N, Genschel J, Iyer RR, Burgers PM, Modrich P. A defined human system that supports bidirectional mismatch-provoked excision. *Mol Cell*. 2004 Jul 2;15(1):31-41. PubMed PMID: 15225546.
163. Kastan MB, Bartek J. Cell-cycle checkpoints and cancer. *Nature*. 2004 Nov 18;432(7015):316-23. PubMed PMID: 15549093.

164. Watanabe N, Broome M, Hunter T. Regulation of the human WEE1Hu CDK tyrosine 15-kinase during the cell cycle. *EMBO J.* 1995 May 1;14(9):1878-91. PubMed PMID: 7743995. Pubmed Central PMCID: 398287.
165. Lew J. MAP kinases and CDKs: kinetic basis for catalytic activation. *Biochemistry.* 2003 Feb 4;42(4):849-56. PubMed PMID: 12549901.
166. Shiloh Y. ATM and related protein kinases: safeguarding genome integrity. *Nat Rev Cancer.* 2003 Mar;3(3):155-68. PubMed PMID: 12612651.
167. Burger K, Muhl B, Harasim T, Rohrmoser M, Malamoussi A, Orban M, et al. Chemotherapeutic drugs inhibit ribosome biogenesis at various levels. *J Biol Chem.* 2010 Apr 16;285(16):12416-25. PubMed PMID: 20159984. Pubmed Central PMCID: 2852979.
168. Li J, Stern DF. Regulation of CHK2 by DNA-dependent protein kinase. *J Biol Chem.* 2005 Mar 25;280(12):12041-50. PubMed PMID: 15668230.
169. Shang ZF, Huang B, Xu QZ, Zhang SM, Fan R, Liu XD, et al. Inactivation of DNA-dependent protein kinase leads to spindle disruption and mitotic catastrophe with attenuated checkpoint protein 2 Phosphorylation in response to DNA damage. *Cancer Res.* 2010 May 1;70(9):3657-66. PubMed PMID: 20406977.
170. Yang S, Jeong JH, Brown AL, Lee CH, Pandolfi PP, Chung JH, et al. Promyelocytic leukemia activates Chk2 by mediating Chk2 autophosphorylation. *J Biol Chem.* 2006 Sep 8;281(36):26645-54. PubMed PMID: 16835227.
171. Lee JS, Collins KM, Brown AL, Lee CH, Chung JH. hCds1-mediated phosphorylation of BRCA1 regulates the DNA damage response. *Nature.* 2000 Mar 9;404(6774):201-4. PubMed PMID: 10724175.
172. Zhang J, Willers H, Feng Z, Ghosh JC, Kim S, Weaver DT, et al. Chk2 phosphorylation of BRCA1 regulates DNA double-strand break repair. *Mol Cell Biol.* 2004 Jan;24(2):708-18. PubMed PMID: 14701743. Pubmed Central PMCID: 343805.
173. Bahassi EM, Ovesen JL, Riesenber AL, Bernstein WZ, Hasty PE, Stambrook PJ. The checkpoint kinases Chk1 and Chk2 regulate the functional associations between hBRCA2 and Rad51 in response to DNA damage. *Oncogene.* 2008 Jun 26;27(28):3977-85. PubMed PMID: 18317453.
174. Tan Y, Raychaudhuri P, Costa RH. Chk2 mediates stabilization of the FoxM1 transcription factor to stimulate expression of DNA repair genes. *Mol Cell Biol.* 2007 Feb;27(3):1007-16. PubMed PMID: 17101782. Pubmed Central PMCID: 1800696.

175. Falck J, Mailand N, Syljuasen RG, Bartek J, Lukas J. The ATM-Chk2-Cdc25A checkpoint pathway guards against radioresistant DNA synthesis. *Nature*. 2001 Apr 12;410(6830):842-7. PubMed PMID: 11298456.
176. Chehab NH, Malikzay A, Appel M, Halazonetis TD. Chk2/hCds1 functions as a DNA damage checkpoint in G1 by stabilizing p53. *Genes & Development*. 2000;14(3):278-88.
177. Inoue Y, Kitagawa M, Taya Y. Phosphorylation of pRB at Ser612 by Chk1/2 leads to a complex between pRB and E2F-1 after DNA damage. *EMBO J*. 2007 Apr 18;26(8):2083-93. PubMed PMID: 17380128. Pubmed Central PMCID: 1852778.
178. Bruno T, De Nicola F, Iezzi S, Lecis D, D'Angelo C, Di Padova M, et al. Chk1 phosphorylation by ATM/ATR and Chk2 kinases activates p53 transcription and the G2/M checkpoint. *Cancer Cell*. 2006 Dec;10(6):473-86. PubMed PMID: 17157788.
179. Raleigh JM, O'Connell MJ. The G(2) DNA damage checkpoint targets both Wee1 and Cdc25. *Journal of Cell Science*. 2000 May;113 (Pt 10):1727-36. PubMed PMID: 10769204.
180. Yonish-Rouach E, Resnitzky D, Lotem J, Sachs L, Kimchi A, Oren M. Wild-type p53 induces apoptosis of myeloid leukaemic cells that is inhibited by interleukin-6. *Nature*. 1991 Jul 25;352(6333):345-7. PubMed PMID: 1852210.
181. Toledo F, Krummel KA, Lee CJ, Liu CW, Rodewald LW, Tang M, et al. A mouse p53 mutant lacking the proline-rich domain rescues Mdm4 deficiency and provides insight into the Mdm2-Mdm4-p53 regulatory network. *Cancer Cell*. 2006 Apr;9(4):273-85. PubMed PMID: 16616333.
182. Reinhardt HC, Schumacher B. The p53 network: cellular and systemic DNA damage responses in aging and cancer. *Trends in Genetics : TIG*. 2012 Mar;28(3):128-36. PubMed PMID: 22265392. Pubmed Central PMCID: 4120491.
183. Yoshida K, Miki Y. The cell death machinery governed by the p53 tumor suppressor in response to DNA damage. *Cancer Science*. 2010 Apr;101(4):831-5. PubMed PMID: 20132225.
184. Haupt Y, Maya R, Kazanietz A, Oren M. Mdm2 promotes the rapid degradation of p53. *Nature*. 1997 May 15;387(6630):296-9. PubMed PMID: 9153395.
185. Moll UM, Petrenko O. The MDM2-p53 interaction. *Mol Cancer Res*. 2003 Dec;1(14):1001-8. PubMed PMID: 14707283.
186. Cox LS, Lane DP. Tumour suppressors, kinases and clamps: how p53 regulates the cell cycle in response to DNA damage. *Bioessays*. 1995 Jun;17(6):501-8. PubMed PMID: 7575491.

187. Abbas T, Dutta A. p21 in cancer: intricate networks and multiple activities. *Nat Rev Cancer*. 2009 Jun;9(6):400-14. PubMed PMID: 19440234. Pubmed Central PMCID: 2722839.
188. Yu J, Zhang L. PUMA, a potent killer with or without p53. *Oncogene*. 2008 Dec;27 Suppl 1(Suppl 1):S71-83. PubMed PMID: 19641508. Pubmed Central PMCID: 2860432.
189. Youle RJ, Strasser A. The BCL-2 protein family: opposing activities that mediate cell death. *Nature Reviews Molecular Cell Biology*. 2008 Jan;9(1):47-59. PubMed PMID: 18097445.
190. Green DR. Apoptotic pathways: ten minutes to dead. *Cell*. 2005;121(5):671-4.
191. Zhang J, Huang K, O'Neill KL, Pang X, Luo X. Bax/Bak activation in the absence of Bid, Bim, Puma, and p53. *Cell Death Dis*. 2016 Jun 16;7(6):e2266. PubMed PMID: 27310874. Pubmed Central PMCID: 5143395.
192. Speidel D. Transcription-independent p53 apoptosis: an alternative route to death. *Trends Cell Biol*. 2010 Jan;20(1):14-24. PubMed PMID: 19879762.
193. Chandrasekaran A, Idelchik M, Melendez JA. Redox control of senescence and age-related disease. *Redox Biol*. 2017 Apr;11:91-102. PubMed PMID: 27889642. Pubmed Central PMCID: 5126126.
194. van Deursen JM. The role of senescent cells in ageing. *Nature*. 2014 May 22;509(7501):439-46. PubMed PMID: 24848057. Pubmed Central PMCID: 4214092.
195. Schosserer M, Grillari J, Breitenbach M. The Dual Role of Cellular Senescence in Developing Tumors and Their Response to Cancer Therapy. *Frontiers in Oncology*. 2017;7:278. PubMed PMID: 29218300. Pubmed Central PMCID: 5703792.
196. Campisi J. Replicative senescence: an old lives' tale? *Cell*. 1996 Feb 23;84(4):497-500. PubMed PMID: 8598035.
197. Bernadotte A, Mikhelson VM, Spivak IM. Markers of cellular senescence. Telomere shortening as a marker of cellular senescence. *Aging (Albany NY)*. 2016 Jan;8(1):3-11. PubMed PMID: 26805432. Pubmed Central PMCID: 4761709.
198. d'Adda di Fagagna F, Teo SH, Jackson SP. Functional links between telomeres and proteins of the DNA-damage response. *Genes Dev*. 2004 Aug 1;18(15):1781-99. PubMed PMID: 15289453.

199. Xue W, Zender L, Miething C, Dickins RA, Hernando E, Krizhanovsky V, et al. Senescence and tumour clearance is triggered by p53 restoration in murine liver carcinomas. *Nature*. 2007 Feb 8;445(7128):656-60. PubMed PMID: 17251933. Pubmed Central PMCID: 4601097.
200. Prieur A, Peeper DS. Cellular senescence in vivo: a barrier to tumorigenesis. *Curr Opin Cell Biol*. 2008 Apr;20(2):150-5. PubMed PMID: 18353625.
201. Artandi SE, Attardi LD. Pathways connecting telomeres and p53 in senescence, apoptosis, and cancer. *Biochemical and Biophysical Research Communications*. 2005 Jun 10;331(3):881-90. PubMed PMID: 15865944.
202. Lu Y, Ma W, Li Z, Lu J, Wang X. The interplay between p16 serine phosphorylation and arginine methylation determines its function in modulating cellular apoptosis and senescence. *Sci Rep*. 2017 Jan 25;7:41390. PubMed PMID: 28120917. Pubmed Central PMCID: 5264599.
203. Iida M, Nakamura M, Tokuda E, Toyosawa D, Niwa T, Ohuchi N, et al. The p21 levels have the potential to be a monitoring marker for ribociclib in breast cancer. *Oncotarget*. 2019 Aug 6;10(47):4907-18. PubMed PMID: 31448056. Pubmed Central PMCID: 6690670.
204. Kiwerska K, Szyfter K. DNA repair in cancer initiation, progression, and therapy—a double-edged sword. *J Appl Genet*. 2019 Nov;60(3-4):329-34. PubMed PMID: 31468363. Pubmed Central PMCID: 6803590.
205. Pessina F, Gioia U, Brandi O, Farina S, Ceccon M, Francia S, et al. DNA Damage Triggers a New Phase in Neurodegeneration. *Trends in Genetics : TIG*. 2021 Apr;37(4):337-54. PubMed PMID: 33020022. Epub 2020/10/07.
206. Madabhushi R, Pan L, Tsai LH. DNA damage and its links to neurodegeneration. *Neuron*. 2014 Jul 16;83(2):266-82. PubMed PMID: 25033177. Pubmed Central PMCID: 5564444.
207. Maynard S, Fang EF, Scheibye-Knudsen M, Croteau DL, Bohr VA. DNA Damage, DNA Repair, Aging, and Neurodegeneration. *Cold Spring Harbor Perspectives in Medicine*. 2015 Sep 18;5(10). PubMed PMID: 26385091. Pubmed Central PMCID: 4588127.
208. Zhao J. Cancer stem cells and chemoresistance: The smartest survives the raid. *Pharmacol Ther*. 2016 Apr;160:145-58. PubMed PMID: 26899500. Pubmed Central PMCID: 4808328.
209. Zahreddine H, Borden KL. Mechanisms and insights into drug resistance in cancer. *Front Pharmacol*. 2013;4:28. PubMed PMID: 23504227. Pubmed Central PMCID: 3596793.

210. Ahmed AA, Etemadmoghadam D, Temple J, Lynch AG, Riad M, Sharma R, et al. Driver mutations in TP53 are ubiquitous in high grade serous carcinoma of the ovary. *J Pathol.* 2010 May;221(1):49-56. PubMed PMID: 20229506. Pubmed Central PMCID: 3262968.
211. Bensaad K, Tsuruta A, Selak MA, Vidal MN, Nakano K, Bartrons R, et al. TIGAR, a p53-inducible regulator of glycolysis and apoptosis. *Cell.* 2006 Jul 14;126(1):107-20. PubMed PMID: 16839880.
212. Zhang C, Lin M, Wu R, Wang X, Yang B, Levine AJ, et al. Parkin, a p53 target gene, mediates the role of p53 in glucose metabolism and the Warburg effect. *Proc Natl Acad Sci U S A.* 2011 Sep 27;108(39):16259-64. PubMed PMID: 21930938. Pubmed Central PMCID: 3182683.
213. Gualberto A, Aldape K, Kozakiewicz K, Tlsty TD. An oncogenic form of p53 confers a dominant, gain-of-function phenotype that disrupts spindle checkpoint control. *Proc Natl Acad Sci U S A.* 1998 Apr 28;95(9):5166-71. PubMed PMID: 9560247. Pubmed Central PMCID: 20232.
214. Murphy KL, Dennis AP, Rosen JM. A gain of function p53 mutant promotes both genomic instability and cell survival in a novel p53-null mammary epithelial cell model. *FASEB J.* 2000 Nov;14(14):2291-302. PubMed PMID: 11053251.
215. Caulin C, Nguyen T, Lang GA, Goepfert TM, Brinkley BR, Cai WW, et al. An inducible mouse model for skin cancer reveals distinct roles for gain- and loss-of-function p53 mutations. *The Journal of Clinical Investigation.* 2007 Jul;117(7):1893-901. PubMed PMID: 17607363. Pubmed Central PMCID: 1904325.
216. Wang SP, Wang WL, Chang YL, Wu CT, Chao YC, Kao SH, et al. p53 controls cancer cell invasion by inducing the MDM2-mediated degradation of Slug. *Nat Cell Biol.* 2009 Jun;11(6):694-704. PubMed PMID: 19448627.
217. Greer JB, Whitcomb DC. Role of BRCA1 and BRCA2 mutations in pancreatic cancer. *Gut.* 2007;56(5):601-5.
218. Quesada V, Conde L, Villamor N, Ordóñez GR, Jares P, Bassaganyas L, et al. Exome sequencing identifies recurrent mutations of the splicing factor SF3B1 gene in chronic lymphocytic leukemia. *Nature genetics.* 2012;44(1):47-52.
219. Bell D, Berchuck A, Birrer M, Chien J, Cramer DW, Dao F, et al. Integrated genomic analyses of ovarian carcinoma. *Nature.* 2011;474:609–15.
220. Masutani C, Kusumoto R, Yamada A, Dohmae N, Yokoi M, Yuasa M, et al. The XPV (xeroderma pigmentosum variant) gene encodes human DNA polymerase eta. *Nature.* 1999 Jun 17;399(6737):700-4. PubMed PMID: 10385124.

221. Cleaver JE. Defective repair replication of DNA in xeroderma pigmentosum. 1968. *DNA Repair*. 2004;3(2):183-7.
222. Kastan MB, Lim DS. The many substrates and functions of ATM. *Nature Reviews Molecular Cell Biology*. 2000 Dec;1(3):179-86. PubMed PMID: 11252893.
223. Mavrou A, Tsangaris GT, Roma E, Kolialexi A. The ATM gene and ataxia telangiectasia. *Anticancer Res*. 2008 Jan-Feb;28(1B):401-5. PubMed PMID: 18383876.
224. Alfarouk KO, Stock CM, Taylor S, Walsh M, Muddathir AK, Verduzco D, et al. Resistance to cancer chemotherapy: failure in drug response from ADME to P-gp. *Cancer Cell International*. 2015;15:71. PubMed PMID: 26180516. Pubmed Central PMCID: 4502609.
225. Rueff J, Rodrigues AS. Cancer Drug Resistance: A Brief Overview from a Genetic Viewpoint. *Methods in Molecular Biology*. 2016;1395:1-18. PubMed PMID: 26910065.
226. Traverso N, Ricciarelli R, Nitti M, Marengo B, Furfaro AL, Pronzato MA, et al. Role of glutathione in cancer progression and chemoresistance. *Oxidative Medicine and Cellular Longevity*. 2013;2013:972913. PubMed PMID: 23766865. Pubmed Central PMCID: 3673338.
227. Huang D, Duan H, Huang H, Tong X, Han Y, Ru G, et al. Cisplatin resistance in gastric cancer cells is associated with HER2 upregulation-induced epithelial-mesenchymal transition. *Sci Rep*. 2016 Feb 5;6:20502. PubMed PMID: 26846307. Pubmed Central PMCID: 4742832.
228. Kurrey NK, Jalgaonkar SP, Joglekar AV, Ghanate AD, Chaskar PD, Doiphode RY, et al. Snail and slug mediate radioresistance and chemoresistance by antagonizing p53-mediated apoptosis and acquiring a stem-like phenotype in ovarian cancer cells. *Stem Cells*. 2009 Sep;27(9):2059-68. PubMed PMID: 19544473.
229. Viale A, De Franco F, Orleth A, Cambiaghi V, Giuliani V, Bossi D, et al. Cell-cycle restriction limits DNA damage and maintains self-renewal of leukaemia stem cells. *Nature*. 2009 Jan 1;457(7225):51-6. PubMed PMID: 19122635.
230. Mansoori B, Mohammadi A, Davudian S, Shirjang S, Baradaran B. The Different Mechanisms of Cancer Drug Resistance: A Brief Review. *Adv Pharm Bull*. 2017 Sep;7(3):339-48. PubMed PMID: 29071215. Pubmed Central PMCID: 5651054.
231. Kelderman S, Schumacher TN, Haanen JB. Acquired and intrinsic resistance in cancer immunotherapy. *Mol Oncol*. 2014 Sep 12;8(6):1132-9. PubMed PMID: 25106088. Pubmed Central PMCID: 5528612.

232. Lippert TH, Ruoff HJ, Volm M. Intrinsic and acquired drug resistance in malignant tumors. The main reason for therapeutic failure. *Arzneimittelforschung*. 2008;58(6):261-4. PubMed PMID: 18677966.
233. Quintas-Cardama A, Kantarjian HM, Cortes JE. Mechanisms of primary and secondary resistance to imatinib in chronic myeloid leukemia. *Cancer Control*. 2009 Apr;16(2):122-31. PubMed PMID: 19337198.
234. Challagundla KB, Wise PM, Neviani P, Chava H, Murtadha M, Xu T, et al. Exosome-mediated transfer of microRNAs within the tumor microenvironment and neuroblastoma resistance to chemotherapy. *Journal of the National Cancer Institute*. 2015 Jul;107(7). PubMed PMID: 25972604. Pubmed Central PMCID: 4651042.
235. Morgan MA, Lawrence TS. Molecular Pathways: Overcoming Radiation Resistance by Targeting DNA Damage Response Pathways. *Clin Cancer Res*. 2015 Jul 1;21(13):2898-904. PubMed PMID: 26133775. Pubmed Central PMCID: 4494107.
236. De Angelis PM, Svendsrud DH, Kravik KL, Stokke T. Cellular response to 5-fluorouracil (5-FU) in 5-FU-resistant colon cancer cell lines during treatment and recovery. *Molecular Cancer*. 2006 May 18;5:20. PubMed PMID: 16709241. Pubmed Central PMCID: 1524802.
237. Bhome R, Bullock MD, Al Saihati HA, Goh RW, Primrose JN, Sayan AE, et al. A top-down view of the tumor microenvironment: structure, cells and signaling. *Frontiers in Cell and Developmental Biology*. 2015;3:33. PubMed PMID: 26075202. Pubmed Central PMCID: 4448519.
238. Luqmani YA. Mechanisms of drug resistance in cancer chemotherapy. *Medical principles and practice : International Journal of the Kuwait University, Health Science Centre*. 2005;14 Suppl 1(1):35-48. PubMed PMID: 16103712.
239. Correia AL, Bissell MJ. The tumor microenvironment is a dominant force in multidrug resistance. *Drug resistance updates : Reviews and Commentaries in Antimicrobial and Anticancer Chemotherapy*. 2012 Feb-Apr;15(1-2):39-49. PubMed PMID: 22335920. Pubmed Central PMCID: 3658318.
240. Mumenthaler SM, Foo J, Choi NC, Heise N, Leder K, Agus DB, et al. The Impact of Microenvironmental Heterogeneity on the Evolution of Drug Resistance in Cancer Cells. *Cancer Informatics*. 2015;14(Suppl 4):19-31. PubMed PMID: 26244007. Pubmed Central PMCID: 4504404.
241. Eiro N, Fernandez-Gomez J, Sacristan R, Fernandez-Garcia B, Lobo B, Gonzalez-Suarez J, et al. Stromal factors involved in human prostate cancer development, progression and castration resistance. *Journal of Cancer Research and Clinical Oncology*. 2017 Feb;143(2):351-9. PubMed PMID: 27787597.

242. Bizzarri M, Cucina A, Conti F, D'Anselmi F. Beyond the oncogene paradigm: understanding complexity in cancerogenesis. *Acta Biotheor.* 2008 Sep;56(3):173-96. PubMed PMID: 18288572.
243. Bissell MJ, Kenny PA, Radisky DC. Microenvironmental regulators of tissue structure and function also regulate tumor induction and progression: the role of extracellular matrix and its degrading enzymes. *Cold Spring Harbor Symposia on Quantitative Biology.* 2005;70:343-56. PubMed PMID: 16869771. Pubmed Central PMCID: 3004779.
244. Acerbi I, Cassereau L, Dean I, Shi Q, Au A, Park C, et al. Human breast cancer invasion and aggression correlates with ECM stiffening and immune cell infiltration. *Integr Biol (Camb).* 2015 Oct;7(10):1120-34. PubMed PMID: 25959051. Pubmed Central PMCID: 4593730.
245. Wang S, Jia J, Liu D, Wang M, Wang Z, Li X, et al. Matrix Metalloproteinase Expressions Play Important role in Prediction of Ovarian Cancer Outcome. *Sci Rep.* 2019 Aug 12;9(1):11677. PubMed PMID: 31406154. Pubmed Central PMCID: 6691000.
246. Grossman JG, Nywening TM, Belt BA, Panni RZ, Krasnick BA, DeNardo DG, et al. Recruitment of CCR2(+) tumor associated macrophage to sites of liver metastasis confers a poor prognosis in human colorectal cancer. *Oncoimmunology.* 2018;7(9):e1470729. PubMed PMID: 30228938. Pubmed Central PMCID: 6140580.
247. Corso S, Giordano S. Cell-autonomous and non-cell-autonomous mechanisms of HGF/MET-driven resistance to targeted therapies: from basic research to a clinical perspective. *Cancer Discov.* 2013 Sep;3(9):978-92. PubMed PMID: 23901039.
248. Dolcetti L, Peranzoni E, Ugel S, Marigo I, Fernandez Gomez A, Mesa C, et al. Hierarchy of immunosuppressive strength among myeloid-derived suppressor cell subsets is determined by GM-CSF. *Eur J Immunol.* 2010 Jan;40(1):22-35. PubMed PMID: 19941314.
249. Movahedi K, Guillems M, Van den Bossche J, Van den Bergh R, Gysemans C, Beschin A, et al. Identification of discrete tumor-induced myeloid-derived suppressor cell subpopulations with distinct T cell-suppressive activity. *Blood.* 2008 Apr 15;111(8):4233-44. PubMed PMID: 18272812.
250. Elkabets M, Ribeiro VS, Dinarello CA, Ostrand-Rosenberg S, Di Santo JP, Apte RN, et al. IL-1beta regulates a novel myeloid-derived suppressor cell subset that impairs NK cell development and function. *Eur J Immunol.* 2010 Dec;40(12):3347-57. PubMed PMID: 21110318. Pubmed Central PMCID: 3373225.
251. Rodriguez PC, Ochoa AC. Arginine regulation by myeloid derived suppressor cells and tolerance in cancer: mechanisms and therapeutic perspectives. *Immunol Rev.* 2008 Apr;222:180-91. PubMed PMID: 18364002. Pubmed Central PMCID: 3546504.

252. Markowitz J, Wang J, Vangundy Z, You J, Yildiz V, Yu L, et al. Nitric oxide mediated inhibition of antigen presentation from DCs to CD4(+) T cells in cancer and measurement of STAT1 nitration. *Sci Rep*. 2017 Nov 13;7(1):15424. PubMed PMID: 29133913. Pubmed Central PMCID: 5684213.
253. Barcus CE, Holt EC, Keely PJ, Eliceiri KW, Schuler LA. Dense collagen-I matrices enhance pro-tumorigenic estrogen-prolactin crosstalk in MCF-7 and T47D breast cancer cells. *PLoS One*. 2015;10(1):e0116891. PubMed PMID: 25607819. Pubmed Central PMCID: 4301649.
254. Haldorsen IS, Stefansson I, Grüner R, Husby JA, Magnussen IJ, Werner HM, et al. Increased microvascular proliferation is negatively correlated to tumour blood flow and is associated with unfavourable outcome in endometrial carcinomas. *British Journal of Cancer*. 2014;110(1):107-14.
255. Cui L, Tse K, Zahedi P, Harding SM, Zafarana G, Jaffray DA, et al. Hypoxia and cellular localization influence the radiosensitizing effect of gold nanoparticles (AuNPs) in breast cancer cells. *Radiat Res*. 2014 Nov;182(5):475-88. PubMed PMID: 25361396.
256. Muller-Edenborn K, Leger K, Glaus Garzon JF, Oertli C, Mirsaidi A, Richards PJ, et al. Hypoxia attenuates the proinflammatory response in colon cancer cells by regulating I κ B. *Oncotarget*. 2015 Aug 21;6(24):20288-301. PubMed PMID: 25978030. Pubmed Central PMCID: 4653005.
257. Cao Z, Ding BS, Guo P, Lee SB, Butler JM, Casey SC, et al. Angiocrine factors deployed by tumor vascular niche induce B cell lymphoma invasiveness and chemoresistance. *Cancer Cell*. 2014 Mar 17;25(3):350-65. PubMed PMID: 24651014. Pubmed Central PMCID: 4017921.
258. Ho YH, Del Toro R, Rivera-Torres J, Rak J, Korn C, Garcia-Garcia A, et al. Remodeling of Bone Marrow Hematopoietic Stem Cell Niches Promotes Myeloid Cell Expansion during Premature or Physiological Aging. *Cell Stem Cell*. 2019 Sep 5;25(3):407-18 e6. PubMed PMID: 31303548. Pubmed Central PMCID: 6739444.
259. Moschoi R, Imbert V, Nebout M, Chiche J, Mary D, Prebet T, et al. Protective mitochondrial transfer from bone marrow stromal cells to acute myeloid leukemic cells during chemotherapy. *Blood*. 2016 Jul 14;128(2):253-64. PubMed PMID: 27257182.
260. Marlein CR, Piddock RE, Mistry JJ, Zaitseva L, Hellmich C, Horton RH, et al. CD38-Driven Mitochondrial Trafficking Promotes Bioenergetic Plasticity in Multiple Myeloma. *Cancer Res*. 2019 May 1;79(9):2285-97. PubMed PMID: 30622116.
261. Ye H, Adane B, Khan N, Sullivan T, Minhajuddin M, Gasparetto M, et al. Leukemic Stem Cells Evade Chemotherapy by Metabolic Adaptation to an Adipose Tissue Niche. *Cell Stem Cell*. 2016 Jul 7;19(1):23-37. PubMed PMID: 27374788. Pubmed Central PMCID: 4938766.

262. Gordon S, Pluddemann A. Tissue macrophages: heterogeneity and functions. *BMC Biol.* 2017 Jun 29;15(1):53. PubMed PMID: 28662662. Pubmed Central PMCID: 5492929.
263. Orihuela R, McPherson CA, Harry GJ. Microglial M1/M2 polarization and metabolic states. *Br J Pharmacol.* 2016 Feb;173(4):649-65. PubMed PMID: 25800044. Pubmed Central PMCID: 4742299.
264. Shi J, Wu Z, Li Z, Ji J. Roles of Macrophage Subtypes in Bowel Anastomotic Healing and Anastomotic Leakage. *Journal of Immunology Research.* 2018;2018:6827237.
265. Mantovani A, Sica A, Allavena P, Garlanda C, Locati M. Tumor-associated macrophages and the related myeloid-derived suppressor cells as a paradigm of the diversity of macrophage activation. *Hum Immunol.* 2009 May;70(5):325-30. PubMed PMID: 19236898.
266. Benoit M, Desnues B, Mege JL. Macrophage polarization in bacterial infections. *Journal of Immunology.* 2008 Sep 15;181(6):3733-9. PubMed PMID: 18768823.
267. Fairweather D, Cihakova D. Alternatively activated macrophages in infection and autoimmunity. *J Autoimmun.* 2009 Nov-Dec;33(3-4):222-30. PubMed PMID: 19819674. Pubmed Central PMCID: 2783278.
268. Makita N, Hizukuri Y, Yamashiro K, Murakawa M, Hayashi Y. IL-10 enhances the phenotype of M2 macrophages induced by IL-4 and confers the ability to increase eosinophil migration. *Int Immunol.* 2015 Mar;27(3):131-41. PubMed PMID: 25267883.
269. Yang Z, Ming XF. Functions of arginase isoforms in macrophage inflammatory responses: impact on cardiovascular diseases and metabolic disorders. *Frontiers in Immunology.* 2014;5:533. PubMed PMID: 25386179. Pubmed Central PMCID: 4209887.
270. Monteleone I, Pallone F, Monteleone G. Interleukin-23 and Th17 cells in the control of gut inflammation. *Mediators Inflamm.* 2009;2009:297645. PubMed PMID: 19503799. Pubmed Central PMCID: 2688649.
271. Dieci MV, Miglietta F, Guarneri V. Immune Infiltrates in Breast Cancer: Recent Updates and Clinical Implications. *Cells.* 2021 Jan 23;10(2). PubMed PMID: 33498711. Pubmed Central PMCID: 7911608.
272. Pages F, Galon J, Dieu-Nosjean MC, Tartour E, Sautes-Fridman C, Fridman WH. Immune infiltration in human tumors: a prognostic factor that should not be ignored. *Oncogene.* 2010 Feb 25;29(8):1093-102. PubMed PMID: 19946335.
273. Gupta V, Yull F, Khabele D. Bipolar Tumor-Associated Macrophages in Ovarian Cancer as Targets for Therapy. *Cancers (Basel).* 2018;29(10):366. Pubmed Central PMCID: PMC6210537.

274. Cai QC, Liao H, Lin SX, Xia Y, Wang XX, Gao Y, et al. High expression of tumor-infiltrating macrophages correlates with poor prognosis in patients with diffuse large B-cell lymphoma. *Med Oncol*. 2012 Dec;29(4):2317-22. PubMed PMID: 22198695.
275. Scott DW, Steidl C. The classical Hodgkin lymphoma tumor microenvironment: macrophages and gene expression-based modeling. *Hematology American Society of Hematology Education Program*. 2014 Dec 5;2014(1):144-50. PubMed PMID: 25696847.
276. Zhang W, Wang L, Zhou D, Cui Q, Zhao D, Wu Y. Expression of tumor-associated macrophages and vascular endothelial growth factor correlates with poor prognosis of peripheral T-cell lymphoma, not otherwise specified. *Leuk Lymphoma*. 2011 Jan;52(1):46-52. PubMed PMID: 21077742.
277. Lin CN, Wang CJ, Chao YJ, Lai MD, Shan YS. The significance of the co-existence of osteopontin and tumor-associated macrophages in gastric cancer progression. *BMC Cancer*. 2015 Mar 15;15:128. PubMed PMID: 25872762. Pubmed Central PMCID: 4384326.
278. Zeisberger SM, Odermatt B, Marty C, Zehnder-Fjallman AH, Ballmer-Hofer K, Schwendener RA. Clodronate-liposome-mediated depletion of tumour-associated macrophages: a new and highly effective antiangiogenic therapy approach. *Br J Cancer*. 2006 Aug 7;95(3):272-81. PubMed PMID: 16832418. Pubmed Central PMCID: 2360657.
279. Verollet C, Charriere GM, Labrousse A, Cougoule C, Le Cabec V, Maridonneau-Parini I. Extracellular proteolysis in macrophage migration: losing grip for a breakthrough. *Eur J Immunol*. 2011 Oct;41(10):2805-13. PubMed PMID: 21953638.
280. Murdoch C, Muthana M, Coffelt SB, Lewis CE. The role of myeloid cells in the promotion of tumour angiogenesis. *Nat Rev Cancer*. 2008 Aug;8(8):618-31. PubMed PMID: 18633355.
281. Guruvayoorappan C. Tumor versus tumor-associated macrophages: how hot is the link? *Integr Cancer Ther*. 2008 Jun;7(2):90-5. PubMed PMID: 18550889.
282. Ben-Baruch A. Inflammation-associated immune suppression in cancer: the roles played by cytokines, chemokines and additional mediators. *Seminars in Cancer Biology*. 2006 Feb;16(1):38-52. PubMed PMID: 16139507.
283. Flavell RA, Sanjabi S, Wrzesinski SH, Licona-Limon P. The polarization of immune cells in the tumour environment by TGFbeta. *Nat Rev Immunol*. 2010 Aug;10(8):554-67. PubMed PMID: 20616810. Pubmed Central PMCID: 3885992.

284. Zhang F, Wang H, Wang X, Jiang G, Liu H, Zhang G, et al. TGF-beta induces M2-like macrophage polarization via SNAIL-mediated suppression of a pro-inflammatory phenotype. *Oncotarget*. 2016 Aug 9;7(32):52294-306. PubMed PMID: 27418133. Pubmed Central PMCID: 5239552.
285. Regis S, Dondero A, Caliendo F, Bottino C, Castriconi R. NK Cell Function Regulation by TGF-beta-Induced Epigenetic Mechanisms. *Frontiers in Immunology*. 2020;11:311. PubMed PMID: 32161594. Pubmed Central PMCID: 7052483.
286. Castriconi R, Cantoni C, Della Chiesa M, Vitale M, Marcenaro E, Conte R, et al. Transforming growth factor beta 1 inhibits expression of NKp30 and NKG2D receptors: consequences for the NK-mediated killing of dendritic cells. *Proc Natl Acad Sci U S A*. 2003 Apr 1;100(7):4120-5. PubMed PMID: 12646700. Pubmed Central PMCID: 153058.
287. Ito M, Minamiya Y, Kawai H, Saito S, Saito H, Nakagawa T, et al. Tumor-derived TGFbeta-1 induces dendritic cell apoptosis in the sentinel lymph node. *Journal of Immunology*. 2006 May 1;176(9):5637-43. PubMed PMID: 16622033.
288. Konkel JE, Zhang D, Zanvit P, Chia C, Zangarle-Murray T, Jin W, et al. Transforming Growth Factor-beta Signaling in Regulatory T Cells Controls T Helper-17 Cells and Tissue-Specific Immune Responses. *Immunity*. 2017 Apr 18;46(4):660-74. PubMed PMID: 28423340.
289. Sanjabi S, Oh SA, Li MO. Regulation of the Immune Response by TGF-beta: From Conception to Autoimmunity and Infection. *Cold Spring Harbor Perspectives in Biology*. 2017 Jun 1;9(6). PubMed PMID: 28108486. Pubmed Central PMCID: 5453394.
290. Maeda H, Shiraishi A. TGF-beta contributes to the shift toward Th2-type responses through direct and IL-10-mediated pathways in tumor-bearing mice. *The Journal of Immunology*. 1996;156(1):73-78.
291. Sato T, Terai M, Tamura Y, Alexeev V, Mastrangelo MJ, Selvan SR. Interleukin 10 in the tumor microenvironment: a target for anticancer immunotherapy. *Immunol Res*. 2011 Dec;51(2-3):170-82. PubMed PMID: 22139852.
292. Jonuleit H, Schmitt E, Schuler G, Knop J, Enk AH. Induction of interleukin 10-producing, nonproliferating CD4(+) T cells with regulatory properties by repetitive stimulation with allogeneic immature human dendritic cells. *The Journal of Experimental Medicine*. 2000 Nov 6;192(9):1213-22. PubMed PMID: 11067871. Pubmed Central PMCID: 2193357.
293. Qin Z, Noffz G, Mohaupt M, Blankenstein T. Interleukin-10 prevents dendritic cell accumulation and vaccination with granulocyte-macrophage colony-stimulating factor gene-modified tumor cells. *Journal of Immunology*. 1997 Jul 15;159(2):770-6. PubMed PMID: 9218594.

294. Sica A, Sacconi A, Bottazzi B, Polentarutti N, Vecchi A, van Damme J, et al. Autocrine production of IL-10 mediates defective IL-12 production and NF-kappa B activation in tumor-associated macrophages. *Journal of Immunology*. 2000 Jan 15;164(2):762-7. PubMed PMID: 10623821.
295. Couper KN, Blount DG, Riley EM. IL-10: the master regulator of immunity to infection. *Journal of Immunology*. 2008 May 1;180(9):5771-7. PubMed PMID: 18424693.
296. D'Andrea A, Aste-Amezaga M, Valiante NM, Ma X, Kubin M, Trinchieri G. Interleukin 10 (IL-10) inhibits human lymphocyte interferon gamma-production by suppressing natural killer cell stimulatory factor/IL-12 synthesis in accessory cells. *The Journal of Experimental Medicine*. 1993 Sep 1;178(3):1041-8. PubMed PMID: 8102388. Pubmed Central PMCID: 2191152.
297. Trifunovic J, Miller L, Debeljak Z, Horvat V. Pathologic patterns of interleukin 10 expression--a review. *Biochem Med (Zagreb)*. 2015;25(1):36-48. PubMed PMID: 25672465. Pubmed Central PMCID: 4401305.
298. Ma X, Yan W, Zheng H, Du Q, Zhang L, Ban Y, et al. Regulation of IL-10 and IL-12 production and function in macrophages and dendritic cells. *F1000Research*. 2015;4. PubMed PMID: 26918147. Pubmed Central PMCID: 4754024.
299. Rahim SS, Khan N, Boddupalli CS, Hasnain SE, Mukhopadhyay S. Interleukin-10 (IL-10) mediated suppression of IL-12 production in RAW 264.7 cells also involves c-rel transcription factor. *Immunology*. 2005 Mar;114(3):313-21. PubMed PMID: 15720433. Pubmed Central PMCID: 1782084.
300. Mannino MH, Zhu Z, Xiao H, Bai Q, Wakefield MR, Fang Y. The paradoxical role of IL-10 in immunity and cancer. *Cancer Lett*. 2015 Oct 28;367(2):103-7. PubMed PMID: 26188281.
301. Mumm JB, Oft M. Pegylated IL-10 induces cancer immunity: the surprising role of IL-10 as a potent inducer of IFN-gamma-mediated CD8(+) T cell cytotoxicity. *Bioessays*. 2013 Jul;35(7):623-31. PubMed PMID: 23666891.
302. Rodriguez PC, Quiceno DG, Zabaleta J, Ortiz B, Zea AH, Piazuelo MB, et al. Arginase I production in the tumor microenvironment by mature myeloid cells inhibits T-cell receptor expression and antigen-specific T-cell responses. *Cancer Res*. 2004 Aug 15;64(16):5839-49. PubMed PMID: 15313928.
303. Bak SP, Alonso A, Turk MJ, Berwin B. Murine ovarian cancer vascular leukocytes require arginase-1 activity for T cell suppression. *Mol Immunol*. 2008 Dec;46(2):258-68. PubMed PMID: 18824264. Pubmed Central PMCID: 2613193.

304. Albaugh VL, Pinzon-Guzman C, Barbul A. Arginine-Dual roles as an onconutrient and immunonutrient. *Journal of surgical oncology*. 2017 Mar;115(3):273-80. PubMed PMID: 27861915. Pubmed Central PMCID: 6486789.
305. Wang H, Li P, Wang L, Xia Z, Huang H, Lu Y, et al. High numbers of CD68+ tumor-associated macrophages correlate with poor prognosis in extranodal NK/T-cell lymphoma, nasal type. *Ann Hematol*. 2015 Sep;94(9):1535-44. PubMed PMID: 25990795.
306. Xu X, Li Z, Liu J, Zhu F, Wang Z, Wang J, et al. The prognostic value of tumour-associated macrophages in Non-Hodgkin's lymphoma: A systematic review and meta-analysis. *Scandinavian Journal of Immunology*. 2020 Jan;91(1):e12814. PubMed PMID: 31419843.
307. Tan KL, Scott DW, Hong F, Kahl BS, Fisher RI, Bartlett NL, et al. Tumor-associated macrophages predict inferior outcomes in classic Hodgkin lymphoma: a correlative study from the E2496 Intergroup trial. *Blood*. 2012 Oct 18;120(16):3280-7. PubMed PMID: 22948049. Pubmed Central PMCID: 3476539.
308. Martin-Moreno AM, Roncador G, Maestre L, Mata E, Jimenez S, Martinez-Torrecedrada JL, et al. CSF1R Protein Expression in Reactive Lymphoid Tissues and Lymphoma: Its Relevance in Classical Hodgkin Lymphoma. *PLoS One*. 2015;10(6):e0125203. PubMed PMID: 26066800. Pubmed Central PMCID: 4466308.
309. Guo B, Cen H, Tan X, Ke Q. Meta-analysis of the prognostic and clinical value of tumor-associated macrophages in adult classical Hodgkin lymphoma. *BMC Med*. 2016 Oct 17;14(1):159. PubMed PMID: 27745550. Pubmed Central PMCID: 5066288.
310. Carey CD, Gusenleitner D, Lipschitz M, Roemer MGM, Stack EC, Gjini E, et al. Topological analysis reveals a PD-L1-associated microenvironmental niche for Reed-Sternberg cells in Hodgkin lymphoma. *Blood*. 2017 Nov 30;130(22):2420-30. PubMed PMID: 28893733. Pubmed Central PMCID: 5766840.
311. Li YL, Shi ZH, Wang X, Gu KS, Zhai ZM. Tumor-associated macrophages predict prognosis in diffuse large B-cell lymphoma and correlation with peripheral absolute monocyte count. *BMC Cancer*. 2019 Nov 6;19(1):1049. PubMed PMID: 31694577. Pubmed Central PMCID: 6836332.
312. Mantovani A, Marchesi F, Malesci A, Laghi L, Allavena P. Tumour-associated macrophages as treatment targets in oncology. *Nature Reviews Clinical Oncology*. 2017 Jul;14(7):399-416. PubMed PMID: 28117416. Pubmed Central PMCID: 5480600.
313. Dagogo-Jack I, Shaw AT. Tumour heterogeneity and resistance to cancer therapies. *Nature reviews Clinical oncology*. 2018 Feb;15(2):81-94. PubMed PMID: 29115304.

314. Cullinane CA, Borneman T, Smith DD, Chu DZ, Ferrell BR, Wagman LD. The surgical treatment of cancer: a comparison of resource utilization following procedures performed with a curative and palliative intent. *Cancer*. 2003 Nov 15;98(10):2266-73. PubMed PMID: 14601098.
315. Tohme S, Simmons RL, Tsung A. Surgery for Cancer: A Trigger for Metastases. *Cancer Res*. 2017 Apr 1;77(7):1548-52. PubMed PMID: 28330928. Pubmed Central PMCID: 5380551.
316. Domchek SM, Friebel TM, Singer CF, Evans DG, Lynch HT, Isaacs C, et al. Association of risk-reducing surgery in BRCA1 or BRCA2 mutation carriers with cancer risk and mortality. *JAMA*. 2010 Sep 1;304(9):967-75. PubMed PMID: 20810374. Pubmed Central PMCID: 2948529.
317. Lee CK. Evolving role of radiation therapy for hematologic malignancies. *Hematology/Oncology Clinics of North America*. 2006 Apr;20(2):471-503. PubMed PMID: 16730303.
318. Burger K, Eick D. Functional ribosome biogenesis is a prerequisite for p53 destabilization: impact of chemotherapy on nucleolar functions and RNA metabolism. *Biol Chem*. 2013 Sep;394(9):1133-43. PubMed PMID: 23640940. Epub 2013/05/04.
319. Kondo N, Takahashi A, Ono K, Ohnishi T. DNA damage induced by alkylating agents and repair pathways. *J Nucleic Acids*. 2010 Nov 21;2010:543531. PubMed PMID: 21113301. Pubmed Central PMCID: 2989456.
320. Amjad MT, Chidharla A, Kasi A. Cancer Chemotherapy. 2023 Feb 27. In: StatPearls [Internet]. Treasure Island (FL); StatPearls Publishing LLC.; 2023 Jan. PMID: 33232037.
321. Robinson AD, Eich ML, Varambally S. Dysregulation of de novo nucleotide biosynthetic pathway enzymes in cancer and targeting opportunities. *Cancer Lett*. 2020 Feb 1;470:134-40. PubMed PMID: 31733288.
322. Jordan MA, Thrower D, Wilson L. Mechanism of inhibition of cell proliferation by Vinca alkaloids. *Cancer Res*. 1991 Apr 15;51(8):2212-22. PubMed PMID: 2009540.
323. Fanale D, Bronte G, Passiglia F, Calo V, Castiglia M, Di Piazza F, et al. Stabilizing versus destabilizing the microtubules: a double-edge sword for an effective cancer treatment option? *Analytical Cellular Pathology*. 2015;2015:690916. PubMed PMID: 26484003. Pubmed Central PMCID: 4592889.
324. Madsen ML, Due H, Ejksjaer N, Jensen P, Madsen J, Dybkaer K. Aspects of vincristine-induced neuropathy in hematologic malignancies: a systematic review. *Cancer Chemother Pharmacol*. 2019 Sep;84(3):471-85. PubMed PMID: 31214762. Pubmed Central PMCID: 6682573.

325. Morth C, Valachis A, Sabaa AA, Molin D, Flogegard M, Enblad G. Does the omission of vincristine in patients with diffuse large B cell lymphoma affect treatment outcome? *Ann Hematol.* 2018 Nov;97(11):2129-35. PubMed PMID: 30091025. Pubmed Central PMCID: 6182738.
326. French SL, Sikes ML, Hontz RD, Osheim YN, Lambert TE, El Hage A, et al. Distinguishing the roles of Topoisomerases I and II in relief of transcription-induced torsional stress in yeast rRNA genes. *Mol Cell Biol.* 2011 Feb;31(3):482-94. PubMed PMID: 21098118. Pubmed Central PMCID: 3028620.
327. Delgado JL, Hsieh CM, Chan NL, Hiasa H. Topoisomerases as anticancer targets. *The Biochemical Journal.* 2018 Jan 23;475(2):373-98. PubMed PMID: 29363591. Pubmed Central PMCID: 6110615.
328. Pentheroudakis G, Goussia A, Voulgaris E, Nikolaidis K, Ioannidou E, Papoudou-Bai A, et al. High levels of topoisomerase II α protein expression in diffuse large B-cell lymphoma are associated with high proliferation, germinal center immunophenotype, and response to treatment. *Leuk Lymphoma.* 2010 Jul;51(7):1260-8. PubMed PMID: 20497003.
329. Saeidnia S. *New Approaches to Natural Anticancer Drugs.* SpringerBriefs in Pharmaceutical Science & Drug Development. 2015 ed. Cham, Switzerland: Springer 2015. p. 106.
330. Cragg GM, Newman DJ. *Natural Products Drug Discovery and Development at the United States National Cancer Institute.* In: Lin Y, editor. *Drug Discovery and Traditional Chinese Medicine: Science, Regulation, and Globalization.* Boston, MA: Springer US; 2001. p. 19-32.
331. Parcesepe P, Giordano G, Laudanna C, Febbraro A, Pancione M. Cancer-Associated Immune Resistance and Evasion of Immune Surveillance in Colorectal Cancer. *Gastroenterology Research and Practice.* 2016;2016:6261721. PubMed PMID: 27006653. Pubmed Central PMCID: 4781955.
332. Vinay DS, Ryan EP, Pawelec G, Talib WH, Stagg J, Elkord E, et al. Immune evasion in cancer: Mechanistic basis and therapeutic strategies. *Seminars in Cancer Biology.* 2015 Dec;35 Suppl:S185-S98. PubMed PMID: 25818339.
333. Leget GA, Czuczman MS. Use of rituximab, the new FDA-approved antibody. *Curr Opin Oncol.* 1998 Nov;10(6):548-51. PubMed PMID: 9818234.
334. Maloney DG, Grillo-Lopez AJ, White CA, Bodkin D, Schilder RJ, Neidhart JA, et al. IDEC-C2B8 (Rituximab) anti-CD20 monoclonal antibody therapy in patients with relapsed low-grade non-Hodgkin's lymphoma. *Blood.* 1997 Sep 15;90(6):2188-95. PubMed PMID: 9310469.
335. Pennock GK, Chow LQ. The Evolving Role of Immune Checkpoint Inhibitors in Cancer Treatment. *Oncologist.* 2015 Jul;20(7):812-22. PubMed PMID: 26069281. Pubmed Central PMCID: 4492230.

336. Pardoll DM. The blockade of immune checkpoints in cancer immunotherapy. *Nat Rev Cancer*. 2012 Mar 22;12(4):252-64. PubMed PMID: 22437870. Pubmed Central PMCID: 4856023.
337. Noguchi T, Ward JP, Gubin MM, Arthur CD, Lee SH, Hundal J, et al. Temporally Distinct PD-L1 Expression by Tumor and Host Cells Contributes to Immune Escape. *Cancer Immunology Research*. 2017 Feb;5(2):106-17. PubMed PMID: 28073774. Pubmed Central PMCID: 5510474.
338. Juneja VR, McGuire KA, Manguso RT, LaFleur MW, Collins N, Haining WN, et al. PD-L1 on tumor cells is sufficient for immune evasion in immunogenic tumors and inhibits CD8 T cell cytotoxicity. *The Journal of Experimental Medicine*. 2017 Apr 3;214(4):895-904. PubMed PMID: 28302645. Pubmed Central PMCID: 5379970.
339. Beatty GL, Gladney WL. Immune escape mechanisms as a guide for cancer immunotherapy. *Clin Cancer Res*. 2015 Feb 15;21(4):687-92. PubMed PMID: 25501578. Pubmed Central PMCID: 4334715.
340. Kim HR, Ha SJ, Hong MH, Heo SJ, Koh YW, Choi EC. PD-L1 expression on immune cells, but not on tumor cells, is a favorable prognostic factor for head and neck cancer patients. *Sci Rep* 2016; 6(36956).
341. Wang X, Yang L, Huang F, Zhang Q, Liu S, Ma L, et al. Inflammatory cytokines IL-17 and TNF-alpha up-regulate PD-L1 expression in human prostate and colon cancer cells. *Immunol Lett*. 2017 Apr;184:7-14. PubMed PMID: 28223102. Pubmed Central PMCID: 5362328.
342. Garcia-Diaz A, Shin DS, Moreno BH, Saco J, Escuin-Ordinas H, Rodriguez GA, et al. Interferon Receptor Signaling Pathways Regulating PD-L1 and PD-L2 Expression. *Cell Rep*. 2017 May 9;19(6):1189-201. PubMed PMID: 28494868. Pubmed Central PMCID: 6420824.
343. Xue S, Hu M, Li P, Ma J, Xie L, Teng F, et al. Relationship between expression of PD-L1 and tumor angiogenesis, proliferation, and invasion in glioma. *Oncotarget*. 2017 Jul 25;8(30):49702-12. PubMed PMID: 28591697. Pubmed Central PMCID: 5564800.
344. Solinas C, Aiello M, Rozali E, Lambertini M, Willard-Gallo K, Migliori E. Programmed cell death-ligand 2: A neglected but important target in the immune response to cancer? *Translational Oncology*. 2020 Oct;13(10):100811. PubMed PMID: 32622310. Pubmed Central PMCID: 7332529.
345. Zhong X, Tumang JR, Gao W, Bai C, Rothstein TL. PD-L2 expression extends beyond dendritic cells/macrophages to B1 cells enriched for V(H)11/V(H)12 and phosphatidylcholine binding. *Eur J Immunol*. 2007 Sep;37(9):2405-10. PubMed PMID: 17683117.

346. Messal N, Serriari NE, Pastor S, Nunes JA, Olive D. PD-L2 is expressed on activated human T cells and regulates their function. *Mol Immunol.* 2011 Sep;48(15-16):2214-9. PubMed PMID: 21752471.
347. Kim ES, Kim JE, Patel MA, Mangraviti A, Ruzevick J, Lim M. Immune Checkpoint Modulators: An Emerging Antiglioma Armamentarium. *Journal of Immunology Research.* 2016;2016:4683607. PubMed PMID: 26881264. Pubmed Central PMCID: 4736366.
348. Yokosuka T, Takamatsu M, Kobayashi-Imanishi W, Hashimoto-Tane A, Azuma M, Saito T. Programmed cell death 1 forms negative costimulatory microclusters that directly inhibit T cell receptor signaling by recruiting phosphatase SHP2. *The Journal of Experimental Medicine.* 2012 Jun 4;209(6):1201-17. PubMed PMID: 22641383. Pubmed Central PMCID: 3371732.
349. Sheppard KA, Fitz LJ, Lee JM, Benander C, George JA, Wooters J, et al. PD-1 inhibits T-cell receptor induced phosphorylation of the ZAP70/CD3zeta signalosome and downstream signaling to PKCtheta. *FEBS Lett.* 2004 Sep 10;574(1-3):37-41. PubMed PMID: 15358536.
350. Kao C, Oestreich KJ, Paley MA, Crawford A, Angelosanto JM, Ali MA, et al. Transcription factor T-bet represses expression of the inhibitory receptor PD-1 and sustains virus-specific CD8+ T cell responses during chronic infection. *Nat Immunol.* 2011 May 29;12(7):663-71. PubMed PMID: 21623380. Pubmed Central PMCID: 3306165.
351. Palaga T, Miele L, Golde TE, Osborne BA. TCR-mediated Notch signaling regulates proliferation and IFN-gamma production in peripheral T cells. *Journal of Immunology.* 2003 Sep 15;171(6):3019-24. PubMed PMID: 12960327.
352. Iwasaki M, Tanaka Y, Kobayashi H, Murata-Hirai K, Miyabe H, Sugie T, et al. Expression and function of PD-1 in human gammadelta T cells that recognize phosphoantigens. *Eur J Immunol.* 2011 Feb;41(2):345-55. PubMed PMID: 21268005.
353. Zhang J, Medeiros LJ, Young KH. Cancer Immunotherapy in Diffuse Large B-Cell Lymphoma. *Frontiers in Oncology.* 2018;8:351. PubMed PMID: 30250823. Pubmed Central PMCID: 6140403.
354. Mahoney KM, Rennert PD, Freeman GJ. Combination cancer immunotherapy and new immunomodulatory targets. *Nature reviews Drug Discovery.* 2015 Aug;14(8):561-84. PubMed PMID: 26228759.
355. Sadelain M, Riviere I, Riddell S. Therapeutic T cell engineering. *Nature.* 2017 May 24;545(7655):423-31. PubMed PMID: 28541315. Pubmed Central PMCID: 5632949.
356. Srivastava S, Riddell SR. Engineering CAR-T cells: Design concepts. *Trends Immunol.* 2015 Aug;36(8):494-502. PubMed PMID: 26169254. Pubmed Central PMCID: 4746114.

357. Milone MC, Fish JD, Carpenito C, Carroll RG, Binder GK, Teachey D, et al. Chimeric receptors containing CD137 signal transduction domains mediate enhanced survival of T cells and increased antileukemic efficacy in vivo. *Molecular therapy : The Journal of the American Society of Gene Therapy*. 2009 Aug;17(8):1453-64. PubMed PMID: 19384291. Pubmed Central PMCID: 2805264.
358. Zhong XS, Matsushita M, Plotkin J, Riviere I, Sadelain M. Chimeric antigen receptors combining 4-1BB and CD28 signaling domains augment PI3kinase/AKT/Bcl-XL activation and CD8+ T cell-mediated tumor eradication. *Molecular therapy : The Journal of The American Society of Gene Therapy*. 2010 Feb;18(2):413-20. PubMed PMID: 19773745. Pubmed Central PMCID: 2839303.
359. Davila ML, Riviere I, Wang X, Bartido S, Park J, Curran K, et al. Efficacy and toxicity management of 19-28z CAR T cell therapy in B cell acute lymphoblastic leukemia. *Science Translational Medicine*. 2014 Feb 19;6(224):224ra25. PubMed PMID: 24553386. Pubmed Central PMCID: 4684949.
360. Bonifant CL, Jackson HJ, Brentjens RJ, Curran KJ. Toxicity and management in CAR T-cell therapy. *Molecular Therapy Oncolytics*. 2016;3:16011. PubMed PMID: 27626062. Pubmed Central PMCID: 5008265.
361. Pegram HJ, Lee JC, Hayman EG, Imperato GH, Tedder TF, Sadelain M, et al. Tumor-targeted T cells modified to secrete IL-12 eradicate systemic tumors without need for prior conditioning. *Blood*. 2012 May 3;119(18):4133-41. PubMed PMID: 22354001. Pubmed Central PMCID: 3359735.
362. Pehlivan KC, Duncan BB, Lee DW. CAR-T Cell Therapy for Acute Lymphoblastic Leukemia: Transforming the Treatment of Relapsed and Refractory Disease. *Curr Hematol Malig Rep*. 2018 Oct;13(5):396-406. PubMed PMID: 30120708.
363. Frey NV. Chimeric antigen receptor T cells for acute lymphoblastic leukemia. *Am J Hematol*. 2019 May;94(S1):S24-S7. PubMed PMID: 30784101.
364. Neelapu SS, Locke FL, Bartlett NL, Lekakis L, Miklos D, Jacobson CA, et al. Kte-C19 (anti-CD19 CAR T Cells) Induces Complete Remissions in Patients with Refractory Diffuse Large B-Cell Lymphoma (DLBCL): Results from the Pivotal Phase 2 Zuma-1. *Blood*. 2016;128(22):LBA-6-LBA-.
365. Kochenderfer JN, Dudley ME, Kassim SH, Somerville RP, Carpenter RO, Stetler-Stevenson M, et al. Chemotherapy-refractory diffuse large B-cell lymphoma and indolent B-cell malignancies can be effectively treated with autologous T cells expressing an anti-CD19 chimeric antigen receptor. *J Clin Oncol*. 2015 Feb 20;33(6):540-9. PubMed PMID: 25154820. Pubmed Central PMCID: 4322257
366. Hopfinger G, Jager U, Worel N. CAR-T Cell Therapy in Diffuse Large B Cell Lymphoma: Hype and Hope. *Hemasphere*. 2019 Apr;3(2):e185. PubMed PMID: 31723824. Pubmed Central PMCID: 6746029.

367. Wolchok JD, Saenger Y. The mechanism of anti-CTLA-4 activity and the negative regulation of T-cell activation. *Oncologist*. 2008;13 Suppl 4(suppl 4):2-9. PubMed PMID: 19001145.
368. Hannani D, Vetizou M, Enot D, Rusakiewicz S, Chaput N, Klatzmann D, et al. Anticancer immunotherapy by CTLA-4 blockade: obligatory contribution of IL-2 receptors and negative prognostic impact of soluble CD25. *Cell Res*. 2015 Feb;25(2):208-24. PubMed PMID: 25582080. Pubmed Central PMCID: 4650573.
369. Wang XY, Zuo D, Sarkar D, Fisher PB. Blockade of cytotoxic T-lymphocyte antigen-4 as a new therapeutic approach for advanced melanoma. *Expert Opinion on Pharmacotherapy*. 2011 Dec;12(17):2695-706. PubMed PMID: 22077831. Pubmed Central PMCID: 3711751.
370. Riha P, Rudd CE. CD28 co-signaling in the adaptive immune response. *Self Nonself*. 2010 Jul;1(3):231-40. PubMed PMID: 21487479. Pubmed Central PMCID: 3047785.
371. Boise LH, Minn AJ, Noel PJ, June CH, Accavitti MA, Lindsten T, et al. CD28 costimulation can promote T cell survival by enhancing the expression of Bcl-XL. *Immunity*. 1995 Jul;3(1):87-98. PubMed PMID: 7621080.
372. Mueller DL, Seiffert S, Fang W, Behrens TW. Differential regulation of bcl-2 and bcl-x by CD3, CD28, and the IL-2 receptor in cloned CD4+ helper T cells. A model for the long-term survival of memory cells. *Journal of Immunology*. 1996 Mar 1;156(5):1764-71. PubMed PMID: 8596025.
373. Qureshi OS, Kaur S, Hou TZ, Jeffery LE, Poulter NS, Briggs Z, et al. Constitutive clathrin-mediated endocytosis of CTLA-4 persists during T cell activation. *J Biol Chem*. 2012 Mar 16;287(12):9429-40. PubMed PMID: 22262842. Pubmed Central PMCID: 3308817.
374. Chuang E, Fisher TS, Morgan RW, Robbins MD, Duerr JM, Vander Heiden MG, et al. The CD28 and CTLA-4 receptors associate with the serine/threonine phosphatase PP2A. *Immunity*. 2000 Sep;13(3):313-22. PubMed PMID: 11021529.
375. Guntermann C, Alexander DR. CTLA-4 suppresses proximal TCR signaling in resting human CD4(+) T cells by inhibiting ZAP-70 Tyr(319) phosphorylation: a potential role for tyrosine phosphatases. *Journal of Immunology*. 2002 May 1;168(9):4420-9. PubMed PMID: 11970985.
376. Calvo CR, Amsen D, Kruisbeek AM. Cytotoxic T lymphocyte antigen 4 (CTLA-4) interferes with extracellular signal-regulated kinase (ERK) and Jun NH2-terminal kinase (JNK) activation, but does not affect phosphorylation of T cell receptor zeta and ZAP70. *The Journal of Experimental Medicine*. 1997 Nov 17;186(10):1645-53. PubMed PMID: 9362525. Pubmed Central PMCID: 2199134.

377. Joshi M, Ansell SM. Activating the Antitumor Immune Response in Non-Hodgkin Lymphoma Using Immune Checkpoint Inhibitors. *Journal of Immunology Research*. 2020;2020:8820377. PubMed PMID: 33294467. Pubmed Central PMCID: 7690999 publication of this paper.
378. Qin S, Dong B, Yi M, Chu Q, Wu K. Prognostic Values of TIM-3 Expression in Patients With Solid Tumors: A Meta-Analysis and Database Evaluation. *Frontiers in Oncology*. 2020;10:1288. PubMed PMID: 32850398. Pubmed Central PMCID: 7417611.
379. Lucca LE, Axisa PP, Singer ER, Nolan NM, Dominguez-Villar M, Hafler DA. TIGIT signaling restores suppressor function of Th1 Tregs. *JCI Insight*. 2019 Feb 7;4(3). PubMed PMID: 30728325. Pubmed Central PMCID: 6413794.
380. Karabon L, Partyka A, Jasek M, Lech-Maranda E, Grzybowska-Izydorczyk O, Bojarska-Junak A, et al. Intragenic Variations in BTLA Gene Influence mRNA Expression of BTLA Gene in Chronic Lymphocytic Leukemia Patients and Confer Susceptibility to Chronic Lymphocytic Leukemia. *Arch Immunol Ther Exp (Warsz)*. 2016 Dec;64(Suppl 1):137-45. PubMed PMID: 27933341. Pubmed Central PMCID: 5334439.
381. Metayer LE, Vilalta A, Burke GAA, Brown GC. Anti-CD47 antibodies induce phagocytosis of live, malignant B cells by macrophages via the Fc domain, resulting in cell death by phagoptosis. *Oncotarget*. 2017 Sep 22;8(37):60892-903. PubMed PMID: 28977832. Pubmed Central PMCID: 5617392.
382. Lindberg FP, Gresham HD, Schwarz E, Brown EJ. Molecular cloning of integrin-associated protein: an immunoglobulin family member with multiple membrane-spanning domains implicated in alpha v beta 3-dependent ligand binding. *J Cell Biol*. 1993 Oct;123(2):485-96. PubMed PMID: 7691831. Pubmed Central PMCID: 2119833.
383. Chao MP, Alizadeh AA, Tang C, Jan M, Weissman-Tsukamoto R, Zhao F, et al. Therapeutic antibody targeting of CD47 eliminates human acute lymphoblastic leukemia. *Cancer Res*. 2011 Feb 15;71(4):1374-84. PubMed PMID: 21177380. Pubmed Central PMCID: 3041855.
384. Chao MP, Alizadeh AA, Tang C, Myklebust JH, Varghese B, Gill S, et al. Anti-CD47 antibody synergizes with rituximab to promote phagocytosis and eradicate non-Hodgkin lymphoma. *Cell*. 2010 Sep 3;142(5):699-713. PubMed PMID: 20813259. Pubmed Central PMCID: 2943345.
385. Bouwstra R, He Y, de Boer J, Kooistra H, Cendrowicz E, Fehrmann RSN, et al. CD47 Expression Defines Efficacy of Rituximab with CHOP in Non-Germinal Center B-cell (Non-GCB) Diffuse Large B-cell Lymphoma Patients (DLBCL), but Not in GCB DLBCL. *Cancer Immunology Research*. 2019 Oct;7(10):1663-71. PubMed PMID: 31409608.

386. Catalan R, Orozco-Morales M, Hernandez-Pedro NY, Guijosa A, Colin-Gonzalez AL, Avila-Moreno F, et al. CD47-SIRPalpha Axis as a Biomarker and Therapeutic Target in Cancer: Current Perspectives and Future Challenges in Nonsmall Cell Lung Cancer. *Journal of Immunology Research*. 2020;2020:9435030. PubMed PMID: 33015199. Pubmed Central PMCID: 7520676
387. Kaur S, Kuznetsova SA, Pendrak ML, Sipes JM, Romeo MJ, Li Z, et al. Heparan sulfate modification of the transmembrane receptor CD47 is necessary for inhibition of T cell receptor signaling by thrombospondin-1. *J Biol Chem*. 2011 Apr 29;286(17):14991-5002. PubMed PMID: 21343308. Pubmed Central PMCID: 3083209.
388. Thomas AM, Santarsiero LM, Lutz ER, Armstrong TD, Chen YC, Huang LQ, et al. Mesothelin-specific CD8(+) T cell responses provide evidence of in vivo cross-priming by antigen-presenting cells in vaccinated pancreatic cancer patients. *The Journal of Experimental Medicine*. 2004 Aug 2;200(3):297-306. PubMed PMID: 15289501. Pubmed Central PMCID: 2211979.
389. Chen DS, Mellman I. Oncology meets immunology: the cancer-immunity cycle. *Immunity*. 2013 Jul 25;39(1):1-10. PubMed PMID: 23890059.
390. Vansteenkiste J, Zielinski M, Linder A, Dahabre J, Esteban E, Malinowski W, et al. Final results of a multi-center, double-blind, randomized, placebo-controlled phase II study to assess the efficacy of MAGE-A3 immunotherapeutic as adjuvant therapy in stage IB/II non-small cell lung cancer (NSCLC). *Journal of Clinical Oncology*. 2007;25(18_suppl):7554.
391. Copier J, Dalglish A. Whole-cell vaccines: A failure or a success waiting to happen? *Curr Opin Mol Ther*. 2010 Feb;12(1):14-20. PubMed PMID: 20140812.
392. Palucka K, Banchereau J. Cancer immunotherapy via dendritic cells. *Nat Rev Cancer*. 2012 Mar 22;12(4):265-77. PubMed PMID: 22437871. Pubmed Central PMCID: 3433802.
393. Higano CS, Schellhammer PF, Small EJ, Burch PA, Nemunaitis J, Yuh L, et al. Integrated data from 2 randomized, double-blind, placebo-controlled, phase 3 trials of active cellular immunotherapy with sipuleucel-T in advanced prostate cancer. *Cancer*. 2009 Aug 15;115(16):3670-9. PubMed PMID: 19536890.
394. Chang GC, Lan HC, Juang SH, Wu YC, Lee HC, Hung YM, et al. A pilot clinical trial of vaccination with dendritic cells pulsed with autologous tumor cells derived from malignant pleural effusion in patients with late-stage lung carcinoma. *Cancer*. 2005 Feb 15;103(4):763-71. PubMed PMID: 15637694.

395. Escobar A, Lopez M, Serrano A, Ramirez M, Perez C, Aguirre A, et al. Dendritic cell immunizations alone or combined with low doses of interleukin-2 induce specific immune responses in melanoma patients. *Clinical and Experimental Immunology*. 2005 Dec;142(3):555-68. PubMed PMID: 16297169. Pubmed Central PMCID: 1809550.
396. Abediankenari S, Janbabaei Mollae G, Ghasemi M, Yousefzadeh Y, Bahrami M, Alimoghaddam K. Vaccination of diffuse large B- cell lymphoma patients with antigen-primed dendritic cells. *Acta Medica Iranica*. 2013 May 30;51(5):284-8. PubMed PMID: 23737309.
397. Rampazzo C, Miazzi C, Franzolin E, Pontarin G, Ferraro P, Frangini M, et al. Regulation by degradation, a cellular defense against deoxyribonucleotide pool imbalances. *Mutation Research*. 2010 Nov 28;703(1):2-10. PubMed PMID: 20561600.
398. Bestor AC, Roniger M, Oren YS, Im MM, Sarni D, Chaoat M, et al. Nucleotide deficiency promotes genomic instability in early stages of cancer development. *Cell*. 2011 Apr 29;145(3):435-46. PubMed PMID: 21529715. Pubmed Central PMCID: 3740329.
399. Uhlin U, Eklund H. Structure of ribonucleotide reductase protein R1. *Nature*. 1994 Aug 18;370(6490):533-9. PubMed PMID: 8052308.
400. Greene BL, Kang G, Cui C, Bennati M, Nocera DG, Drennan CL, et al. Ribonucleotide Reductases: Structure, Chemistry, and Metabolism Suggest New Therapeutic Targets. *Annu Rev Biochem*. 2020 Jun 20;89:45-75. PubMed PMID: 32569524. Pubmed Central PMCID: 7316142.
401. Minnihan EC, Nocera DG, Stubbe J. Reversible, long-range radical transfer in E. coli class Ia ribonucleotide reductase. *Accounts of Chemical Research*. 2013 Nov 19;46(11):2524-35. PubMed PMID: 23730940. Pubmed Central PMCID: 3823682.
402. Knittel G, Liedgens P, Korovkina D, Seeger JM, Al-Baldawi Y, Al-Maarri M, et al. B-cell-specific conditional expression of Myd88p.L252P leads to the development of diffuse large B-cell lymphoma in mice. *Blood*. 2016 Jun 2;127(22):2732-41. PubMed PMID: 27048211. Pubmed Central PMCID: 4891954.
403. Jiang H, Pritchard JR, Williams RT, Lauffenburger DA, Hemann MT. A mammalian functional-genetic approach to characterizing cancer therapeutics. *Nat Chem Biol*. 2011 Feb;7(2):92-100. PubMed PMID: 21186347. Pubmed Central PMCID: 3070540.
404. Cepko C, Pear W. Overview of the retrovirus transduction system. *Current Protocols in Molecular Biology*. 2001 May;Chapter 9:Unit9 PubMed PMID: 18265289. Epub 2008/02/12.

405. Graham FL, van der Eb AJ. A new technique for the assay of infectivity of human adenovirus 5 DNA. *Virology*. 1973;52(2):456-467.
406. Leskov I, Pallasch CP, Drake A, Iliopoulou BP, Souza A, Shen CH, et al. Rapid generation of human B-cell lymphomas via combined expression of Myc and Bcl2 and their use as a preclinical model for biological therapies. *Oncogene*. 2013 Feb 21;32(8):1066-1072. PubMed PMID: 22484426. Pubmed Central PMCID: 4117216.
407. Harris AW, Pinkert CA, Crawford M, Langdon WY, Brinster RL, Adams JM. The E mu-myc transgenic mouse. A model for high-incidence spontaneous lymphoma and leukemia of early B cells. *Journal of Experimental Medicine*. 1988;167(2):353-71.
408. Hertlein E, Beckwith KA, Lozanski G, Chen TL, Towns WH, Johnson AJ, et al. Characterization of a new chronic lymphocytic leukemia cell line for mechanistic in vitro and in vivo studies relevant to disease. *PLoS One*. 2013;8(10):e76607. PubMed PMID: 24130782. Pubmed Central PMCID: 3793922.
409. Weiskopf K, Weissman IL. Macrophages are critical effectors of antibody therapies for cancer. *mAbs*. 2015;7(2):303-10. PubMed PMID: 25667985. Pubmed Central PMCID: 4622600.
410. Zajd CM, Ziemba AM, Miralles GM, Nguyen T, Feustel PJ, Dunn SM, et al. Bone Marrow-Derived and Elicited Peritoneal Macrophages Are Not Created Equal: The Questions Asked Dictate the Cell Type Used. *Frontiers in Immunology*. 2020;11:269. PubMed PMID: 32153579. Pubmed Central PMCID: 7047825.
411. Andreu N, Phelan J, de Sessions PF, Cliff JM, Clark TG, Hibberd ML. Primary macrophages and J774 cells respond differently to infection with *Mycobacterium tuberculosis*. *Sci Rep*. 2017 Feb 8;7:42225. PubMed PMID: 28176867. Pubmed Central PMCID: 5296737.
412. Barreto L, Caminero F, Cash L, Makris C, Lamichhane P, Deshmukh RR. Resistance to Checkpoint Inhibition in Cancer Immunotherapy. *Translational Oncology*. 2020 Mar;13(3):100738. PubMed PMID: 32114384. Pubmed Central PMCID: 7047187.
413. Nurieva R, Thomas S, Nguyen T, Martin-Orozco N, Wang Y, Kaja M-K, et al. T-cell tolerance or function is determined by combinatorial costimulatory signals. *The EMBO Journal*. 2006;25(11):2623-33.
414. Hodi FS, O'Day SJ, McDermott DF, Weber RW, Sosman JA, Haanen JB, et al. Improved survival with ipilimumab in patients with metastatic melanoma. *N Engl J Med*. 2010 Aug 19;363(8):711-23. PubMed PMID: 20525992. Pubmed Central PMCID: 3549297.

415. Weiskopf K, Jahchan NS, Schnorr PJ, Cristea S, Ring AM, Maute RL, et al. CD47-blocking immunotherapies stimulate macrophage-mediated destruction of small-cell lung cancer. *The Journal of Clinical Investigation*. 2016;126(7):2610-20.
416. Swoboda A, Nanda R. Immune Checkpoint Blockade for Breast Cancer. *Cancer Treatment and Research*. 2018;173:155-65. PubMed PMID: 29349763. Pubmed Central PMCID: 6061922.
417. Ansell S, Gutierrez ME, Shipp MA, Gladstone D, Moskowitz A, Borello I, et al. A Phase 1 Study of Nivolumab in Combination with Ipilimumab for Relapsed or Refractory Hematologic Malignancies (CheckMate 039). *Blood*. 2016;128(22):183.
418. Lesokhin AM, Ansell SM, Armand P, Scott EC, Halwani A, Gutierrez M, et al. Nivolumab in Patients With Relapsed or Refractory Hematologic Malignancy: Preliminary Results of a Phase Ib Study. *J Clin Oncol*. 2016 Aug 10;34(23):2698-704. PubMed PMID: 27269947. Pubmed Central PMCID: 5019749
419. Zhao XW, van Beek EM, Schornagel K, Van der Maaden H, Van Houdt M, Otten MA, et al. CD47-signal regulatory protein-alpha (SIRPalpha) interactions form a barrier for antibody-mediated tumor cell destruction. *Proc Natl Acad Sci U S A*. 2011 Nov 8;108(45):18342-7. PubMed PMID: 22042861. Pubmed Central PMCID: 3215076.
420. Bai J, Gao Z, Li X, Dong L, Han W, Nie J. Regulation of PD-1/PD-L1 pathway and resistance to PD-1/PD-L1 blockade. *Oncotarget*. 2017 Dec 15;8(66):110693-707. PubMed PMID: 29299180. Pubmed Central PMCID: 5746415.
421. Mosser DM, Edwards JP. Exploring the full spectrum of macrophage activation. *Nat Rev Immunol*. 2008 Dec;8(12):958-69. PubMed PMID: 19029990. Pubmed Central PMCID: 2724991.
422. Nathan CF, Murray HW, Wiebe ME, Rubin BY. Identification of interferon-gamma as the lymphokine that activates human macrophage oxidative metabolism and antimicrobial activity. *The Journal of Experimental Medicine*. 1983 Sep 1;158(3):670-89. PubMed PMID: 6411853. Pubmed Central PMCID: 2187114.
423. Mantovani A, Sica A, Sozzani S, Allavena P, Vecchi A, Locati M. The chemokine system in diverse forms of macrophage activation and polarization. *Trends Immunol*. 2004 Dec;25(12):677-86. PubMed PMID: 15530839.
424. Murray PJ, Allen JE, Biswas SK, Fisher EA, Gilroy DW, Goerdt S, et al. Macrophage activation and polarization: nomenclature and experimental guidelines. *Immunity*. 2014 Jul 17;41(1):14-20. PubMed PMID: 25035950. Pubmed Central PMCID: 4123412.

425. Paltridge JL, Belle L, Khew-Goodall Y. The secretome in cancer progression. *Biochimica Et Biophysica Acta*. 2013 Nov;1834(11):2233-41. PubMed PMID: 23542208.
426. Xue H, Lu B, Lai M. The cancer secretome: a reservoir of biomarkers. *J Transl Med*. 2008 Sep 17;6:52. PubMed PMID: 18796163. Pubmed Central PMCID: 2562990.
427. Ries LAG, Harkins D, Krapcho M, Mariotto A, Miller BA, Feuer EJ, et al. SEER Cancer Statistics Review, 1975–2003. https://seer.cancer.gov/csr/1975_2003/, based on November 2005 SEER data submission, posted to the SEER web site, 2006: National Cancer Institute, 2006.
428. Gunawardana C, Austen B, Powell JE, Fegan C, Wandroo F, Jacobs A, et al. South Asian chronic lymphocytic leukaemia patients have more rapid disease progression in comparison to White patients. *Br J Haematol*. 2008 Aug;142(4):606-9. PubMed PMID: 18503582.
429. Damle RN, Wasil T, Fais F, Ghiotto F, Valetto A, Allen SL, et al. Ig V Gene Mutation Status and CD38 Expression As Novel Prognostic Indicators in Chronic Lymphocytic Leukemia. *Blood*. 1999;94(6):1840-7.
430. Wiestner A, Rosenwald A, Barry TS, Wright G, Davis RE, Henrickson SE, et al. ZAP-70 expression identifies a chronic lymphocytic leukemia subtype with unmutated immunoglobulin genes, inferior clinical outcome, and distinct gene expression profile. *Blood*. 2003 Jun 15;101(12):4944-51. PubMed PMID: 12595313.
431. Rosenwald A, Alizadeh AA, Widhopf G, Simon R, Davis RE, Yu X, et al. Relation of gene expression phenotype to immunoglobulin mutation genotype in B cell chronic lymphocytic leukemia. *The Journal of Experimental Medicine*. 2001 Dec 3;194(11):1639-47. PubMed PMID: 11733578. Pubmed Central PMCID: 2193523.
432. Crespo M, Bosch F, Villamor N, Bellosillo B, Colomer D, Rozman M, et al. ZAP-70 expression as a surrogate for immunoglobulin-variable-region mutations in chronic lymphocytic leukemia. *N Engl J Med*. 2003 May 1;348(18):1764-75. PubMed PMID: 12724482.
433. Fleming AF. Leukaemias in Africa. *Leukemia*. 1993 Aug;7 Suppl 2:S138-41. PubMed PMID: 8361219.
434. Omoti CE, Awodu OA, Bazuaye GN. Chronic lymphoid leukaemia: clinico-haematological correlation and outcome in a single institution in Niger Delta region of Nigeria. *Int J Lab Hematol*. 2007 Dec;29(6):426-32. PubMed PMID: 17988297.

435. Ministry of Health Ghana. National strategy for cancer control in Ghana [internet]. Ministry of Health Ghana; 2011 Feb [cited 2023 Jul 26]. Available from: <https://aaopenplatform.accessaccelerated.org/resource-library/content/national-strategy-cancer-control-ghana>.
436. Founou CR, Nwobegahay J, Gandji R, Tsayem CJ. Chronic Lymphocytic Leukemia in a Black African Man: A Cameroonian Case Report. *J Leuk*. 2019; 7(1).
437. Sall A, Toure AO, Sall FB, Ndour M, Fall S, Sene A, et al. Characteristics of chronic lymphocytic leukemia in Senegal. *BMC Hematol*. 2016;16:10. PubMed PMID: 27110362. Pubmed Central PMCID: 4841974.
438. Addai-Mensah O, Gyamfi D, Duneeh RV, Danquah KO, Annani-Akollor ME, Boateng L, et al. Determination of Haematological Reference Ranges in Healthy Adults in Three Regions in Ghana. *Biomed Res Int*. 2019;2019:7467512. PubMed PMID: 30868073. Pubmed Central PMCID: 6379879.
439. Dreger P, Corradini P, Kimby E, Michallet M, Milligan D, Schetelig J, et al. Indications for allogeneic stem cell transplantation in chronic lymphocytic leukemia: the EBMT transplant consensus. *Leukemia*. 2007 Jan;21(1):12-7. PubMed PMID: 17109028.
440. Rai KR, Sawitsky A, Cronkite EP, Chanana AD, Levy RN, Pasternack BS. Clinical staging of chronic lymphocytic leukemia. *Blood*. 1975 Aug;46(2):219-34. PubMed PMID: 1139039.
441. Binet JL, Lepage M, Dighiero G, Charron D, D'Athis P, Vaugier G, et al. A clinical staging system for chronic lymphocytic leukemia: prognostic significance. *Cancer*. 1977 Aug;40(2):855-64. PubMed PMID: 890666.
442. Grzywnowicz M, Karczmarczyk A, Skorka K, Zajac M, Zaleska J, Chocholska S, et al. Expression of Programmed Death 1 Ligand in Different Compartments of Chronic Lymphocytic Leukemia. *Acta Haematol*. 2015;134(4):255-62. PubMed PMID: 26159545.
443. Kraus M, Alimzhanov MB, Rajewsky N, Rajewsky K. Survival of resting mature B lymphocytes depends on BCR signaling via the Igalpha/beta heterodimer. *Cell*. 2004 Jun 11;117(6):787-800. PubMed PMID: 15186779.
444. Schweighoffer E, Tybulewicz VL. Signalling for B cell survival. *Curr Opin Cell Biol*. 2018 Apr;51:8-14. PubMed PMID: 29149682.
445. Matutes E, Owusu-Ankomah K, Morilla R, Garcia Marco J, Houlihan A, Que TH, et al. The immunological profile of B-cell disorders and proposal of a scoring system for the diagnosis of CLL. *Leukemia*. 1994 Oct;8(10):1640-5. PubMed PMID: 7523797. Pubmed Central PMCID: 7523797.

446. Rassenti LZ, Huynh L, Toy TL, Chen L, Keating MJ, Gribben JG, et al. ZAP-70 compared with immunoglobulin heavy-chain gene mutation status as a predictor of disease progression in chronic lymphocytic leukemia. *N Engl J Med*. 2004 Aug 26;351(9):893-901. PubMed PMID: 15329427.
447. Chen L, Widhopf G, Huynh L, Rassenti L, Rai KR, Weiss A, et al. Expression of ZAP-70 is associated with increased B-cell receptor signaling in chronic lymphocytic leukemia. *Blood*. 2002 Dec 15;100(13):4609-14. PubMed PMID: 12393534.
448. Gobessi S, Laurenti L, Longo PG, Sica S, Leone G, Efremov DG. ZAP-70 enhances B-cell-receptor signaling despite absent or inefficient tyrosine kinase activation in chronic lymphocytic leukemia and lymphoma B cells. *Blood*. 2007 Mar 1;109(5):2032-9. PubMed PMID: 17038529.
449. Montserrat E. New prognostic markers in CLL. *Hematology American Society of Hematology Education Program*. 2006:279-84. PubMed PMID: 17124073.
450. Deaglio S, Vaisitti T, Aydin S, Bergui L, D'Arena G, Bonello L, et al. CD38 and ZAP-70 are functionally linked and mark CLL cells with high migratory potential. *Blood*. 2007 Dec 1;110(12):4012-21. PubMed PMID: 17699742.
451. Del Poeta G, Maurillo L, Venditti A, Buccisano F, Epiceno AM, Capelli G, et al. Clinical significance of CD38 expression in chronic lymphocytic leukemia. *Blood*. 2001 Nov 1;98(9):2633-9. PubMed PMID: 11675331.
452. Kröber A, Seiler T, Benner A, Bullinger L, Brückle E, Lichter P, et al. VH mutation status, CD38 expression level, genomic aberrations, and survival in chronic lymphocytic leukemia. *Blood*. 2002;100(4):1410-6.
453. Oscier DG, Gardiner AC, Mould SJ, Glide S, Davis ZA, Ibbotson RE, et al. Multivariate analysis of prognostic factors in CLL: clinical stage, IGVH gene mutational status, and loss or mutation of the p53 gene are independent prognostic factors. *Blood*. 2002 Aug 15;100(4):1177-84. PubMed PMID: 12149195.
454. Chevallier P, Penther D, Avet-Loiseau H, Robillard N, Ifrah N, Mahe B, et al. CD38 expression and secondary 17p deletion are important prognostic factors in chronic lymphocytic leukaemia. *Br J Haematol*. 2002 Jan;116(1):142-50. PubMed PMID: 11841407.
455. Mainou-Fowler T, Dignum HM, Proctor SJ, Summerfield GP. The prognostic value of CD38 expression and its quantification in B cell chronic lymphocytic leukemia (B-CLL). *Leuk Lymphoma*. 2004 Mar;45(3):455-62. PubMed PMID: 15160906.

456. Durig J, Naschar M, Schmucker U, Renzing-Kohler K, Holter T, Huttmann A, et al. CD38 expression is an important prognostic marker in chronic lymphocytic leukaemia. *Leukemia*. 2002 Jan;16(1):30-5. PubMed PMID: 11840260.
457. Fukuda T, Chen L, Endo T, Tang L, Lu D, Castro JE, et al. Antisera induced by infusions of autologous Ad-CD154-leukemia B cells identify ROR1 as an oncofetal antigen and receptor for Wnt5a. *Proc Natl Acad Sci U S A*. 2008 Feb 26;105(8):3047-52. PubMed PMID: 18287027. Pubmed Central PMCID: 2268582.
458. Yu J, Chen L, Cui B, Widhopf GF, 2nd, Shen Z, Wu R, et al. Wnt5a induces ROR1/ROR2 heterooligomerization to enhance leukemia chemotaxis and proliferation. *The Journal of Clinical Investigation*. 2016 Feb;126(2):585-98. PubMed PMID: 26690702. Pubmed Central PMCID: 4731190.
459. Hasan MK, Rassenti L, Widhopf GF, 2nd, Yu J, Kipps TJ. Wnt5a causes ROR1 to complex and activate cortactin to enhance migration of chronic lymphocytic leukemia cells. *Leukemia*. 2019 Mar;33(3):653-61. PubMed PMID: 30568170. Pubmed Central PMCID: 6462876.
460. Kohlmann A, Kipps TJ, Rassenti LZ, Downing JR, Shurtleff SA, Mills KI, et al. An international standardization programme towards the application of gene expression profiling in routine leukaemia diagnostics: the Microarray Innovations in LEukemia study prephase. *Br J Haematol*. 2008 Sep;142(5):802-7. PubMed PMID: 18573112. Pubmed Central PMCID: 2654477.
461. Daneshmanesh AH, Mikaelsson E, Jeddi-Tehrani M, Bayat AA, Ghods R, Ostadkarampour M, et al. Ror1, a cell surface receptor tyrosine kinase is expressed in chronic lymphocytic leukemia and may serve as a putative target for therapy. *International Journal of Cancer*. 2008 Sep 1;123(5):1190-5. PubMed PMID: 18546292.
462. Cui B, Ghia EM, Chen L, Rassenti LZ, DeBoever C, Widhopf GF, 2nd, et al. High-level ROR1 associates with accelerated disease progression in chronic lymphocytic leukemia. *Blood*. 2016 Dec 22;128(25):2931-40. PubMed PMID: 27815263. Pubmed Central PMCID: 5179332.
463. Thorsson V, Gibbs DL, Brown SD, Wolf D, Bortone DS, Ou Yang TH, et al. The Immune Landscape of Cancer. *Immunity*. 2018 Apr 17;48(4):812-30 e14. PubMed PMID: 29628290. Pubmed Central PMCID: 5982584.
464. Sharma P, Wagner K, Wolchok JD, Allison JP. Novel cancer immunotherapy agents with survival benefit: recent successes and next steps. *Nat Rev Cancer*. 2011 Oct 24;11(11):805-12. PubMed PMID: 22020206. Pubmed Central PMCID: 3426440.
465. Boussiotis VA. Molecular and Biochemical Aspects of the PD-1 Checkpoint Pathway. *N Engl J Med*. 2016 Nov 3;375(18):1767-78. PubMed PMID: 27806234. Pubmed Central PMCID: 5575761.

466. Dong H, Strome SE, Salomao DR, Tamura H, Hirano F, Flies DB, et al. Tumor-associated B7-H1 promotes T-cell apoptosis: a potential mechanism of immune evasion. *Nature Medicine*. 2002 Aug;8(8):793-800. PubMed PMID: 12091876.
467. Luhder F, Hoglund P, Allison JP, Benoist C, Mathis D. Cytotoxic T lymphocyte-associated antigen 4 (CTLA-4) regulates the unfolding of autoimmune diabetes. *The Journal of Experimental Medicine*. 1998 Feb 2;187(3):427-32. PubMed PMID: 9449722. Pubmed Central PMCID: 2212113.
468. Ishida Y, Agata Y, Shibahara K, Honjo T. Induced expression of PD-1, a novel member of the immunoglobulin gene superfamily, upon programmed cell death. *EMBO J*. 1992 Nov;11(11):3887-95. PubMed PMID: 1396582. Pubmed Central PMCID: 556898.
469. Andrews LP, Marciscano AE, Drake CG, Vignali DA. LAG3 (CD223) as a cancer immunotherapy target. *Immunol Rev*. 2017 Mar;276(1):80-96. PubMed PMID: 28258692. Pubmed Central PMCID: 5338468.
470. Monney L, Sabatos CA, Gaglia JL, Ryu A, Waldner H, Chernova T, et al. Th1-specific cell surface protein Tim-3 regulates macrophage activation and severity of an autoimmune disease. *Nature*. 2002 Jan 31;415(6871):536-41. PubMed PMID: 11823861.
471. Park R, Winnicki M, Liu E, Chu WM. Immune checkpoints and cancer in the immunogenomics era. *Briefings in Functional Genomics*. 2019 Mar 22;18(2):133-9. PubMed PMID: 30137232. Pubmed Central PMCID: 6488970.
472. Finn OJ. *Cancer Immunology*. *New England Journal of Medicine*. 2008;358(25):2704-15. PubMed PMID: 18565863.
473. Orchard JA, Ibbotson RE, Davis Z, Wiestner A, Rosenwald A, Thomas PW, et al. ZAP-70 expression and prognosis in chronic lymphocytic leukaemia. *Lancet*. 2004 Jan 10;363(9403):105-11. PubMed PMID: 14726163.
474. Bubien JK, Zhou LJ, Bell PD, Frizzell RA, Tedder TF. Transfection of the CD20 cell surface molecule into ectopic cell types generates a Ca²⁺ conductance found constitutively in B lymphocytes. *J Cell Biol*. 1993 Jun;121(5):1121-32. PubMed PMID: 7684739. Pubmed Central PMCID: 2119683.
475. Press OW, Farr AG, Borroz KI, Anderson SK, Martin PJ. Endocytosis and degradation of monoclonal antibodies targeting human B-cell malignancies. *Cancer Res*. 1989 Sep 1;49(17):4906-12. PubMed PMID: 2667754.
476. Uchida J, Lee Y, Hasegawa M, Liang Y, Bradney A, Oliver JA, et al. Mouse CD20 expression and function. *Int Immunol*. 2004 Jan;16(1):119-29. PubMed PMID: 14688067.

477. Skarzynski M, Niemann CU, Lee YS, Martyr S, Maric I, Salem D, et al. Interactions between Ibrutinib and Anti-CD20 Antibodies: Competing Effects on the Outcome of Combination Therapy. *Clin Cancer Res.* 2016 Jan 1;22(1):86-95. PubMed PMID: 26283682. Pubmed Central PMCID: 4703510.
478. Harris AW, Pinkert CA, Crawford M, Langdon WY, Brinster RL, Adams JM. The E mu-myc transgenic mouse. A model for high-incidence spontaneous lymphoma and leukemia of early B cells. *The Journal of Experimental Medicine.* 1988;167(2):353-71.
479. Adams JM, Harris AW, Pinkert CA, Corcoran LM, Alexander WS, Cory S, et al. The c-myc oncogene driven by immunoglobulin enhancers induces lymphoid malignancy in transgenic mice. *Nature.* 1985 Dec 12-18;318(6046):533-8. PubMed PMID: 3906410.
480. Montalvao F, Garcia Z, Celli S, Breart B, Deguine J, Van Rooijen N, et al. The mechanism of anti-CD20-mediated B cell depletion revealed by intravital imaging. *The Journal of Clinical Investigation.* 2013 Dec;123(12):5098-103. PubMed PMID: 24177426. Pubmed Central PMCID: 3859399.
481. Strasser A, Harris AW, Bath ML, Cory S. Novel primitive lymphoid tumours induced in transgenic mice by cooperation between myc and bcl-2. *Nature.* 1990 Nov 22;348(6299):331-3. PubMed PMID: 2250704.
482. Schmitt CA, McCurrach ME, de Stanchina E, Wallace-Brodeur RR, Lowe SW. INK4a/ARF mutations accelerate lymphomagenesis and promote chemoresistance by disabling p53. *Genes Dev.* 1999 Oct 15;13(20):2670-7. PubMed PMID: 10541553. Pubmed Central PMCID: 317110.
483. van Meerten T, van Rijn RS, Hol S, Hagenbeek A, Ebeling SB. Complement-induced cell death by rituximab depends on CD20 expression level and acts complementary to antibody-dependent cellular cytotoxicity. *Clin Cancer Res.* 2006 Jul 1;12(13):4027-35. PubMed PMID: 16818702.
484. Lykken JM, Horikawa M, Minard-Colin V, Kamata M, Miyagaki T, Poe JC, et al. Galectin-1 drives lymphoma CD20 immunotherapy resistance: validation of a preclinical system to identify resistance mechanisms. *Blood.* 2016 Apr 14;127(15):1886-95. PubMed PMID: 26888257. Pubmed Central PMCID: 4832507.
485. Bellesso M, Xavier FD, Costa RO, Pereira J, Siqueira SA, Chamone DA. Disease progression after R-CHOP treatment associated with the loss of CD20 antigen expression. *Revista Brasileira De Hematologia E Hemoterapia.* 2011;33(2):148-50. PubMed PMID: 23284263. Pubmed Central PMCID: 3520640.
486. Pickartz T, Ringel F, Wedde M, Renz H, Klein A, von Neuhoff N, et al. Selection of B-cell chronic lymphocytic leukemia cell variants by therapy with anti-CD20 monoclonal antibody rituximab. *Exp Hematol.* 2001 Dec;29(12):1410-6. PubMed PMID: 11750099.

487. Foran JM, Norton AJ, Micallef IN, Taussig DC, Amess JA, Rohatiner AZ, et al. Loss of CD20 expression following treatment with rituximab (chimaeric monoclonal anti-CD20): a retrospective cohort analysis. *Br J Haematol*. 2001 Sep;114(4):881-3. PubMed PMID: 11564080.
488. Horvat M, Kloboves Prevodnik V, Lavrencak J, Jezersek Novakovic B. Predictive significance of the cut-off value of CD20 expression in patients with B-cell lymphoma. *Oncology Reports*. 2010 Oct;24(4):1101-7. PubMed PMID: 20811695.
489. Johnson NA, Boyle M, Bashashati A, Leach S, Brooks-Wilson A, Sehn LH, et al. Diffuse large B-cell lymphoma: reduced CD20 expression is associated with an inferior survival. *Blood*. 2009 Apr 16;113(16):3773-80. PubMed PMID: 19029441. Pubmed Central PMCID: 2943836.
490. Henry C, Deschamps M, Rohrlich PS, Pallandre JR, Remy-Martin JP, Callanan M, et al. Identification of an alternative CD20 transcript variant in B-cell malignancies coding for a novel protein associated to rituximab resistance. *Blood*. 2010 Mar 25;115(12):2420-9. PubMed PMID: 20089966.
491. Terui Y, Mishima Y, Sugimura N, Kojima K, Sakurai T, Mishima Y, et al. Identification of CD20 C-terminal deletion mutations associated with loss of CD20 expression in non-Hodgkin's lymphoma. *Clin Cancer Res*. 2009 Apr 1;15(7):2523-30. PubMed PMID: 19276251.
492. Beers SA, French RR, Chan HT, Lim SH, Jarrett TC, Vidal RM, et al. Antigenic modulation limits the efficacy of anti-CD20 antibodies: implications for antibody selection. *Blood*. 2010 Jun 24;115(25):5191-201. PubMed PMID: 20223920.
493. Williams ME, Densmore JJ, Pawluczkojczyk AW, Beum PV, Kennedy AD, Lindorfer MA, et al. Thrice-weekly low-dose rituximab decreases CD20 loss via shaving and promotes enhanced targeting in chronic lymphocytic leukemia. *Journal of Immunology*. 2006 Nov 15;177(10):7435-43. PubMed PMID: 17082663.
494. Beum PV, Peek EM, Lindorfer MA, Beurskens FJ, Engelberts PJ, Parren PW, et al. Loss of CD20 and bound CD20 antibody from opsonized B cells occurs more rapidly because of trogocytosis mediated by Fc receptor-expressing effector cells than direct internalization by the B cells. *Journal of Immunology*. 2011 Sep 15;187(6):3438-47. PubMed PMID: 21841127.
495. Boross P, Jansen JH, Pastula A, van der Poel CE, Leusen JH. Both activating and inhibitory Fc gamma receptors mediate rituximab-induced trogocytosis of CD20 in mice. *Immunol Lett*. 2012 Mar 30;143(1):44-52. PubMed PMID: 22285696.
496. Sugimoto T, Tomita A, Hiraga J, Shimada K, Kiyoi H, Kinoshita T, et al. Escape mechanisms from antibody therapy to lymphoma cells: downregulation of CD20 mRNA by recruitment of the HDAC complex and not by DNA methylation. *Biochemical and Biophysical Research Communications*. 2009 Dec 4;390(1):48-53. PubMed PMID: 19769942.

497. Pozzo F, Bittolo T, Arruga F, Bulian P, Macor P, Tissino E, et al. NOTCH1 mutations associate with low CD20 level in chronic lymphocytic leukemia: evidence for a NOTCH1 mutation-driven epigenetic dysregulation. *Leukemia*. 2016 Jan;30(1):182-9. PubMed PMID: 26165233.
498. Ferguson LR, Chen H, Collins AR, Connell M, Damia G, Dasgupta S, et al. Genomic instability in human cancer: Molecular insights and opportunities for therapeutic attack and prevention through diet and nutrition. *Seminars in Cancer Biology*. 2015 Dec;35 Suppl(Suppl):S5-S24. PubMed PMID: 25869442. Pubmed Central PMCID: 4600419.
499. McKinney JA, Wang G, Mukherjee A, Christensen L, Subramanian SHS, Zhao J, et al. Distinct DNA repair pathways cause genomic instability at alternative DNA structures. *Nature Communications*. 2020 Jan 13;11(1):236. PubMed PMID: 31932649. Pubmed Central PMCID: 6957503.
500. Davis AJ, Chen BP, Chen DJ. DNA-PK: a dynamic enzyme in a versatile DSB repair pathway. *DNA Repair (Amst)*. 2014 May;17:21-9. PubMed PMID: 24680878. Pubmed Central PMCID: 4032623.
501. Ruis BL, Fattah KR, Hendrickson EA. The catalytic subunit of DNA-dependent protein kinase regulates proliferation, telomere length, and genomic stability in human somatic cells. *Mol Cell Biol*. 2008 Oct;28(20):6182-95. PubMed PMID: 18710952. Pubmed Central PMCID: 2577426.
502. Jette N, Lees-Miller SP. The DNA-dependent protein kinase: A multifunctional protein kinase with roles in DNA double strand break repair and mitosis. *Prog Biophys Mol Biol*. 2015 Mar;117(2-3):194-205. PubMed PMID: 25550082. Pubmed Central PMCID: 4502593.
503. Smits VA, Gillespie DA. DNA damage control: regulation and functions of checkpoint kinase 1. *The FEBS Journal*. 2015 Oct;282(19):3681-92. PubMed PMID: 26216057.
504. Sorensen CS, Syljuasen RG, Falck J, Schroeder T, Ronnstrand L, Khanna KK, et al. Chk1 regulates the S phase checkpoint by coupling the physiological turnover and ionizing radiation-induced accelerated proteolysis of Cdc25A. *Cancer Cell*. 2003 Mar;3(3):247-58. PubMed PMID: 12676583.
505. Shimuta K, Nakajo N, Uto K, Hayano Y, Okazaki K, Sagata N. Chk1 is activated transiently and targets Cdc25A for degradation at the *Xenopus* midblastula transition. *EMBO J*. 2002 Jul 15;21(14):3694-703. PubMed PMID: 12110582. Pubmed Central PMCID: 125399.
506. Takai H, Naka K, Okada Y, Watanabe M, Harada N, Saito S, et al. Chk2-deficient mice exhibit radioresistance and defective p53-mediated transcription. *EMBO J*. 2002 Oct 1;21(19):5195-205. PubMed PMID: 12356735. Pubmed Central PMCID: 129029.

507. Hirao A, Cheung A, Duncan G, Girard PM, Elia AJ, Wakeham A, et al. Chk2 is a tumor suppressor that regulates apoptosis in both an ataxia telangiectasia mutated (ATM)-dependent and an ATM-independent manner. *Mol Cell Biol.* 2002 Sep;22(18):6521-32. PubMed PMID: 12192050. Pubmed Central PMCID: 135625.
508. Blasiak J. DNA-Damaging Anticancer Drugs - A Perspective for DNA Repair- Oriented Therapy. *Curr Med Chem.* 2017;24(15):1488-503. PubMed PMID: 28120709.
509. Zhou J, Giannakakou P. Targeting microtubules for cancer chemotherapy. *Curr Med Chem Anticancer Agents.* 2005 Jan;5(1):65-71. PubMed PMID: 15720262.
510. Shieh SY, Ikeda M, Taya Y, Prives C. DNA damage-induced phosphorylation of p53 alleviates inhibition by MDM2. *Cell.* 1997 Oct 31;91(3):325-34. PubMed PMID: 9363941.
511. Harper JW, Adami GR, Wei N, Keyomarsi K, Elledge SJ. The p21 Cdk-interacting protein Cip1 is a potent inhibitor of G1 cyclin-dependent kinases. *Cell.* 1993 Nov 19;75(4):805-16. PubMed PMID: 8242751.
512. Matsuoka S, Huang M, Elledge SJ. Linkage of ATM to cell cycle regulation by the Chk2 protein kinase. *Science.* 1998 Dec 4;282(5395):1893-7. PubMed PMID: 9836640.
513. Taylor WR, DePrimo SE, Agarwal A, Agarwal ML, Schonthal AH, Katula KS, et al. Mechanisms of G2 arrest in response to overexpression of p53. *Mol Biol Cell.* 1999 Nov;10(11):3607-22. PubMed PMID: 10564259. Pubmed Central PMCID: 25646.
514. Chan TA, Hwang PM, Hermeking H, Kinzler KW, Vogelstein B. Cooperative effects of genes controlling the G2/M checkpoint. *Genes & Development.* 2000;14(13):1584-8.
515. Kannan K, Kaminski N, Rechavi G, Jakob-Hirsch J, Amariglio N, Givol D. DNA microarray analysis of genes involved in p53 mediated apoptosis: activation of Apaf-1. *Oncogene.* 2001 Jun 7;20(26):3449-55. PubMed PMID: 11423996.
516. Miyashita T, Reed JC. Tumor suppressor p53 is a direct transcriptional activator of the human bax gene. *Cell.* 1995 Jan 27;80(2):293-9. PubMed PMID: 7834749.
517. Nakano K, Vousden KH. PUMA, a novel proapoptotic gene, is induced by p53. *Mol Cell.* 2001 Mar;7(3):683-94. PubMed PMID: 11463392.
518. Oda E, Ohki R, Murasawa H, Nemoto J, Shibue T, Yamashita T, et al. Noxa, a BH3-only member of the Bcl-2 family and candidate mediator of p53-induced apoptosis. *Science.* 2000 May 12;288(5468):1053-8. PubMed PMID: 10807576.

519. Strasser A, Harris AW, Jacks T, Cory S. DNA damage can induce apoptosis in proliferating lymphoid cells via p53-independent mechanisms inhibitable by Bcl-2. *Cell*. 1994 Oct 21;79(2):329-39. PubMed PMID: 7954799.
520. Berggren KL, Restrepo Cruz S, Hixon MD, Cowan AT, Keysar SB, Craig S, et al. MAPKAPK2 (MK2) inhibition mediates radiation-induced inflammatory cytokine production and tumor growth in head and neck squamous cell carcinoma. *Oncogene*. 2019 Nov;38(48):7329-41. PubMed PMID: 31417185. Pubmed Central PMCID: 6883149.
521. Guo M, Sun D, Fan Z, Yuan Y, Shao M, Hou J, et al. Targeting MK2 Is a Novel Approach to Interfere in Multiple Myeloma. *Frontiers in Oncology*. 2019;9:722. PubMed PMID: 31440466. Pubmed Central PMCID: 6694709.
522. Reinhardt HC, Aslanian AS, Lees JA, Yaffe MB. p53-deficient cells rely on ATM- and ATR-mediated checkpoint signaling through the p38MAPK/MK2 pathway for survival after DNA damage. *Cancer Cell*. 2007 Feb;11(2):175-89. PubMed PMID: 17292828. Pubmed Central PMCID: 2742175.
523. Reinhardt HC, Hasskamp P, Schmedding I, Morandell S, van Vugt MA, Wang X, et al. DNA damage activates a spatially distinct late cytoplasmic cell-cycle checkpoint network controlled by MK2-mediated RNA stabilization. *Mol Cell*. 2010 Oct 8;40(1):34-49. PubMed PMID: 20932473. Pubmed Central PMCID: 3030122.
524. Carra G, Lingua MF, Maffeo B, Taulli R, Morotti A. P53 vs NF-kappaB: the role of nuclear factor-kappa B in the regulation of p53 activity and vice versa. *Cellular and Molecular Life Sciences : CMLS*. 2020 Nov;77(22):4449-58. PubMed PMID: 32322927.
525. Ak P, Levine AJ. p53 and NF-kappaB: different strategies for responding to stress lead to a functional antagonism. *FASEB J*. 2010 Oct;24(10):3643-52. PubMed PMID: 20530750.
526. Yamashita A, Ohnishi T, Kashima I, Taya Y, Ohno S. Human SMG-1, a novel phosphatidylinositol 3-kinase-related protein kinase, associates with components of the mRNA surveillance complex and is involved in the regulation of nonsense-mediated mRNA decay. *Genes Dev*. 2001 Sep 1;15(17):2215-28. PubMed PMID: 11544179. Pubmed Central PMCID: 312771.
527. Brumbaugh KM, Otterness DM, Geisen C, Oliveira V, Brognard J, Li X, et al. The mRNA surveillance protein hSMG-1 functions in genotoxic stress response pathways in mammalian cells. *Mol Cell*. 2004 Jun 4;14(5):585-98. PubMed PMID: 15175154.
528. Gehen SC, Staversky RJ, Bambara RA, Keng PC, O'Reilly MA. hSMG-1 and ATM sequentially and independently regulate the G1 checkpoint during oxidative stress. *Oncogene*. 2008 Jul 3;27(29):4065-74. PubMed PMID: 18332866. Pubmed Central PMCID: 2651885.

529. Gubanov E, Issaeva N, Gokturk C, Djureinovic T, Helleday T. SMG-1 suppresses CDK2 and tumor growth by regulating both the p53 and Cdc25A signaling pathways. *Cell Cycle*. 2013 Dec 15;12(24):3770-80. PubMed PMID: 24107632. Pubmed Central PMCID: 3905069.
530. Du Y, Lu F, Li P, Ye J, Ji M, Ma D, et al. SMG1 acts as a novel potential tumor suppressor with epigenetic inactivation in acute myeloid leukemia. *Int J Mol Sci*. 2014 Sep 25;15(9):17065-76. PubMed PMID: 25257528. Pubmed Central PMCID: 4200422.
531. Gonzalez-Estevez C, Felix DA, Smith MD, Paps J, Morley SJ, James V, et al. SMG-1 and mTORC1 act antagonistically to regulate response to injury and growth in planarians. *PLoS Genetics*. 2012;8(3):e1002619. PubMed PMID: 22479207. Pubmed Central PMCID: 3315482.
532. O'Connor L, Strasser A, O'Reilly LA, Hausmann G, Adams JM, Cory S, et al. Bim: a novel member of the Bcl-2 family that promotes apoptosis. *EMBO J*. 1998 Jan 15;17(2):384-95. PubMed PMID: 9430630. Pubmed Central PMCID: 1170389.
533. Kuwana T, Bouchier-Hayes L, Chipuk JE, Bonzon C, Sullivan BA, Green DR, et al. BH3 domains of BH3-only proteins differentially regulate Bax-mediated mitochondrial membrane permeabilization both directly and indirectly. *Mol Cell*. 2005 Feb 18;17(4):525-35. PubMed PMID: 15721256.
534. Marani M, Tenev T, Hancock D, Downward J, Lemoine NR. Identification of novel isoforms of the BH3 domain protein Bim which directly activate Bax to trigger apoptosis. *Mol Cell Biol*. 2002 Jun;22(11):3577-89. PubMed PMID: 11997495. Pubmed Central PMCID: 133811.
535. Gustafsson AS, Abramenkova A, Stenerlow B. Suppression of DNA-dependent protein kinase sensitize cells to radiation without affecting DSB repair. *Mutation Research*. 2014 Nov;769:1-10. PubMed PMID: 25771720.
536. Neal JA, Meek K. Deciphering phenotypic variance in different models of DNA-PKcs deficiency. *DNA Repair (Amst)*. 2019 Jan;73:7-16. PubMed PMID: 30409670. Pubmed Central PMCID: 6312468.
537. Ashley AK, Shrivastava M, Nie J, Amerin C, Troksa K, Glanzer JG, et al. DNA-PK phosphorylation of RPA32 Ser4/Ser8 regulates replication stress checkpoint activation, fork restart, homologous recombination and mitotic catastrophe. *DNA Repair (Amst)*. 2014 Sep;21:131-9. PubMed PMID: 24819595. Pubmed Central PMCID: 4135522.
538. Davis AJ, Chen DJ. DNA double strand break repair via non-homologous end-joining. *Transl Cancer Res*. 2013 Jun;2(3):130-43. PubMed PMID: 24000320. Pubmed Central PMCID: 3758668.

539. Woo RA, McLure KG, Lees-Miller SP, Rancourt DE, Lee PW. DNA-dependent protein kinase acts upstream of p53 in response to DNA damage. *Nature*. 1998 Aug 13;394(6694):700-4. PubMed PMID: 9716137.
540. Zhang Y, Hunter T. Roles of Chk1 in cell biology and cancer therapy. *International Journal Of Cancer*. 2014 Mar 1;134(5):1013-23. PubMed PMID: 23613359. Pubmed Central PMCID: 3852170.
541. Mailand N, Falck J, Lukas C, Syljuasen RG, Welcker M, Bartek J, et al. Rapid destruction of human Cdc25A in response to DNA damage. *Science*. 2000 May 26;288(5470):1425-9. PubMed PMID: 10827953.
542. O'Connell MJ, Raleigh JM, Verkade HM, Nurse P. Chk1 is a wee1 kinase in the G2 DNA damage checkpoint inhibiting cdc2 by Y15 phosphorylation. *EMBO J*. 1997 Feb 3;16(3):545-54. PubMed PMID: 9034337. Pubmed Central PMCID: 1169658.
543. Takai H, Tominaga K, Motoyama N, Minamishima YA, Nagahama H, Tsukiyama T, et al. Aberrant cell cycle checkpoint function and early embryonic death in Chk1^{-/-} mice. *Genes & Development*. 2000;14(12):1439-47.
544. Rodriguez R, Meuth M. Chk1 and p21 cooperate to prevent apoptosis during DNA replication fork stress. *Mol Biol Cell*. 2006 Jan;17(1):402-12. PubMed PMID: 16280359. Pubmed Central PMCID: 1345677.
545. Sidi S, Sanda T, Kennedy RD, Hagen AT, Jette CA, Hoffmans R, et al. Chk1 suppresses a caspase-2 apoptotic response to DNA damage that bypasses p53, Bcl-2, and caspase-3. *Cell*. 2008 May 30;133(5):864-77. PubMed PMID: 18510930. Pubmed Central PMCID: 2719897.
546. Verlinden L, Vanden Bempt I, Eelen G, Drijkoningen M, Verlinden I, Marchal K, et al. The E2F-regulated gene Chk1 is highly expressed in triple-negative estrogen receptor /progesterone receptor /HER-2 breast carcinomas. *Cancer Res*. 2007 Jul 15;67(14):6574-81. PubMed PMID: 17638866.
547. David L, Fernandez-Vidal A, Bertoli S, Grgurevic S, Lepage B, Deshaies D, et al. CHK1 as a therapeutic target to bypass chemoresistance in AML. *Sci Signal*. 2016 Sep 13;9(445):ra90. PubMed PMID: 27625304.
548. Hoglund A, Nilsson LM, Muralidharan SV, Hasvold LA, Merta P, Rudelius M, et al. Therapeutic implications for the induced levels of Chk1 in Myc-expressing cancer cells. *Clin Cancer Res*. 2011 Nov 15;17(22):7067-79. PubMed PMID: 21933891.

549. Sanjiv K, Hagenkort A, Calderon-Montano JM, Koolmeister T, Reaper PM, Mortusewicz O, et al. Cancer-Specific Synthetic Lethality between ATR and CHK1 Kinase Activities. *Cell Rep.* 2016 Jan 12;14(2):298-309. PubMed PMID: 26748709. Pubmed Central PMCID: 4713868.
550. Schuler F, Weiss JG, Lindner SE, Lohmuller M, Herzog S, Spiegl SF, et al. Checkpoint kinase 1 is essential for normal B cell development and lymphomagenesis. *Nature Communications.* 2017 Nov 22;8(1):1697. PubMed PMID: 29167438. Pubmed Central PMCID: 5700047.
551. Derenzini E, Agostinelli C, Imbrogno E, Iacobucci I, Casadei B, Brighenti E, et al. Constitutive activation of the DNA damage response pathway as a novel therapeutic target in diffuse large B-cell lymphoma. *Oncotarget.* 2015 Mar 30;6(9):6553-69. PubMed PMID: 25544753. Pubmed Central PMCID: 4466634.
552. Ennishi D, Mottok A, Ben-Neriah S, Shulha HP, Farinha P, Chan FC, et al. Genetic profiling of MYC and BCL2 in diffuse large B-cell lymphoma determines cell-of-origin-specific clinical impact. *Blood.* 2017 May 18;129(20):2760-70. PubMed PMID: 28351934.
553. Iqbal J, Neppalli VT, Wright G, Dave BJ, Horsman DE, Rosenwald A, et al. BCL2 expression is a prognostic marker for the activated B-cell-like type of diffuse large B-cell lymphoma. *J Clin Oncol.* 2006 Feb 20;24(6):961-8. PubMed PMID: 16418494.
554. Rousseau D, Cannella D, Boulaire J, Fitzgerald P, Fotedar A, Fotedar R. Growth inhibition by CDK-cyclin and PCNA binding domains of p21 occurs by distinct mechanisms and is regulated by ubiquitin-proteasome pathway. *Oncogene.* 1999 May 27;18(21):3290-302. PubMed PMID: 10359535.
555. Miyanishi M, Tada K, Koike M, Uchiyama Y, Kitamura T, Nagata S. Identification of Tim4 as a phosphatidylserine receptor. *Nature.* 2007 Nov 15;450(7168):435-9. PubMed PMID: 17960135.
556. Park D, Tosello-Trampont AC, Elliott MR, Lu M, Haney LB, Ma Z, et al. BAI1 is an engulfment receptor for apoptotic cells upstream of the ELMO/Dock180/Rac module. *Nature.* 2007 Nov 15;450(7168):430-4. PubMed PMID: 17960134.
557. Albert ML, Kim JI, Birge RB. α 5 β 1 integrin recruits the CrkII-Dock180-rac1 complex for phagocytosis of apoptotic cells. *Nat Cell Biol.* 2000 Dec;2(12):899-905. PubMed PMID: 11146654.
558. Dransfield I, Zagorska A, Lew ED, Michail K, Lemke G. Mer receptor tyrosine kinase mediates both tethering and phagocytosis of apoptotic cells. *Cell Death Dis.* 2015 Feb 19;6(2):e1646. PubMed PMID: 25695599. Pubmed Central PMCID: 4669813.

559. Seitz HM, Camenisch TD, Lemke G, Earp HS, Matsushima GK. Macrophages and dendritic cells use different Axl/Mertk/Tyro3 receptors in clearance of apoptotic cells. *Journal of Immunology*. 2007 May 1;178(9):5635-42. PubMed PMID: 17442946.
560. Segawa K, Nagata S. An Apoptotic 'Eat Me' Signal: Phosphatidylserine Exposure. *Trends Cell Biol*. 2015 Nov;25(11):639-50. PubMed PMID: 26437594.
561. Munn DH, Cheung NK. Antibody-independent phagocytosis of tumor cells by human monocyte-derived macrophages cultured in recombinant macrophage colony-stimulating factor. *Cancer Immunology, Immunotherapy : CII*. 1995 Jul;41(1):46-52. PubMed PMID: 7641219.
562. Hoffmann PR, deCathelineau AM, Ogden CA, Leverrier Y, Bratton DL, Daleke DL, et al. Phosphatidylserine (PS) induces PS receptor-mediated macropinocytosis and promotes clearance of apoptotic cells. *J Cell Biol*. 2001 Nov 12;155(4):649-59. PubMed PMID: 11706053. Pubmed Central PMCID: 2198875.
563. Yoon KW, Byun S, Kwon E, Hwang SY, Chu K, Hiraki M, et al. Control of signaling-mediated clearance of apoptotic cells by the tumor suppressor p53. *Science*. 2015 Jul 31;349(6247):1261669. PubMed PMID: 26228159. Pubmed Central PMCID: 5215039.
564. Turenne GA, Paul P, Laflair L, Price BD. Activation of p53 transcriptional activity requires ATM's kinase domain and multiple N-terminal serine residues of p53. *Oncogene*. 2001 Aug 23;20(37):5100-10. PubMed PMID: 11526498.
565. Massol P, Montcourrier P, Guillemot JC, Chavrier P. Fc receptor-mediated phagocytosis requires CDC42 and Rac1. *EMBO J*. 1998 Nov 2;17(21):6219-29. PubMed PMID: 9799231. Pubmed Central PMCID: 1170948.
566. Tosello-Trampont AC, Nakada-Tsukui K, Ravichandran KS. Engulfment of apoptotic cells is negatively regulated by Rho-mediated signaling. *J Biol Chem*. 2003 Dec 12;278(50):49911-9. PubMed PMID: 14514696.
567. Zullo J, Matsumoto K, Xavier S, Ratliff B, Goligorsky MS. The cell secretome, a mediator of cell-to-cell communication. *Prostaglandins & other Lipid Mediators*. 2015 Jul;120:17-20. PubMed PMID: 25936481. Pubmed Central PMCID: 4575600.
568. Beohar N, Rapp J, Pandya S, Losordo DW. Rebuilding the damaged heart: the potential of cytokines and growth factors in the treatment of ischemic heart disease. *Journal of the American College of Cardiology*. 2010 Oct 12;56(16):1287-97. PubMed PMID: 20888519. Pubmed Central PMCID: 3123891.

569. Ranganath SH, Levy O, Inamdar MS, Karp JM. Harnessing the mesenchymal stem cell secretome for the treatment of cardiovascular disease. *Cell Stem Cell*. 2012 Mar 2;10(3):244-58. PubMed PMID: 22385653. Pubmed Central PMCID: 3294273.
570. Gul N, van Egmond M. Antibody-Dependent Phagocytosis of Tumor Cells by Macrophages: A Potent Effector Mechanism of Monoclonal Antibody Therapy of Cancer. *Cancer Res*. 2015 Dec 1;75(23):5008-13. PubMed PMID: 26573795.
571. Penberthy KK, Ravichandran KS. Apoptotic cell recognition receptors and scavenger receptors. *Immunol Rev*. 2016 Jan;269(1):44-59. PubMed PMID: 26683144. Pubmed Central PMCID: 4685734.
572. Green DR, Oguin TH, Martinez J. The clearance of dying cells: table for two. *Cell Death Differ*. 2016 Jun;23(6):915-26. PubMed PMID: 26990661. Pubmed Central PMCID: 4987729.
573. Chatzidoukaki O, Goulielmaki E, Schumacher B, Garinis GA. DNA Damage Response and Metabolic Reprogramming in Health and Disease. *Trends in Genetics : TIG*. 2020 Oct;36(10):777-91. PubMed PMID: 32684438.
574. Lujambio A, Akkari L, Simon J, Grace D, Tschaharganeh DF, Bolden JE, et al. Non-cell-autonomous tumor suppression by p53. *Cell*. 2013 Apr 11;153(2):449-60. PubMed PMID: 23562644. Pubmed Central PMCID: 3702034.
575. Campisi J, d'Adda di Fagagna F. Cellular senescence: when bad things happen to good cells. *Nature Reviews Molecular Cell Biology*. 2007 Sep;8(9):729-40. PubMed PMID: 17667954.
576. Longman D, Jackson-Jones KA, Maslon MM, Murphy LC, Young RS, Stoddart JJ, et al. Identification of a localized nonsense-mediated decay pathway at the endoplasmic reticulum. *Genes Dev*. 2020 Aug 1;34(15-16):1075-88. PubMed PMID: 32616520. Pubmed Central PMCID: 7397857.
577. Gubanov E, Brown B, Ivanov SV, Helleday T, Mills GB, Yarbrough WG, et al. Downregulation of SMG-1 in HPV-positive head and neck squamous cell carcinoma due to promoter hypermethylation correlates with improved survival. *Clin Cancer Res*. 2012 Mar 1;18(5):1257-67. PubMed PMID: 22247495. Pubmed Central PMCID: 4010255.
578. Vallabhapurapu S, Karin M. Regulation and function of NF-kappaB transcription factors in the immune system. *Annu Rev Immunol*. 2009;27:693-733. PubMed PMID: 19302050.
579. Zhao J, Zhang L, Lu A, Han Y, Colangelo D, Bukata C, et al. ATM is a key driver of NF-kappaB-dependent DNA-damage-induced senescence, stem cell dysfunction and aging. *Aging (Albany NY)*. 2020 Mar 22;12(6):4688-710. PubMed PMID: 32201398. Pubmed Central PMCID: 7138542.

580. Mustafa S, Pan L, Marzoq A, Fawaz M, Sander L, Ruckert F, et al. Comparison of the tumor cell secretome and patient sera for an accurate serum-based diagnosis of pancreatic ductal adenocarcinoma. *Oncotarget*. 2017 Feb 14;8(7):11963-76. PubMed PMID: 28060763. Pubmed Central PMCID: 5355318.
581. Creaney J, Dick IM, Leon JS, Robinson BW. A Proteomic Analysis of the Malignant Mesothelioma Secretome Using iTRAQ. *Cancer Genomics & Proteomics*. 2017 Mar-Apr;14(2):103-17. PubMed PMID: 28387650. Pubmed Central PMCID: 5369310.
582. Holohan C, Van Schaeybroeck S, Longley DB, Johnston PG. Cancer drug resistance: an evolving paradigm. *Nat Rev Cancer*. 2013 Oct;13(10):714-26. PubMed PMID: 24060863.
583. Menendez D, Inga A, Resnick MA. The expanding universe of p53 targets. *Nat Rev Cancer*. 2009 Oct;9(10):724-37. PubMed PMID: 19776742.
584. Harris SL, Levine AJ. The p53 pathway: positive and negative feedback loops. *Oncogene*. 2005 Apr 18;24(17):2899-908. PubMed PMID: 15838523.
585. Crump M, Neelapu SS, Farooq U, Van Den Neste E, Kuruvilla J, Westin J, et al. Outcomes in refractory diffuse large B-cell lymphoma: results from the international SCHOLAR-1 study. *Blood*. 2017 Oct 19;130(16):1800-8. PubMed PMID: 28774879. Pubmed Central PMCID: 5649550
586. Ansell SM, Hurvitz SA, Koenig PA, LaPlant BR, Kabat BF, Fernando D, et al. Phase I Study of Ipilimumab, an Anti-CTLA-4 Monoclonal Antibody, in Patients with Relapsed and Refractory B-Cell Non-Hodgkin Lymphoma. *Clinical Cancer Research*. 2009;15(20):6446-53.
587. Kiyasu J, Miyoshi H, Hirata A, Arakawa F, Ichikawa A, Niino D, et al. Expression of programmed cell death ligand 1 is associated with poor overall survival in patients with diffuse large B-cell lymphoma. *Blood*. 2015 Nov 5;126(19):2193-201. PubMed PMID: 26239088. Pubmed Central PMCID: 4635115.
588. Kwiecinska A, Tsesmetzis N, Ghaderi M, Kis L, Saft L, Rassidakis GZ. CD274 (PD-L1)/PDCD1 (PD-1) expression in de novo and transformed diffuse large B-cell lymphoma. *Br J Haematol*. 2018 Mar;180(5):744-8. PubMed PMID: 27879989.
589. Gilad Y, Eliaz Y, Yu Y, Han SJ, O'Malley BW, Lonard DM. Drug-induced PD-L1 expression and cell stress response in breast cancer cells can be balanced by drug combination. *Sci Rep*. 2019 Oct 22;9(1):15099. PubMed PMID: 31641154. Pubmed Central PMCID: 6805932.

590. Ng HY, Li J, Tao L, Lam AK, Chan KW, Ko JMY, et al. Chemotherapeutic Treatments Increase PD-L1 Expression in Esophageal Squamous Cell Carcinoma through EGFR/ERK Activation. *Translational Oncology*. 2018 Dec;11(6):1323-33. PubMed PMID: 30172884. Pubmed Central PMCID: 6122398.
591. Sato H, Niimi A, Yasuhara T, Permata TBM, Hagiwara Y, Isono M, et al. DNA double-strand break repair pathway regulates PD-L1 expression in cancer cells. *Nature Communications*. 2017 Nov 24;8(1):1751. PubMed PMID: 29170499. Pubmed Central PMCID: 5701012.
592. Sato H, Jeggo PA, Shibata A. Regulation of programmed death-ligand 1 expression in response to DNA damage in cancer cells: Implications for precision medicine. *Cancer Science*. 2019 Nov;110(11):3415-23. PubMed PMID: 31513320. Pubmed Central PMCID: 6824998.
593. Carbognin L, Pilotto S, Milella M, Vaccaro V, Brunelli M, Calio A, et al. Differential Activity of Nivolumab, Pembrolizumab and MPDL3280A according to the Tumor Expression of Programmed Death-Ligand-1 (PD-L1): Sensitivity Analysis of Trials in Melanoma, Lung and Genitourinary Cancers. *PloS One*. 2015;10(6):e0130142. PubMed PMID: 26086854. Pubmed Central PMCID: 4472786.
594. Sun D, Ma J, Wang J, Han C, Qian Y, Chen G, et al. Anti-PD-1 therapy combined with chemotherapy in patients with advanced biliary tract cancer. *Cancer Immunology, Immunotherapy : CII*. 2019 Sep;68(9):1527-35. PubMed PMID: 31535160. Pubmed Central PMCID: 6768892.
595. Landre T, Des Guetz G, Chouahnia K, Taleb C, Vergnenegre A, Chouaid C. First-line PD-1/PD-L1 inhibitor plus chemotherapy vs chemotherapy alone for negative or < 1% PD-L1-expressing metastatic non-small-cell lung cancers. *Journal of Cancer Research and Clinical Oncology*. 2020 Feb;146(2):441-8. PubMed PMID: 31686247.
596. Zhou Y, Chen C, Zhang X, Fu S, Xue C, Ma Y, et al. Immune-checkpoint inhibitor plus chemotherapy versus conventional chemotherapy for first-line treatment in advanced non-small cell lung carcinoma: a systematic review and meta-analysis. *Journal for Immunotherapy of Cancer*. 2018 Dec 22;6(1):155. PubMed PMID: 30577837. Pubmed Central PMCID: 6303974.
597. Iwai Y, Hamanishi J, Chamoto K, Honjo T. Cancer immunotherapies targeting the PD-1 signaling pathway. *J Biomed Sci*. 2017 Apr 4;24(1):26. PubMed PMID: 28376884. Pubmed Central PMCID: 5381059.
598. Hartley GP, Chow L, Ammons DT, Wheat WH, Dow SW. Programmed Cell Death Ligand 1 (PD-L1) Signaling Regulates Macrophage Proliferation and Activation. *Cancer Immunology Research*. 2018 Oct;6(10):1260-73. PubMed PMID: 30012633.
599. Beningo KA, Wang YL. Fc-receptor-mediated phagocytosis is regulated by mechanical properties of the target. *Journal of Cell Science*. 2002 Feb 15;115(Pt 4):849-56. PubMed PMID: 11865040.

600. Nirschl CJ, Drake CG. Molecular pathways: coexpression of immune checkpoint molecules: signaling pathways and implications for cancer immunotherapy. *Clin Cancer Res.* 2013 Sep 15;19(18):4917-24. PubMed PMID: 23868869. Pubmed Central PMCID: 4005613.
601. Advani R, Flinn I, Popplewell L, Forero A, Bartlett NL, Ghosh N, et al. CD47 Blockade by Hu5F9-G4 and Rituximab in Non-Hodgkin's Lymphoma. *N Engl J Med.* 2018 Nov 1;379(18):1711-21. PubMed PMID: 30380386. Pubmed Central PMCID: 8058634.
602. Gu S, Ni T, Wang J, Liu Y, Fan Q, Wang Y, et al. CD47 Blockade Inhibits Tumor Progression through Promoting Phagocytosis of Tumor Cells by M2 Polarized Macrophages in Endometrial Cancer. *Journal of Immunology Research.* 2018;2018:6156757. PubMed PMID: 30525058. Pubmed Central PMCID: 6247569.
603. Willingham SB, Volkmer JP, Gentles AJ, Sahoo D, Dalerba P, Mitra SS, et al. The CD47-signal regulatory protein alpha (SIRP α) interaction is a therapeutic target for human solid tumors. *Proc Natl Acad Sci U S A.* 2012 Apr 24;109(17):6662-7. PubMed PMID: 22451913. Pubmed Central PMCID: 3340046
604. Jaiswal S, Jamieson CH, Pang WW, Park CY, Chao MP, Majeti R, et al. CD47 is upregulated on circulating hematopoietic stem cells and leukemia cells to avoid phagocytosis. *Cell.* 2009 Jul 23;138(2):271-85. PubMed PMID: 19632178. Pubmed Central PMCID: 2775564.
605. Olsson M, Bruhns P, Frazier WA, Ravetch JV, Oldenborg PA. Platelet homeostasis is regulated by platelet expression of CD47 under normal conditions and in passive immune thrombocytopenia. *Blood.* 2005 May 1;105(9):3577-82. PubMed PMID: 15665111. Pubmed Central PMCID: 1895021.
606. Oldenborg PA, Gresham HD, Chen Y, Izui S, Lindberg FP. Lethal autoimmune hemolytic anemia in CD47-deficient nonobese diabetic (NOD) mice. *Blood.* 2002 May 15;99(10):3500-4. PubMed PMID: 11986200.
607. Steidl C, Shah SP, Woolcock BW, Rui L, Kawahara M, Farinha P, et al. MHC class II transactivator CIITA is a recurrent gene fusion partner in lymphoid cancers. *Nature.* 2011 Mar 17;471(7338):377-81. PubMed PMID: 21368758. Pubmed Central PMCID: 3902849.
608. Xu Y, Wan B, Chen X, Zhan P, Zhao Y, Zhang T, et al. The association of PD-L1 expression with the efficacy of anti-PD-1/PD-L1 immunotherapy and survival of non-small cell lung cancer patients: a meta-analysis of randomized controlled trials. *Translational Lung Cancer Research.* 2019 Aug;8(4):413-28. PubMed PMID: 31555516. Pubmed Central PMCID: 6749123.
609. Cortez MA, Ivan C, Valdecanas D, Wang X, Peltier HJ, Ye Y, et al. PDL1 Regulation by p53 via miR-34. *Journal of the National Cancer Institute.* 2016 Jan;108(1). PubMed PMID: 26577528. Pubmed Central PMCID: 4862407.

610. Oldenborg PA, Zheleznyak A, Fang YF, Lagenaur CF, Gresham HD, Lindberg FP. Role of CD47 as a marker of self on red blood cells. *Science*. 2000 Jun 16;288(5473):2051-4. PubMed PMID: 10856220.
611. Bartlett NL, Wilson WH, Jung SH, Hsi ED, Maurer MJ, Pederson LD, et al. Dose-Adjusted EPOCH-R Compared With R-CHOP as Frontline Therapy for Diffuse Large B-Cell Lymphoma: Clinical Outcomes of the Phase III Intergroup Trial Alliance/CALGB 50303. *J Clin Oncol*. 2019 Jul 20;37(21):1790-9. PubMed PMID: 30939090. Pubmed Central PMCID: 6774813
612. Younes A, Burke JM, Cheson BD, Diefenbach C, Ferrari S, Hahn UH, et al. Safety and Efficacy of Atezolizumab in Combination with Rituximab Plus CHOP in Previously Untreated Patients with Diffuse Large B-Cell Lymphoma (DLBCL): Updated Analysis of a Phase I/II Study. *Blood*. 2019;134(Supplement_1):2874.
613. Godfrey J, Tumuluru S, Bao R, Leukam M, Venkataraman G, Phillip J, et al. PD-L1 gene alterations identify a subset of diffuse large B-cell lymphoma harboring a T-cell-inflamed phenotype. *Blood*. 2019 May 23;133(21):2279-90. PubMed PMID: 30910787. Pubmed Central PMCID: 6911840
614. Ansell SM, Minnema MC, Johnson P, Timmerman JM, Armand P, Shipp MA, et al. Nivolumab for Relapsed/Refractory Diffuse Large B-Cell Lymphoma in Patients Ineligible for or Having Failed Autologous Transplantation: A Single-Arm, Phase II Study. *J Clin Oncol*. 2019 Feb 20;37(6):481-9. PubMed PMID: 30620669. Pubmed Central PMCID: 6528729.
615. Smith SD, Till BG, Shadman MS, Lynch RC, Cowan AJ, Wu QV, et al. Pembrolizumab with R-CHOP in previously untreated diffuse large B-cell lymphoma: potential for biomarker driven therapy. *Br J Haematol*. 2020 Jun;189(6):1119-26. PubMed PMID: 32030732.
616. Xu-Monette ZY, Wu L, Visco C, Tai YC, Tzankov A, Liu WM, et al. Mutational profile and prognostic significance of TP53 in diffuse large B-cell lymphoma patients treated with R-CHOP: report from an International DLBCL Rituximab-CHOP Consortium Program Study. *Blood*. 2012 Nov 8;120(19):3986-96. PubMed PMID: 22955915. Pubmed Central PMCID: 3496956.
617. Pascual M, Mena-Varas M, Robles EF, Garcia-Barchino MJ, Panizo C, Hervas-Stubbs S, et al. PD-1/PD-L1 immune checkpoint and p53 loss facilitate tumor progression in activated B-cell diffuse large B-cell lymphomas. *Blood*. 2019 May 30;133(22):2401-12. PubMed PMID: 30975638. Pubmed Central PMCID: 6543517.
618. Sica A, Bronte V. Altered macrophage differentiation and immune dysfunction in tumor development. *The Journal of Clinical Investigation*. 2007 May;117(5):1155-66. PubMed PMID: 17476345. Pubmed Central PMCID: 1857267.

619. Goerdts S, Politz O, Schledzewski K, Birk R, Gratchev A, Guillot P, et al. Alternative versus classical activation of macrophages. *Pathobiology*. 1999;67(5-6):222-6. PubMed PMID: 10725788.
620. Roszer T. Understanding the Mysterious M2 Macrophage through Activation Markers and Effector Mechanisms. *Mediators Inflamm*. 2015;2015:816460. PubMed PMID: 26089604. Pubmed Central PMCID: 4452191.
621. Blobel GA, Schiemann WP, Lodish HF. Role of transforming growth factor beta in human disease. *N Engl J Med*. 2000 May 4;342(18):1350-8. PubMed PMID: 10793168.
622. Xuan W, Qu Q, Zheng B, Xiong S, Fan GH. The chemotaxis of M1 and M2 macrophages is regulated by different chemokines. *J Leukoc Biol*. 2015 Jan;97(1):61-9. PubMed PMID: 25359998.
623. Gordon SR, Maute RL, Dulken BW, Hutter G, George BM, McCracken MN, et al. PD-1 expression by tumour-associated macrophages inhibits phagocytosis and tumour immunity. *Nature*. 2017 May 25;545(7655):495-9. PubMed PMID: 28514441. Pubmed Central PMCID: 5931375.
624. Prima V, Kaliberova LN, Kaliberov S, Curiel DT, Kusmartsev S. COX2/mPGES1/PGE2 pathway regulates PD-L1 expression in tumor-associated macrophages and myeloid-derived suppressor cells. *Proc Natl Acad Sci U S A*. 2017 Jan 31;114(5):1117-22. PubMed PMID: 28096371. Pubmed Central PMCID: 5293015.
625. Gimmi CD, Freeman GJ, Gribben JG, Sugita K, Freedman AS, Morimoto C, et al. B-cell surface antigen B7 provides a costimulatory signal that induces T cells to proliferate and secrete interleukin 2. *Proc Natl Acad Sci U S A*. 1991 Aug 1;88(15):6575-9. PubMed PMID: 1650475. Pubmed Central PMCID: 52129.
626. Lam JH, Ng HHM, Lim CJ, Sim XN, Malavasi F, Li H, et al. Expression of CD38 on Macrophages Predicts Improved Prognosis in Hepatocellular Carcinoma. *Frontiers in Immunology*. 2019;10:2093. PubMed PMID: 31552039. Pubmed Central PMCID: 6738266.
627. Nabeshima A, Matsumoto Y, Fukushi J, Iura K, Matsunobu T, Endo M, et al. Tumour-associated macrophages correlate with poor prognosis in myxoid liposarcoma and promote cell motility and invasion via the HB-EGF-EGFR-PI3K/Akt pathways. *Br J Cancer*. 2015 Feb 3;112(3):547-55. PubMed PMID: 25562433. Pubmed Central PMCID: 4453656.
628. Mahmoud SM, Lee AH, Paish EC, Macmillan RD, Ellis IO, Green AR. Tumour-infiltrating macrophages and clinical outcome in breast cancer. *Journal of Clinical Pathology*. 2012 Feb;65(2):159-63. PubMed PMID: 22049225.

629. Jezequel P, Campion L, Spyrtos F, Loussouarn D, Campone M, Guerin-Charbonnel C, et al. Validation of tumor-associated macrophage ferritin light chain as a prognostic biomarker in node-negative breast cancer tumors: A multicentric 2004 national PHRC study. *International Journal of Cancer*. 2012 Jul 15;131(2):426-37. PubMed PMID: 21898387.
630. Arandjelovic S, Ravichandran KS. Phagocytosis of apoptotic cells in homeostasis. *Nat Immunol*. 2015 Sep;16(9):907-17. PubMed PMID: 26287597. Pubmed Central PMCID: 4826466.
631. Thebaud B, Stewart DJ. Exosomes: cell garbage can, therapeutic carrier, or trojan horse? *Circulation*. 2012 Nov 27;126(22):2553-5. PubMed PMID: 23114790.
632. Thery C, Zitvogel L, Amigorena S. Exosomes: composition, biogenesis and function. *Nat Rev Immunol*. 2002 Aug;2(8):569-79. PubMed PMID: 12154376.
633. Jaggi U, Yang M, Matundan HH, Hirose S, Shah PK, Sharifi BG, et al. Increased phagocytosis in the presence of enhanced M2-like macrophage responses correlates with increased primary and latent HSV-1 infection. *PLoS pathogens*. 2020 Oct;16(10):e1008971. PubMed PMID: 33031415. Pubmed Central PMCID: 7575112.
634. Yu X, Harris SL, Levine AJ. The regulation of exosome secretion: a novel function of the p53 protein. *Cancer Res*. 2006 May 1;66(9):4795-801. PubMed PMID: 16651434.
635. Distler JH, Huber LC, Hueber AJ, Reich CF, 3rd, Gay S, Distler O, et al. The release of microparticles by apoptotic cells and their effects on macrophages. *Apoptosis*. 2005 Aug;10(4):731-41. PubMed PMID: 16133865.
636. Aubrey BJ, Kelly GL, Janic A, Herold MJ, Strasser A. How does p53 induce apoptosis and how does this relate to p53-mediated tumour suppression? *Cell Death Differ*. 2018 Jan;25(1):104-13. PubMed PMID: 29149101. Pubmed Central PMCID: 5729529.
637. Sant M, Allemani C, Tereanu C, De Angelis R, Capocaccia R, Visser O, et al. Incidence of hematologic malignancies in Europe by morphologic subtype: results of the HAEMACARE project. *Blood*. 2010 Nov 11;116(19):3724-34. PubMed PMID: 20664057.
638. Duggan MA, Anderson WF, Altekruse S, Penberthy L, Sherman ME. The Surveillance, Epidemiology, and End Results (SEER) Program and Pathology: Toward Strengthening the Critical Relationship. *The American Journal of Surgical Pathology*. 2016 Dec;40(12):e94-e102. PubMed PMID: 27740970. Pubmed Central PMCID: 5106320.
639. Fleming AF. Twenty-five Zambians with leukaemias. *East Afr Med J*. 1989 Mar;66(3):162-6. PubMed PMID: 2591324.

640. Falchi L, Keating MJ, Wang X, Coombs CC, Lanasa MC, Strom S, et al. Clinical characteristics, response to therapy, and survival of African American patients diagnosed with chronic lymphocytic leukemia: joint experience of the MD Anderson Cancer Center and Duke University Medical Center. *Cancer*. 2013 Sep 1;119(17):3177-85. PubMed PMID: 24022787. Pubmed Central PMCID: 4394603.
641. Coombs CC, Rassenti LZ, Falchi L, Slager SL, Strom SS, Ferrajoli A, et al. Single nucleotide polymorphisms and inherited risk of chronic lymphocytic leukemia among African Americans. *Blood*. 2012 Aug 23;120(8):1687-90. PubMed PMID: 22745306. Pubmed Central PMCID: 3429309.
642. Kipps TJ, Stevenson FK, Wu CJ, Croce CM, Packham G, Wierda WG, et al. Chronic lymphocytic leukaemia. *Nature Reviews Disease Primers*. 2017 Jan 19;3(1):16096. PubMed PMID: 28102226. Pubmed Central PMCID: 5336551.
643. Eichhorst B, Robak T, Montserrat E, Ghia P, Niemann CU, Kater AP, et al. Chronic lymphocytic leukaemia: ESMO Clinical Practice Guidelines for diagnosis, treatment and follow-up. *Annals of Oncology : official journal of the European Society for Medical Oncology / ESMO*. 2021 Jan;32(1):23-33. PubMed PMID: 33091559.
644. Eichhorst B, Robak T, Montserrat E, Ghia P, Hillmen P, Hallek M, et al. Chronic lymphocytic leukaemia: ESMO Clinical Practice Guidelines for diagnosis, treatment and follow-up. *Annals of Oncology : official journal of the European Society for Medical Oncology / ESMO*. 2015 Sep;26 Suppl 5:v78-84. PubMed PMID: 26314781.
645. Dong N, Saeed H, Gaballa S, Shah BD, Coghill A, Isenalumhe LL, et al. Survival trend of chronic lymphocytic leukemia and prognostic factors in the United States: An analysis of the National Cancer Database. *Journal of Clinical Oncology*. 2020;38(15_suppl):e20012-e.
646. Pfeil AM, Imfeld P, Pettengell R, Jick SS, Szucs TD, Meier CR, et al. Trends in incidence and medical resource utilisation in patients with chronic lymphocytic leukaemia: insights from the UK Clinical Practice Research Datalink (CPRD). *Ann Hematol*. 2015 Mar;94(3):421-9. PubMed PMID: 25219890.
647. Madu AJ, Korubo K, Okoye A, Ajuba I, Duru AN, Ugwu AO, et al. Presenting features and treatment outcomes of chronic lymphocytic leukaemia in a resource poor Southern Nigeria. *Malawi medical journal : The Journal of Medical Association of Malawi*. 2019 Jun;31(2):144-9. PubMed PMID: 31452848. Pubmed Central PMCID: 6698622.
648. Shamebo M, Gebremedhin A. Chronic lymphocytic leukaemia in Ethiopians. *East Afr Med J*. 1996 Oct;73(10):643-6. PubMed PMID: 8997843.
649. Clegg-Lamptey J, Dakubo J, Attobra YN. Why do breast cancer patients report late or abscond during treatment in Ghana? A pilot study. *Ghana Med J*. 2009;43(3):127-31. Pubmed Central PMCID: 2810246.

650. Hamblin TJ. Autoimmune complications of chronic lymphocytic leukemia. *Semin Oncol.* 2006 Apr;33(2):230-9. PubMed PMID: 16616070.
651. Basabaeen AA, Abdelgader EA, Babekir EA, Eltayeb NH, Altayeb OA, Fadul EA, et al. Clinical presentation and hematological profile among young and old chronic lymphocytic leukemia patients in Sudan. *BMC Research Notes.* 2019 Apr 2;12(1):202. PubMed PMID: 30940190. Pubmed Central PMCID: 6446286.
652. Watson L, Wyld P, Catovsky D. Disease burden of chronic lymphocytic leukaemia within the European Union. *European Journal of Haematology.* 2008 Oct;81(4):253-8. PubMed PMID: 18616512.
653. Mauro FR, Foa R, Giannarelli D, Cordone I, Crescenzi S, Pescarmona E, et al. Clinical characteristics and outcome of young chronic lymphocytic leukemia patients: a single institution study of 204 cases. *Blood.* 1999 Jul 15;94(2):448-54. PubMed PMID: 10397712.
654. Schroers R, Griesinger F, Trumper L, Haase D, Kulle B, Klein-Hitpass L, et al. Combined analysis of ZAP-70 and CD38 expression as a predictor of disease progression in B-cell chronic lymphocytic leukemia. *Leukemia.* 2005 May;19(5):750-8. PubMed PMID: 15759031.
655. Choi Y, Lee JH, Jung CW, Jo JC, Kim JS, Kim I, et al. Treatment outcome and prognostic factors of Korean patients with chronic lymphocytic leukemia: a multicenter retrospective study. *The Korean Journal of Internal Medicine.* 2021 Jan;36(1):194-204. PubMed PMID: 32279477. Pubmed Central PMCID: 7820637.
656. Chan TS, Lee YS, Del Giudice I, Marinelli M, Ilari C, Cafforio L, et al. Clinicopathological features and outcome of chronic lymphocytic leukaemia in Chinese patients. *Oncotarget.* 2017 Apr 11;8(15):25455-68. PubMed PMID: 28424415. Pubmed Central PMCID: 5421943.
657. Gogia A, Gupta R, Sharma A, Kumar L, Raina V, Rani L. Chronic lymphocytic leukemia: An Indian experience. *Journal of Clinical Oncology.* 2019;37(15_suppl):e19007-e.
658. Shenoy PJ, Malik N, Sinha R, Nooka A, Nastoupil LJ, Smith M, et al. Racial differences in the presentation and outcomes of chronic lymphocytic leukemia and variants in the United States. *Clin Lymphoma Myeloma Leuk.* 2011 Dec;11(6):498-506. PubMed PMID: 21889433.
659. Wierda WG, O'Brien S, Wang X, Faderl S, Ferrajoli A, Do KA, et al. Multivariable model for time to first treatment in patients with chronic lymphocytic leukemia. *J Clin Oncol.* 2011 Nov 1;29(31):4088-95. PubMed PMID: 21969505. Pubmed Central PMCID: 4876352.

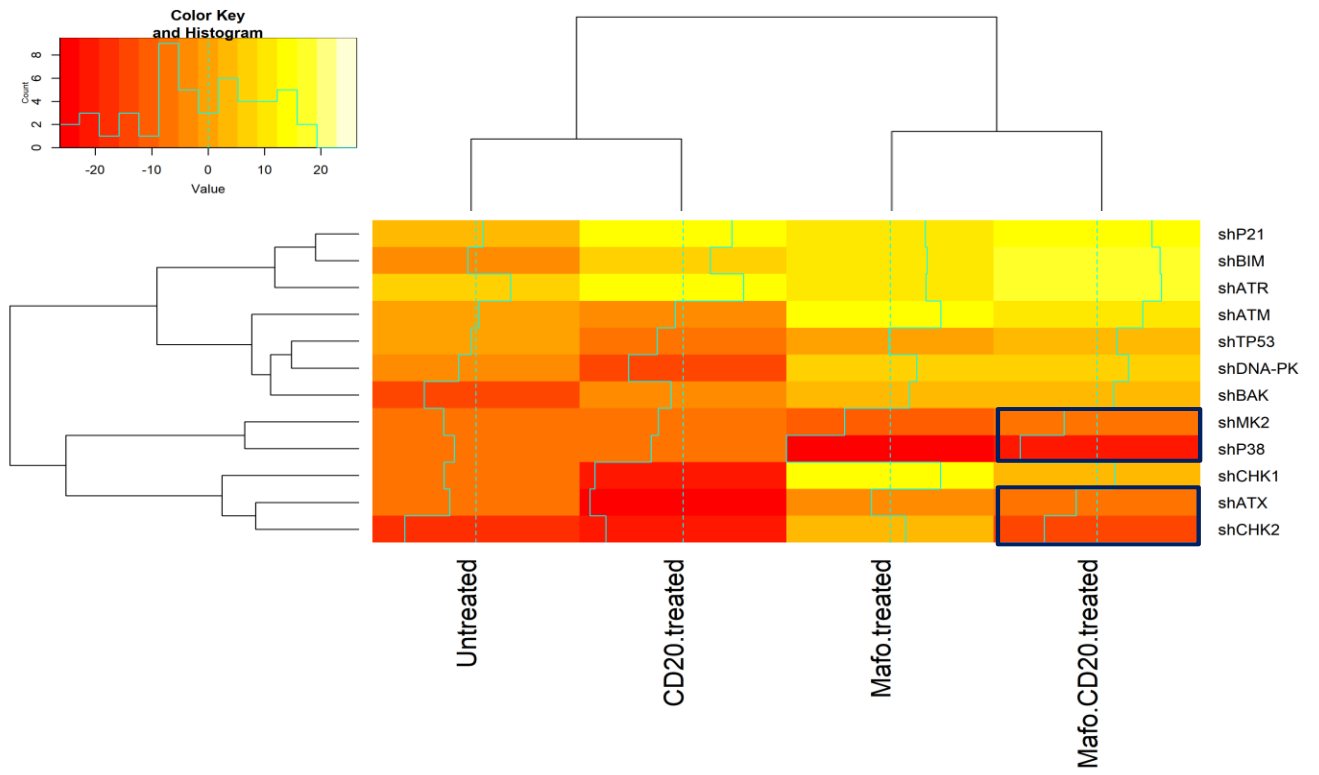
660. Mutala AH, Badu K, Owusu C, Agordzo SK, Tweneboah A, Abbas DA, et al. Impact of malaria on haematological parameters of urban, peri-urban and rural residents in the Ashanti region of Ghana: a cross-sectional study. *AAS Open Research*. 2019;2:27. PubMed PMID: 32704620. Pubmed Central PMCID: 7355218.
661. Shen PU, Fuller SG, Rezuke WN, Sherburne BJ, DiGiuseppe JA. Laboratory, morphologic, and immunophenotypic correlates of surface immunoglobulin heavy chain isotype expression in B-cell chronic lymphocytic leukemia. *Am J Clin Pathol*. 2001 Dec;116(6):905-12. PubMed PMID: 11764081.
662. Geisler CH, Larsen JK, Hansen NE, Hansen MM, Christensen BE, Lund B, et al. Prognostic importance of flow cytometric immunophenotyping of 540 consecutive patients with B-cell chronic lymphocytic leukemia. *Blood*. 1991 Oct 1;78(7):1795-802. PubMed PMID: 1717071.
663. Hamblin TJ, Oscier DG, Stevens JR, Smith JL. Long survival in B-CLL correlates with surface IgM kappa phenotype. *Br J Haematol*. 1987 May;66(1):21-6. PubMed PMID: 3496111.
664. Marantidou F, Dagklis A, Stalika E, Korkolopoulou P, Saetta A, Anagnostopoulos A, et al. Activation-induced cytidine deaminase splicing patterns in chronic lymphocytic leukemia. *Blood Cells, Molecules & Diseases*. 2010 Apr 15;44(4):262-7. PubMed PMID: 20117026.
665. Kimby E, Mellstedt H, Bjorkholm M, Holm G. Surface immunoglobulin pattern of the leukaemic cell population in chronic lymphocytic leukaemia (CLL) in relation to disease activity. *Hematol Oncol*. 1985 Oct-Dec;3(4):261-9. PubMed PMID: 3936768.
666. Rudders RA. B lymphocyte subpopulations in chronic lymphocytic leukemia. *Blood*. 1976 Feb;47(2):229-35. PubMed PMID: 1081895.
667. Hamblin T, Hough D. Chronic lymphatic leukaemia: correlation of immunofluorescent characteristics and clinical features. *Br J Haematol*. 1977 Jul;36(3):359-65. PubMed PMID: 329856.
668. Chen K, Cerutti A. New insights into the enigma of immunoglobulin D. *Immunol Rev*. 2010 Sep;237(1):160-79. PubMed PMID: 20727035. Pubmed Central PMCID: 3048779.
669. Lewis RE, Cruse JM, Pierce S, Lam J, Tadros Y. Surface and cytoplasmic immunoglobulin expression in B-cell chronic lymphocytic leukemia (CLL). *Experimental and Molecular Pathology*. 2005 Oct;79(2):146-50. PubMed PMID: 15963979.
670. Geisberger R, Lamers M, Achatz G. The riddle of the dual expression of IgM and IgD. *Immunology*. 2006 Aug;118(4):429-37. PubMed PMID: 16895553. Pubmed Central PMCID: 1782314.

671. Noviski M, Mueller JL, Satterthwaite A, Garrett-Sinha LA, Brombacher F, Zikherman J. IgM and IgD B cell receptors differentially respond to endogenous antigens and control B cell fate. *Elife*. 2018 Mar 9;7. PubMed PMID: 29521626. Pubmed Central PMCID: 5897097.
672. Lanham S, Hamblin T, Oscier D, Ibbotson R, Stevenson F, Packham G. Differential signaling via surface IgM is associated with VH gene mutational status and CD38 expression in chronic lymphocytic leukemia. *Blood*. 2003 Feb 1;101(3):1087-93. PubMed PMID: 12393552.
673. Guarini A, Chiaretti S, Tavoraro S, Maggio R, Peragine N, Citarella F, et al. BCR ligation induced by IgM stimulation results in gene expression and functional changes only in IgV H unmutated chronic lymphocytic leukemia (CLL) cells. *Blood*. 2008 Aug 1;112(3):782-92. PubMed PMID: 18487510.
674. Schreiber RD, Old LJ, Smyth MJ. Cancer immunoediting: integrating immunity's roles in cancer suppression and promotion. *Science*. 2011 Mar 25;331(6024):1565-70. PubMed PMID: 21436444.

10 APPENDICES

APPENDIX A

A.  Increased phagocytosis



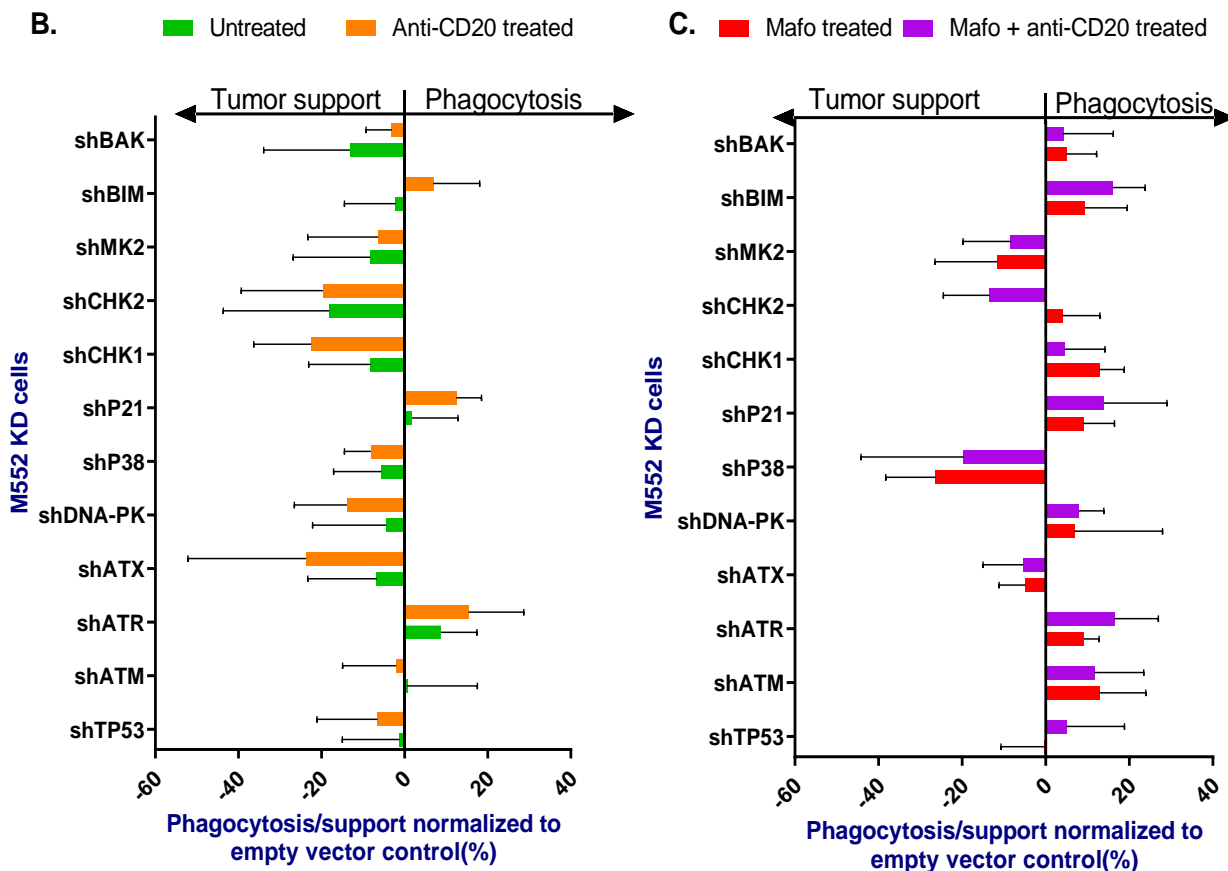


Figure34: Critical DDR genes regulate tumor cells phagocytosis by J774.1A macrophages

A. Overview of phagocytosis pattern of M552 KD cells under different treatment conditions cocultured with murine J774.1A macrophages. Colour shades depict continuum of deep red to light yellow representing highly reduced phagocytosis/ tumor support to enhanced phagocytosis respectively. Broken green line for each condition represent empty vector control (shCtrl) and the solid stepped lines indicate quantitatively, average phagocytosis of the KD cell of all biological replicates relative to the empty vector control for the indicated gene. The violet box in the mafosphamide-anti-CD20 combination treatment highlights identified DDR genes mediating treatment resistance/refractory in this model. (n=5).

- B. Detailed quantitative presentation of M552 KD cells under different treatment conditions cocultured with J774.1 anti-CD20 monotherapy treatment (yellow). Phagocytosis of KD cells in all conditions is normalized to the empty vector (shCtrl) control cells (n=5).
- C. Detailed quantitative presentation of M552 KD cells under different treatment conditions cocultured with J774.1A macrophages. Tumor cells were mafosphamide pretreatment (red) and mafosphamide pretreatment in combination with anti-CD20 mAb (purple). Phagocytosis of the KD cells in all conditions are normalized to the empty vector (shCtrl) control cells (n=5).

APPENDIX B

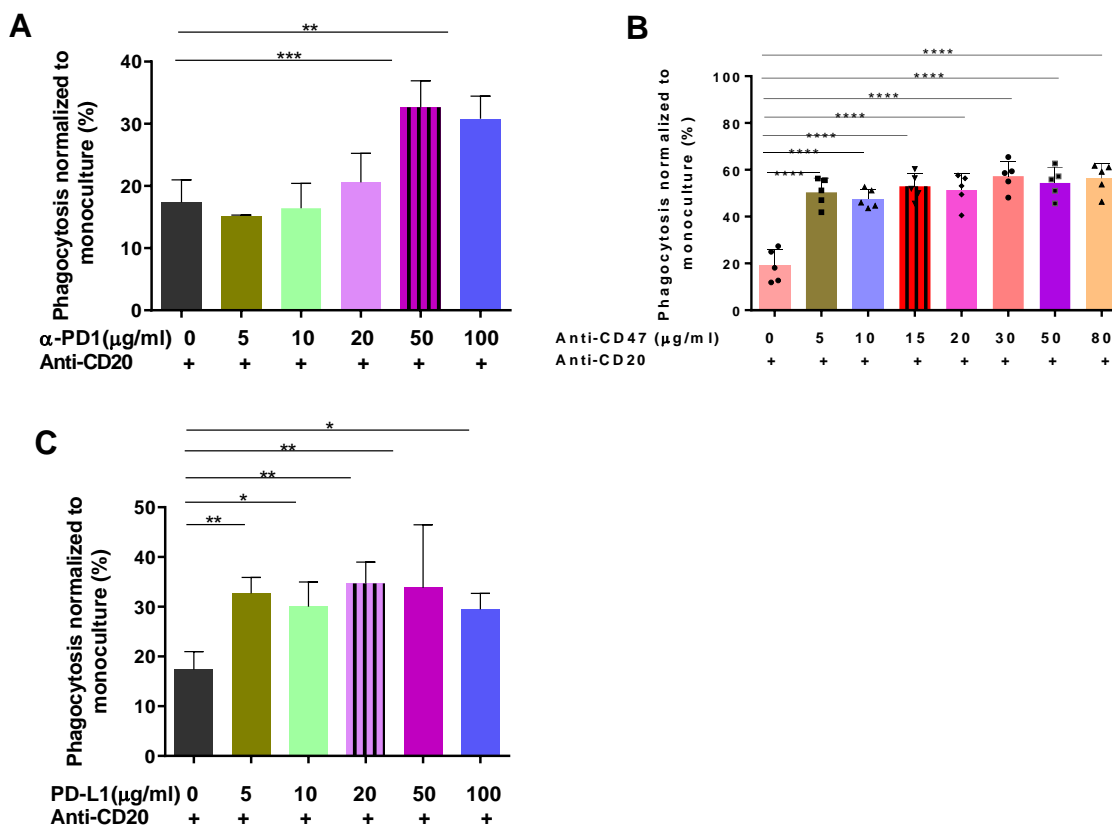


Figure 35: Optimization for functionally relevant concentration of immune checkpoint inhibitors

- A. level of anti-CD20 dependent macrophage-mediated tumor cells phagocytosis induced by increasing anti-PD-1 concentration.
- B. level of anti-CD20 dependent macrophage-mediated tumor cells phagocytosis induced by increasing anti-CD47 concentration.
- C. level of anti-CD20 dependent macrophage-mediated tumor cells phagocytosis induced by increasing anti-PD-L1 concentration.

APPENDIX C

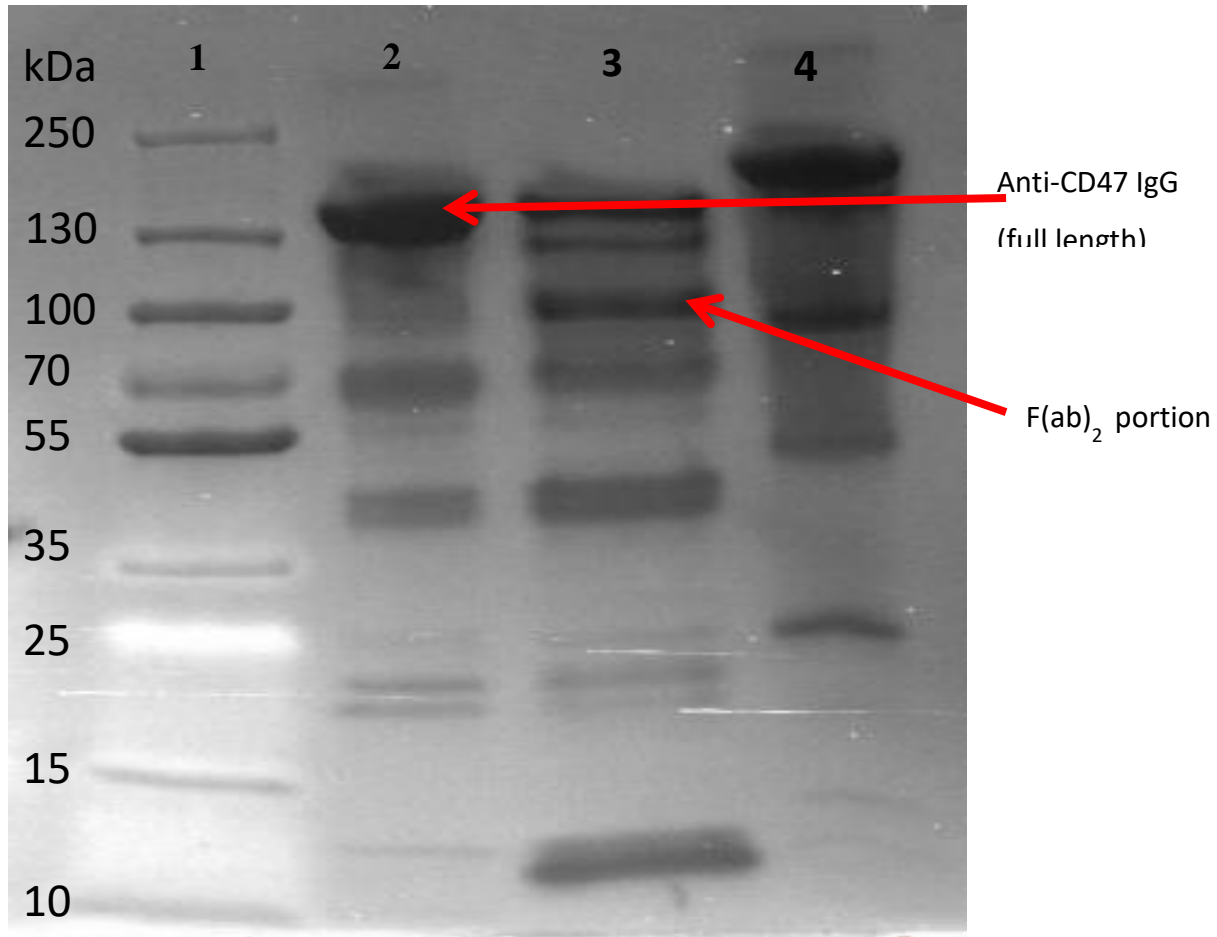


Figure36: Full length and F(ab)₂ fractionated anti-CD47 antibody stained by Coomassie blue

Proteins were electrophorised on 4-12% gradient SDS-Page gel under non-reducing conditions at 160v for 1hr, 0.1%, stained with Coomassie blue for 1hr, destained with several changes of destaining solution overnight and visualized on a BioRad imager.

1 = 10-250kDa protein ladder

2 = Anti-CD47 IgG (full length)

3 = F(ab)₂ portion

4 = Rat IgG2a,k isotype control

APPENDIX D

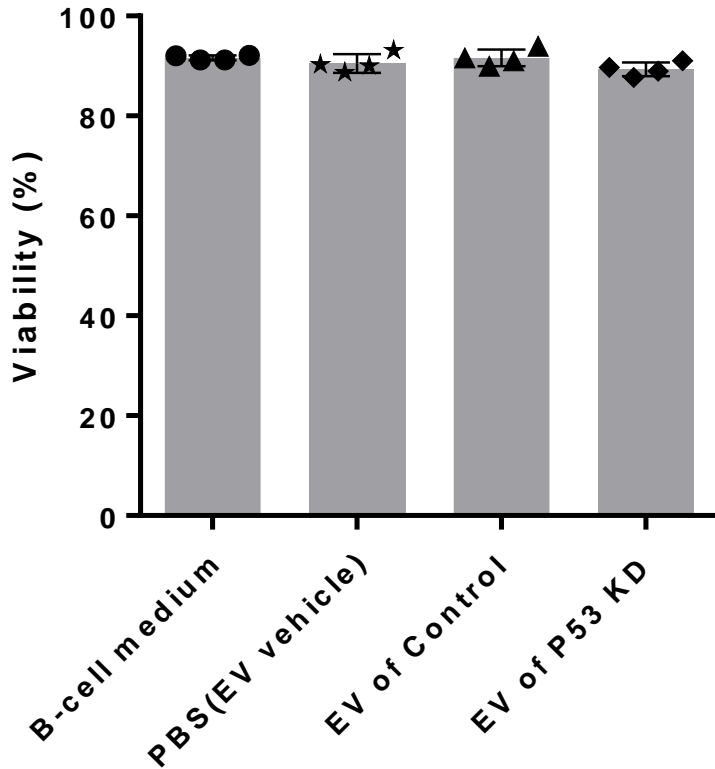


Figure37: Viability of M552 cell cocultured with extracellular vesicles or PBS (vehicle control)

Monocultures of control cells (empty vector) with 5 μ l of B-cell medium, PBS, exosome vesicles from control or p53 KD cells were stained with annexin V/ 7-AAD after 16hrs and enumerated by flow cytometry.

Abbreviations

~	Approximately
μl	Microliter
53BP1	p53 binding protein 1
7-AAD	7- Aminoactinomycin D
A	Adenine
Ab	Antibody
ADCP	Antibody dependent cell phagocytosis
AICP	Antibody independent cellular phagocytosis
Ag	Antigen
AKT	Protein kinase B
ALL	Acute lymphoid leukemia
AML	Acute myeloid leukemia
APC	Antigen presenting cell
APS	Ammonium per sulfate
ASAP	Acute secretory activating phenotype
AT	Ataxia telangiectasia
ATM	Ataxia telangiectasia mutated
ATR	Ataxia telangiectasia and Rad3 related
ATRIP	ATR-interacting protein
BAD	BCL-2 associated agonist of cell death
BAX	Bcl-2 associated X- protein
BCL-2/6/X	B cell lymphoma 2/6/X
BCR	B-cell receptor
BID	BH3 interacting domain death agonist
BIK	BCL-2 interacting killer
BIM	BCL-2 Interacting Mediator of cell death
BL	Burkitt's lymphoma
BLNK	B cell linker

BM	Bone marrow
BMF	BCL-2 modifying factor
BMSC	Bone marrow stromal cell
bp	Base pair
BRCA1,	Breast cancer gene 1
BRCA2,	Breast cancer gene 2
BSA	Bovine serum albumin
BTK	Bruton's tyrosine kinase
C	Cytosine
Ca ²⁺	Calcium ion
CAF	Cancer associated fibroblast
CAR-T	Chimeric antigen receptor T-cell
CBP	CREB binding protein
CCL	C-C motif ligand
CCND1	Cyclin D1
CD	Cluster of Differentiation
CDK	Cyclin-dependent kinase
cDNA	Complementary DNA
CHK1	Checkpoint kinase 1
CHK2	Checkpoint kinase 2
CLL	Chronic lymphoid leukemia
CM	Conditioned Media
CML	Chronic myeloid leukemia
CSF1	Colony Stimulating Factor 1
Ctrl	Control
CTX	Cyclophosphamide
CXCL	C-X-C motif ligand
DC	Dendritic cell
DDR	DNA damage response
DHL	Double hit lymphoma

DLBCL	Diffuse large B cell lymphoma
DMSO	Dimethyl sulfoxide
DNA	Deoxyribonucleic acid
DNA-PK	DNA-dependent protein kinase
DNA-PKc	DNA-dependent protein kinase catalytic subunit
DOX	Doxorubicin
DSB	Double strand break
EDTA	Ethylenediaminetetraacetic acid
EGF	Epithelial growth factors
EMT	Epithelial to mesenchymal transition
Eomes	Eomesodermin homolog
EPOCH/EPOCH-R	Etoposide, prednisolone, vincristine (oncovin), cyclophosphamide,
ERK	Extracellular signal regulated kinase
XPO1	Exportin-1
FBS	Fetal bovine serum
FcR	Fc receptor
FCR	Fludarabine-cyclophosphamide-rituximab treatment
FISH	Fluorescent in-situ hybridization
G1 and G2	Gap 1 and Gap 2
GADD45	Growth arrest and DNA damage inducible 45
GATA-3	GATA binding protein 3
GC	Germinal center
GFP	Green fluorescent protein
GM-CSF	Granulocyte macrophage colony stimulating factor
H2AX	Histone 2A family member X
HAT	Histone acetyltransferase
HCL	Hairy cell leukemic
HIF-1 and HIF-2	Hypoxia-Inducible Factor 1 and 2
HIF1a	Hypoxia inducible factor 1 alpha
HR	Homologous recombination

hr	Hour
HRK	Harakiri
HSC	Hematopoietic stem cells
ICL	Interstrand cross link repair
IFN γ	Interferon gamma
Ig	Immunoglobulin
IGF1	Insulin like growth factor 1
IgG	Immunoglobulin G
IgVH	Immunoglobulin heavy chain variable region
IHC	Immunohistochemistry
IL	Interleukin
iNOS	Inducible nitric oxide synthase
IR	Ionizing radiation
IRF	Interferon regulator factor
ITAM	Immunoreceptor tyrosine based activation motif
KD	Knock-down
kDa	Kilo Dalton
LB	Lysogenic broth
LPS	Lipopolysaccharide
LTR	Long terminal repeat
LYN	Lck/Yes novel tyrosine kinase
M	Mitosis
M	Molar
mA	Milli ampere
MACS	Magnetic activated cell sorting
MBL	Monoclonal B-cell lymphocytosis
MCL1	Myeloid cell leukemia 1
M-CSF	Macrophage colony stimulating factor
MDC1	Mediator of DNA Damage Checkpoint 1
MDM2	Mouse double minute protein 2

MDSC	Myeloid derived suppressor cells
MEF	Mouse embryonic fibroblast
MFI	Median fluorescent intensity
mg	Milligram
min	Minute
miR	Micro RNA
MK2	Mitogen activated protein kinase 2
ml	Milliliter
mm	Millimeter
mM	Millimolar
MyD88	Myeloid differentiation primary response gene 88
MMP	Matrix metalloproteinase
MMR	Mismatch repair
MRN	Mre11/Rad50/Nijmegen breakage syndrome
mRNA	Messenger ribonucleic acid
MSC	Mesenchymal stem cell
Mut	Mutator
MYC	(Avian) Myelocytomatosis viral oncogene homolog
n	Number of replicates
NBS	Nijmegen breakage syndrome
NER	Nucleotide excision repair
NFAT	Nuclear factor of activated T- cells
NF- κ B	Nuclear factor kappa-light-chain-enhancer of activated B cells
NHEJ	Non-homologous end joining
NHL	Non-Hodgkin's lymphoma
NK cell	Natural killer cell
NLC	Nurse like cell
nM	Nanomolar
NO	Nitric oxide
PAGE	Polyacrylamide gel electrophoresis

PARP	Poly (ADP-ribose) polymerase
PBMC	Peripheral blood mononuclear cells
PBS	Phosphate buffered saline
PCNA	Proliferating cell nuclear antigen
PCR	Polymerase chain reaction
PDGF	Platelet-derived growth factor
PD-L1	Programmed cell death protein ligand 1
PI3-K	Phosphatidylinositide 3 kinase
PIKK	Phosphatidylinositol 3-kinase-like protein kinase
PKC	Protein kinase C
PLCy	Phospholipase C gamma
pRB	Phosphorylated retinoblastoma
PS	Phosphatidylserine
PUMA	p53 upregulated modulator of apoptosis
RAD50	RAD50 double strand break repair protein
RAD51C	RAD51 homolog C
RAG1/2	Recombination activating gene 1 and 2
R-CHOP	Rituximab-Cyclophosphamide-Hydroxydaunorubicin-vincristine- Prednisone
ROS	Reactive oxygen species
RPA	Replication protein A2
Rpm	Revolutions per minute
S	Synthesis
SASP	Senescent associated secretory phenotype
SDF1	Stromal cell derived factor 1
SDS	Sodium dodecyl sulfate
sec	Second
SF3B1	Splicing factor 3 β subunit 1
SHIP 1	SH-2 containing Inositol 5' polyphosphate 1
SIRP- α	Signal regulatory protein Alpha

Src	Rous sarcoma oncogene cellular homolog
SSB	Single strand break
STAT	Signal transducer and activator of transcription
SYK	Spleen tyrosine kinase
T	Thymine
TAE	Tris acetate ethylene diamine tetraacetic acid
TAM	Tumor-associated macrophages
T-bet	T-box protein expressed in T-cells
TBST	Tris buffered saline with Tween-20
TCL1	T-cell leukemia 1
TCR	T-cell receptor
TEMED	Tetramethylethylenediamine
TF	Transcription factor
TGF	Transforming growth factor
TH cell	T helper cell
TILs	Tumor infiltrating lymphocytes
TLR	Toll-like receptor
TNF	Tumor necrosis factor
T-PLL	T-cell prolymphocytic leukemia
Tris	Tris (hydroxymethyl) aminomethane
U	Units
U	Uracil
UV	Ultra violet
V	Volt
V(D)J	Variability, diversity and joining genes
VCAM1	Vascular cell adhesion molecule 1
VEGF	Vascular endothelial growth factor
WIP1	Wild type p53 induced phosphatase
g	Acceleration of gravity
XLF	XRCC4-like factor

XP	Xeroderma pigmentosum
XRCC4	Cross-complementing protein 4
ZAP-70	Zeta chain associated protein kinase 70kDa

List of Figures

Figure 1: Diagrammatic representation of vector construct	67
Figure 2: Diagrammatic depiction of ADCP and AICP experimental setup.....	81
Figure 3: Characterization of E μ -Myc and OSU-CLL cell lines by CD20 antigen expression and sensitivity to genotoxic substances.....	88
Figure 4: Genotoxic pretreatment of Eu-Myc cells induces a higher ADCP.....	90
Figure 5: ADCP of Eu-Myc cells reduces in culture regardless of genotoxic pretreatment.....	91
Figure 6: Eu-Myc cells show reduced Fc gamma mediated phagocytosis	93
Figure 7: Suppressed Cd20 expression causes diminished anti-CD20 specific phagocytosis of.....	95
Figure 8: Baseline characterization of sub-clones of MyD88 cell line.....	98
Figure 9: Characterization of M552 cell line by genotoxic agents and phagocytic patterns in coculture with different murine macrophages	100
Figure 10: Efficiency of shRNA mediated knockdowns of DNA damage response genes in M552 clone cell	102
Figure 11: Proliferation pattern of untreated and mafosphamide pretreated M552 KD cells.....	104
Figure 12: Sensitivity of M552 cell lines harboring DDR genes KD to mafosphamide	106
Figure 13: Critical genes in DDR regulate phagocytosis of tumor cells by peritoneal macrophages.....	111
Figure 14: DDR genes regulation of tumor cells phagocytosis by DDR genes in coculture with by Bone marrow derived macrophages	114
Figure 15: Pattern of phagocytosis of DDR KD M552 lymphoma cells of mouse peritoneal, bone marrow and J774.1A macrophages under different treatment condition.....	118
Figure 16: Secretome of control cells with functional DDR restores phagocytosis of DDR KD cells.....	122
Figure 17: Impact of genotoxic stress on phagocytosis of empty vector control cells (shCTRL) cocultured in CM of DDR KD cells	125
Figure 18: Expression patterns of immune checkpoint antigens of MyD88 cells unstressed and sub-lethally stressed with mafosphamide	127

Figure 19: Levels of phagocytosis of M552 cells cocultured with effector macrophages under immune checkpoint inhibitors combinatory treatment.....	130
Figure 20: F(ab) ₂ fragment of anti-CD47 effectively induces higher ADCP through blockade of CD47-Sirp- α	133
Figure 21: Immune checkpoint expression of DDR genes KD cells exposed to varied treatment.....	136
Figure 22: Levels of phagocytosis of genotoxic stressed empty vector control and DDR KD cells of M552 coculture with primary murine peritoneal macrophages. Cocultures were treated with anti-CD20 mAb and immune checkpoint inhibitors.....	139
Figure 23: Levels of phagocytosis of genotoxic stressed empty vector control and DDR KD cells of M552 coculture with primary murine bone marrow macrophages and J774.1A macrophages. Cocultures were treated with anti-CD20 mAb and immune checkpoint inhibitors	142
Figure 25: Phenotypic characteristics of mouse peritoneal macrophages cocultured with poorly phagocytosed tumor cells harboring KD of DNA damage response genes.	146
Figure 26: TP53 KD changes the functional effect of the exosomal response to immune checkpoint antibody combinations.....	148
Figure 27: Complete blood count profile of CLL patients.....	154
Figure 28: Binet staging criteria and stratification of Ghanaian CLL patients.....	156
Figure 29: Surface immunoglobulin expression pattern in CLL patients.....	160
Figure 30: Prognostic assessment of CLL patients using ZAP-70 and CD38 expression.....	163
Figure 31: The expression levels of surface immunoglobulin in various groups defined by published prognostic factors.....	165
Figure 32: Comparative analysis of immune checkpoint proteins expression with published prognostic factors in CLL.....	168
Figure 33: Clinical stage in CLL is independent of immune checkpoints and prognostic markers	170

List of Tables

Table 1: Recipe for preparation of stacking and separation gel.....	71
Table 2: Antibody panel for staining surface marker of murine macrophages for purity check ..	73
Table 3: Extra-and Intracellular markers for murine macrophage phenotype determination	75
Table 4: Antibody panel for immunophenotyping of CLL cohort	78
Table 5: Optimized concentrations for different cell types	80
Table 6: Antibody panel for assessment of immune checkpoint antigens expression	82
Table 7: Optimized concentration of immune checkpoint inhibitors.....	83
Table 8: Basic demographics of recruited patients	152
Table 9: Stratification of full blood count of CLL patients by the normal reference ranges	154

Erklärung

Ich versichere, dass ich die von mir vorgelegte Dissertation selbstständig angefertigt, die benutzten Quellen und Hilfsmittel vollständig angegeben und die Stellen der Arbeit - einschließlich Tabellen, Karten und Abbildungen -, die anderen Werken im Wortlaut oder dem Sinn nach entnommen sind, in jedem Einzelfall als Entlehnung kenntlich gemacht habe; dass diese Dissertation noch keiner anderen Fakultät oder Universität zur Prüfung vorgelegen hat; dass sie - abgesehen von unten angegebenen Teilpublikationen - noch nicht veröffentlicht worden ist sowie, dass ich eine solche Veröffentlichung vor Abschluss des Promotionsverfahrens nicht ohne Genehmigung der Dekanin / dem Dekan vornehmen werde. Die Bestimmungen dieser Ordnung sind mir bekannt. Die von mir vorgelegte Dissertation ist von Prof. Dr. Christian P. Pallasch betreut worden.

Overview of publications

Izquierdo E, Vorholt D, Blakemore S, **Sackey B**, Nolte JL, Barbarino V, Schmitz J, Nickel N, Bachurski D, Lobastova L, Nikolic M, Michalik M, Brinker R, Merkel O, Franitza M, Georgomanolis T, Neuhaus R, Koch M, Nasada N, Knittel G, Chapuy B, Ludwig N, Meese E, Frenzel L, Reinhardt HC, Peifer M, Rebollido-Rios R, Bruns H, Krüger M, Hallek M, Pallasch CP. **Extracellular vesicles and PD-L1 suppress macrophages, inducing therapy resistance in TP53-deficient B-cell malignancies.** Blood. 2022 Jun 23;139(25):3617-3629. doi: 10.1182/blood.2021014007. PMID: 35344582.

Ich versichere, dass ich alle Angaben wahrheitsgemäß nach bestem Wissen und Gewissen gemacht habe und verpflichte mich, jedmögliche, die obigen Angaben betreffenden Veränderungen, dem Promotionsausschuss unverzüglich mitzuteilen.



Datum: 21.06.2023

Unterschrift

Curriculum vitae

PERSONAL INFORMATION

Name: Benedict Sackey

Address: AG Pallasch

CECAD Forschungszentrum

Joseph-Stelzmann-Str. 26

50931 Köln

Nationality: Ghanaian

Mobile: +233244963713

Email: askabuka@yahoo.com

bsackey@smail.uni-koeln.de

EDUCATION

Doctoral student

April, 2016 -

IPHS, Faculty of Medicine, University of Cologne

26th Aug.– 1st Oct. 2009

NUPAD, School of Medicine, Federal University of Minas Gerais,
Belo Horizonte, Brazil.

Certificate

Newborn Screening for Sickle Cell Disease and other
Haemoglobinopathies.

May, 2007-Aug.2008

Liverpool School of Tropical Medicine, U.K.

Certificate

Professional Diploma, Project Design and Management.

Thesis Topic

*“Evaluating Pre -Analytical Errors Affecting the Quality of
Specimen for Laboratory Investigations at KATH”.*

Aug, 2003 – June, 2008

Kwame Nkrumah University of Science and Technology
Kumasi, Ghana. (School of Medical Sciences)

Certificate

Master of Philosophy in Clinical Biochemistry.

Thesis Topic

*“A study to Elucidate the Impact of Direct Nutritional Intervention
/Supportive Therapy on the Health and Quality of Life of People
Living with HIV/AIDS”.*

Sept, 1998-Jun, 2002

Kwame Nkrumah University of Science and Technology
Kumasi, Ghana. (College of Health Sciences).

Certificate

Bsc. (Hons.) Medical Laboratory Technology

Dissertation: “*Granulocytosis Causes Sickle Cell Crisis*”.
Jan, 1994-Nov. 1996 St. John’s Secondary School, Sekondi, W/R.
Certificate Senior Secondary School Certificate
Jul, 1991-1993 Nana Katabra “A” Junior Secondary School Kojokrom, W/R.
Certificate Basic Education Certificate.

WORK EXPERIENCE

Oct., 2011 Lecturer - Haematology, Department of Medical Diagnostics, KNUST- Kumasi.
2009 – 2012. Laboratory Manager, Garden City Hospital, Asokore-Mampong – Kumasi.
2010 – 2011 Haematology Tutor – DOSONEC Health Care Institute, Patasi-Kumasi, Ghana
2003 – 2011 Biomedical Scientist - Haematology Department, Komfo Anokye Teaching
Hospital, Kumasi Ashanti Region
2005 – 2008 Biomedical Scientist - Clinical Laboratory Component, Sickle Cell Foundation of
Ghana - Center Sickle Cell Disease, (Kumasi).
2003-2009 Demonstrator (Haematology) – Department of Medical Laboratory Technology,
Kwame Nkrumah University of Science and Technology.
2002 – 2003 Clinical Intern- Komfo Anokye Teaching Hospital, Kumasi - Ghana.

APPOINTMENTS

Aug 2012 – March, 2015 Examination Officer – Faculty of Allied Health Sciences, KNUST
March, 2012-Aug. 2012 Chief Invigilator – Faculty of Allied Health Sciences, KNUST
Oct., 2011-Aug. 2012 Examination officer –Dept. of Medical Lab. Technology,
KNUST
Dec, 2010 Member – National Technical Advisory Committee on Newborn
Screening for Sickle Cell Disease, Ghana
13th August, 2009 External Examiner - Professional Qualifying Examination of
Medical Laboratory Technician Program, Rural Health Training
School, Kintampo
July, 2009 Member - National Accreditation Board AccreditationPanel

- Jan., 2009 Member - Strategic Scale-up of National Newborn Screening for Sickle Cell Disease Programme, Ghana Health Service.
- Oct., 2003 – 2011 Quality Control Officer - Haematology Dept. Komfo Anokye Teaching Hospital

PUBLICATIONS

1. Selleh PK, Anto EO, Boadu WIO, **Sackey B**, Boateng LA, Nkansah C, Nsafoah F, Saasi AR, Mintaah S, Wiafe YA, Derigubah C, Korsah EE, Frimpong J, Ansah E, Tamakloe VCKT, Adu P, Boachie J, Addai-Mensah O. Quality of glycemc control in type 2 diabetes mellitus (T2DM) and its association with markers of coagulation and inhibitors of fibrinolysis: A case-control study in the Upper West Region, Ghana. *Health Sci Rep.* 2023 Jun 7;6(6):e1297. doi: 10.1002/hsr2.1297. PMID: 37292102; PMCID: PMC10246457.
2. Abdul G, Osei-Wusu W, Asare GA, Daud S, Opoku S, Tamakloe VCKT, Frimpong J, **Sackey B**, Boadu WIO, Paintsil V, Annani-Akollor ME, Wiafe YA, Anto EO, Addai-Mensah O. Biomarkers of oxidative stress and its nexus with haemoglobin variants and adverse foeto-maternal outcome among women with preeclampsia in a Ghanaian population: A multi-centre prospective study. *PLoS One.* 2023 Mar 30;18(3):e0283638. doi: 10.1371/journal.pone.0283638. PMID: 36996011; PMCID: PMC10062654.
3. Owusu-Poku, Ama, Gyamfi, Daniel, Togbe, Eliezer, Opoku, Stephen, Ephraim, Richard & Asibey, Jocelyn, **Sackey, Benedict**, Boadu, Wina, Annani-akollor, Max, Anto, Enoch, Addai-Mensah, Otchere. (2022). Interplay between foetal haemoglobin, micronutrients and oxidative stress biomarkers in sickle cell anaemia children. *Human Nutrition & Metabolism.* 30. 200173. 10.1016/j.hnm.2022.200173
4. Osei-Owusu, W., D. O. Ntiamoah, G. A. Akuffo, S. Mintaah, M. Owusu, **B. Sackey**, L. Antwi-Boateng, G. Abdul, M. Annani-Akollor, E.-W. Owiredu, A. Y. Debrah and O. Addai-Mensah (2021). "Coagulation abnormalities in childhood acute lymphoblastic leukemia:

assessing the impact of L-asparaginase therapy in Ghana." *Thrombosis Journal* **19**(1): 44.
<https://doi.org/10.1186/s12959-021-00297-4>

5. Abbam G, Tandoh S, Tetteh M, Afrifah DA, Annani-Akollor ME, Owiredu E-W, Gyasi C , Adu-Gyamfi C, **Sackey B**, Debrah AY, Otchere Addai-Mensah et al. (2021). Reference intervals for selected haematological and biochemical parameters among apparently healthy adults in different eco-geographical zones in Ghana. *PLoS ONE* 16(1): e0245585. <https://doi.org/10.1371/journal.pone.0245585>
6. Boateng L.A, Schonewille H., **Sackey B.**, Owusu-Ofori S. Afriyie, E. (2015). Prevalence of red blood cell antibodies among transfused patients at Komfo Anokye Teaching (KATH) Hospital, Ghana. *Journal of Science and Technology, Ghana*.
7. Ackah-Bonwin E, **Sackey B**, Boateng A I, (2013). Pre-analytical errors in the haematology laboratory, Komfo Anokye Teaching Hospital. *Proceedings of 1st Regional Conference of Ghana Association of Biomedical Scientist*.
8. Opoku-Okrah C, Sam DK, Nkum B, Dogbe EE, Antwi-Boateng L, Sackey B, Gyamfi D, Danquah KO. Sports anaemia and anthropometric evaluation of footballers at Kwame Nkrumah University of Science and Technology (KNUST). *Pan Afr Med J*. 2016 May 9;24:25. doi: 10.11604/pamj.2016.24.25.7244. PMID: 27583089; PMCID: PMC4992372.
9. Yeboah F.A, **Sackey B** Oti-Boateng P. (2007). Impact of direct nutritional intervention and palliative care on the health status of people living with HIV/AIDS in rural and urban poor of Ghana. *IAS (Sydney) · Abstract: A-042-0113-00872*.

Date: 21.06.2023



Signature